To the Graduate Council:

I am submitting herewith a thesis written by Sara Bier entitled " Geology of the Southeastern South Mountains, North Carolina." I have examined the final copy of this thesis for form and content and recommend that it be accepted in partial fulfillment of the requirements for the degree of Master of Science, with a major in Geology.

Dr. Robert D. Hatcher, Jr.

We have read this thesis and recommend its acceptance:

Dr. Harry McSween

Dr. Lawrence Taylor

Accepted for the Council:

Interim Vice Provost and
Dean of the Graduate School

GEOLOGY OF THE SOUTHEASTERN SOUTH MOUNTAINS, NORTH CAROLINA

A Thesis

Presented for the

Master of Science

Degree

The University of Tennessee, Knoxville

Sara Bier

August, 2001

This thesis is dedicated to my dog and best friend,
the best little dog that ever was born.

Josie

ACKNOWLEDGMENTS

These few pages of gratitude will never adequately thank all the individuals that made this thesis possible. First, I would like to thank my advisor, Dr. Robert D. Hatcher, Jr., for his wisdom and guidance while deciphering the Inner Piedmont "soup". I am most grateful for the opportunity to pursue research that required over a year of hiking in the Carolina hills creating a geologic map. I would also like to thank my other committee members, Dr. Lawrence Taylor and Dr. Hap McSween, for their ability to make petrology exciting. They are indeed the best teachers I've ever had.

Thanks to the Science Alliance Center of Excellence and the EDMAP component of the National Cooperative Mapping Program for financial support.

Thanks to the South Mountains State Park staff, especially Walt and Jeremy, for providing me with transportation, a cabin, and watching out for me. I want to thank the communities of Casar, Moriah, and Golden Valley for letting me traverse their mountains and for the lively conversation and memorable horseback trips.

I owe an immense amount of gratitude to the "Hatchery". Thanks to Scott Giorgis for an introduction to fieldwork in the South Mountains. Thanks to Jen Whisner for being a source of inspiration and female companionship, and to her husband, Chris, for his ceaseless energy and humor. Thanks to Camilo Montes for the occasional coffee breaks, his limitless knowledge and patience when dealing with three dimensional challenges, and also to his wife, Sara, for not letting us fall at Obed. Thanks to Brendan Bream for his endless assistance, even when 3000 miles away. Thanks to both Brendan and Katy Bream for their friendship and support. I owe the biggest thanks to Nancy Meadows, my fairy godmother. Without her unconditional support and huge heart (not to mention her amazing ability to keep the Hatchery happy), this never would have happened.

Other Tennessee folks deserving of thanks include Dr. William Dunne, Theresa Mathes, Mike Wyatt, Steve Tavernier, Keith Milam, Dana Miller, Amy Robinson, and Amber Johnstone. I am especially grateful for Heather Gastineau's friendship; the hospitality and the companionship during the all-nighters.

I would also like to acknowledge the four individuals, Dr. Keith Mann, Dr. Lawrence Mutti, Dr. Robert Washburn, and Dr. Thomas Laudon, who inspired and fed my geologic enthusiasm (and got me into this mess).

I thank Wesley Shepherd for the couch and cornbread and Drippy and Skippy for the welcome distractions. My sister and friend Jessica deserves a million thanks for the home, the dogs, the pizza, the bike, the hikes, the river, and most of all for the company. Thanks to Mom for her incredible listening skills, patience, and unconditional love. Thanks to Dad for his hospitality, his curiosity, his spirit of adventure, and his belief in me. Thanks to Rebecca, Jessica, and Jonathan for being my favorite people in the whole world as well as my siblings. Thanks to my entire family: Mom, Dad, Rebecca, Jessica, Jonathan, Josie, Allie, Belle, Patrick, and Secan for their love and support and most of all, for the much-needed reminders of what's truly important.

Lastly, I want to thank Scott Williams for his companionship, serenading distractions, patience, support, and love.

ABSTRACT

Stratigraphic, geochemical, and structural data from across the North Carolina Inner Piedmont provide insight into the history of the southern Appalachian crystalline core. Detailed geologic mapping and compilation of over 500 km^2 (300 mi^2) of previous mapping reveal a similar package of metasedimentary rocks to those found in the western Inner Piedmont. This sequence consists of the Tallulah Falls Formation, which includes both a sillimanite schist middle member and a metagraywacke-schist upper member. Isolated and disseminated bodies of the Walker Top orthogneiss (granite to granodiorite) and the Toluca Granite were also recognized throughout the central and eastern Inner Piedmont.

Crystallization ages, preliminary zircon and monazite ages, mineral assemblages, petrographic textures, garnet chemical zoning profiles, and temperature and pressure estimates of rocks in and around the study area suggest a single prograde metamorphic event that occurred as a result of the Acadian orogeny. Metamorphic conditions estimated from electron microprobe data using a garnet-biotite geothermometer and garnet-aluminumsilicate-silica-plagioclase and garnet-plagioclase-muscovite-biotite geobarometers. They range from 610-645°C and from 3.8 ± 0.8 kbar to 5.4 ± 0.8 kbar. These conditions are consistent with mineral assemblages present and regional isograds, and support a model of Barrovian metamorphism for the Inner Piedmont.

A deformational framework for this portion of the Inner Piedmont in North Carolina includes five deformational events. Rare D_1 intrafolial folds and foliation are attributed to the Taconic orogeny. Penetrative D_2 structures include foliation, lineation, tight to isoclinal and reclined to recumbent folds, sheath folds, and Type-F thrust sheets. D_3 folds and Type-C thrust faults probably constitute the latter portion of ductile Acadian deformation. D_4 broad open folds formed during the Alleghanian orogeny. D_5 fractures are a result of Mesozoic uplift and extension.

A portion of the North Carolina Inner Piedmont from the Brevard fault zone to the eastern Inner Piedmont is divisible into three fault-bounded domains. The easternmost domain is subdivided into five subdomains based on homogenous fabrics. Foliation reflects a regional change in strike from NE-SW in the western flank to N-S in the central Inner Piedmont back to NE-SW in the southeastern part of the terranes. Lineations are aligned NE-SW (orogen parallel) in the western Inner Piedmont and E-W in the central Inner Piedmont and probably indicate transport direction. The structural data and map patterns compiled in this study are best explained by crustal flow during oblique collision.

TABLE OF CONTENTS

CHAPTER	PAGE
I. INTRODUCTION	1
Regional setting	2
Previous work	2
Lithologic units	2
Metamorphism	5
Structure	5
Location	6
Methodology	6
II. LITHOLOGIC UNITS AND STRATIGRAPHY	9
Tallulah Falls Formation	9
Tallulah Falls metagraywacke-schist	11
Tallulah Falls aluminous schist	14
Toluca Granite	16
Walker Top orthogneiss	21
III. METAMORPHISM	28
Regional metamorphism	28
Timing	30
Migmatization	30
Petrography	31
Tallulah Falls Formation	31
Walker Top orthogneiss	33
Toluca Granite	33
Electron Microprobe Analyses	34
Temperature estimates	34
Pressure estimates	36
Chemical zoning in garnets	40
Conclusions	47
IV. MESOSCOPIC STRUCTURE	48
Mesoscale structures	48
Foliations	48
Lineations	49
Folds	52
Joints	55
IV. REGIONAL STRUCTURAL ANALYSIS	57
Introduction	57
Deformation events	59
D_1 deformation	59
D_2 deformation	62
D_3 deformation	69
D_4 deformation	71
D_5 deformation	71
Cross sections	71
Section A-A'	72
Section B-B'	72
Section C-C'	73
Section D-D'	73

TABLE OF CONTENTS

CHAPTER		PAGE
	Deformational synthesis and tectonic summary	73
VI.	CONCLUSIONS	77
	REFERENCES CITED	79
	APPENDICES	86
	Appendix A. Modal Analyses: Methodology	87
	Appendix B. XRF Analyses: Methodology and Precision of Results	90
	Appendix C. Structural data for portions of the Benn Knob and Casar quadrangles	101
	Appendix D. Compiled structural data for the Casar, Lawndale, Shelby and Boiling Springs quadrangles	127
	VITA	162

LIST OF TABLES

TABLE	PAGE
2-1. Modes of the Tallulah Falls Formation	13
2-2. Modes of the Toluca Granite	19
2-3. XRF analyses and CIPW norms for the Toluca Granite	20
2-4. Modes of the Walker Top orthogneiss	26
2-5. XRF analyses and CIPW norms for the Walker Top orthogneiss	27
3-1. Analyses of the Tallulah Falls Formation (BK 959) used for geothermobarometric estimations	35
3-2. Biotite and garnet analyses in the Walker Top orthogneiss (BK 337) used for geothermobarometric estimations	38
3-3. Analyses of plagioclase and muscovite in the Walker Top orthogneiss (BK 337) used for geothermobarometric estimations	39
3-4. Analyses plotted in Figure 3-4; garnet D zoning in the Tallulah Falls Formation (Sample BK 82)	44
3-5. Analyses plotted in Figure 3-5; garnet zoning in the Walker Top orthogneiss	45
3-6. Analyses plotted in Figure 3-6; garnet zoning in the Toluca Granite	46
5-1. Deformational framework and related events for the central and western Inner Piedmont, North Carolina	60
B-1. SIAL protocol used for bulk chemical analyses	95
B-2. SIAL conditions of X-ray fluorescence	96
B-3. XRF analyses of the Toluca Granite	97
B-4. XRF analyses of the Walker Top orthogneiss	98
B-5. XRF analyses and certificate value of standards	99

LIST OF FIGURES

FIGURE		PAGE
1-1.	Simplified tectonic map of the southern Appalachians	3
1-2.	Location of and access to the study area	7
2-1.	Generalized stratigraphic column for the study area	10
2-2.	Photograph and photomicrograph of Tallulah Falls metagraywacke	12
2-3.	Photographs and photomicrograph of Tallulah Falls sillimanite schist	15
2-4.	IUGS modal classification of Toluca Granite and Walker Top orthogneiss	17
2-5.	Photographs and photomicrograph of Toluca Granite	18
2-6.	Major element discrimination diagram distinguishing orth- and paragneisses in metamorphic terranes	22
2-7.	Nb-Y and Rb-(Y + Nb) variation diagrams for the Toluca Granite and Walker Top orthogneiss	23
2-8.	Photograph and photomicrograph of the Walker Top orthogneiss	25
3-1.	Metamorphic isograd map of North and South Carolina	29
3-2.	Petrogenetic grid for aluminous rocks	32
3-3.	Petrogenetic grid with metamorphic conditions determined by mineral phases present and temperature and pressure estimates calculated from electron microprobe data	37
3-4.	Rim to tim garnet traverse in Sample BK 252	41
3-5.	Near-rim weight percent oxide composition of the garnet in Sample BK-337	42
3-6.	Traverse of a garnet in the Toluca Granite	43
4-1.	Scatter plot, fabric diagrams, and dip histograms for all foliation measurements obtained in the study area	50
4-2.	Plots of preferred mineral orientation lineations from the study area	51
4-3.	Mesoscale fold measurements from the study area	53
4-4.	Photographs of folds in the study area	54
4-5.	Distribution of all joint measurements collected from the study area	56
5-1.	Simplified tectonic map of the southern Appalachians	58
5-2	Index map to domains	61
5-3.	S_1 and S_2 foliation relationships	63
5-4.	Lower hemisphere, equal-area contoured diagrams of poles to foliation for the study area	64
5-5.	Lower hemisphere, equal-area contoured diagrams of lineations and directions of regional scale sheath fold axes in the study area	66
5-6.	Lower hemisphere, equal-area contoured diagrams of fold axes in the study area	68
5-7.	F_{2b} fold in the Tallulah Falls metagraywacke showing thickened hinges and attenuated limbs	70
A-1.	Chart for judging the reliability of point-counting results	89

LIST OF PLATES

PLATE	PAGE
I. Geologic map and cross sections of portions of the Benn Knob and Casar 7.5-minute quadrangles, North Carolina	in pocket
II. Station map of portions of the Benn Knob and Casar 7.5-minute quadrangles, North Carolina	in pocket
III. Compiled geologic map of the Casar, Polkville, Lawndale, Boiling Springs and Shelby 7.5-minute quadrangles, North Carolina	in pocket
IV. Station map of the Casar, Polkville, Lawndale, Boiling Springs, and Shelby 7.5-minute quadrangles, North Carolina	in pocket
V. Detailed geologic mapping in the western and central Inner Piedmont North Carolina	in pocket

CHAPTER 1

INTRODUCTION

The crystalline cores of orogens contain a wealth of information about their tectonic and metamorphic histories. Since recognition of the Inner Piedmont as the locus of the Acadian orogeny in the southern Appalachians (Davis, 1993; Hatcher, 1993), continued detailed mapping of the area is the first step to resolving the history of the crystalline southern Appalachians. The South Mountains, with their moderate relief, and thus excellent exposure, have proven to be an excellent location to conduct this geologic study.

Detailed mapping in the western Inner Piedmont enabled previous workers (Davis, 1993; Hill, 1999) to recognize a primary lithostratigraphic sequence. Recognition of this sequence by later workers (Bream, 1999; Giorgis, 1999; Hill, 1999; Williams, 2000) in the western Inner Piedmont of North Carolina warranted detailed mapping in the southeastern South Mountains, south and east of previous study areas.

This work is a culmination of two field seasons of detailed mapping of ~110 km^2 (~66 mi^2) in the southeastern South Mountains between Morganton and Shelby, North Carolina, and structural, petrographic, and geochemical analyses of the mapped lithologic units. The lithologic units, which include metagraywacke, sillimanite schist, the Walker Top orthogneiss, and the Toluca Granite, are described in Chapter 2. Chapter 3 discusses the metamorphic history of the study area, with a focus on geothermobarometric estimates from electron microprobe data. Mesoscale structures in the study area are discussed in Chapter 4. A regional structural analysis of the western and central Inner Piedmont, North Carolina, is presented in Chapter 5. Conclusions are stated in Chapter 6.

REGIONAL SETTING

The Inner Piedmont comprises the highly deformed and metamorphosed core of the Acadian orogen in the southern Appalachians (Hatcher, 1993). The terrane is separated from the eastern Blue Ridge by the Brevard fault zone and from the Carolina terrane to the southeast by the Central Piedmont suture (Fig. 1-1).

PREVIOUS WORK

Previous mapping adjacent to and in the study area has been conducted by Overstreet *et al.* (1963a, 1963b), Verseput (1980), Goldsmith *et al.* (1988), Giorgis (1999), and Williams (2000). Overstreet *et al.* (1963b) mapped the Shelby 15-minute quadrangle and the southern portion of the Casar quadrangle (Overstreet *et al.*, 1963a). Verseput (1980) mapped the South Mountains State Park that lies in the northeast corner of the Benn Knob quadrangle. Goldsmith *et al.* (1988) published the Charlotte 1° X 2° quadrangle. Giorgis (1999) mapped 160 km^2 spanning parts of four quadrangles: Dysartsville, Glen Alpine, Morganton South, and the northwest corner of Benn Knob. Williams (2000) mapped the eastern portion of Glenwood, the southern portion of Dysartsville, and the northern portion of Sunshine quadrangles.

LITHOLOGIC UNITS

Multiple episodes of deformation and high grades of metamorphism in the Inner Piedmont have made recognition of primary igneous or sedimentary structures difficult, but a distinct stratigraphic order has been resolved west of the study area. It consists mainly of metagraywacke, aluminous schist, and amphibolite (Tallulah Falls Formation), overlain by a

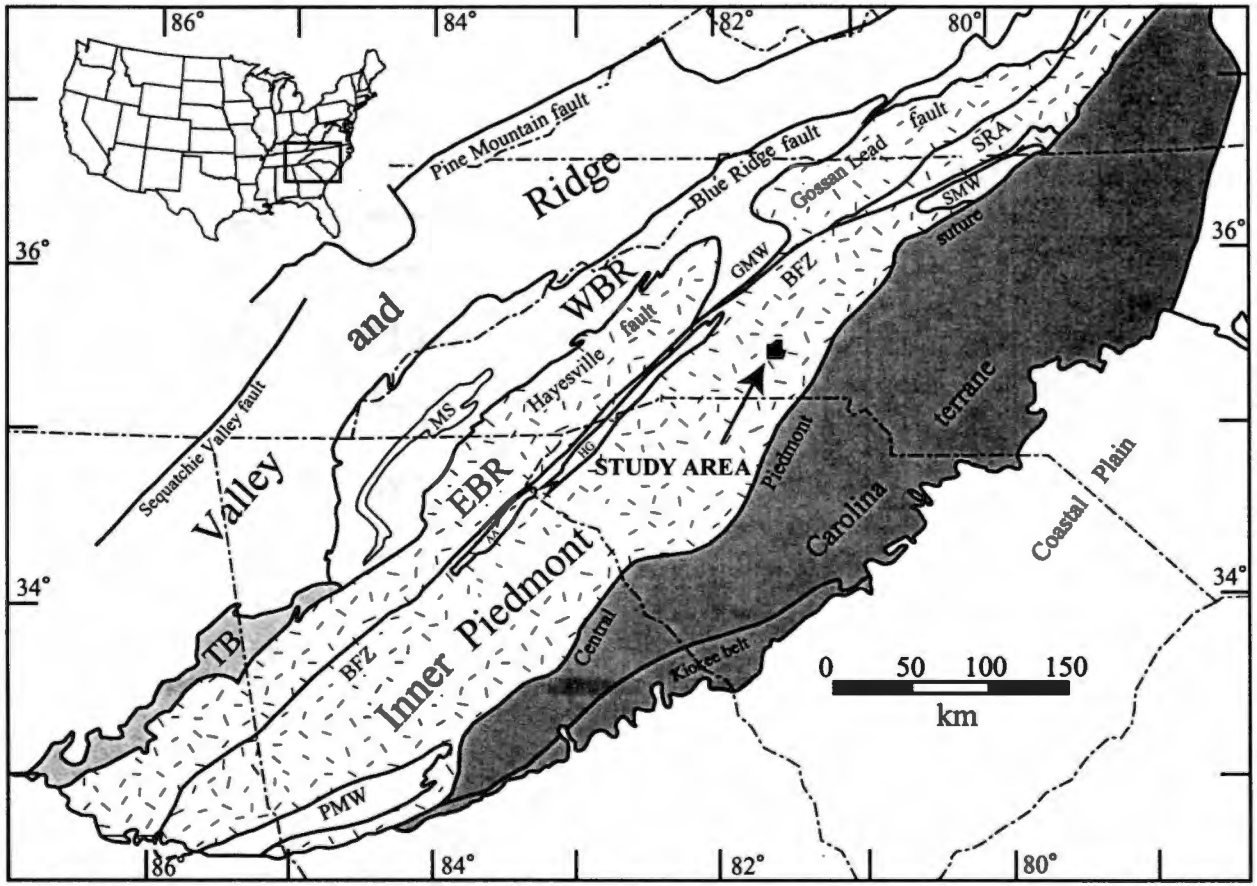


Figure 1-1. Simplified tectonic map of the southern Appalachians. The study area is in black. TB-Talladega belt. MS-Murphy syncline. WBR-Western Blue Ridge. GMW-Grandfather Mountain Window. EBR-Eastern Blue Ridge. BFZ-Brevard fault zone. AA-Alto allochthon. HG-Henderson Gneiss. SMW-Sauratown Mountain window. SRA-Smith River allochthon. PMW-Pine Mountain window. Modified from Hatcher *et al.* (1990).

different amphibolite and quartzite (Poor Mountain Formation; Hatcher, 1993). Similar marker units (i.e., sillimanite schist) suggest that the lower sequence is related to the assemblage present in the easternmost Blue Ridge (Tallulah Falls-Ashe Formation; Hatcher, 1989).

The basal cover sequence is the Tallulah Falls Formation that rests on either oceanic or continental basement (Hatcher, 1993). This formation can be divided into several distinct members: a metagraywacke, amphibolite, and two-mica schist member; a kyanite/sillimanite-garnet-mica schist member; and a metagraywacke and two-mica schist member (Hatcher, 1993). Previous workers in the area recognized similar lithologies (e.g., sillimanite schist, biotite schist, and biotite gneiss) but subdivided them differently (Overstreet *et al.*, 1963a, 1963b; Verseput, 1980; Davis, 1993; Yanagihara, 1994).

Stratigraphically overlying the Tallulah Falls Formation is the Poor Mountain Formation. The Poor Mountain Formation was broken down into four major units by Schufflebarger (1961) and Hatcher (1969): the Brevard-Poor Mountain transitional member consists of garnet-mica schist and metasiltstone; the Poor Mountain amphibolite consists of laminated amphibolite and hornblende gneiss; and the quartzite and marble members (Hatcher, 1969, 1993) are made up of interbedded quartzite, amphibolite, and marble. These units are in contact with the Tallulah Falls Formation northwest of, but not within, the study area.

Granitoids occur throughout the Inner Piedmont (Goldsmith *et al.*, 1988; Nelson *et al.*, 1998), and the South Mountains are no exception. The Walker Top orthogneiss and the Toluca Granite have been recognized and mapped in the study area. The Toluca Granite is a gray, medium-grained, biotite granite that occasionally contains megacrysts of garnet and feldspar (Overstreet *et al.*, 1963a, 1963b; Verseput, 1980). The Walker Top orthogneiss is a feldspar-megacrystic granite to granodiorite that was once thought to be potentially basement but has been determined to be a post-peak-metamorphic-catazonal pluton with an Ordovician crystallization age (Giorgis, 1999; Vinson, 1999).

Quaternary deposits in this area consist of alluvium and colluvium. Typical alluvium consists of well-sorted channel, point bar, and flood plain deposits derived from the local bedrock. Colluvium is generally poorly sorted with grain sizes as large as boulders. Landslide lobes are another Quaternary feature common in the study area.

METAMORPHISM

The core of the Inner Piedmont underwent intense metamorphism with metamorphic grade decreasing toward the western and eastern flanks of the belt (Butler, 1991; Hatcher, 1993). Some workers have suggested two separate episodes of metamorphism (Lemmon, 1973; Roper and Dunn, 1973). Recent work suggests only one progressive upper-amphibolite facies (sillimanite-grade) metamorphic event occurred here (Davis, 1993; Yanagihara, 1994) and Pb isotopic age dates from monazite grains (Dennis and Wright, 1997) and zircons (Bream, pers. comm., 2000) suggest that it was Acadian.

STRUCTURE

The Inner Piedmont is structurally characterized by a stack of westward-vergent Type-F (fold-related) thrust sheets, generated by the cutting out of the common limb between a plastic antiform and synform (Hatcher and Hooper, 1992). Cooling allows these thrust sheets to gain additional strength and coherence, thus permitting greater transport, and transforms Type-F thrust sheets into Type-T, then Type-C (composite) thrust sheets.

Studies by Davis *et al.* (1991), Davis (1993), and Yanagihara (1994) in North Carolina, and Hatcher (1969, 1972, 1978, 1989) in South Carolina indicate five separate deformation events. The detailed mapping and compilation of my study also supports five deformation events, with slight modification.

According to Goldsmith *et al.* (1988), there is a strong northwest trend in the structure of the Benn Knob quadrangle. They defined a dominant foliation and horizontal fold axes that trend north-northeast (Goldsmith *et al.*, 1988). In South Mountains State Park, in the northeast corner of Benn Knob quadrangle, Verseput (1980) mapped north-south axes of tight recumbent folds and a later set of east-west-trending axes of open folds. He also recognized an earlier folding event from the presence of intrafolial folds.

LOCATION

The study area was chosen for its location between recent 1:12,000-scale geologic mapping in the western Inner Piedmont (Bream, 1999; Giorgis, 1999; Hill, 1999; Williams, 2000) and earlier detailed mapping of the interior Inner Piedmont (Overstreet *et al.*, 1963a, 1963b). The study area is located approximately 100 km (60 mi) east of Asheville and 42 km (25 mi) southwest of Hickory, North Carolina (Fig. 1-2). Access is limited due to the rural nature of the area, the expanding South Mountains State Park, and recent increase in State Forest Service gamelands. The southwest corner of the study area is accessible via Interstate 40 to U.S. 64 to State Road 226. Interstate 40 to State Road 18 to State Road 10 provides access to the eastern portion of the study area. Interior access is limited to secondary gravel roads or trails (by bicycle, horse, or foot).

METHODOLOGY

This study consisted of both field and laboratory components. Detailed mapping began in January, 1999, and continued through April, 1999. A second field season began in January, 2000, and continued through May, 2000.

Mapping was done at a 1:12,000 scale and compiled at a 1:24,000 scale using standard and enlarged U.S.G.S. 7.5 minute topographic quadrangles. Foliations, joints, lineations, and

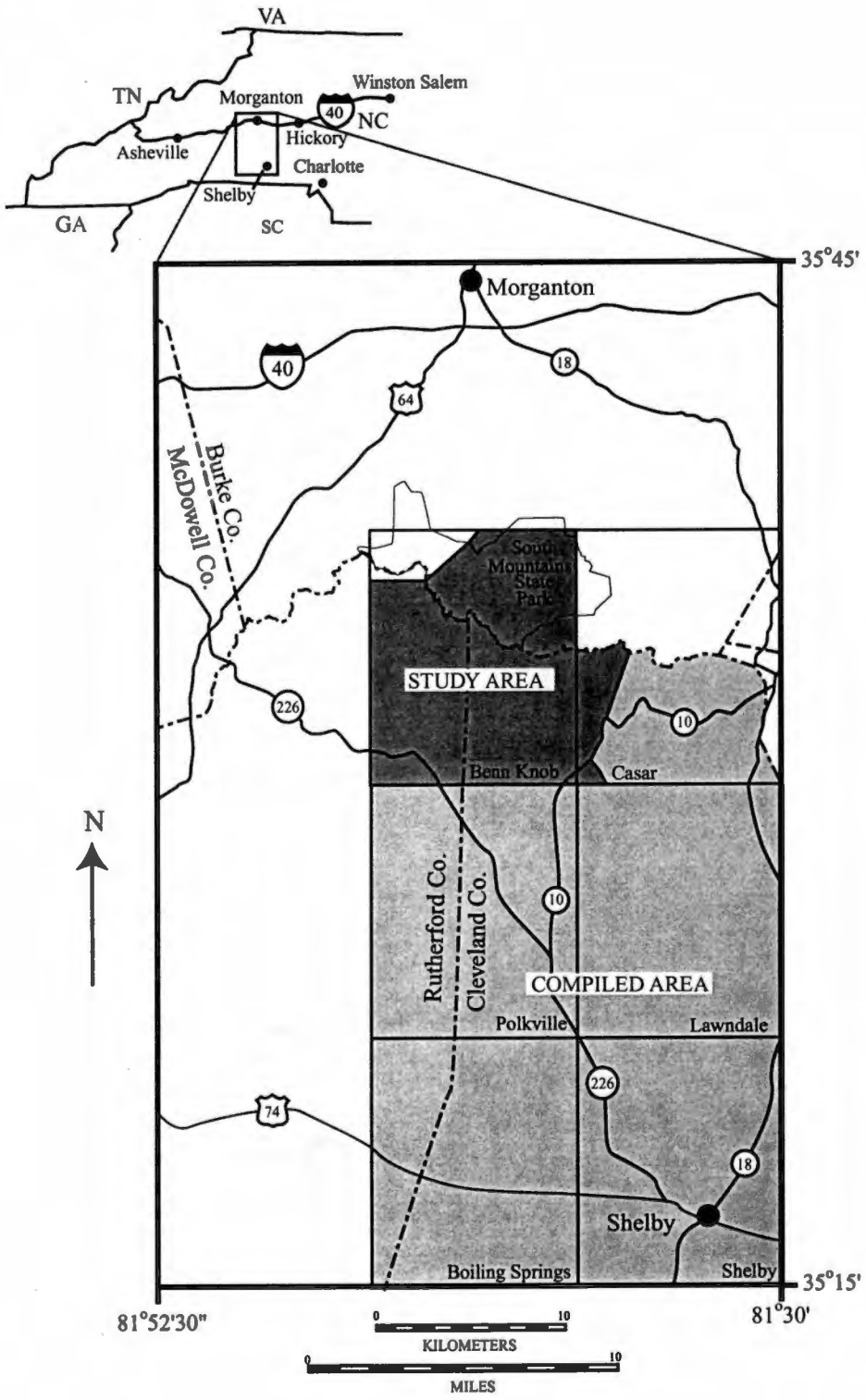


Figure 1-2. Location of and access to the study area. The dark gray area was mapped in this study. The light gray area was compiled from Overstreet *et al.* (1963).

folds were measured using a Brunton compass. Structural data and geologic contacts were compiled using Adobe Illustrator™ and Adobe Photoshop™ onto a raster image of the topographic base. Stereonets were created using GeoOrient created by Rod Holcombe (University of Queensland, Australia) to assist in structural analysis.

Laboratory work involved petrographic, bulk chemical, and microgeochemical analyses. Petrographic analysis was done using a Lietz Orthoplan Pol™ polarizing microscope. Point counting methodology and uncertainties are discussed in Appendix A. Reflected images were taken using an Olympus BH-2™ polarizing microscope.

Bulk chemical analyses were collected using an EG&G Ortec™ energy dispersive X-ray fluorescence spectrometer. Methods used to obtain bulk chemical analyses are discussed in Appendix B. Magma 2.3 [copyright by the Regents of the University of California, written by Ken Woheltz (Los Alamos National Laboratory and University of New Mexico)] was used to determine the CIPW normative mineralogy from bulk chemical analyses.

Microgeochemical data were collected on a CAMECA SX-52 in the University of Tennessee Electron Microprobe Facility. An acceleration voltage of 15 kV and a beam current of 20 nA were used for all analyses. Beam size varied depending on the mineral phase being analyzed; a 5 μm beam was used for biotite, muscovite, and plagioclase, and a 2 μm beam was used for garnet. A peak counting time of 20 seconds was used for all analyses, except for Fe in plagioclase and Na in garnet where a counting time of 30 seconds was used. Some garnet cation totals indicate the presence of Fe^{3+}, but all iron was calculated as Fe^{2+} due to uncertainty in Fe^{3+} electron microprobe calculations (Sobolev et al., 1999). Microgeochemical data were used in geothermobarometric estimations assisted by Thermobarometry v. 2.0 software written by Matthew J. Kohn and Frank S. Spear.

CHAPTER 2

LITHOLOGIC UNITS AND STRATIGRAPHY

The stratigraphy of the central Inner Piedmont is difficult to resolve because of its migmatitic and polydeformational history, but it is not impossible to resolve. Lithologies found within the study area include both paragneisses and orthogneisses. The paragneiss sequence consists of lithologies that may be equivalent to the Tallulah Falls Formation, which was originally recognized in the eastern Blue Ridge and then correlated across the Brevard fault zone into the western Inner Piedmont (Hatcher, 1972; Hopson and Hatcher, 1988; Davis, 1993; Yanagihara, 1994; Hill, 1999). Orthogneiss units include the Walker Top orthogneiss (Giorgis, 1999) and the Toluca Granite (Goldsmith *et al.*, 1988).

Stratigraphic relationships within the study area are presented in Figure 2-1. No basement was recognized in the study area. The aluminous schist member of the Tallulah Falls separates the lower and upper members. The Poor Mountain Formation that overlies the Tallulah Falls Formation in the western Inner Piedmont is not present east of the Brindle Creek thrust (Plate 1). The Walker Top orthogneiss and the Toluca Granite occur as disseminated pods throughout the hanging wall of the Brindle Creek thrust.

TALLULAH FALLS FORMATION

Hatcher (1971) first recognized and mapped the Tallulah Falls Formation in the eastern Blue Ridge of northeastern Georgia. Hatcher (1972, 1987), Davis (1993), and Hill (1999) correlated lithologies within the western Inner Piedmont with the Tallulah Falls Formation. This correlation has suggested that the Brevard fault zone is not a terrane boundary (Hill, 1999). The eastern Blue Ridge and Inner Piedmont terranes are both part of the Tugaloo terrane (Hatcher et al., 1999). The Tallulah Falls sequence consists of three members: a metagraywacke-schist-

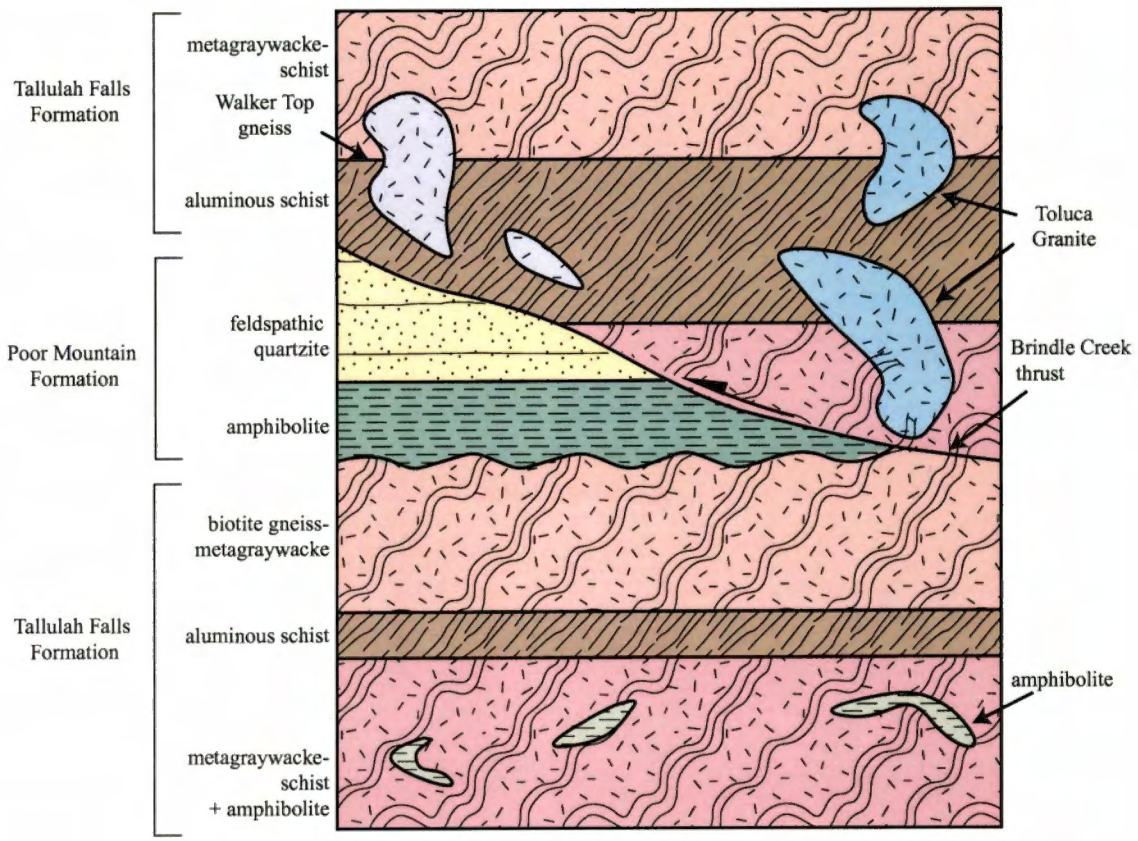


Figure 2-1. Generalized stratigraphic column for the study area.

amphibolite member (lower Tallulah Falls), an aluminous schist member, and a metagraywacke-schist member (upper Tallulah Falls).

Tallulah Falls metagraywacke-schist

Previous workers in the South Mountains (Bream, 1999; Hill, 1999) identified larger amounts of amphibolite in the lower Tallulah Falls relative to the upper member. Giorgis (1999) and Williams (2000) subdivided the lower and upper members based entirely on the stratigraphic position relative to the sillimanite-mica schist marker unit. Due to the lack of amphibolite and the change in the sillimanite schist marker unit in the study area, the metagraywacke-schist is correlated with the upper Tallulah Falls member.

In outcrop, the upper Tallulah Falls member is gray and contains migmatitic quartzofeldspathic gneiss interlayered with biotite-muscovite schist (Fig. 2-2). Rare occurrences of calc-silicate are present and were observed as float. The well-developed foliation is defined by the alignment of biotite, muscovite, and quartz. Compositional banding is defined by alternating quartzofeldspathic and biotite-muscovite schist bands ranging from one centimeter to several meters thick.

Modal analyses of the Tallulah Falls Formation are presented in Table 2-1. The mineral assemblage of the upper Tallulah Falls member is plagioclase (An_{20-30}) + quartz + biotite + muscovite + sillimanite ± garnet. Zircon and chlorite occur as accessory or trace minerals. Biotite (0.5-3 mm) and muscovite (0.25-1.5 mm) define the foliation and are segregated into layers that alternate with quartz (0.1-2 mm) and plagioclase (An_{20-30}, 0.2-3 mm) layers. Biotite often defines microscale structures (Fig. 2-2).

(a)



(b)

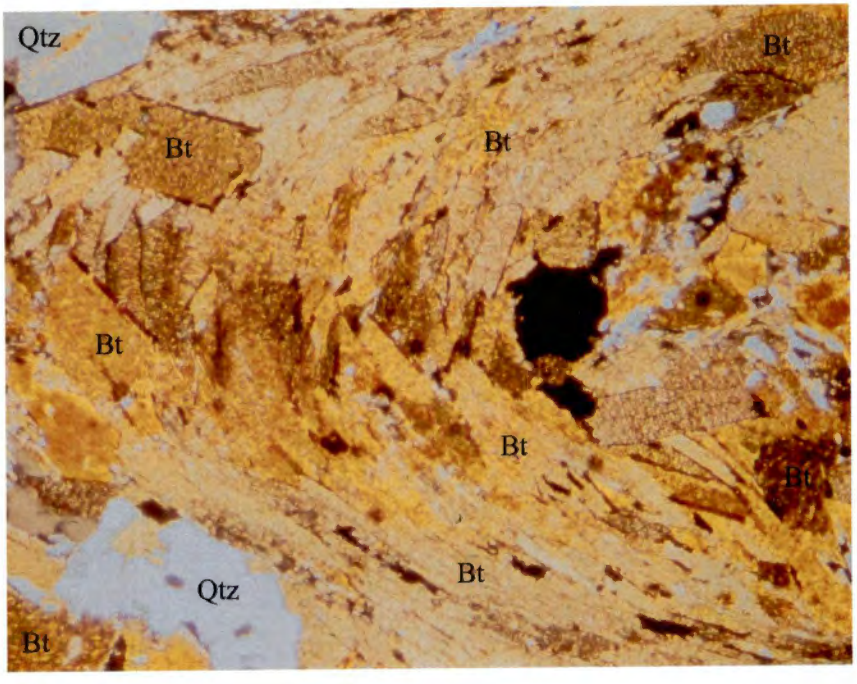


Figure 2-2. Photograph and photomicrograph of Tallulah Falls metagraywacke. (a) Tallulah Falls migmatitic metagraywacke near Gibbs Gap, Benn Knob quadrangle (Plate 1). (b) Sample BK 375 from Shinny Creek, Benn Knob quadrangle (Plate 1). Microfold defined by biotite. Field of view is 4.25 mm. Qtz-quartz, Bt-biotite.

Table 2-1. Modes of the Tallulah Falls Formation. Trace (tr) minerals are less than 0.1% of the thin section. Point counting methodology and uncertainties are discussed Appendix A.

	Tallulah Falls sillimanite schist				Tallulah Falls metagraywacke-schist				
	BK 572	**BK 575**	**BK 1226**	**BK 1345**	**BK 112**	**BK 305**	**BK 320**	**BK 375**	**BK 959**
points counted	2153	2072	2172	2559	2480	2346	2540	2087	2028
Quartz	–	31.9	19.4	22.6	39.5	22.5	20.1	19.1	38.3
Plagioclase	–	7.1	6.3	15.2	15.9	21.7	29.9	32.4	21.8
Muscovite	7.1	6.5	23.4	41.1	4.2	3.6	8.9	8.4	3.1
Biotite	–	25.1	2.6	3.6	32.4	37.8	38.1	35.1	34.8
Sillimanite	34.5	16.7	41.8	11.7	4.9	6.1	0.3	1.6	–
Garnet	1.9	12.8	3.9	3.8	3.1	7.8	1.9	1.0	1.8
Tourmaline	39.7	–	–	–	–	–	–	–	–
Kyanite	12.6	–	–	–	–	–	–	–	–
Rutile	4.5	–	–	–	–	–	–	–	–
Chlorite	–	–	2.4	tr	–	–	–	0.6	tr
Epidote	–	–	–	1.9	–	–	–	–	–
Opaques	tr	tr	tr	tr	tr	tr	0.3	1.1	tr
Zircon	tr	tr	tr	tr	tr	0.5	0.3	0.7	tr
Total	100.3	100.1	99.8	99.9	100.0	100.0	99.8	100.0	99.8

Tallulah Falls aluminous schist

The aluminous schist member occurs as a marker unit in the western Inner Piedmont (e.g., Hill, 1999). My work indicates that it thickens dramatically to the central Inner Piedmont, in the hanging wall of the Brindle Creek thrust. This thickness increase could be the result of an original facies change of the Tallulah Falls Formation or complex folding of the unit, and is most likely a combination of both.

The aluminous schist member of the Tallulah Falls Formation consists of sillimanite schist and sillimanite gneiss in the study area. In outcrop, the sillimanite schist and gneiss are gray to grayish-brown purple and weather to tan, yellow ochre, and purple-brown saprolite (Fig. 2-3). The well-developed foliation of the unit is defined by the alignment of micas, predominantly muscovite, sillimanite, and quartz. The sillimanite (up to 5 cm) occurs in mats that are concordant with the foliation but rarely displays a strong lineation. Sillimanite also occurs as pseudomorphs after kyanite (Fig. 2-3).

Modal analyses of the middle member of the Tallulah Falls are presented in Table 2-1. The assemblage of the Tallulah Falls sillimanite schist is muscovite + quartz + plagioclase (An_{20-35}) + sillimanite + biotite + garnet ± tourmaline (Fig. 2-3). Chlorite and epidote occur as accessory minerals, commonly as an alteration of plagioclase. Zircon, apatite, and opaques are present in trace amounts. The muscovite is bimodal in size, occurring as large grains (1-3 mm) and fine grain (0.2 mm) alteration within mats of sillimanite. Both fibrolitic and prismatic sillimanite were recognized in thin sections. Fibrolite was often associated with muscovite layers while the prismatic sillimanite occurred throughout the sections.

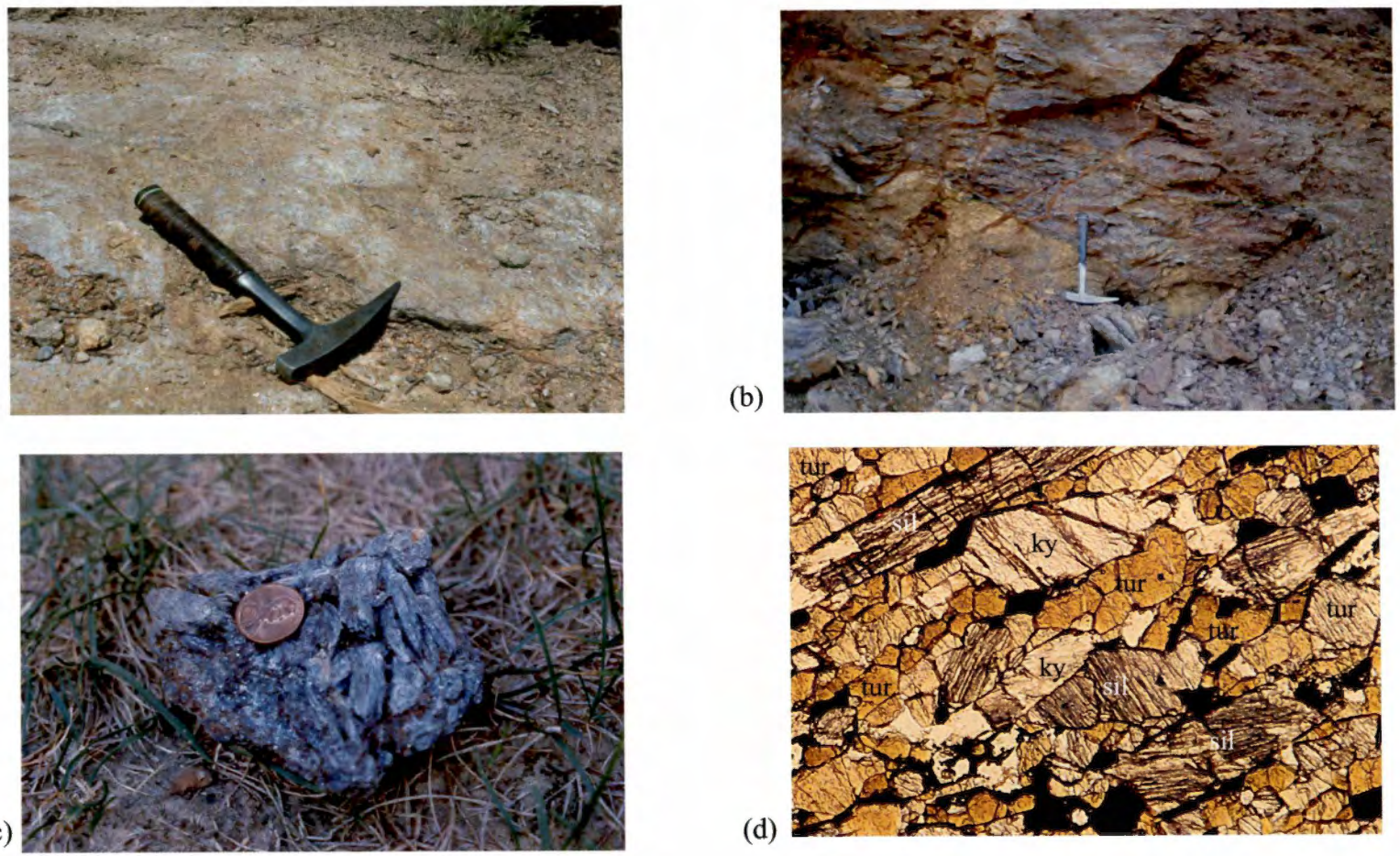


Figure 2-3. Photographs and photomicrograph of Tallulah Falls sillimanite schist. a) Tallulah Falls sillimanite schist near near Horse Ridge (Plate 1). b) Tallulah Falls sillimanite schist saprolite near Dogwood Stamp Mountain, Benn Knob quadrangle (Plate 1). c) Sample BK-1310 from Benn Knob (Plate 1). Sillimanite pseudomorphs of kyanite. d) Sample BK-572 from Huckleberry Mountain, Benn Knob quadrangle (Plate 1). Prismatic sillimanite, kyanite, and anhedral tourmaline. Field of view is 1.7 mm.

TOLUCA GRANITE

Keith and Sterrett (1931) originally recognized the Toluca Granite (Goldsmith *et al.*, 1988) and called it the Whiteside Granite. Griffitts and Overstreet (1952) subdivided the Whiteside Granite into the Toluca Quartz Monzonite and the Cherryville Quartz Monzonite. The Toluca quartz monzonite was renamed the Toluca Granite by Goldsmith *et al.* (1988) to adhere to Streckeisen's (1976) IUGS classification (Fig. 2-4). Preliminary ion microprobe analyses suggest Grenville inheritance and the $^{238}U/^{206}Pb$ zircon age date of the Toluca Granite is 379-388 Ma (B. R. Bream, unpublished data).

Griffitts and Overstreet (1952) noted that individual bodies of the Toluca Granite range from inches to thousands of feet in thickness and from a few feet to miles in length. The bodies mapped in this study also vary widely in size, possibly indicating original sills rather than a large contiguous pluton. The Toluca Granite is medium gray and weathers to light gray and tan saprolite. The unit is moderately to strongly foliated (Fig. 2-5), and, although bodies lie parallel to the foliation of the Tallulah Falls Formation, the foliation of the Toluca Granite is not always parallel to the contacts. This may be due to incomplete transpostion, relict magmatic foliation, or a rheological difference between the orthogneiss and the country rock.

Modal analyses of the Toluca Granite are presented in Table 2-2. The mineral assemblage of the Toluca Granite is plagioclase (An_{25-35}) + microcline + quartz + muscovite + biotite + garnet. Minor constituents include garnet and sillimanite. Zircon, monazite, xenotime, apatite, and opaques occur as accessory or trace minerals. The Toluca Granite is medium- to coarse-grained (1-4 mm) and usually equigranular but sometimes porphyritic with megacrysts of either garnet or feldspar (Fig. 2-5). Myrmekite occurs at the rims of some microcline megacrysts. The weak foliation is defined by the alignment of muscovite, biotite, and quartz.

Bulk chemical analyses of the Toluca Granite are found in Table 2-3. A discussion of XRF analyses and the accuracy and precision of the data is in Appendix B. Due to the high grade

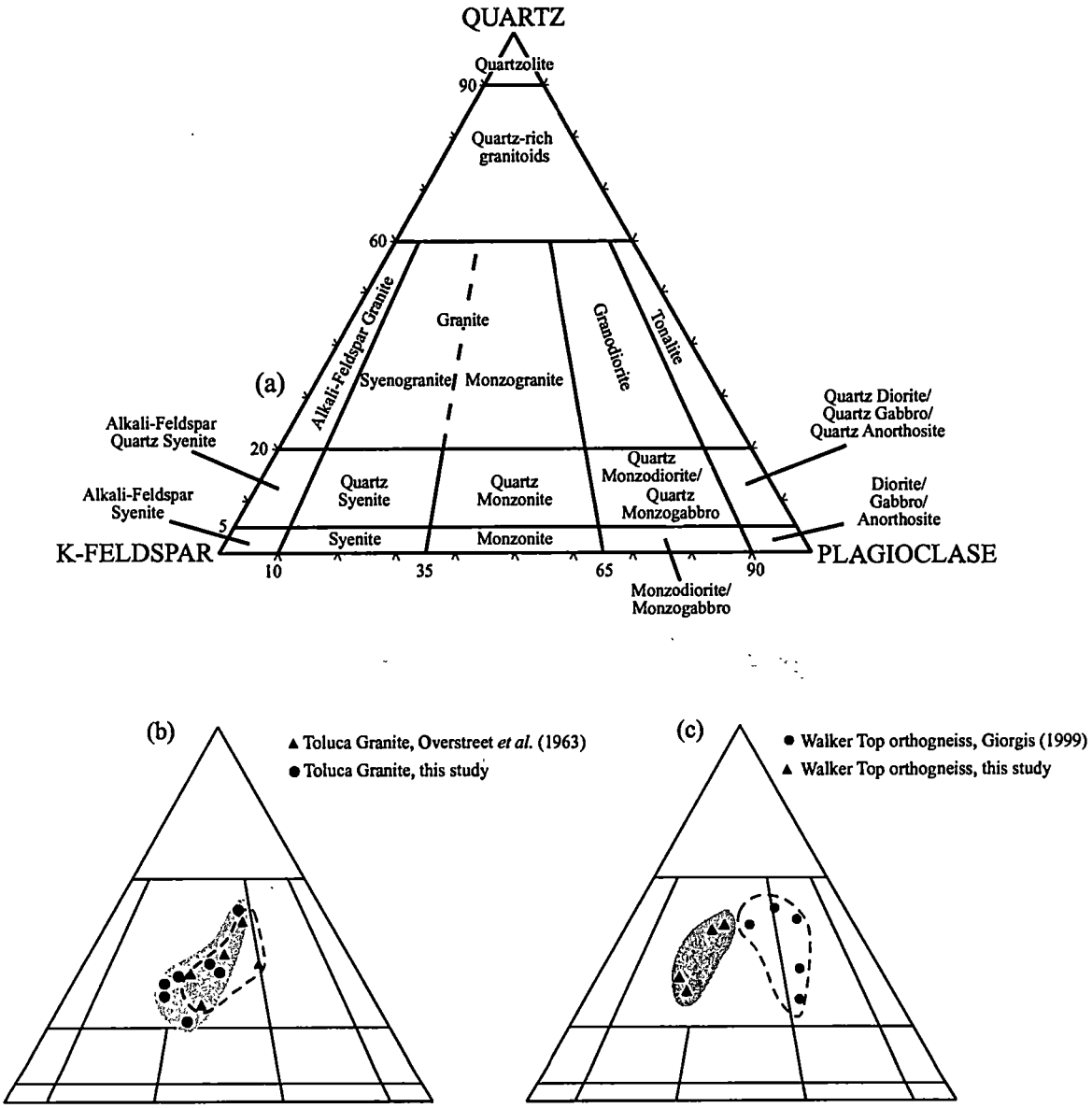


Figure 2-4. IUGS modal classification of Toluca Granite and Walker Top orthogneiss. (a) IUGS igneous classification after Streckeisen (1976) (b) Toluca Granite. Dashed line encloses data from Overstreet *et al.* (1963b). (c) Walker Top orthogneiss. Dashed line encloses data from Giorgis (1999). The difference in data sets is attributed to different point counting techniques (Appendix A).

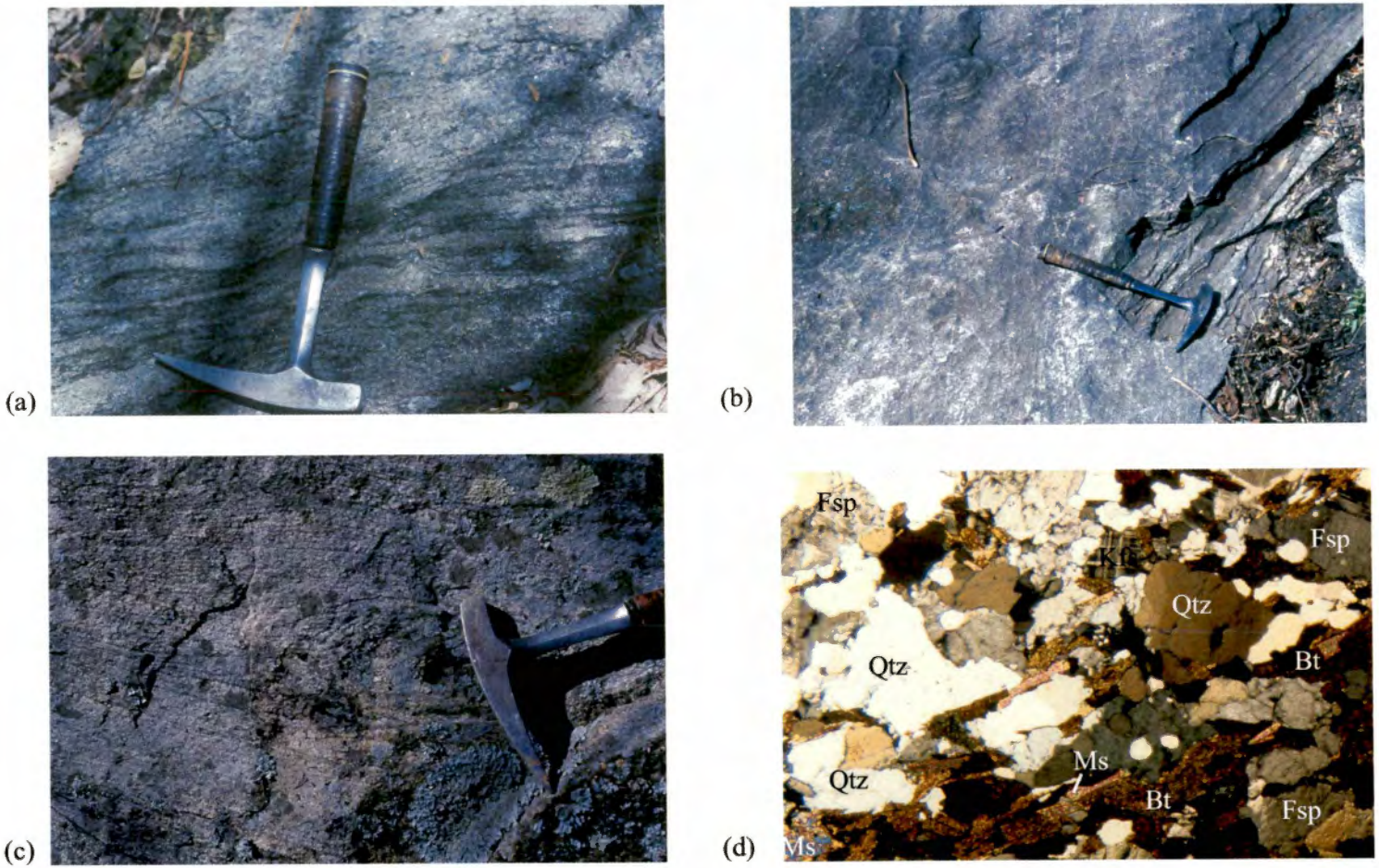


Figure 2-5. Photographs and photomicrograph of the Toluca Granite. (a) Toluca Granite near Black Mountain, Benn Knob quadrangle (Plate 1). (b) A xenolith of foliated biotite gneiss (around hammer head) within weakly foliated Toluca Granite near Shinny Creek, Benn Knob quadrangle. (c) Toluca Granite near Wards Gap, Benn Knob quadrangle (Plate 1) (d) Sample CA 63. Field of view is 1.7 mm. Fsp-feldspar (plagioclase), Kfs-Kfeldspar (microcline), Qtz-quartz, Ms-muscovite, Bt-biotite.

Table 2-2. Modes of the Toluca Granite. Trace (tr) minerals are less than 0.1% of the thin section. Point counting methodology and uncertainties are discussed in Appendix A.

	BK 372	BK 431	BK 1052	BK 1079	BK 1357	CA 40	CA 63	*Samples from Overstreet et al. (1963b)*					
points counted	2292	2174	3027	2685	2097	2005	2214						
Quartz	20.8	24.9	20.7	20.1	19.3	17.2	24.1	*26*	*31*	*23*	*26*	*38*	*31*
Plagioclase	41.8	30.3	29.7	29.1	31.3	31.2	18.8	*35*	*40*	*31*	*41*	*35*	*25*
Microcline	14.8	24.5	24.1	43.8	34.9	41.5	38.2	*23*	*28*	*34*	*16*	*20*	*38*
Muscovite	6.7	13.2	21.7	2.2	11.4	2.7	11.8	*8*	–	–	*4*	–	–
Biotite	15.9	7.1	1.7	4.8	1.4	5.3	4.3	*8*	*1*	*4*	*13*	*5*	*2*
Garnet	–	tr	tr	–	–	0.9	2.8	–	–	*8*	–	*2*	*4*
Sillimanite	–	tr	2.1	–	1.7	0.5	tr	–	–	–	–	–	–
Myrmekite	tr	–	–	tr	tr	0.7	tr	–	–	–	–	–	–
Total	100.0	100.0	100.0	100.0	100.0	100.0	100.0	100.0	100.0	100.0	100.0	100.0	100.0

Table 2-3. XRF analyses and CIPW norms for the Toluca Granite. The number in parentheses represents 1σ of the least digit cited. Accuracy and precision of analyses are discussed in Appendix B.

Sample number	BK 238	BK 372	BK 431	BK 529	BK 955	BK 1052	BK 1079	BK 1357	BK 1365	CA 40	CA 63	CA-AR1	TOL-1**
Number of replicate analyses	9	9	9	9	4	4	4	4	4	4	4	4	
Oxides-weight percent													
SiO_2	74.4 (8)	69.0 (8)	76.7 (8)	76.3 (8)	74.9 (9)	77.1 (12)	72.3 (9)	77.8 (12)	74.9 (8)	75.7 (8)	70.6 (8)	76.7 (22)	73.14
TiO_2	0.32 (1)	0.49 (1)	0.10 (1)	0.11 (1)	nd	0.03 (2)	0.27 (1)	0.06 (0)	0.08 (1)	0.01 (2)	0.39 (1)	0.12 (1)	0.12
Al_2O_3	14.3 (3)	16.5 (2)	16.4 (3)	15.4 (2)	17.5 (3)	16.4 (2)	15.4 (3)	16.1 (3)	16.9 (3)	15.9 (3)	17.3 (2)	16.4 (3)	15.04
Fe_2O_3	2.08 (3)	3.37 (10)	1.02 (3)	1.00 (2)	0.74 (2)	0.88 (21)	2.38 (3)	1.23 (2)	0.70 (2)	0.88 (1)	2.91 (18)	2.13 (6)	2.10
MnO	0.01 (0)	0.02 (0)	0.01 (0)	0.01 (0)	0.03 (0)	0.01 (0)	0.02 (0)	nd	nd	nd	0.03 (0)	0.02 (0)	0.04
MgO	0.96 (3)	1.82 (3)	0.46 (8)	0.46 (8)	0.23 (12)	0.49 (8)	1.26 (1)	0.49 (6)	0.64 (7)	0.43 (8)	0.86 (7)	0.79 (8)	0.26
CaO	1.21 (0)	2.27 (1)	0.58 (1)	0.91 (1)	0.53 (1)	0.43 (1)	1.32 (0)	0.28 (1)	1.86 (2)	0.57 (6)	0.50 (1)	2.08 (1)	2.22
Na_2O	2.10 (5)	3.32 (10)	3.22 (14)	3.05 (13)	3.50 (9)	2.81 (19)	2.06 (12)	4.03 (8)	3.97 (4)	2.57 (4)	1.49 (9)	3.37 (9)	3.56
K_2O	1.21 (0)	3.82 (7)	5.84 (13)	6.28 (9)	6.06 (10)	5.40 (8)	7.18 (12)	4.43 (7)	4.16 (6)	5.62 (8)	7.63 (1)	3.92 (14)	3.63
P_2O_5	0.01 (0)	0.18 (2)	0.06 (4)	0.10 (3)	0.12 (3)	0.17 (2)	0.20 (0)	0.10 (2)	0.07 (0)	0.19 (1)	0.26 (1)	0.09 (2)	0.03
	96.6	101	104	104	104	104	102	105	103	102	102	106	100
Trace elements-ppm													
Ba	682 (17)	614 (46)	561 (42)	797 (32)	482 (22)	204 (91)	961 (75)	274 (94)	499 (81)	770 (64)	462 (97)	823 (64)	661
Co	5 (0)	6 (0)	3 (0)	3 (0)	26 (0)	3 (0)	5 (0)	3 (0)	3 (0)	3 (0)	5 (0)	4 (0)	1.8
Cr	nd	15 (2)	nd	nd	64 (6)	nd	nd	nd	nd	nd	12 (5)	nd	na
Cu	nd	11 (3)	3 (0)	2 (4)	3 (6)	nd	2 (2)	nd	nd	nd	6 (10)	nd	nd
Mo	5 (1)	5 (1)	8 (1)	10 (1)	9 (1)	12 (1)	6 (0)	9 (1)	8 (3)	12 (0)	5 (0)	6 (1)	nd
Nb	9 (0)	11 (1)	8 (0)	11 (0)	4 (1)	15 (1)	9 (0)	16 (2)	7 (1)	13 (0)	14 (0)	7 (1)	4
Ni	8 (2)	19 (2)	6 (2)	3 (2)	3 (2)	3 (2)	8 (1)	3 (1)	5 (3)	1 (2)	12 (7)	5 (1)	2
Pb	31 (2)	26 (2)	45 (3)	39 (3)	89 (5)	37 (4)	32 (2)	42 (3)	35 (2)	40 (3)	39 (4)	28 (1)	29
Rb	155 (3)	217 (3)	166 (1)	197 (2)	215 (3)	297 (4)	255 (3)	130 (3)	130 (2)	376 (3)	346 (3)	142 (5)	102
S	75 (7)	42 (1)	47 (1)	73 (7)	363 (14)	12 (8)	136 (4)	69 (18)	136 (15)	6 (9)	113 (5)	nd (8)	na
Sr	151 (1)	62 (1)	215 (2)	62 (1)	306 (4)	42 (2)	191 (1)	129 (2)	232 (5)	41 (1)	72 (1)	194 (2)	199
V	16 (1)	30 (1)	10 (1)	10 (1)	15 (21)	6 (7)	17 (0)	6 (5)	9 (9)	5 (1)	21 (3)	14 (1)	10
Y	18 (1)	36 (1)	23 (1)	37 (1)	18 (1)	31 (1)	27 (2)	23 (9)	10 (5)	34 (1)	39 (0)	15 (0)	8
Zn	48 (2)	70 (4)	41 (2)	36 (4)	36 (3)	42 (3)	39 (3)	42 (2)	43 (5)	43 (4)	56 (8)	44 (1)	31
Zr	176 (4)	115 (24)	124 (2)	115 (2)	49 (0)	53 (2)	147 (3)	50 (7)	111 (4)	54 (1)	288 (4)	134 (1)	126
*Total Fe												**Sample analyzed at ACTLABS	
Normative mineralogy													
Quartz	52.36	25.99	33.25	31.58	29.70	38.35	27.22	35.58	30.76	37.34	29.34	35.32	32.09
Corundum	7.37	3.11	3.87	2.17	4.51	5.56	2.32	4.41	2.66	5.01	6.30	3.05	1.29
Orthoclase	7.14	22.55	34.47	37.07	35.77	31.88	42.38	26.15	24.56	33.17	45.04	23.14	21.43
Albite	17.75	28.06	27.22	25.78	29.59	23.75	17.41	34.07	33.56	21.72	12.59	28.49	30.09
Anorthite	5.93	10.09	2.49	3.86	1.85	1.03	5.25	0.74	8.77	1.60	0.80	9.73	10.81
Hypersthene	5.14	9.04	2.60	2.55	1.79	2.57	6.46	3.05	2.55	2.43	6.12	5.14	3.82
Magnetite	0.30	0.49	0.15	0.15	0.11	0.13	0.35	0.18	0.10		0.42	0.31	0.31
Ilmenite	0.61	0.93	0.19	0.21		0.06	0.51	0.11	0.15	0.13	0.74	0.23	0.23
Apatite		0.39	0.13	0.22	0.26	0.37	0.44	0.22	0.15	0.41	0.57	0.20	0.07

Calculated using Magma 2.3 software written by Ken Wohletz, copyright by the Regents of California (1996)
Calculated assuming Fe^{3+}/Fe^{2+} ratio = 0.1

of metamorphism in the study area, distinguishing ortho- from paragneisses is difficult. The major element discrimination diagram of Werner (1987) supports interpretation of the Toluca Granite as having an igneous protolith (Fig. 2-6). As shown in Figure 2-4, modal analyses of the Toluca Granite lie entirely within the granitic field of Streckeisen's (1976) IUGS classification.

Trace element data from the Toluca Granite cluster on variation diagrams from Pearce *et al.*, (1984) (Fig. 2-7). The Nb-Y tectonic discrimination diagram suggests that the Toluca Granite is either a volcanic arc or syncollisional granite. The Rb-(Nb + Y) tectonic diagram is inconclusive regarding a tectonic setting for the Toluca Granite since data plot at the junction of three tectonic fields. It is most likely either a syncollisional or volcanic arc granite, both orogenic, rather than an anorogenic within-plate granite.

WALKER TOP ORTHOGNEISS

The Walker Top orthogneiss was mapped by Goldsmith *et al.* (1988) as a less foliated, less sheared, garnetiferous version of the Henderson Gneiss, which outcrops in the western Inner Piedmont. The Walker Top orthogneiss and Henderson Gneiss both contain megacrysts of microcline and plagioclase (An_{20-30}) surrounded by a coarse-grained equigranular matrix of biotite, feldspar, and quartz. The Walker Top orthogneiss has been recognized as a distinct unit separate from the Henderson Gneiss because of spatial and textural differences. Feldspar megacrysts in the Henderson Gneiss are lenticular, whereas the feldspar megacrysts in the Walker Top gneiss are subhedral. Microcline megacrysts in both the Walker Top orthogneiss and the Henderson Gneiss have myrmekitic rims and pressure shadows. Bulk chemical analyses suggested a strong genetic correlation between the Henderson Gneiss and the Walker Top orthogneiss (Giorgis, 1999). $^{238}U/^{206}Pb$ age dates determined from the ion microprobe for the Walker Top orthogneiss are approximately 470 Ma (Vinson, 1999).

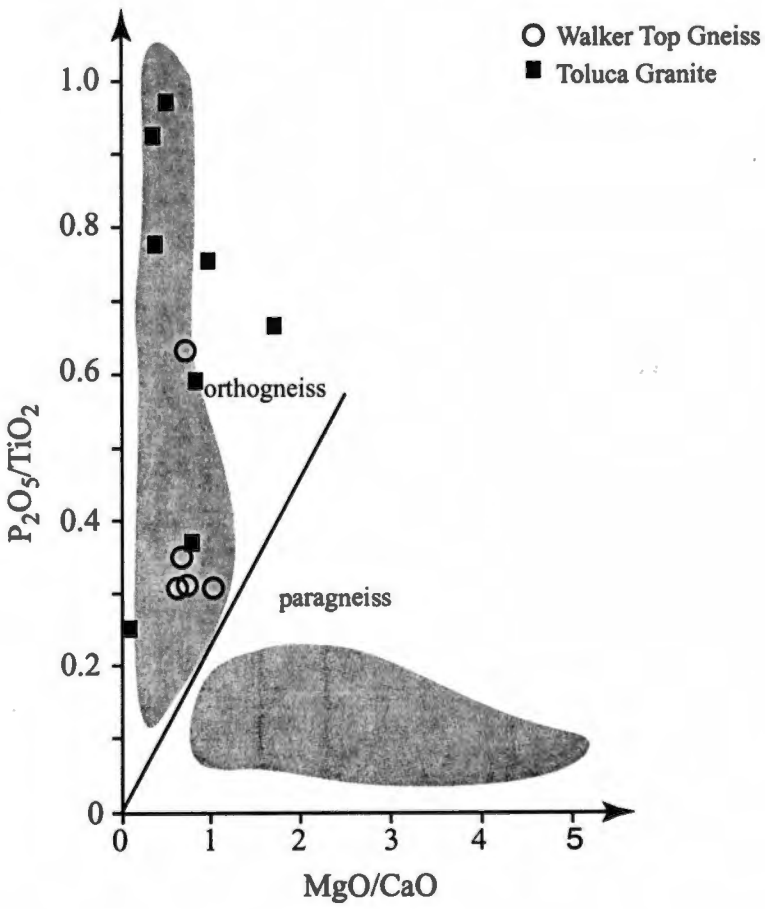


Figure 2-6. Major element discrimination diagram distinguishing ortho- and paragneisses in metamorphic terranes. Shaded areas are data from the Saxonian granulite massif used to construct the diagram. Data and diagram from Werner (1987).

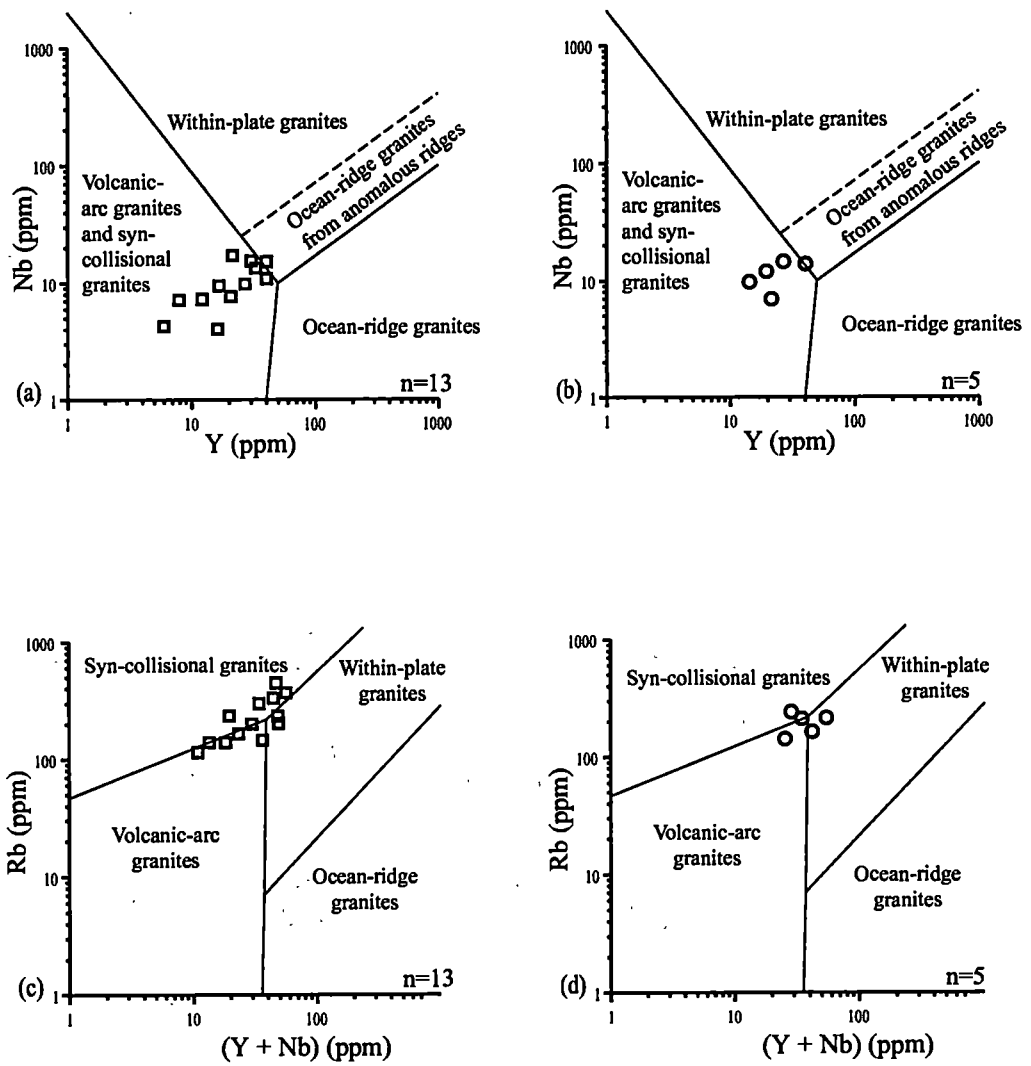


Figure 2-7. Nb-Y and Rb-(Y + Nb) variation diagrams for the Toluca Granite and the Walker Top orthogneiss. Diagram from Pearce *et al.* (1984). (a) Nb-Y variation diagram for Toluca Granite. (b) Nb-Y discriminant diagram for Walker Top orthogneiss. (c) Rb-(Y + Nb) variation diagram for Toluca Granite. (d) Rb-(Y + Nb) variation diagram for Walker Top orthogneiss.

The Walker Top orthogneiss is medium to dark gray and has conspicuous subhedral microcline and plagioclase megacrysts (Fig. 2-8). Orientation of the megacrysts resembles a flow pattern rather than metamorphic foliation (Goldsmith *et al.*, 1988). A weak foliation is defined by alignment of biotite in the groundmass. The matrix consists of fine- to medium-grained biotite, quartz, and plagioclase (An_{20-30}).

Modal analyses of the Walker Top orthogneiss are found in Table 2-4. The mineral assemblage of the Walker Top orthogneiss is microcline + plagioclase (An_{20-30}) + quartz + biotite + muscovite. Zircon, apatite, epidote-clinozoisite, and opaques occur as trace minerals. The microcline and plagioclase are present as both megacrysts and part of the coarse-grained matrix. Myrmekite and rapakivi textures are found at the rims of the microcline megacrysts (2-6 cm) (Fig. 2-8) which are much larger than the plagioclase megacryts (1-4 cm). Biotite (1-3 mm), muscovite (0.5-2 mm), quartz (0.5-3 mm), and plagioclase (0.5-2 mm) define the foliation.

Bulk chemical analyses of the Walker Top orthogneiss are presented in Table 2-5. Appendix B is a discussion of the accuracy and precision of XRF analyses. The major element discrimination diagram of Werner (1987) supports a magmatic origin for the Walker Top orthogneiss (Fig. 2-6). Modal analyses reveal that the Walker Top orthogneiss ranges from granodioritic to granitic in composition (Fig. 2-4).

The Nb-Y tectonic discrimination diagram of Pearce *et al.* (1984) suggests that the Walker Top orthogneiss is either a syncollisional or volcanic-arc related granite (Fig. 2-7). On the Rb-(Y+Nb) tectonic disrimination diagram, data plot at the junction of three tectonic fields: volcanic-arc granites, syn-collisional granites, and within-plate granites. The Walker Top orthogneiss is most likely an orogenic granite, either a volcanic-arc or syncollisional granite rather than an anorogenic within-plate granite.

(a)



(b)

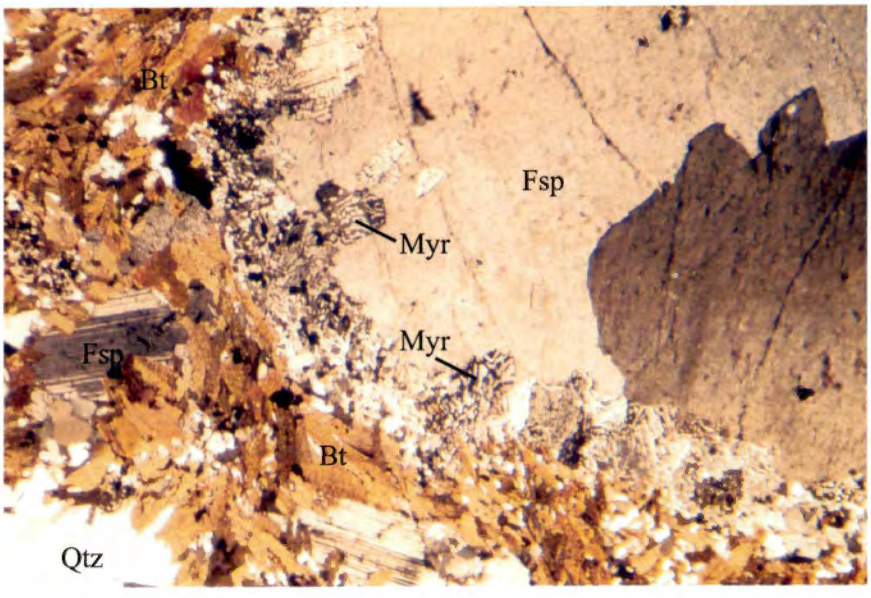


Figure 2-8 Photograph and photomicrograph of Walker Top orthogneiss. (a) Walker Top orthogneiss near Richland Mountain, Benn Knob quadrangle (Plate 1). (b) Sample BK 151 near Camp Knob, Benn Knob quadrangle (Plate 1). Microcline megacryst with myrmekitic rim in a matrix of plagioclase (An_{20-30}), quartz, and biotite. Field of view is 11.1 mm. Bt-biotite, Fsp-feldspar, Myr-myrmekite, Qtz-quartz.

Table 2-4. Modes of the Walker Top gneiss. Trace (tr) minerals are less than 0.1% of the thin section. Point counting methodology and uncertainties are discussed in Appendix A.

					Samples from Giorgis (1999)				
	BK 151	**BK 283**	**BK 301**	**BK 409**	***MS 53***	***D 341***	***BK 111***	***D 708***	***MS 26***
points counted	2130	2173	2413	2413	*1014*	*1022*	*1024*	*1019*	*1023*
Quartz	15.2	16.0	16.3	13.7	*21.6*	*27.8*	*20.5*	*30.7*	*38.1*
Plagioclase	24.8	28.9	35.3	30.9	*35.2*	*35.3*	*34.3*	*24*	*21.1*
Microcline	32.8	37.1	24.8	32.8	*10.3*	*8.8*	*17.9*	*12.5*	*16.6*
Muscovite	2.1	2.8	1.9	1.0	*5.0*	*0.5*	*7*	*3.8*	*5.8*
Biotite	21.5	12.5	19.8	19.7	*26.5*	*26*	*19*	*27.5*	*15.4*
Garnet	–	0.5	0.3	–	*tr*	*tr*	–	–	*1.2*
Myrmekite	3	1.8	1.6	1.8	*1.0*	*0.9*	*1.2*	*1.2*	*1.6*
Zircon	tr	tr	tr	tr	*tr*	*tr*	–	*tr*	*tr*
Opaque	0.6	0.4	tr	tr	*tr*	*tr*	–	*tr*	–
Epidote-Clinozoisite	–	–	tr	tr	–	–	–	–	–
Apatite								*tr*	
Total	100.0	100.0	100.0	99.9	99.6	99.3	99.9	99.7	99.8

Table 2-5. XRF analyses and CIPW norms for the Walker Top gneiss. The number in parentheses represents 1σ of the least digit cited. Accuracy and precision of XRF analyses are discussed in Appendix B.

Sample number	BK 501	BK 408	BK 396	BK 409	BK 301
Number of replicate analyses	10	10	10	9	9
Oxides-weight percent					
SiO_2	68.1 (9)	68.7 (7)	70.7 (8)	75.2 (8)	74.2 (9)
TiO_2	0.56 (0)	0.58 (1)	0.65 (0)	0.21 (1)	0.45 (1)
Al_2O_3	17.4 (12)	17.0 (3)	15.4 (2)	15.5 (3)	15.3 (2)
Fe_2O_3*	3.57 (1)	3.40 (15)	3.62 (15)	1.35 (4)	2.48 (7)
MnO	0.03 (0)	0.04 (1)	0.04 (1)	0.01 (0)	0.02 (6)
MgO	1.36 (1)	1.38 (7)	1.12 (6)	0.77 (7)	1.20 (11)
CaO	2.31 (0)	2.12 (1)	1.13 (1)	1.11 (1)	1.73 (1)
Na_2O	3.37 (20)	2.64 (11)	2.42 (9)	2.23 (9)	2.56 (15)
K_2O	4.17 (10)	4.64 (7)	5.95 (11)	6.84 (10)	4.96 (10)
P_2O_5	0.17 (0)	0.20 (4)	0.20 (3)	0.13 (4)	0.14 (3)
Oxide-Total	101	101	101	103	103
Trace elements-ppm					
Ba	666 (50)	871 (42)	56 (30)	1160 (20)	1147 (36)
Co	7 (0)	6 (0)	64 (0)	34 (0)	49 (1)
Cr	20 (5)	13 (5)	16 (4)	nd (1)	3 (3)
Cu	14 (4)	7 (4)	10 (4)	2 (4)	5 (5)
Mo	3 (1)	2 (1)	2 (1)	6 (1)	5 (2)
Nb	15 (4)	13 (1)	14 (7)	7 (0)	10 (5)
Ni	18 (2)	12 (2)	12 (3)	5 (2)	8 (5)
Pb	33 (2)	22 (2)	30 (2)	32 (2)	25 (8)
Rb	171 (38)	220 (7)	222 (5)	239 (5)	144 (2)
S	74 (11)	25 (11)	82 (7)	72 (12)	53 (9)
Sr	197 (36)	177 (13)	117 (2)	171 (2)	201 (3)
V	35 (2)	32 (2)	30 (10)	15 (5)	25 (1)
Y	27 (1)	21 (1)	41 (3)	22 (9)	15 (1)
Zn	79 (5)	56 (2)	55 (3)	32 (2)	49 (3)
Zr	300 (17)	334 (8)	360 (10)	362 (53)	202 (4)
* Total Fe					
Normative mineralogy					
Quartz	23.93	27.56	28.24	32.12	34.02
Corundum	3.55	4.26	3.40	2.72	2.91
Orthoclase	24.62	27.39	35.12	40.38	29.28
Albite	28.49	22.32	20.46	18.85	21.64
Anorthite	10.35	9.22	4.31	4.66	7.67
Hypersthene	8.11	7.88	7.47	3.70	6.17
Magnetite	0.52	0.49	0.53	0.20	0.36
Ilmenite	1.07	1.10	1.24	0.40	0.86
Apatite	0.37	0.44	0.44	0.28	0.31

Calculated using Magma 2.3 software written by Ken Wohletz, copyright by the Regents of California (1996)

Calculated assuming Fe^{3+}/Fe^{2+} ratio = 0.1

CHAPTER 3

METAMORPHISM

The crystalline rocks found in the innermost portions of mountain chains can provide valuable insight into the metamorphic and tectonic history of an orogen. Mineral assemblages, petrographic textures, and electron microprobe analyses constrain metamorphic conditions of paragneisses and orthogneisses in the central Inner Piedmont. Pressure and temperature estimates for rocks in the study area increase our understanding of the thermal-metamorphic peak and deformation processes that may occur before, during, and after the peak in the Inner Piedmont, which was likely produced by the Acadian orogeny (Dennis and Wright, 1997).

REGIONAL METAMORPHISM

The Inner Piedmont is dominated by sillimanite-grade regional metamorphism with grade decreasing to kyanite and garnet on the northwestern flank of the belt (Butler, 1991; Fig. 3-1). Previous workers interpreted the metamorphic gradient to be structurally inverted with sillimanite-grade rocks thrust northwestward over lower grade kyanite-grade rocks (Griffin, 1974; Butler, 1991; Hatcher and Goldberg, 1991). Butler (1991) recognized that the isograds in the central Inner Piedmont must be nearly horizontal, remaining in the first sillimanite zone, neither rising to second sillimanite (sillimanite + Kfeldspar) nor falling to kyanite grade over a 60 km wide area. The study area lies within this vast first sillimanite zone region.

The protoliths for the Tallulah Falls Formation consist of immature quartzofeldspathic sediments (metagraywacke-schist) and a pelitic unit (aluminous schist) (Bream, 1999). The Walker Top orthogneiss and the Toluca Granite have been interpreted to have magmatic origins (Griffitts and Overstreet, 1952; Giorgis. 1999), but because of their aluminum contents, may indeed be the product of regional-scale migmatization. This hypothesis requires further detailed

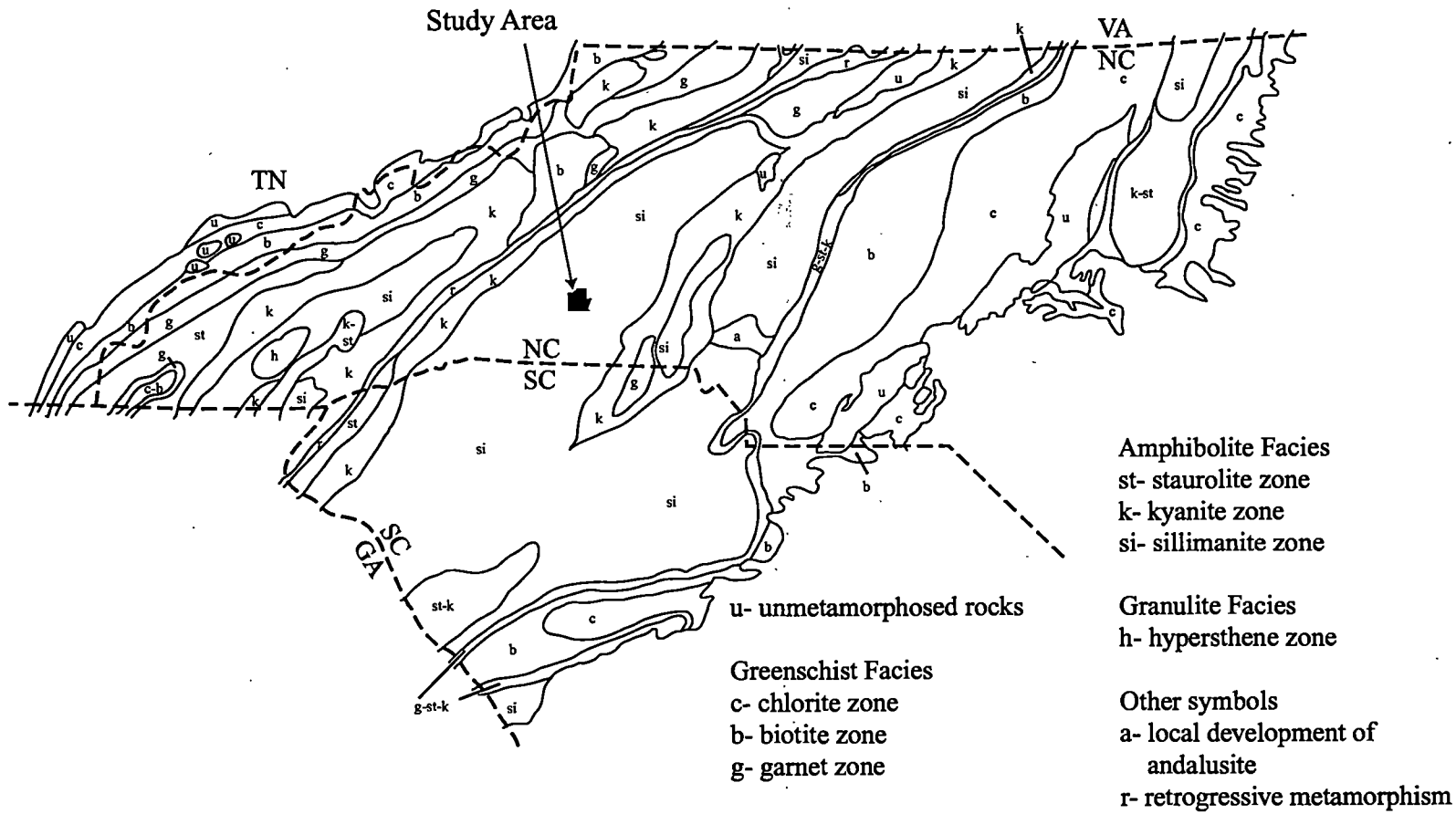


Figure 3-1. Metamorphic isograd map of North and South Carolina. Isograds represent the first occurrence of the index mineral (modified from Butler, 1991).

study.

Timing

Timing of metamorphism in the Inner Piedmont is delimited by ages of deformed and undeformed granitic intrusives in the region. A granitic intrusion associated with the Henderson Gneiss with a Rb-Sr age of 429 ± 22 Ma (Odom and Russell, 1975) was subjected to high-grade metamorphism and intense deformation in what has been interpreted to be the result of the Acadian orogeny (Lemmon, 1982). Core and rim $^{206}Pb/^{238}U$ zircon ages of the deformed Dysartsville gneiss (Bream *et al.*, 2001) also support an Acadian event for peak deformation and metamorphism of the Inner Piedmont. The non-foliated (post-peak deformation) Cherryville Granite in the eastern Inner Piedmont has a Rb-Sr whole rock age of 351 ± 10 Ma (Kish, 1983) and provides an upper constraint on timing of the major orogenic event. Based on the crystallization ages, peak metamorphism and deformation in the Inner Piedmont occurred in the Devonian as a result of the Acadian orogeny.

Pegmatites found throughout the study area display no deformational fabric nor contain evidence of metamorphism. These coarse-grained intrustives crosscut the foliation of the Tallulah Falls Formation and the Toluca Granite. The pegmatites may be related to the Cherryville granite (Griffitts and Overstreet, 1952).

Migmatization

The Inner Piedmont has long been recognized as a high-grade migmatitic terrane (e.g., Griffin, 1974 and Hatcher, 1993). Migmatic rocks are sparse in the western Inner Piedmont and are restricted to localized zones, usually within the lower Tallulah Falls member (Hill, 1999). Williams (2000) recognized a concentrated zone of migmatization along the footwall boundary of the Brindle Creek thrust. Migmatization is pervasive and consistent throughout the study area.

Increasing migmatization from the western to central Inner Piedmont in North Carolina is similar to the trend recognized by Griffin (1974) in South Carolina.

PETROGRAPHY

The dominant mineral assemblage in the paragneiss sequence consists of plagioclase, quartz, biotite, muscovite, sillimanite, kyanite, and garnet; this assemblage is used to constrain mimimum metamorphic conditions. The abundance of micas suggests that water was present during metamorphism. Migmatitic outcrops are prevalent throughout the study area, indicating that metamorphic conditions were at or above the wet granitic solidus. Lack of K-feldspar and the abundance of muscovite suggest that metamorphic conditions remained below the second sillimanite isograd. The mineral assemblage constrains minimum P-T conditions to be between 610-725 °C and between 3 and 8 kbar (Fig. 3-2). These conditions are consistent with those determined by previous workers (e. g., Butler, 1991; Davis, 1993; Giorgis, 1999).

Tallulah Falls Formation

Gneissic banding in the Tallulah Falls metagraywacke-schist is defined by alternating layers of quartzofeldspathic material and micaceous layers. In the Tallulah Falls aluminous schist, the foliation is defined by biotite and muscovite.

Plagioclase (An_{20-35}) occurs as subhedral porphyroblasts (1-2 mm) as well as anhedral grains (0.2-0.5 mm) in the matrix of the Tallulah Falls Formation. Twinned grains are rare and occur only in the matrix. Sericitization is minimal. Quartz is present as anhedral grains (0.1-0.4 mm) in the matrix and as subhedral grains (0.5-1 mm) in veins.

Biotite, muscovite, sillimanite, and kyanite are the primary phases in the micaceous layers. Biotite (0.2-1 mm), muscovite (0.3-1 mm), and kyanite (0.5-2 mm) define the foliation. The biotite and muscovite are euhedral, while the kyanite has been partially altered to muscovite.

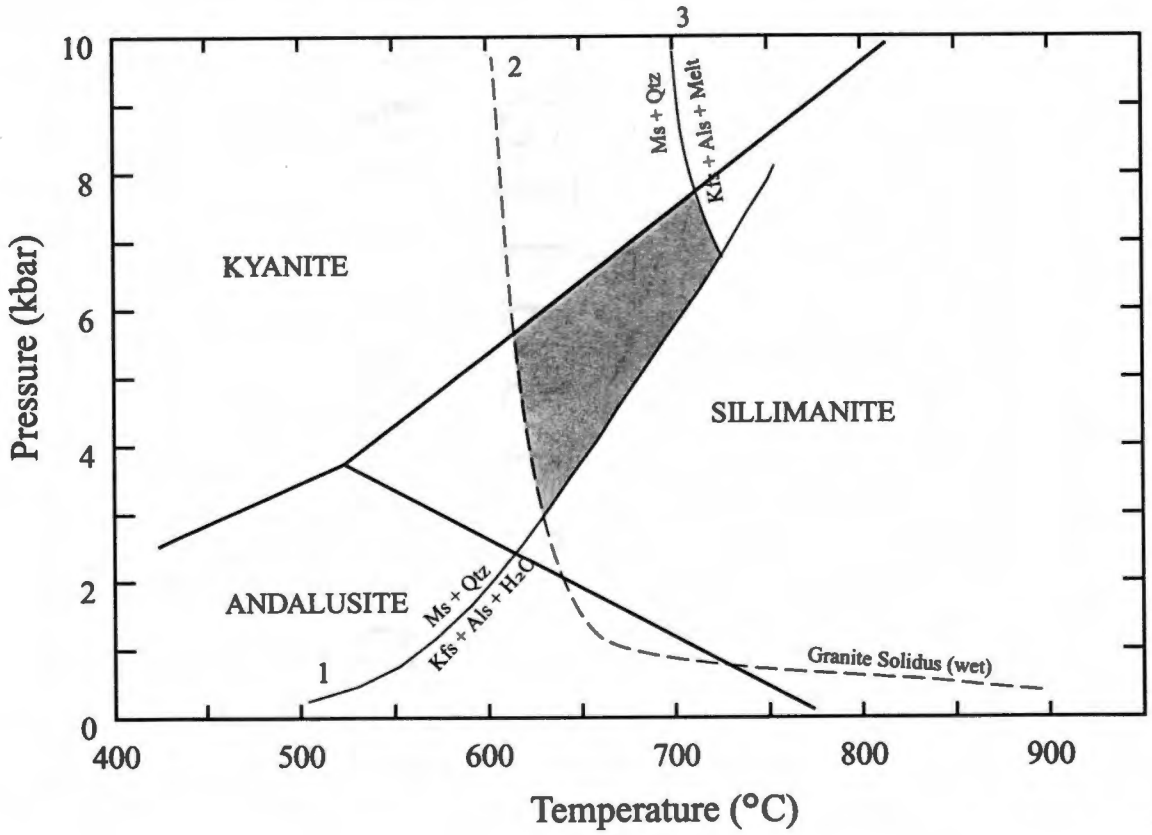


Figure 3-2. Petrogenetic grid for aluminous rocks. The shaded region represents minimum P-T conditions based on mineral phases present in the study area. Reaction sources: 1: Chatterjee and Johannes (1974); 2. Raymond (1995); 3. Thompson (1982). The aluminumsilicate phase diagram is after Holdaway (1971). Ms - Muscovite. Qtz - quartz. Kfs- K-feldspar. Als - Al_2SiO_5.

Sillimanite is present as euhedral prismatic rhombs (0.2-1 mm) in mats within the bioite-muscovite-kyanite foliation. There are rare occurrences of fibrolite intergrown with muscovite and biotite. The coexistence of kyanite and sillimanite is common at sillimanite-grade conditions. Sillimanite in the reaction kyanite = sillimanite rarely overgrows kyanite, but nucleates and grows within muscovite and biotite (Spear, 1993).

Garnets in the Tallulah Falls Formation occur as subhedral fractured porphyroblasts (0.5-2 mm). Iron oxide from weathering is usually present on the rims and along fractures. Biotite, quartz, and feldspar all occur as inclusions. Biotite-muscovite-kyanite foliation wraps around the garnet porphyroblasts, but shear-sense indicators (tails or inclusion trails) are absent.

Walker Top orthogneiss

The Walker Top orthogneiss is a megacrystic granite to granodiorite. Plagioclase (An_{20-30}) and microcline megacrysts (2 mm-10 cm) are subhedral and show little to no preferred orientation. Goldsmith *et al.* (1988) suggested that the orientation of the megacrysts resembled a flow pattern rather than metamorphic foliation. Microcline megacrysts are rimmed with myrmekite. Micas (0.1-4 mm), primarily biotite, in the groundmass define a weak foliation. The quartz (0.1-2 mm) and feldpar (0.1-2 mm) in the groundmass are sub- to anhedral; and plagioclase is sometimes untwinned. Anhedral, fractured garnets (1-8 mm) contain inclusions of biotite, quartz, and feldspar and are wrapped by the weak foliation defined by the biotite.

Toluca Granite

The Toluca Granite is a medium- to coarse-grained, equigranular to porphyritic, weakly to non-foliated granite. Garnet megacrysts contain no inclusions and are euhedral and undeformed. Feldspar megacrysts are also euhedral. In the groundmass, microcline (0.5-2 mm), plagioclase(An_{25-35}) (0.5-3 mm), and quartz (0.1-1.5 mm) are anhedral to subhedral. Twinned and

untwinned feldspars are present in the Toluca Granite. The biotite and muscovite (0.2-0.5 mm) rarely show preferred orientation or layering.

ELECTRON MICROPROBE ANALYSES

Detailed geochemical analyses of garnet, biotite, muscovite and plagioclase were performed using the four-spectrometer CAMECA SX-52 electron microprobe in the University of Tennessee Microprobe Facility. Analyses chosen for pressure and temperature estimates were obtained from line traverses across grain boundaries. The points were selected based on proximity to the rim boundary, cation totals, and weight percent totals. In all cases, analyses were within 6 μm of the grain boundary.

Temperature estimates

The exchange of Fe and Mg between garnet and biotite is the basis of the geothermometer used to determine the equilibrium temperature of both the Tallulah Falls Formation and the Walker Top orthogneiss. The reaction that describes this exchange is

almandine + phlogopite = pyrope + annite (Spear, 1993)

Ferry and Spear (1978) determined the partitioning of Fe and Mg between synthetic garnets and biotite at 2.07 kbar and determined the following equation for T (temperature):

$$ln\ K = -2109/T\ (°K) + 0.782$$

Berman (1990) modified Ferry and Spear's (1978) equation to accommodate mixing properties of Ca-Mg-Fe-Mn garnets. This geothermometer has an uncertainty of ± 20 °C.

Compositions of garnet, biotite, and plagioclase in the Tallulah Falls Formation used in geothermometry and geobarometry estimations are presented in Table 3-1. Using Ferry and Spear's (1978) model and Berman's (1990) corrections for mixing properties, the equilibrium temperature estimate of the Tallulah Falls Formation (Sample BK 959) in the study area is 645 ±

Table 3-1. Analyses of the Tallulah Falls Formation (BK 959) used for geothermobarometric calculations.

Garnet analyses

	gBm1	gBm2	gBf2
weight % oxides			
SiO_2	37.4	37.3	36.6
TiO_2	< 0.03	< 0.03	< 0.03
Al_2O_3	21.3	21.4	20.9
Cr_2O_3	< 0.03	0.05	0.06
MgO	3.54	3.66	3.77
CaO	2.01	1.71	1.65
MnO	4.68	4.71	4.24
FeO	31.4	31.6	31.9
Na_2O	< 0.03	< 0.03	< 0.03
TOTAL	100	100	99.1
cations based on 12 oxygen			
Si	2.991	2.981	2.971
Ti	0.000	0.000	0.000
Al	2.007	2.013	1.999
Cr	0.001	0.003	0.004
Mg	0.421	0.436	0.456
Ca	0.172	0.146	0.144
Mn	0.316	0.319	0.291
Fe	2.094	2.110	2.163
Na	0.001	0.004	0.000
TOTAL	8.003	8.012	8.028
Mg #*	0.003	0.009	0.014
<py>	14.02	14.48	14.93
<gr>	5.73	4.85	4.72
<sp>	10.52	10.59	9.53
<al>	69.73	70.08	70.83

*Mg # = Mg cation # / (Mg cation # + Fe cation #)

Biotite analyses

	m1gB	m2gB
weight % oxides		
SiO_2	34.5	35.1
TiO_2	3.95	3.23
Al_2O_3	18.7	18.8
MgO	9.76	10.03
CaO	< 0.03	0.03
MnO	0.10	0.07
FeO	17.3	16.8
Na_2O	0.13	0.11
K_2O	9.61	9.89
H_2O	3.91	3.92
TOTAL	98.0	98.0
cations based on 22 oxygen and 2 H_2O		
Si	5.293	5.375
Ti	0.456	0.372
Al	3.386	3.381
Cr	2.231	2.287
Mg	0.004	0.005
Ca	0.012	0.008
Mn	2.216	2.152
Fe	0.039	0.033
Na	1.881	1.930
K	15.52	15.54
TOTAL	7.988	8.004
Mg #*	0.093	0.132

Feldspar analyses

	f2gB
weight % oxides	
SiO_2	56.5
Al_2O_3	25.5
CaO	8.61
FeO	0.4
Na_2O	6.77
K_2O	0.09
TOTAL	97.9
cations based on 8 oxygen	
Si	5.293
Al	3.386
Ca	0.012
Fe	0.039
Na	1.881
K	15.52
TOTAL	7.988

20 °C (Fig. 3-3).

Compositions of garnet, biotite, muscovite, and plagioclase used in geothermometry and geobarometry estimations are presented in Tables 3-2 and 3-3. Using Ferry and Spear's (1978) model and Berman's (1990) corrections for mixing properties, equilibrium temperature estimates of the Walker Top orthogneiss (Sample BK 337) range from 525 to 640 °C (Fig. 3-3).

Pressure estimates

Two different barometers were used to estimate pressures for the Tallulah Falls Formation and the Walker Top orthogneiss because of the differences in mineral assemblages. The garnet-aluminumsilicate-silica-plagioclase (GASP) barometer was used for the Tallulah Falls Formation. The GASP equation determines pressure based on the following reaction:

anorthite = grossular + sillimanite + quartz

The plagioclase-garnet-muscovite-biotite barometer was used for the Walker Top orthogneiss because of the lack of an aluminum silicate. This barometer is based on the change in the Al coordination number from 6 to 4 and Mg-Fe coordination number from 8 to 6. There are both Mg- and Fe-dependent barometers as illustrated by the following equilibria:

muscovite + pyrope + grossular = anorthite + phlogopite

that yields: $\Delta G = 0 = 1482 - 40.67\,(T) + 1.738\,(P+1)$ where G is Gibbs free energy.

muscovite + pyrope + grossular = anorthite + phlogopite

that yields: $\Delta G = 0 = 28849 - 37.23\,(T) + 1.802\,(P+1)$ where G is Gibbs free energy.

Uncertainty in the pressure estimates based on the above equations depends on the uncertainty of temperature estimates and mineral entropies, solid solution of biotite and muscovite, and variable contents of anorthite. The pressure estimates obtained from this geobarometer have a standard deviation of ± 800 bars (Ghent and Stout, 1981).

Using Koziol's (1995) GASP barometer and the temperature estimate from the Ferry and

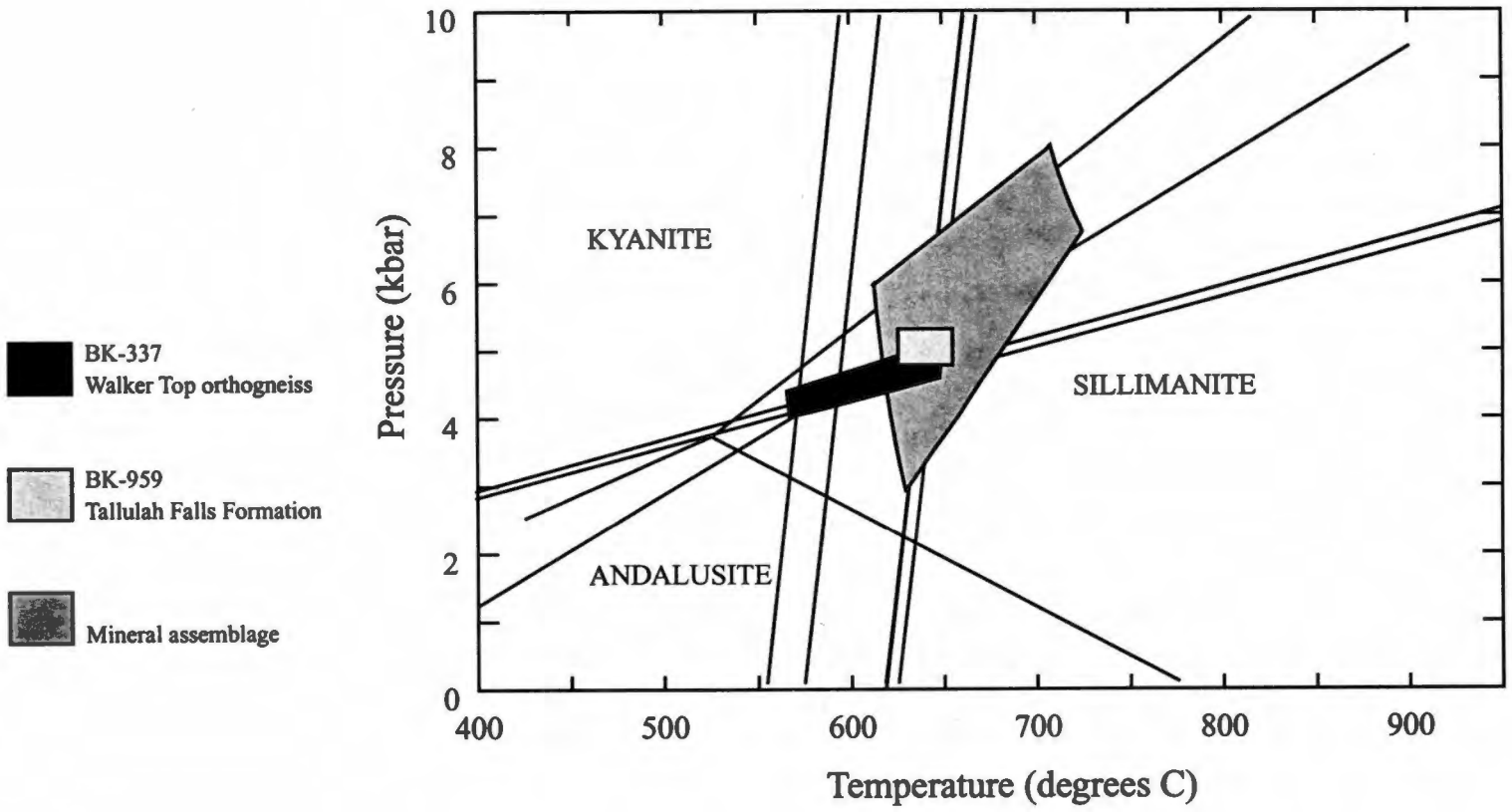


Figure 3-3. Petrogenetic grid with metamorphic conditions as determined by mineral phases present and temperature and pressure estimates calculated from electron microprobe data. Each line represents either a temperature or pressure estimates of an analyzed mineral pair. The aluminum silicate phase diagram is after Holdaway (1971).

Table 3-2. Analyses of garnet and biotite in the Walker Top orthogneiss (BK 337) used for geothermobarometric estimations. (P) refers to analyses used to estimate pressure.

Garnet Analyses

	g2b2 (P)	(P)	g8b9	g9b7	g11b10
weight % oxides					
SiO_2	36.3	36.7	36.8	36.9	36.5
TiO_2	< 0.03	< 0.03	< 0.03	< 0.03	< 0.03
Al_2O_3	20.6	20.8	20.8	20.8	20.9
Cr_2O_3	< 0.03	< 0.03	< 0.03	< 0.03	< 0.03
MgO	1.70	1.10	1.26	1.52	1.76
CaO	2.50	2.66	3.16	3.26	2.91
MnO	6.03	9.32	8.27	7.26	4.81
FeO	32.5	29.5	30.2	30.6	33.0
Na_2O	< 0.03	< 0.03	< 0.03	< 0.03	< 0.03
TOTAL	99.6	100	100	100	99.9
cations based on 12 oxygen					
Si	2.967	2.987	2.987	2.991	2.973
Ti	0.017	0.001	0.001	0.002	0.001
Al	1.986	2.001	1.986	1.983	2.002
Cr	0.001	0.002	0.000	0.001	0.000
Mg	0.208	0.134	0.153	0.184	0.214
Ca	0.219	0.232	0.274	0.283	0.254
Mn	0.418	0.643	0.568	0.498	0.332
Fe	2.223	2.008	2.046	2.073	2.250
Na	0.007	0.003	0.003	0.000	0.001
total	8.046	8.011	8.018	8.015	8.027
Mg #*	0.086	0.063	0.070	0.082	0.087
<py>	6.78	4.44	5.03	6.06	7.02
<gr>	7.14	7.69	9.01	9.32	8.33
<sp>	13.62	21.31	18.68	16.39	10.89
<al>	72.46	66.56	67.28	68.24	73.77

*Mg # = Mg cation #/ (Mg cation # + Fe cation #)

Biotite Analyses

	(P)	b2g2 (P)	b7g9	b8g8	b10g11
weight % oxides					
SiO_2	34.9	35.3	34.8	35.2	35.0
TiO_2	1.3	1.18	2.72	2.76	1.56
Al_2O_3	18.3	19.2	17.5	17.4	18.0
Cr_2O_3	< 0.03	< 0.03	< 0.03	< 0.03	< 0.03
MgO	6.89	6.46	6.34	6.39	6.64
CaO	0.14	0.14	< 0.03	< 0.03	< 0.03
MnO	0.16	0.13	0.25	0.27	0.11
FeO	23.0	22.3	24.5	23.8	23.5
Na_2O	0.07	0.04	0.05	0.06	0.05
K_2O	9.44	8.61	9.69	9.58	9.58
H_20	3.42	3.6	3.74	3.57	3.55
TOTAL	97.7	97.0	99.5	99.1	98.0
cations based on 22 oxygen and 2 H_2O					
Si	5.487	5.532	5.426	5.486	5.475
Ti	0.154	0.139	0.319	0.323	0.185
Al	3.397	3.551	3.218	3.192	3.357
Cr	0.002	0.001	0.004	0.003	0.000
Mg	1.613	1.613	1.476	1.484	1.561
Ca	0.004	0.011	0.000	0.002	0.002
Mn	0.022	0.017	0.033	0.035	0.014
Fe	3.025	2.927	3.195	3.107	3.096
Na	0.020	0.011	0.015	0.018	0.016
K	1.891	1.721	1.931	1.905	1.929
Total	15.62	15.52	15.62	15.56	15.64
Mg# *	0.348	0.355	0.316	0.323	0.335

Table 3-3. Analyses of plagioclase and muscovite in the Walker Top orthogneiss (BK 337) used in geobarometry estimations.

Feldspar analyses		
	F-2	**F-3**
weight % oxides		
SiO_2	61.0	60.6
Al_2O_3	24.5	24.3
FeO	0.21	0.26
CaO	5.98	5.93
Na_2O	8.31	8.27
K_2O	0.13	0.11
TOTAL	100	99.5
cations based on 8 oxygen		
Si	2.711	2.711
Al	1.281	1.279
Fe	0.007	0.009
Ca	0.285	0.284
Na	0.714	0.717
K	0.007	0.006
TOTAL	5.006	5.006
<ab>	71.0	71.2
<or>	0.72	0.59
<an>	28.3	28.2

Muscovite analyses		
	M-1	**M-3**
weight % oxides		
SiO_2	45.3	45.7
TiO_2	0.92	0.60
Al_2O_3	33.5	33.7
Cr_2O_3	< 0.03	< 0.03
MgO	0.90	0.93
CaO	< 0.03	< 0.03
MnO	< 0.03	< 0.03
FeO	2.13	2.47
Na_2O	0.31	0.41
K_2O	10.7	10.9
H_2O	4.38	4.24
TOTAL	97.2	98.4
cations based on 22 oxygen and 2 H_2O		
Si	6.170	6.178
Ti	0.094	0.061
Al	5.384	5.372
Cr	0.000	0.002
Mg	0.183	0.187
Ca	0.001	0.001
Mn	0.000	0.002
Fe	0.243	0.279
Na	0.082	0.107
K	1.854	1.875
TOTAL	14.01	14.06

Spear (1978) with Berman's (1990) calculations, a pressure estimate for the Tallulah Falls Formation (Sample BK 959) is 5.2 ± 1 kbar (Fig. 3-3).

Based on Ghent and Stout's (1981) plagioclase-biotite-garnet-muscovite barometer and temperature estimates from the Ferry and Spear (1978) with Berman's (1990) calculations, pressure estimates for the Walker Top gneiss (Sample BK-337) range from 3.8 ± 0.8 to 5.4 ± 0.8 kbar (Fig. 3-3).

Chemical zoning in garnets

Chemical zoning in garnets from the Tallulah Falls Formation, the Walker Top orthogneiss, and the Toluca Granite was determined using electron microprobe analyses. Zoning profiles of FeO, MgO, MnO, and CaO help to further understand the metamorphic history of the study area (Figs. 3-4, 3-5, 3-6).

Garnets in the Tallulah Falls Formation are primarily almandine (>75 %) and pyrope (>15 %) (Table 3-4). Garnets are homogenous in the interior and display minor zoning at the rims. FeO (34.8-33.8 %) and MgO (4.51-4.47 %) decrease toward the rim of the garnet, whereas CaO (0.98-1.07 %) increases (Table 3-4). This type of zoning suggests diffusional zoning rather than growth zoning (Spear, 1993).

The garnet in the Walker Top orthogneiss consists mostly of almandine (>55 %) and spessartine (>15 %) (Table 3-5). The garnet is extremely heterogeneous with a conspicuous zoning pattern (Fig. 3-5). FeO (33.3 - 29.2 %) and MgO (2.55 – 0.08 %) decrease toward the rim of the garnet, whereas MnO (3.41-9.23 %) and CaO (2.62-3.22 %) increase. The Mn content from the Walker Top orthogneiss is significantly higher than that in the garnets in both the Tallulah Falls Formation and Toluca Granite.

Garnets in the Toluca Granite consist of almandine (>67 %), spessartine (>15 %), and pyrope (>15 %) (Table 3-6). The garnets are homogeneous in the core and show no consistent

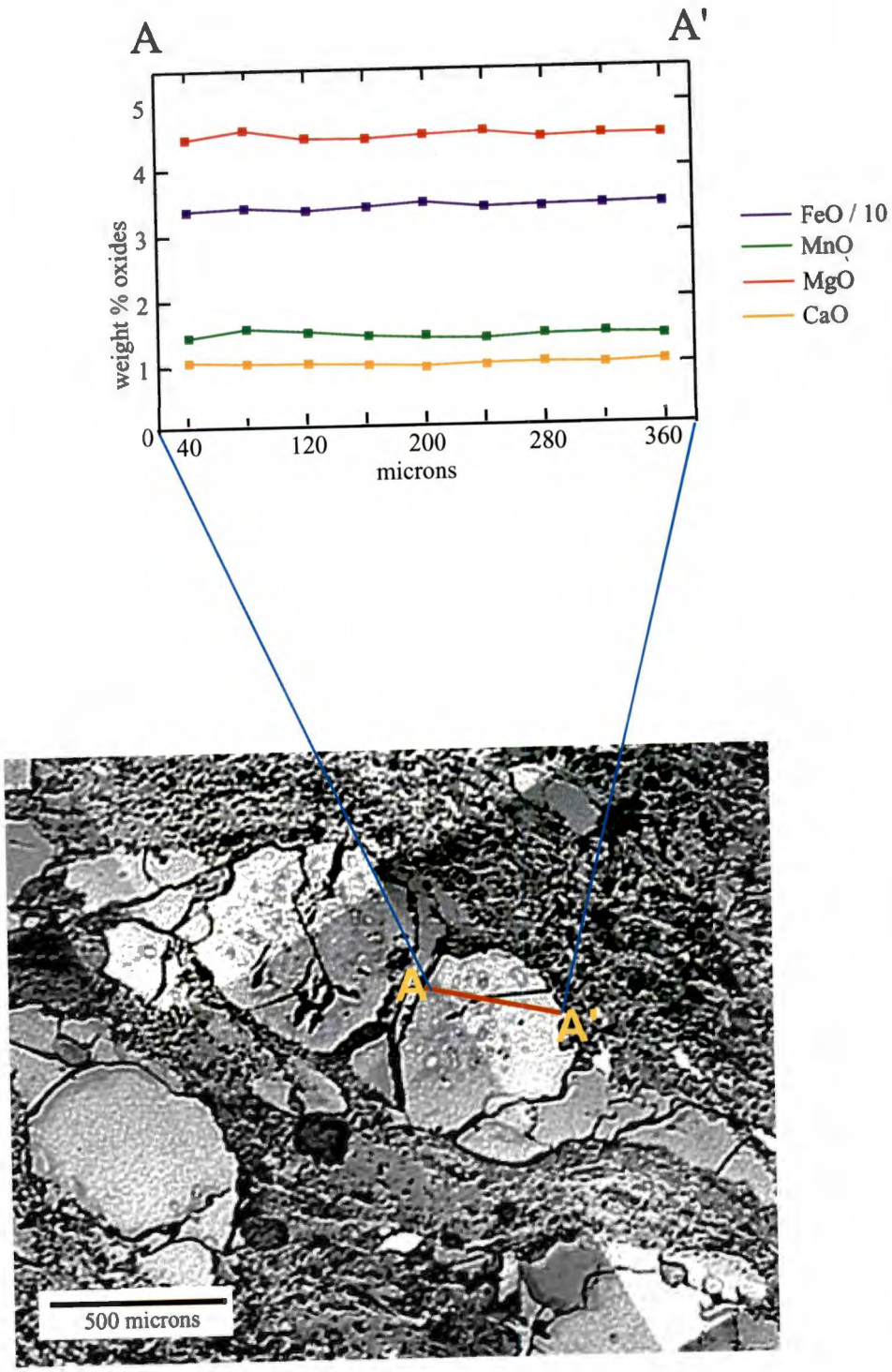


Figure 3-4. Rim to rim garnet traverse in Sample BK 52. The image is a photomicrograph of the garnets taken in reflected light. Analyses were collected every 40 microns from A to A'.

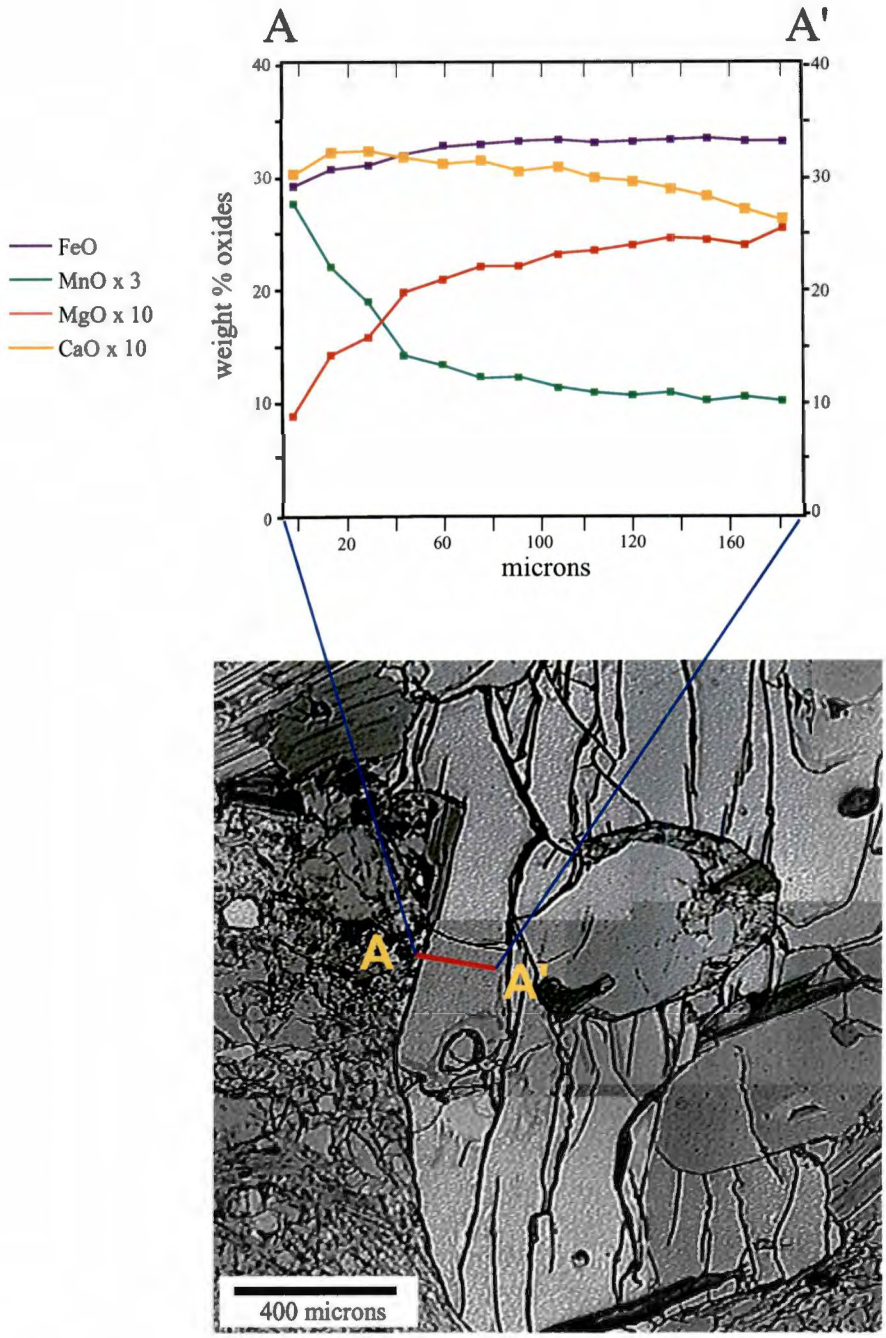


Figure 3-5. Near-rim weight percent oxide composition of the garnet in Sample BK-337. The image is a photomicrograph of the garnet taken in reflected light. Analyses were collected every 15 microns along the traverse from A to A'.

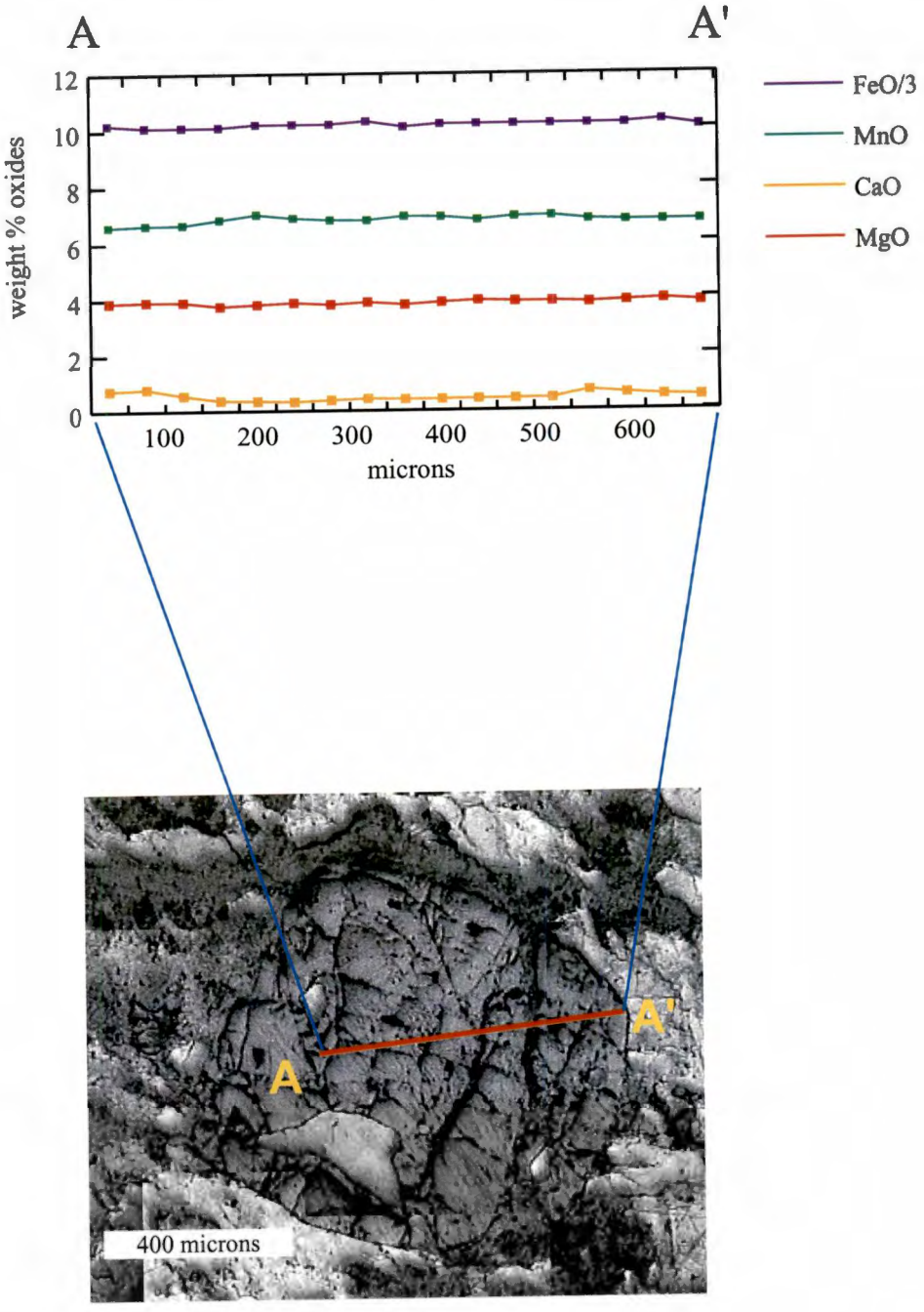


Figure 3-6. Traverse of a garnet in the Toluca Granite. The image is a photomicrograph of the garnets taken in reflected light. Analyses were collected every 40 microns from A to A'.

Table 3-4. Analyses plotted in Figure 3-4: Garnet D zoning in the Tallulah Falls Formation (Sample BK 82). The number in parenthese represents 1σ of the least digit cited.

	A								A'	AVG
weight % oxides										
SiO_2	37.8	37.8	37.4	37.5	37.7	37.6	37.3	37.3	37.3	37.5(2)
TiO_2	< 0.03	< 0.03	< 0.03	< 0.03	< 0.03	< 0.03	< 0.03	< 0.03	< 0.03	
Al_2O_3	21.6	21.6	21.3	21.6	21.4	21.4	21.4	21.5	21.4	21.4(1)
Cr_2O_3	< 0.03	< 0.03	< 0.03	< 0.03	< 0.03	< 0.03	< 0.03	< 0.03	< 0.03	
MgO	4.47	4.60	4.47	4.46	4.51	4.55	4.46	4.44	4.49	4.50(5)
CaO	1.07	1.04	1.03	1.01	0.98	1.01	1.02	1.00	1.04	1.02(2)
MnO	1.44	1.57	1.52	1.45	1.41	1.39	1.44	1.45	1.43	1.46(6)
FeO	33.8	34.2	33.7	34.2	34.8	34.0	34.2	34.3	34.5	34.2(3)
Na_2O	< 0.03	< 0.03	< 0.03	< 0.03	< 0.03	< 0.03	< 0.03	< 0.03	< 0.03	
TOTAL	100	101	99.5	100	101	99.9	99.8	100	100	
cations based on 12 oxygen										
Si	3.000	2.986	2.999	2.984	2.991	2.997	2.982	2.981	2.977	2.987(8)
Ti	0.000	0.002	0.000	0.003	0.000	0.001	0.000	0.002	0.001	0.001(1)
Al	2.022	2.017	2.008	2.022	1.997	2.008	2.019	2.019	2.009	2.012(8)
Cr	0.001	0.002	0.002	0.000	0.000	0.001	0.000	0.000	0.002	0.001(1)
Mg	0.529	0.542	0.534	0.529	0.533	0.541	0.533	0.529	0.535	0.535(5)
Ca	0.091	0.088	0.089	0.086	0.083	0.086	0.087	0.086	0.089	0.087(2)
Mn	0.097	0.105	0.103	0.097	0.095	0.094	0.097	0.098	0.096	0.068(4)
Fe	2.248	2.260	2.260	2.278	2.309	2.268	2.288	2.291	2.305	2.282(19)
Na	0.000	0.002	0.000	0.003	0.003	0.001	0.002	0.000	0.004	0.004(2)
TOTAL	7.988	8.004	7.995	8.002	8.011	7.997	8.008	8.006	8.018	8.005(7)
Mg #*	0.190	0.193	0.191	0.188	0.188	0.193	0.189	0.188	0.188	0.190(2)
<py>	17.84	18.10	17.88	17.69	17.65	18.10	17.74	17.61	17.69	17.81(19)
<gr>	3.07	2.94	2.98	2.88	2.75	2.88	2.90	2.86	2.94	2.89(7)
<sp>	3.27	3.51	3.45	3.24	3.15	3.14	3.23	3.26	3.17	3.27(14)
<al>	75.82	75.46	75.69	76.19	76.46	75.88	76.14	76.26	76.20	76.03(33)

*Mg # = Mg cation # / (Mg cation # + Fe cation #)

Table 3-5. Analyses plotted for Figure 3-5. Garnet zoning in the Walker Top orthogneiss. The number in parentheses represent 1σ of the least digit cited.

	A													A'	AVG
weight % oxides															
SiO_2	37.4	36.9	36.9	37.0	37.1	37.1	36.9	37.0	37.1	36.9	37.1	37.0	36.9	36.8	37.0(1)
TiO_2	< 0.03	< 0.03	< 0.03	< 0.03	< 0.03	< 0.03	< 0.03	< 0.03	< 0.03	< 0.03	< 0.03	< 0.03	< 0.03	< 0.03	
Al_2O_3	21.0	21.0	20.8	20.7	20.8	20.9	20.8	21.0	20.8	20.8	20.8	20.8	20.8	20.6	20.8(1)
Cr_2O_3	< 0.03	< 0.03	< 0.03	< 0.03	< 0.03	< 0.03	< 0.03	< 0.03	< 0.03	< 0.03	< 0.03	< 0.03	< 0.03	< 0.03	
MgO	0.88	1.42	1.58	1.99	2.10	2.21	2.21	2.33	2.35	2.40	2.47	2.45	2.40	2.55	2.19(33)
CaO	3.02	3.22	3.23	3.18	3.13	3.14	3.06	3.09	2.99	2.97	2.91	2.83	2.72	2.62	3.00(19)
MnO	9.23	7.34	6.29	4.75	4.43	4.06	4.12	3.82	3.64	3.58	3.63	3.39	3.53	3.41	4.30(120)
FeO	29.2	30.7	31.0	32.0	32.6	32.9	33.2	33.3	33.1	33.3	33.4	33.5	33.3	33.3	32.7(9)
Na_2O	< 0.03	< 0.03	< 0.03	< 0.03	< 0.03	< 0.03	< 0.03	< 0.03	< 0.03	< 0.03	< 0.03	< 0.03	< 0.03	< 0.03	
TOTAL	101	101	99.8	99.6	100	100	100	101	100	99.9	100	100	99.6	99.3	
cations based on 12 oxygen															
Si	3.013	2.984	2.996	3.003	2.995	2.992	2.985	2.979	2.995	2.987	2.993	2.992	2.993	2.997	2.992(6)
Ti	0.003	0.004	0.003	0.002	0.000	0.003	0.002	0.001	0.001	0.003	0.001	0.001	0.002	0.001	0.002(1)
Al	1.996	1.996	1.992	1.979	1.984	1.983	1.979	1.990	1.985	1.982	1.975	1.986	1.985	1.978	1.984(6)
Cr	0.001	0.001	0.000	0.000	0.001	0.000	0.000	0.001	0.000	0.000	0.002	0.000	0.001	0.000	0.000(1)
Mg	0.106	0.171	0.192	0.241	0.253	0.266	0.267	0.280	0.283	0.290	0.296	0.295	0.291	0.309	0.264(41)
Ca	0.261	0.278	0.281	0.276	0.270	0.271	0.264	0.267	0.259	0.258	0.251	0.245	0.236	0.228	0.260(16)
Mn	0.631	0.502	0.432	0.327	0.303	0.277	0.282	0.261	0.249	0.246	0.248	0.232	0.242	0.235	0.295(82)
Fe	1.970	2.075	2.109	2.176	2.205	2.219	2.242	2.243	2.238	2.252	2.251	2.262	2.258	2.265	2.215(60)
Na	0.006	0.005	0.002	0.000	0.002	0.001	0.006	0.003	0.002	0.000	0.002	0.000	0.004	0.000	0.002(2)
TOTAL	7.987	8.016	8.007	8.004	8.013	8.012	8.027	8.025	8.012	8.018	8.019	8.013	8.012	8.013	8.015(6)
Mg #*	0.051	0.076	0.083	0.100	0.103	0.107	0.106	0.111	0.112	0.114	0.116	0.115	0.114	0.120	0.106(13)
<py>	3.57	5.65	6.37	7.98	8.35	8.77	8.74	9.18	9.34	9.52	9.72	9.72	9.61	10.17	8.71(134)
<gr>	8.79	9.19	9.32	9.14	8.91	8.94	8.64	8.75	8.55	8.47	8.24	8.08	7.80	7.51	8.57(55)
<sp>	21.3	16.6	14.3	10.8	10.0	9.13	9.23	8.55	8.22	8.08	8.14	7.65	7.99	7.74	9.73(274)
<al>	66.4	68.6	70.0	72.1	72.7	73.2	73.4	73.5	73.9	73.9	73.9	74.6	74.6	74.6	73.0(18)

*Mg # = Mg cation # / (Mg cation # + Fe cation #)

Table 3-6. Analyses plotted in Figure 3-6. Garnet zoning in the Toluca Granite. The number in parentheses represents 1σ of the least digit cited.

A																	A'	AVG
weight % oxide																		
SiO_2	37.1	36.8	37.1	37.3	36.8	36.9	36.8	36.6	36.6	36.9	36.9	36.8	36.7	37.0	37.0	36.9	36.8	36.8(2)
TiO_2	0.03	<0.03	<0.03	<0.03	<0.03	<0.03	0.03	<0.03	<0.03	<0.03	<0.03	<0.03	<0.03	0.03	<0.03	<0.03	<0.03	
Al_2O_3	21.1	21.1	21.3	21.4	21.0	21.1	21.1	21.1	21.1	21.1	21.0	21.1	21.3	21.1	21.1	21.1	21.1	21.1(1)
Cr_2O_3	<0.03	<0.03	<0.03	<0.03	<0.03	<0.03	<0.03	<0.03	<0.03	<0.03	<0.03	<0.03	<0.03	<0.03	0.04	<0.03	0.07	
MgO	3.88	3.91	3.90	3.75	3.81	3.87	3.80	3.88	3.79	3.87	3.93	3.89	3.89	3.85	3.90	3.95	3.86	3.87(5)
CaO	0.72	0.77	0.54	0.36	0.34	0.31	0.36	0.41	0.39	0.39	0.40	0.40	0.41	0.67	0.57	0.49	0.46	0.47(14)
MnO	6.61	6.66	6.67	6.85	7.03	6.90	6.83	6.82	6.95	6.93	6.82	6.93	6.95	6.82	6.78	6.77	6.78	6.83(11)
FeO	30.6	30.4	30.2	30.4	30.6	30.7	30.6	30.8	30.2	30.5	30.7	30.7	30.5	30.5	30.6	30.8	30.4	30.5(2)
Na_2O	<0.03	0.05	0.06	<0.03	<0.03	0.03	0.04	0.05	0.05	0.05	0.04	0.04	0.07	<0.03	<0.03	<0.03	<0.03	
TOTAL	100.0	99.7	99.8	100.1	99.6	99.8	99.6	99.7	99.1	99.7	99.8	99.9	99.8	99.9	100.0	100.0	99.5	
cations based on 12 oxygen																		
Si	2.983	2.971	2.982	2.988	2.978	2.977	2.973	2.961	2.970	2.975	2.977	2.970	2.963	2.977	2.975	2.970	2.975	2.974(6)
Ti	0.002	0.000	0.000	0.000	0.000	0.001	0.002	0.001	0.000	0.001	0.000	0.000	0.001	0.002	0.001	0.000	0.001	0.001(1)
Al	1.996	2.009	2.019	2.027	2.000	2.008	2.013	2.014	2.023	2.010	2.000	2.007	2.023	1.999	2.003	2.006	2.009	2.011(9)
Cr	0.000	0.000	0.001	0.000	0.000	0.000	0.002	0.001	0.000	0.001	0.000	0.000	0.000	0.001	0.002	0.000	0.005	0.001(1)
Mg	0.465	0.471	0.467	0.449	0.460	0.465	0.458	0.468	0.459	0.465	0.473	0.468	0.467	0.462	0.468	0.473	0.465	0.465(6)
Ca	0.062	0.066	0.047	0.031	0.030	0.027	0.031	0.035	0.034	0.033	0.035	0.034	0.036	0.057	0.049	0.042	0.040	0.039(11)
Mn	0.450	0.455	0.455	0.466	0.482	0.471	0.468	0.467	0.478	0.473	0.466	0.473	0.475	0.465	0.462	0.462	0.464	0.468(8)
Fe	2.057	2.050	2.032	2.036	2.070	2.067	2.068	2.080	2.051	2.056	2.070	2.071	2.055	2.056	2.060	2.074	2.057	2.060(13)
Na	0.002	0.007	0.009	0.003	0.003	0.005	0.006	0.007	0.007	0.008	0.006	0.007	0.011	0.000	0.001	0.001	0.004	0.005(3)
TOTAL	8.017	8.029	8.012	8.000	8.023	8.021	8.021	8.034	8.022	8.022	8.027	8.030	8.031	8.019	8.021	8.028	8.020	8.023(8)
Mg # *	0.184	0.187	0.187	0.181	0.182	0.184	0.181	0.184	0.183	0.184	0.186	0.184	0.185	0.183	0.185	0.186	0.184	0.184(2)
<py>	15.3	15.5	15.6	15.1	15.1	15.3	15.1	15.3	15.2	15.4	15.5	15.4	15.4	15.2	15.4	15.5	15.4	15.3(1)
<gr>	2.0	2.2	1.6	1.0	1.0	0.9	1.0	1.1	1.1	1.1	1.1	1.1	1.2	1.9	1.6	1.4	1.3	1.3(3)
<sp>	14.8	15.0	15.2	15.6	15.8	15.5	15.5	15.3	15.8	15.6	15.3	15.5	15.7	15.3	15.2	15.1	15.3	15.4(3)
<al>	67.8	67.4	67.7	68.3	68.0	68.2	68.4	68.2	67.9	67.9	68.0	68.0	67.8	67.6	67.8	68.0	68.0	67.9(3)

* Mg # = Mg cation # / (Mg cation # + Fe cation #)

chemical zoning at the rim (Fig. 3-6).

CONCLUSIONS

Garnets in both the Tallulah Falls Formation and the Toluca Granite are homogeneous throughout the interior of the grain and show minor diffusional zoning at the rims. The garnet in the Walker Top orthogneiss is heterogeneous and shows conspicuous chemical zoning. The chemical zonation in the garnets of the Walker Top orthogneiss may indicate that the Walker Top orthogneiss experienced a different metamorphic history than the Tallulah Falls Formation or the Toluca Granite.

Crystallization ages, preliminary $^{206}Pb/^{238}U$ zircon ages, mineral assemblages, petrographic textures, and temperature and pressure estimates from electron microprobe data of rocks in the Inner Piedmont suggest a single prograde metamorphic event occurred as a result of the Acadian orogeny. Metamorphic conditions estimated from electron microprobe data range from 610 ± 20 °C to 645 ± 20 °C and from 3.8 ± 0.8 kbar to 5.4 kbar ± 0.8 kbar. These conditions are consistent with regional isograds and support a Barrovian model of metamorphism for the Inner Piedmont.

CHAPTER 4

MESOSCOPIC STRUCTURE

Rocks of the Inner Piedmont record multiple episodes of deformation, and the map patterns reflect the complex overprinting of structures. This chapter describes the mesoscale structures (foliations, lineations, folds, and joints) within the study area (Plate 1). A regional structural analysis addressing the temporal relationships of deformational events is presented in Chapter 5.

MESOSCALE STRUCTURES

Foliations

The foliation in the field area has been recognized as the dominant foliation in the western Inner Piedmont (e.g., Hatcher, 1970; Conley and Drummond, 1975, Bream, 1999; Giorgis, 1999; Hill, 1999; Williams, 2000). In the Tallulah Falls metagraywacke-schist unit, foliation is defined by the parallel alignment of quartz, feldspar, biotite, muscovite, kyanite, and sillimanite. Foliation in the Tallulah Falls sillimanite schist is defined by the parallel alignment of muscovite, quartz, and sillimanite. The Walker Top orthogneiss and the Toluca Granite are both weakly to nonfoliated. Where foliation is recognized in the orthogneiss units, it is defined by the alignment of biotite, muscovite, quartz, and feldspar.

Compositional layering is present in the Tallulah Falls Formation. In the metagraywacke-schist unit, compositional layering is enhanced by migmatization and metamorphic differentiation. Banding is defined by felsic (quartz and feldspar) and mafic (biotite) layers. In the sillimanite schist unit, layers of quartz alternate with micaceous layers. In both members of the Tallulah Falls Formation, compositional layering is parallel to foliation,

consistent with previous work in the western Inner Piedmont (e.g.: Whisnant, 1975; Bream, 1999).

Mesoscopic shear zones were recognized at isolated outcrops. Outcrops with S-C fabrics showed no geographical correlation and thus do not delineate a major shear zone. The shear sense of these localized shear zones is consistently top to the northwest.

Over 1,700 foliation measurements were collected in parts of the Benn Knob and Casar quadrangles (Plate 1, Plate 2) and are compiled in Appendix C. Poles to foliation were plotted and contoured on an equal-area net (Fig. 4-1). Foliations generally strike N-S (mean = 001°), are oblique to the orogen, and dip gently to the east (mean = 11°; Fig. 4-1). In the northernmost portion of the Benn Knob quadrangle, the strike of dominant foliation changes from NNW-SSE to NNE-SSW (Plate 1).

Lineations

Mineral lineations in the field area were observed primarily in the Tallulah Falls sillimanite schist unit in the field area. Although sillimanite needles are usually randomly oriented, it is the dominant mineral that defines the lineation measured. Quartz, feldspar, biotite, and muscovite also frequently define a lineation. Previous workers in the western Inner Piedmont (e.g., Davis, 1993; Giorgis, 1999) interpreted aligned muscovite, amphibole, feldspar, quartz and biotite to be mineral stretching lineations. This interpretation is based on the orientation of independent kinematic indicators parallel to the mineral lineations (Davis, 1993). The paucity of kinematic indicators (winged porphyroclasts, asymmetric folds, snowball garnets, etc.) complicates genetic interpretation of the mineral lineations in the study area.

Lineations plot roughly in the plane of foliation (Figs. 4-1, 4-2), indicating that lineation formation was syn- to late-foliation formation. Mineral lineations in the study area trend WNW-ESE (mean = 114°) and plunge to the SE (mean = 18°) (Fig. 4-2). The data are consistent with

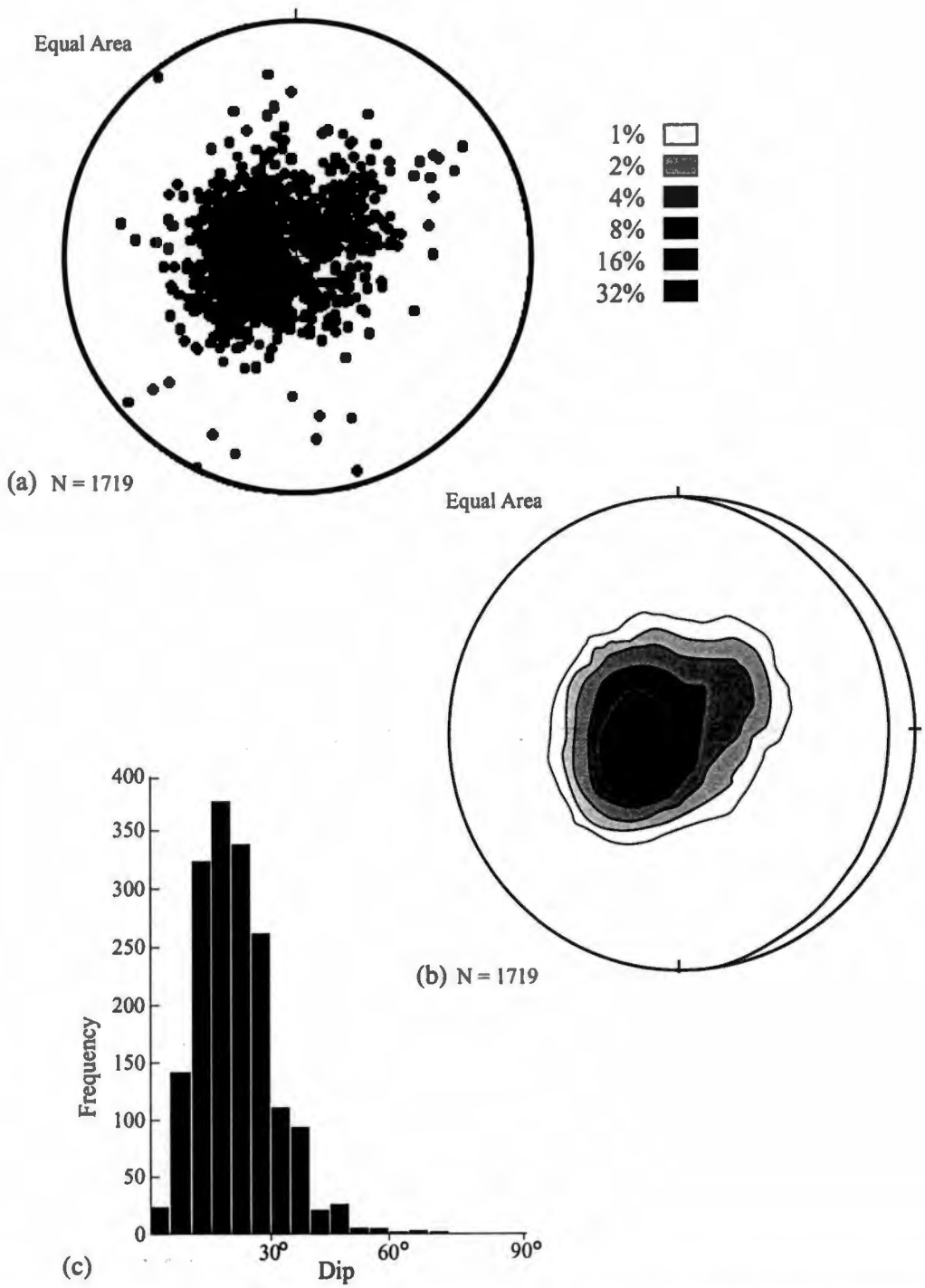


Figure 4-1. Scatter plot, fabric diagrams, and dip histogram for all foliation measurements obtained in the study area. (a) Lower hemisphere equal-area scatter plot of poles to foliation. (b) Lower hemisphere, equal-area contoured diagram of poles to foliation. The vector mean is 279°, 89°. The strike and dip of the plane to this point is 001° 11° to the east. (c) Histogram of foliation dip values in five degree intervals.

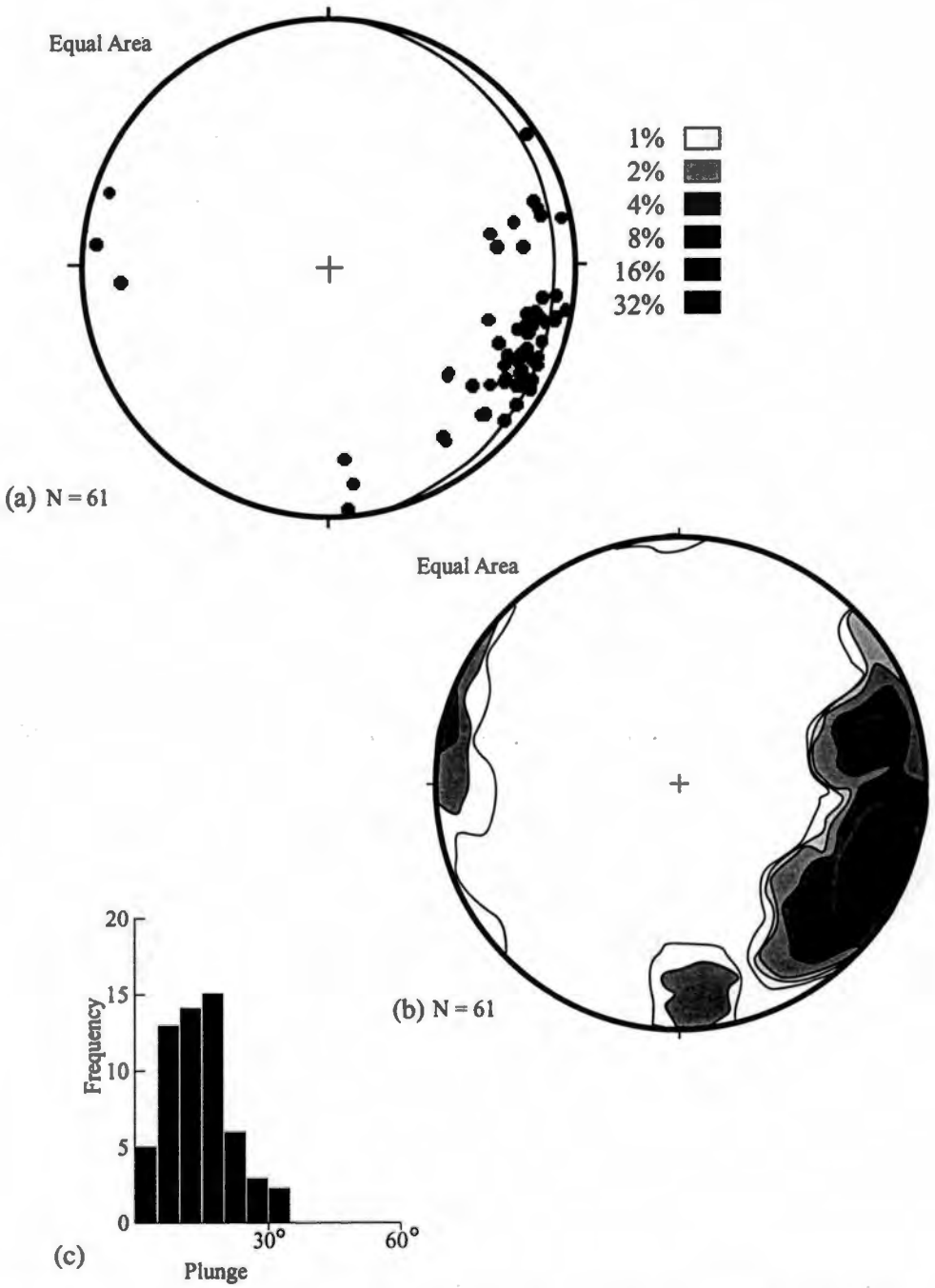


Figure 4-2. Plots of preferred mineral orientation lineations from the study area. (a) Lower hemisphere, equal-area scatter plot. (b) Lower hemisphere, equal-area contoured diagram of lineations. The mean vector lineation trends 114° and plunges 18°. (c) Histogram showing frequency of plunge values for lineations in five degree intervals.

the regional lineation trend outlined by Hatcher (1998) that indicates a NE-SW lineation adjacent to the Brevard fault zone that becomes more E-W into the core of the Inner Piedmont. A WNW-ESE trend, in combination with the assumption that these are stretching lineations, indicates a transport direction that has a WNW-ESE axis, which is consistent with tectonic models proposed by Davis (1993) and Hill (1999).

Folds

A wide variety of mesoscale folds were recognized in the study area. Axes of isoclinal to tight (20°-80°) recumbent folds have two trends, NNW and NE (Fig. 4-3). These reclined to recumbent folds all verge to the west and have axial planes roughly parallel to the regional foliation, and fold compositional layering. These passive-flow and flexural-flow folds often have attenuated limbs and thickened hinges (Fig. 4-4). The parallel nature of lineations and tight fold axes suggest that the structures formed as part of a synchronous deformation event.

Axes of broad, open (120°-160°), symmetrical folds scatter on the fabric diagram (Fig. 4-3), but show a dominant trend to the SE. Axes of this fold set are generally subhorizontal to gently plunging. Because constant thickness is maintained in the hinges and limbs and layers show homogeneous deformation, flexural slip during buckling is the probable fold mechanism. This later fold set warps earlier tight to isoclinal folds and creates map-scale interference fold patterns.

Sheath and noncylindrical folds have been recognized by previous workers in the Inner Piedmont (e.g.: Davis, 1993; Hill, 1999; Bream, 1999). These folds were not recognized at the outcrop scale in my study area but map patterns support their existence.

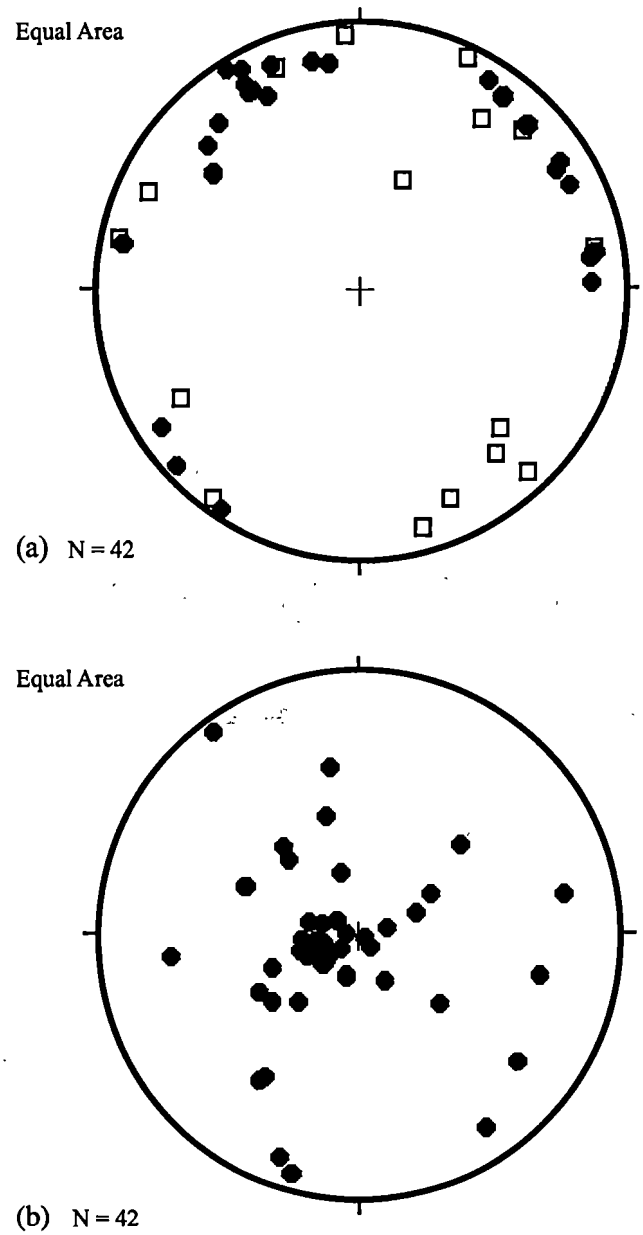


Figure 4-3. Mesoscale fold measurements from the study area. (a) Lower hemisphere, equal-area scatter plot of fold axes. Closed circles are tight to isoclinal folds; open squares are open folds. (b) Lower hemisphere, equal-area scatter plot of poles to axial surfaces.

(a)



(b)



Figure 4-4. Photographs of folds in the study area. (a) Tight flexural flow folds within a hinge of a similar isoclinal fold of Tallulah Falls metagraywacke-schist near Painter Knob, station BK 1375. (b) Tight similar folds in the Toluca Granite near Benn Knob, station BK 1370.

Joints

Fracture orientation data were collected from unfilled joints at the outcrop scale throughout the field area and are listed in Appendix C. The frequency, density, or spacing of joints was not addressed in this study. Three fracture sets occur in the study area (Fig. 4-5): an ESE-WNW set, a SE-NW set, and a SW-NE set. Joints must have formed after the last ductile deformational event because they cut all other structures (e.g., foliation and folds) in the field area. Garihan *et al.* (1993) and Curl (1998) associated at least some of these fractures with Mesozoic uplift and extension in the southern Appalachians. The orientation of fracture sets could influence surface and groundwater flow characteristics (Snipes, 1980, 1981).

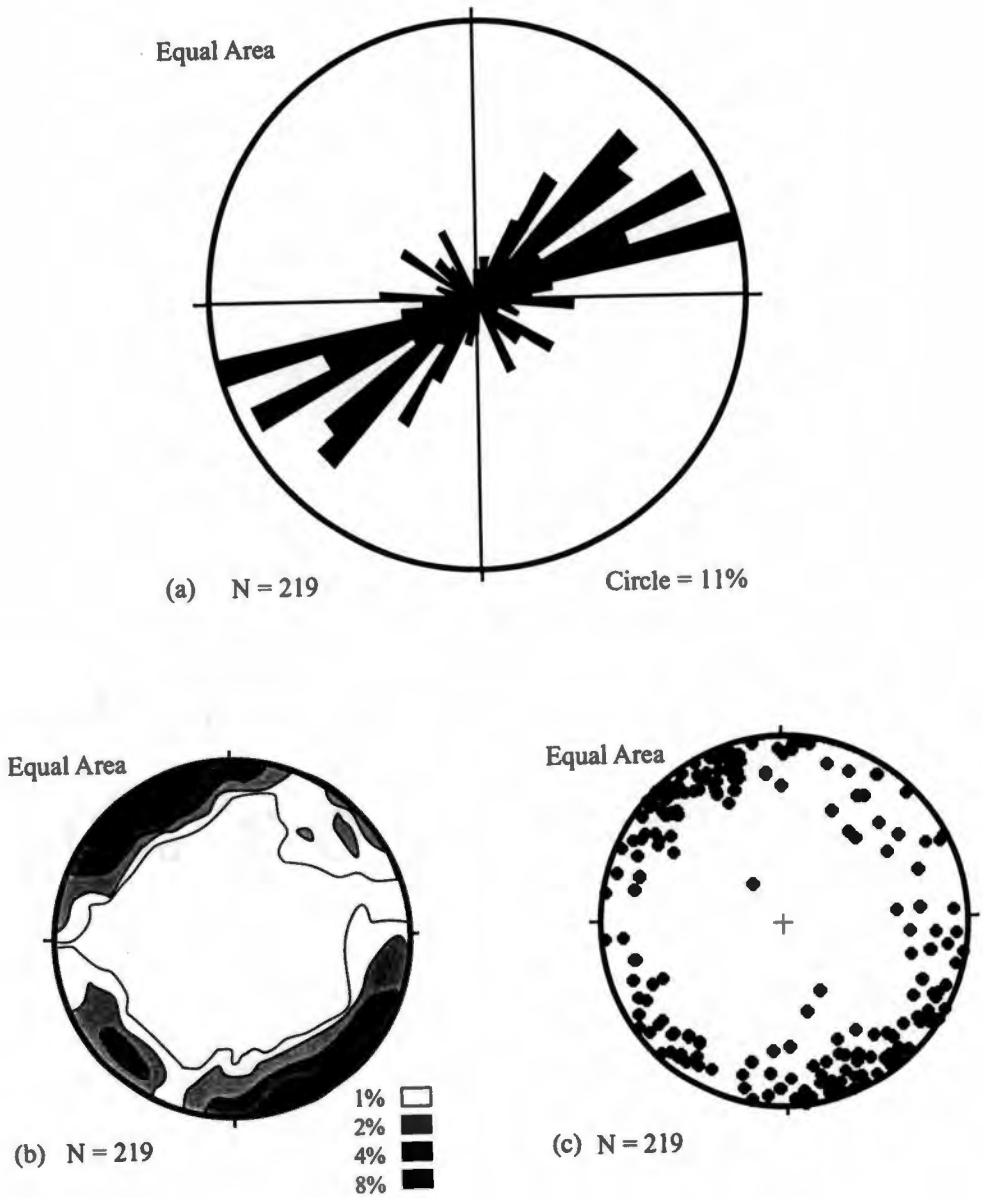


Figure 4-5. Distribution of all joint measurements collected from the study area. (a) Rose diagram. (b) Lower hemisphere, equal-area contoured diagram of poles to joints. (c) Lower hemisphere, equal-area scatter plot of poles to joints.

CHAPTER 5

REGIONAL STRUCTURAL ANALYSIS

INTRODUCTION

Rocks of the Inner Piedmont have been subjected to a complex deformational history, recording multiple episodes of folding and faulting. This chapter presents a deformational framework for the Inner Piedmont that addresses the relative timing of regional structures, using mesoscale and macroscale data. The analyzed area extends from the Brevard fault zone to the eastern Inner Piedmont (Fig. 5-1) and contains distinct changes in style, structural orientation, and displacement direction (Davis, 1993).

Granitoid crystallization ages and U-Pb ages of monazite and zircon separates from the eastern Blue Ridge and Inner Piedmont help to delimit the timing of deformation. Early and middle Paleozoic granitoids with foliation concordant to regional structures have been dated at 500 Ma (Odom and Fullagar, 1973), 460 Ma (McSween *et al.*, 1991), 438 Ma (Odom and Russell, 1975), 423 Ma (Harper and Fullagar, 1981), and 409 Ma (McSween *et al.*, 1991). Preliminary U-Pb data on monazites separated from metapelites in South Carolina indicate two separate metamorphism events at ca. 360 Ma and ca. 320 Ma (Dennis and Wright, 1997). Electron microprobe age dating of monazite separates from migmatites in the Athens gneiss, Georgia yield ages of 330 ± 10 Ma (Mirante and Patino-Douce, 2000). U-Pb data on zircon rims from lithologies from across the Blue Ridge and Inner Piedmont yield ages of ca. 325-380 Ma (Carrigan *et al.*, 2001). Therefore peak deformation in the Inner Piedmont occurred between 320 and 409 Ma, as a result of the Alleghanian and Acadian orogenies.

Structures parallel, normal, and oblique to the orogen have been recognized in the Inner Piedmont for decades (e.g., Reed and Bryant, 1964; Hatcher, 1972; Roper and Dunn, 1973; and Griffin, 1974). Davis (1993) suggested that this structural pattern was a result of a "thrust-

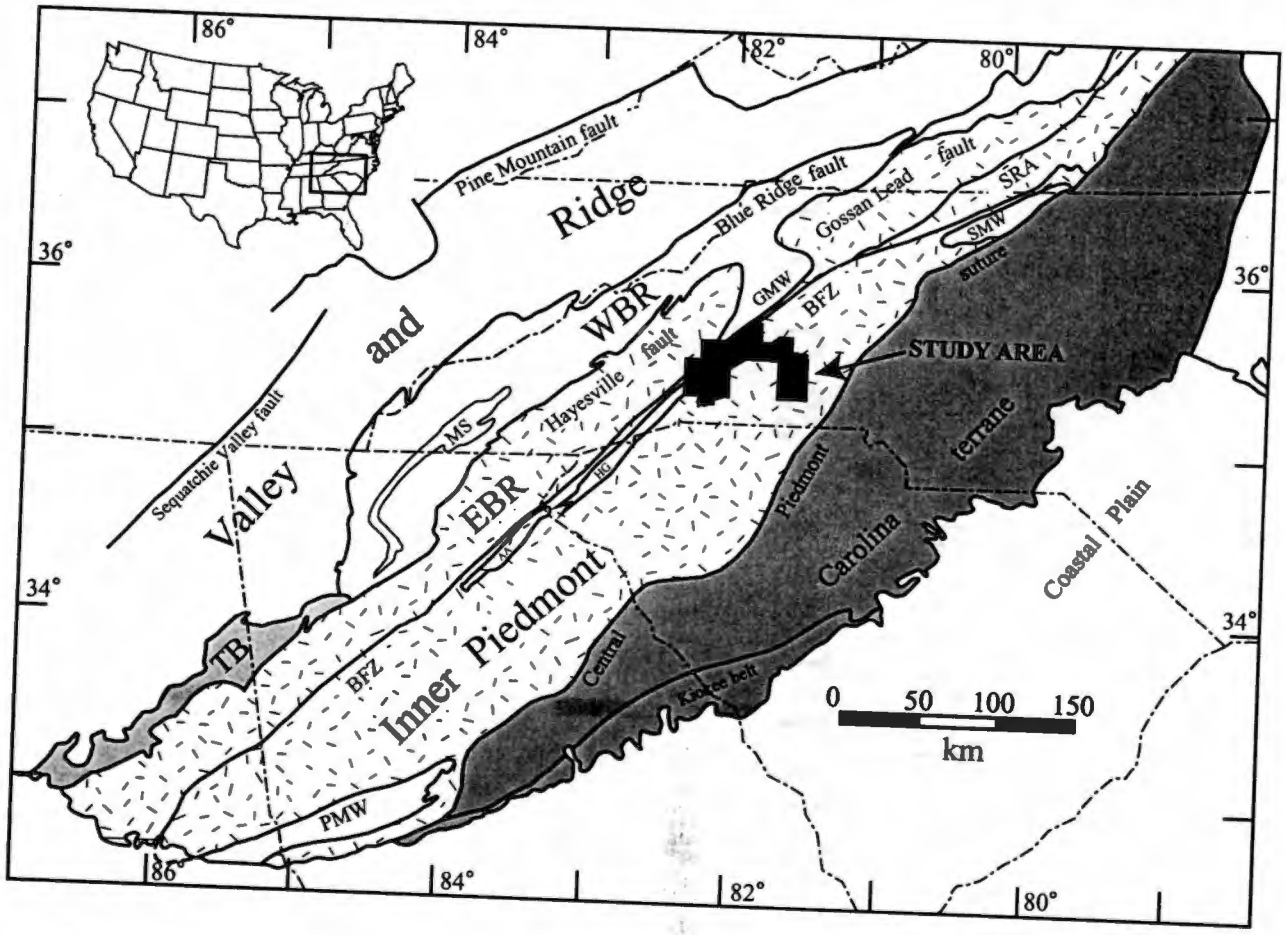


Figure 5-1. Simplified tectonic map of the southern Appalachians. The compiled study area is in black. TB-Talladega belt. MS-Murphy syncline. WBR-Western Blue Ridge. GMW-Grandfather Mountain Window. EBR-Eastern Blue Ridge. BFZ-Brevard fault zone. AA-Alto allochthon. HG-Henderson Gneiss. SMW-Sauratown Mountain window. SRA-Smith River allochthon. PMW-Pine Mountain window. Modified from Hatcher *et al.* (1990).

wrench partitioned deformation . . . and is a manifestation of an early oblique convergence within the southern Appalachians." The deformational framework outlined by Davis (1993) and subsequently modified by Yanagihara (1994), Bream (1999), Hill (1999), Giorgis (1999), and Williams (2000) identifies five deformational events. Compilation of recent detailed mapping from the above workers with that of Overstreet *et al.* (1963a, 1963b) (Plate 3 and Plate 5) also supports five deformational events, although they are slightly modified (Table 5-1).

This compilation has been divided into three domains for structural analysis based on thrust sheets and subdivisions thereof (Fig. 5-2). The Brevard fault zone bounds Domain I to the northwest and the Mill Spring thrust forms the southeast boundary. The Mill Spring thrust to the west and the Brindle Creek thrust to the east form the boundary of Domain II. Domain III is composed of the hanging wall of the Brindle Creek thrust. Due to the heterogeneity of structural fabrics and orientations, Domain III is subdivided into 5 subdomains (IIIa, IIIb, IIIc, IIId, and IIIe). Structures will be discussed in chronological order of deformation events (D_1-D_5).

DEFORMATION EVENTS

D_1 Deformation

The D_1 deformation event occurred prior to the main phase of recrystallization (Davis, 1993) and because of the penetrative deformation associated with later events, evidence of the D_1 event is rare. Hopson and Hatcher (1988) recognized D_1 in the Alto allochthon, Georgia, as the presence of a folding event, F_1, which produced an axial planar foliation, S_1. In the Columbus Promontory, Davis (1993) recognized compositional layering of the Poor Mountain Formation preserved in F_1 folds in a small window within the Tumblebug Creek thrust sheet.

Truncated folds in the footwall of the Tumblebug Creek thrust provide macroscale evidence of D_1 (Bream, 1999) (Plate 5). A regional recumbent antiform in the hanging wall of

Table 5-1. Deformational framework and related events for the central and western Inner Piedmont, North Carolina. (modified from Williams, 2000; Bream, 1999; Giorgis, 1999; Yanagihara, 1994; and Davis 1993). BCT-Brindle Creek thrust. MST-Mill Spring thrust. TCT-Tumblebug Creek thrust. SMT-Sugarloaf Mountain thrust.

DEFORMATION EVENTS		STRUCTURES			OROGENIC EVENTS
		FABRICS	FOLDS	FAULTS	
D_5		joints	———	———	Mesozoic Uplift and Extension
D_4	b	joints	F_{4b} open, upright; trend NW	———	ALLEGHANIAN
	a	joints	F_{4a} open, upright; trend N to NE	———	
D_3		S_3	F_3 tight reclined to upright trend N to NE	final movement of faults as Type-C thrusts	ACADIAN
D_2	b	S_2 L_2	F_{2b} tight to isoclinal, reclined to recumbent; sheath folds	initial movement on the SMT, MST, and BCT as Type-F thrusts	
	a	S_2	F_{2a} upright folds	TCT	
D_1		S_1	F_1 intrafolial folds, map scale in TCT footwall and BCT hanging wall	———	TACONIAN

prograde metamorphism

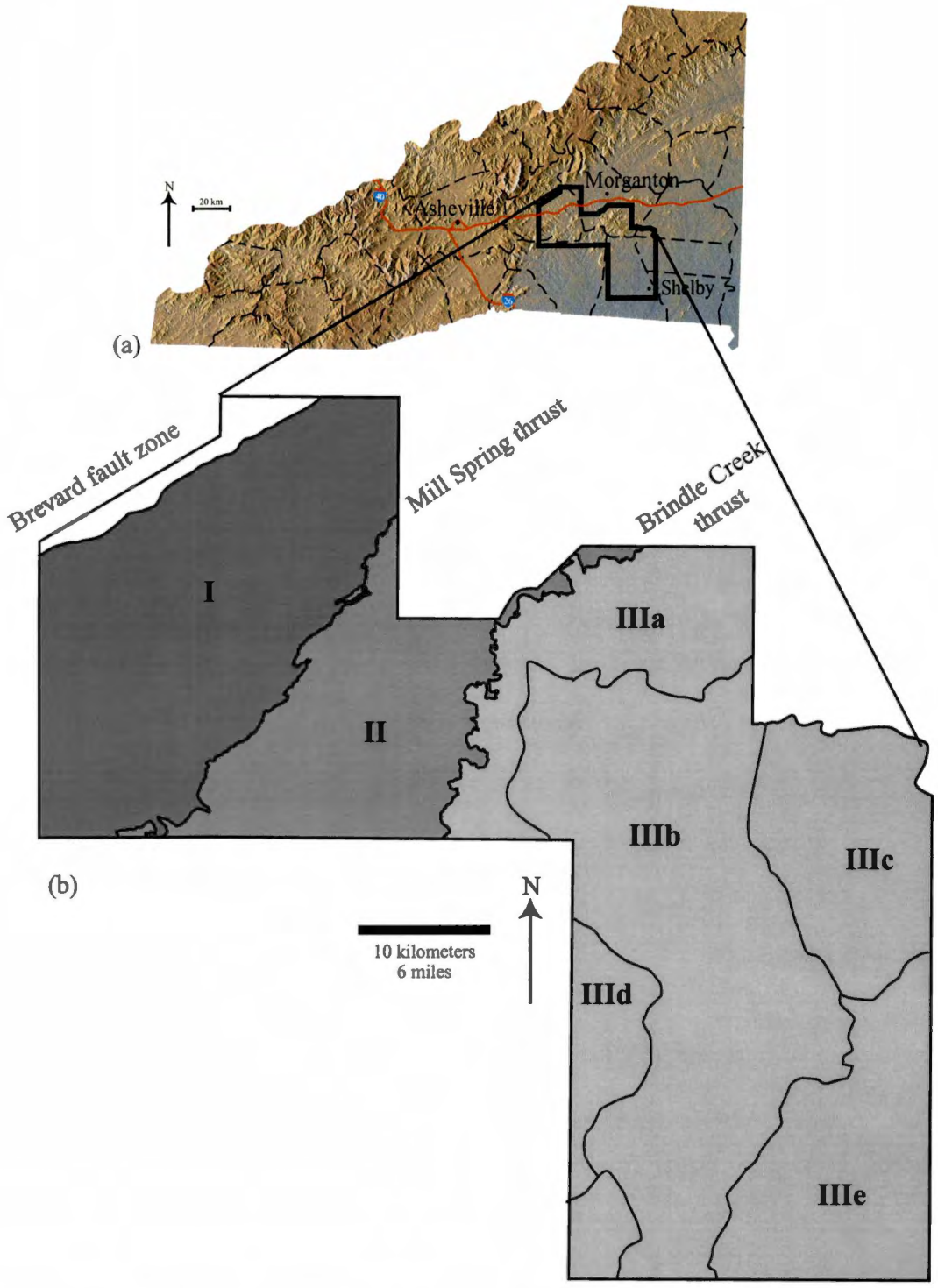


Figure 5-2. Index map to domains. (a) Geographic location of the study area. (b) Domains within the study area. See text for details.

the Brindle Creek thrust also resulted from this early episode of deformation (Plate1, Plate 5). Stratigraphic constraints necessitate the existence of this early folding episode. The majority of the metagraywacke in the hanging wall of the Brindle Creek thrust has been correlated with the upper Tallulah Falls member due to the lack of amphibolite. A regional scale antiform serves as an explanation for the dominance of the upper Tallulah Falls member in the eastern portion of the study area (Plate 5). The antiform trends SW-NE, verges northwest, and comprises the hanging wall of the Brindle Creek thrust. The localization of the Walker Top orthogneiss has been interpreted to represent the core of the fold that abuts the Brindle Creek thrust (Plate 5).

Mesoscale evidence of D_1 deformation in the study area (Domains I, II, and III) includes truncated folds and foliation within amphibolite boudins (Fig. 5-3) and rootless, intrafolial folds. These have been recognized as the most defining mesoscale criterion for this early episode of deformation (Hopson and Hatcher, 1988; Davis, 1993; Yanagihara, 1994; Curl, 1998; Bream, 1999; Hill, 1999; Giorgis, 1999; Williams, 2000).

D_2 Deformation

D_2 is the most penetrative deformation event in the Inner Piedmont, a polyphase event at or near peak metamorphism (e.g., Davis, 1993; Hill, 1999; Bream, 1999). This event is characterized by the formation of a dominant foliation, a prominent preferred mineral lineation, reclined to recumbent, tight to isoclinal folds, sheath folds, and Type-F thrust faults. D_2 is interpreted to be "a progressive episode, in which heterogeneous and slightly diachronous deformation occurred as a continuum" (Hill, 1999).

Equal-area fabric diagrams of over 10,000 foliations are presented in Figure 5-4. Near the Brevard fault zone, S_2 foliation strikes parallel to the fault zone and dips moderately (~40°) to the southeast. The average S_2 foliation in Domain I is roughly orogen-parallel and strikes N41E and dips 25° SE. The average foliation in the Mill Spring thrust sheet strikes N19E and dips 22°

(a)



(b)

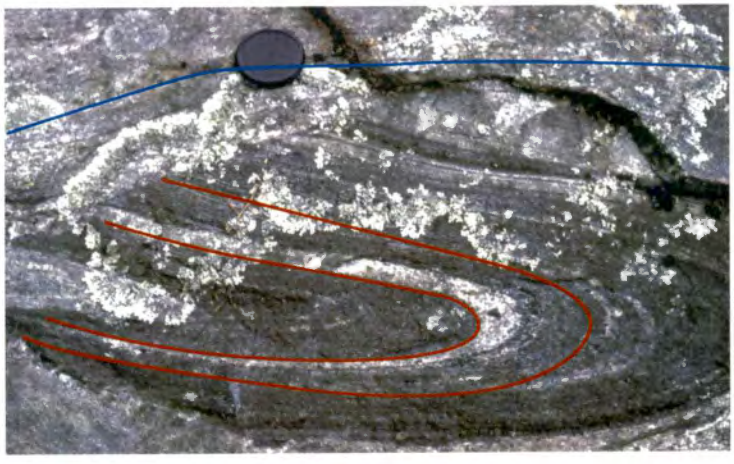


Figure 5-3. S_1 and S_2 foliation relationships. S_1 is outlined in red. S_2 is outlined in blue. (a) Foliated amphibolite boudin within Dysartsville orthogneiss one mile south of Vein Mountain Church (Glenwood quadrangle). S_1 foliation within amphibolite boudin and S_2 foliation within the Dysartsville orthogneiss. Modified from Williams (2000). (b) Isoclinal flexural-flow fold in an amphibolite boudin in the lower Tallulah Falls member from the west face of Burkemont Mountain (Morganton South quadrangle). Modified from Giorgis (1999).

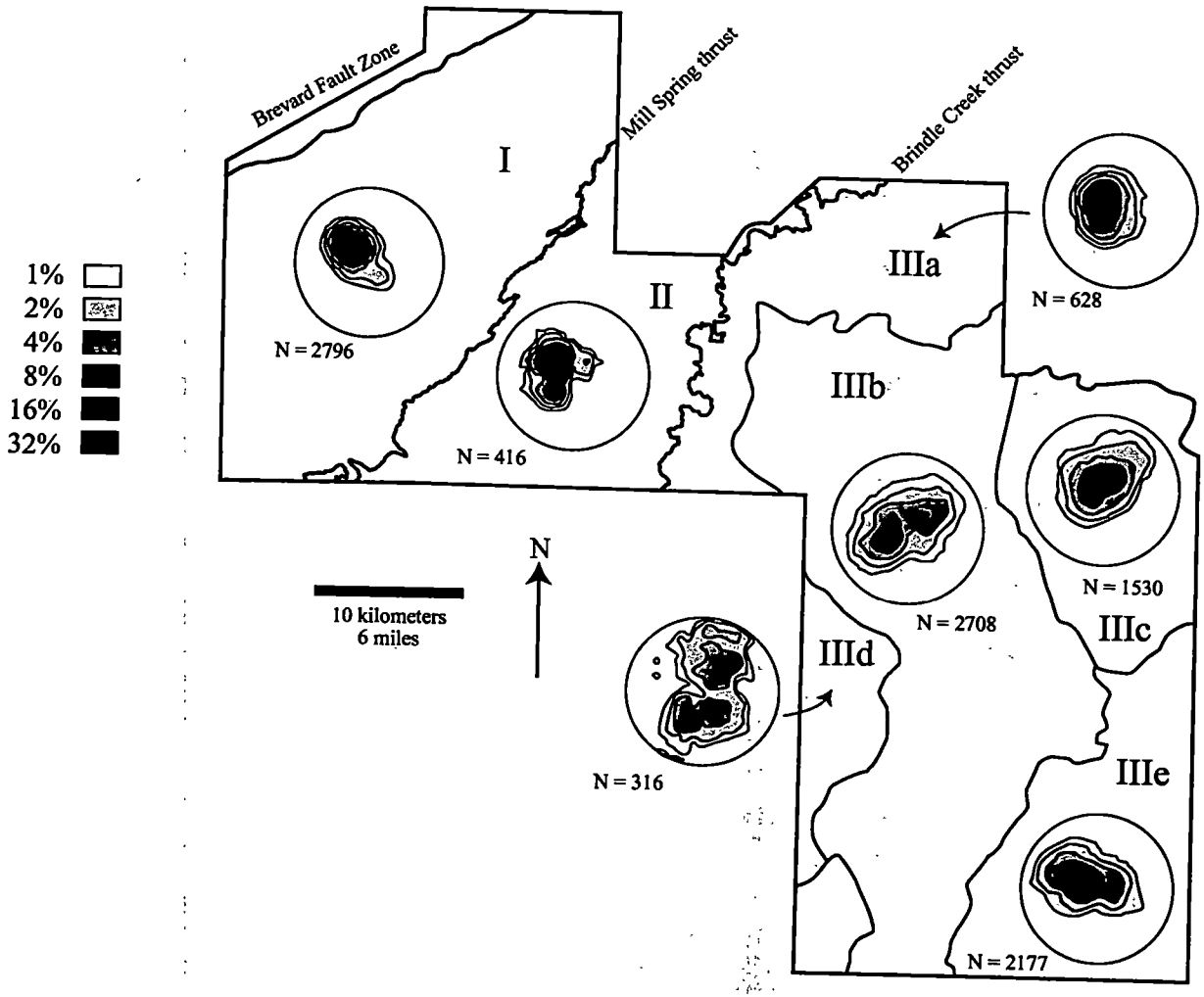


Figure 5-4. Lower hemisphere, equal-area contoured diagrams of poles to foliation for the study area. See text for further discussion.

SE. In the Brindle Creek thrust sheet, the mean foliation in Domain IIIa strikes N10E and dips 11° SE. Domains IIIb, IIIc, and IIId strike NE-SW and dip shallowly to the southwest. Domain IIId reflects a later (D_5) open fold in the eastern portions of the Polkville and Boiling Springs 7.5-minute quadrangles. The foliations reflect a regional change in strike from NE-SW in the western flank to N-S in the central Inner Piedmont back to NE-SW in the southeastern part of the terrane.

In the western Inner Piedmont, lineations were interpreted to be mineral stretching lineations (e.g., Davis, 1993; Giorgis, 1999) based on the orientation of independent kinematic indicators (snowball garnets, asymmetric folds, winged porphyroclasts, boudinage, etc.) parallel to the mineral lineations (Davis, 1993). L_2 lineations are defined by elongate and rodded quartz, micas, amphiboles, and feldspars in the western Inner Piedmont (Domains I and II) and by elongate micas, quartz rods, and sillimanite needles in the central and eastern Inner Piedmont.

Over 800 lineations are plotted on lower hemisphere, equal-area stereonets in Figure 5-5. Lineations in Domain I and II trend NE-SW, roughly parallel to the trend of F_2 fold axes. Whisnant (1975) observed the parallel nature of the isoclinal fold axes and the lineations in the western Inner Piedmont and interpreted isoclinal folding and lineation formation to be synchronous. An alternative explanation for the lineation trends in the study area involves transport parallel to axes of regional sheath folds (e.g., Bream, 1999). Structural data and map patterns in this study support a genetic association between mesoscopic sheath folds and lineations (Fig. 5-5).

Davis (1993) was able to distinguish D_{2a} folds and D_{2b} folds based on truncated footwall structures, transposition of D_{2a} folds into S_2 and the abrupt structural and metamorphic relationships fold across D_{2b} folds. This division is supported by initial folding of the Tumblebug Creek thrust (a D_{2a} fault) in a Type-F thrust relationship that is then truncated by the Sugarloaf Mountain thrust, a D_{2b} fault (Bream, 1999).

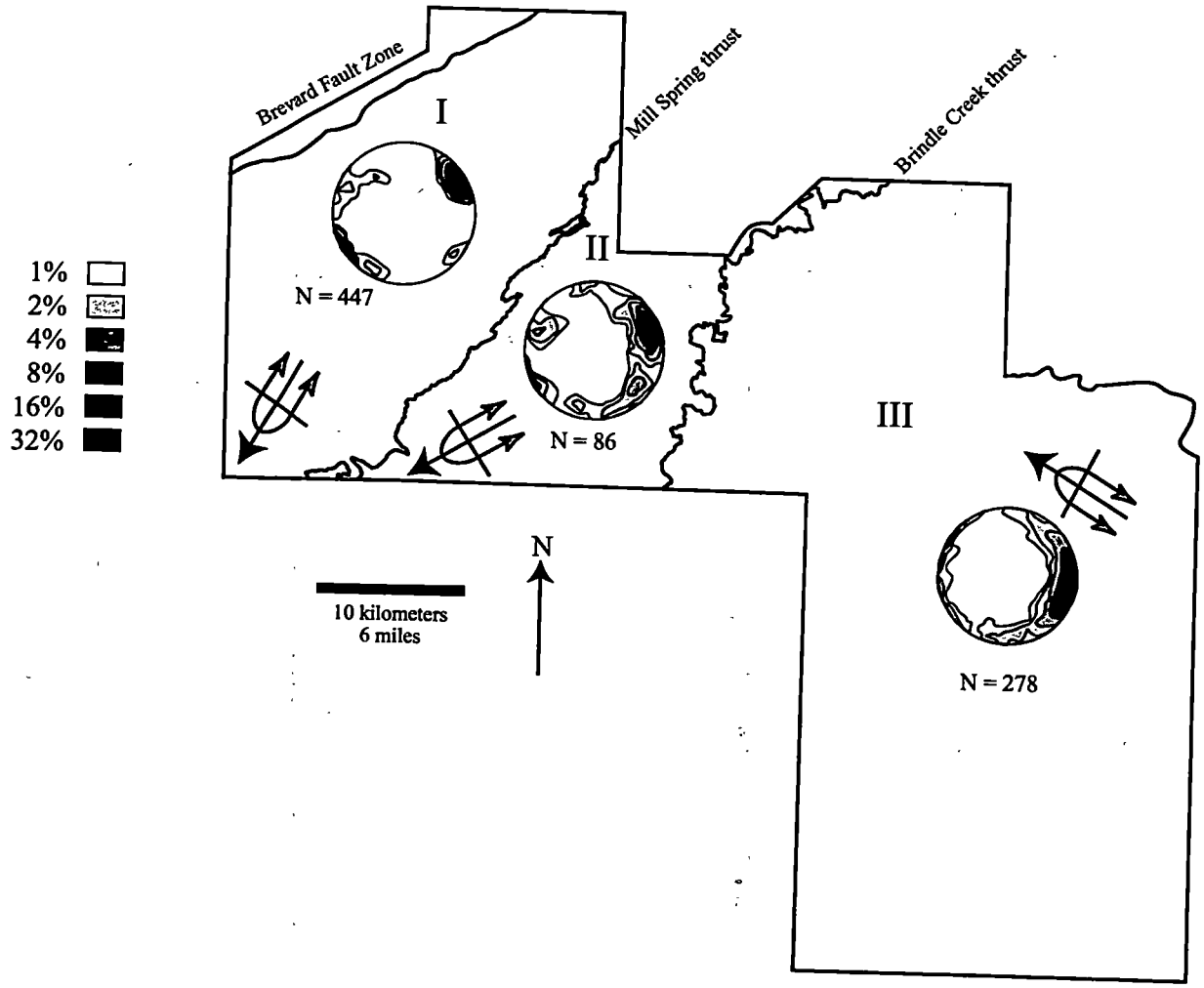


Figure 5-5. Lower hemisphere, equal-area contoured diagrams of lineations and directions of regional scale sheath fold axes in the study area. See text for further discussion.

D_{2a} is characterized by upright isoclinal folds (Davis, 1993) and pre-peak metamorphism emplacement of the Henderson Gneiss on the Tumblebug Creek thrust. Timing of displacement on the Tumblebug Creek thrust (and later deformation) is constrained by the age of the Henderson Gneiss, 470 Ma (Vinson, 1999). Therefore, the most intense deformation and metamorphic conditions occurred after 470 Ma.

Mesoscopic and macroscopic sheath folds recognized throughout the study area have been attributed to the D_{2b} event. At the outcrop scale, these are identified by their characteristic eye or anvil shape (Davis, 1993). Bream (1999) recognized regional-scale sheath folding within the Henderson Gneiss (Plate 5) because of the map pattern at both southeast and northeast terminations. The outcrop pattern can be explained by northwest-directed thrusting on the Tumblebug Creek thrust prior to later southwest-directed sheath folding. Convincing structural evidence in support of large-scale sheath folds is the strong NE-SW-oriented mineral stretching lineation (Bream, 1999).

Large-scale sheath folds are recognized in each of the thrust sheets in the composite study area. The axes of these sheath folds are nearly parallel to the lineation trends of the respective domains (Fig. 5-5). Map patterns and fabric diagrams support a transport direction that is NE-SW in the western Inner Piedmont that becomes more E-W in the central and eastern Inner Piedmont, which is consistent with tectonic models proposed by Davis (1993) and Hill (1999). The spread in the lineations may be related to later D_3 and D_4 folding. A conspicuous northwest-directed lineation in the study area may be the result of D_3 thrust emplacement.

Equal-area stereonets of fold axes (F_1-F_4) are presented in Figure 5-6. Due to the dominant D_2 deformation at both the meso- and macroscales, trends on the stereonets are primarily attributed to F_2 folding events. The most common folds indicative of D_{2b} deformation are tight to isoclinal, reclined to recumbent folds with westward vergence. F_{2b} folds in Domain III show a wide variety of orientations. Regional map patterns reflect a strong N-NW trend of

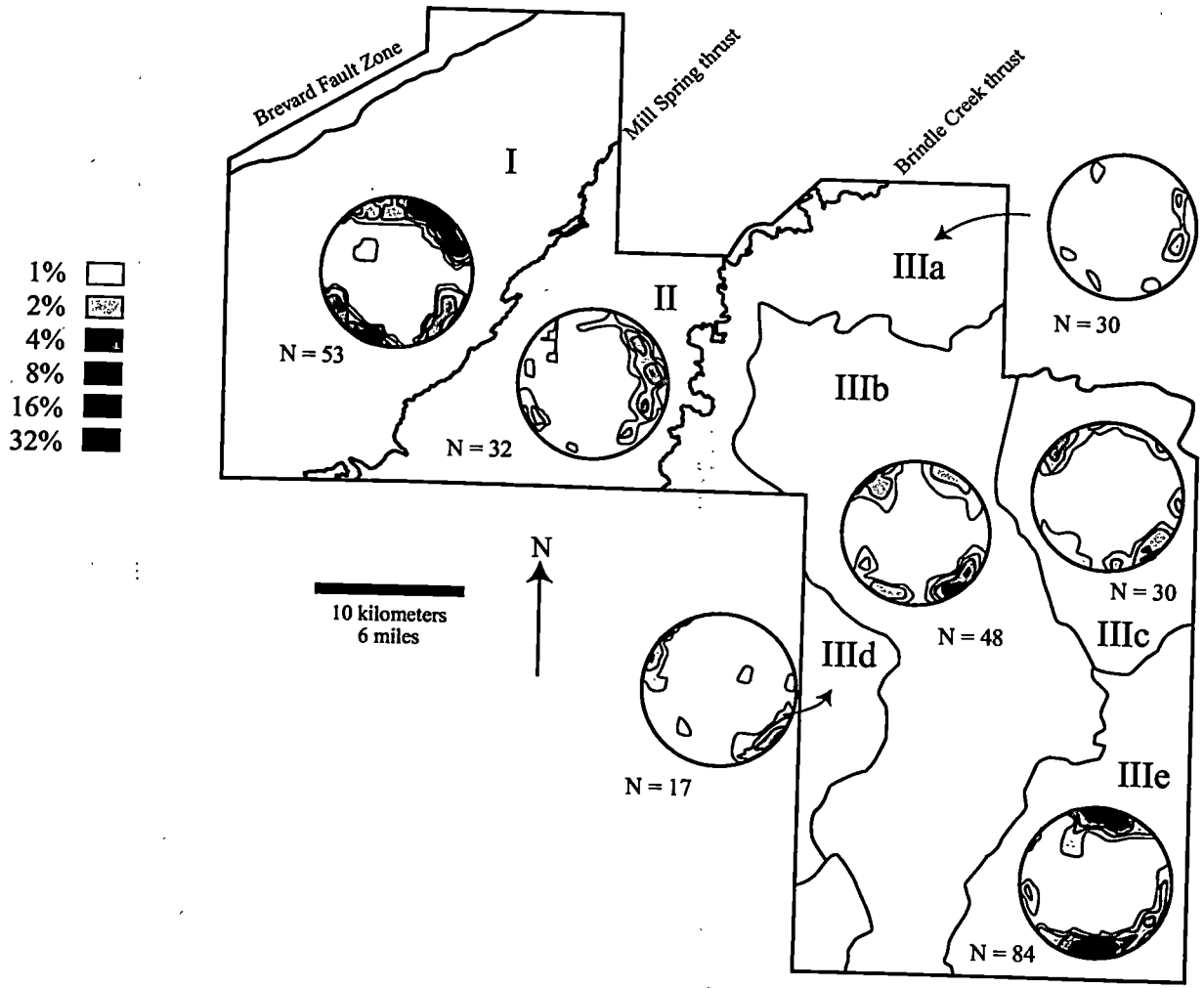


Figure 5-6. Lower hemisphere, equal-area contoured diagrams of fold axes in the study area. See text for further discussion.

tight to isoclinal, reclined to recumbent F_{2b} folds (Plate 5). F_{2b} folds in the western portion of Domain III (IIIa) trend E, but become NW-SE in Domains IIIb, IIIc, IIId, and N-S in Domain IIIe (Fig. 5-6). F_{2b} folds are tight to isoclinal, reclined to recumbent, and trend NE, parallel to the orogen. At the outcrop scale, F_{2b} folds have thickened hinges and attenuated limbs indicative of flexural flow folding (Fig. 5-7).

The Mill Spring thrust, Sugarloaf Mountain thrust, and Brindle Creek thrust are examples of Type-F thrust faults that formed when the common limb of an F_{2b} antiform-synform pair is removed, and the fault then accommodates displacement. Initial movement on these faults is interpreted to have occurred late during D_{2b}.

D_3 Deformation

D_3 deformation occurred after peak metamorphism, but prior to complete cooling of the rocks (Hopson and Hatcher, 1988). D_3 structures are oriented parallel and subparallel to D_2 structures in Domains I and II. Davis (1993) noted that F_3 folds are common in the western Inner Piedmont but not penetrative. These folds include outcrop-scale undulations that locally produce crenulation cleavage (Davis, 1993). Bream (1999) observed that D_3 folds have moderately inclined axial surfaces and maintain constant thickness in the limbs and hinges. D_3 folds were not conspicuous in Domain III, and may not be parallel to NW-SE- and W-E-oriented D_2 structures.

Final emplacement of thrust sheets as coherent packages took place during D_3. In the study area, this includes emplacement of the Sugarloaf Mountain thrust, the Mill Spring thrust, and the Brindle Creek thrust. Earlier F_2 folds are truncated by each of these thrusts (Plate 5), which indicates final emplacement occurred after peak metamorphism during D_2.

D_3 deformation is likely the tail end of the Acadian orogenic event but may indeed by a result of the Alleghanian orogeny.



Figure 5-7. F_{2b} fold in Tallulah Falls metagraywacke showing thickened hinges and attenuated limbs. Flexural-flow fold south of Cove Mountain (Dysartsville quadrangle, from Williams, 2000)

D_4 Deformation

D_4 produced similar, open, upright folds that overprint earlier (F_1-F_3) folds. This event produced map-scale folds and dome-and-basin interference patterns in the study area. F_{4a} folds trend NE and are orogen-parallel while F_{4b} folds trend NW, perpendicular to earlier structures. Bream (1999) suggested that D_{4a} may be the end member of D_3 deformation, however D_4 structures are probably evidence of the Alleghanian orogeny in the Inner Piedmont. The brittle nature and similar style of these open folds suggests they formed in the same deformational event. The perpendicular nature of these two fold sets can be explained by a spasmodic episode of deformation (Whitten, 1966). Deformation during this event is coeval with or predates joints in the study area.

D_5 Deformation

Several dominant fracture sets have been recognized in the study area. Unfilled fractures are typically planar with small apertures. Garihan *et al.* (1993) and Curl (1998) associate these fractures with later (Mesozoic) brittle faulting in the southern Appalachians. Fracture orientations in the study area are parallel to the N50°-N70° fault system that produced the Marietta-Tryon graben in South Carolina (Garihan *et al.*, 1993).

CROSS SECTIONS

Sections A-A', B-B', C-C', and D-D' are located in Plate 5. Locations of sections A-A', B-B', and C-C' were chosen based on the locations of previous lines by Bream (1999), Giorgis (1999), and Williams (2000). Section D-D' was drawn perpendicular to major structures on the Shelby 15' quadrangle.

Section A-A'

Section line A-A' is located in the Glenwood, Sugar Hill, and Dysartsville quadrangles and illustrates the subsurface geometry of the Tumblebug Creek thrust, the Sugarloaf Mountain thrust, and the Mill Spring thrust. In this cross section, the folds found in the footwall of the Tumblebug Creek thrust represent the earliest episode of deformation (D_1). The Tumblebug Creek thrust emplaced the Henderson Gneiss over the Tallulah Falls Formation during D_{2a}. The Mill Spring thrust was active during D_{2b} as a Type-F (of Hatcher and Hooper, 1992) and then evolved into a Type-T thrust. The Sugarloaf Mountain thrust crosscuts the Tumblebug Creek thrust and is also attributed to D_{2b} deformation. The contact between the Dysartsville orthogneiss and the Tallulah Falls Formation is drawn as concordant because the contact at the surface appears to parallel foliation in most areas. The open folding of the tight-to-isoclinal folds and the faults in the section is a result of D_4 deformation.

Section B-B'

Section line B-B' is also located in the Sugar Hill, Glenwood, and Dysartsville quadrangles and depicts the subsurface geometry of the Tumblebug Creek thrust, Mill Spring thrust, and the Brindle Creek thrust. This section illustrates the northeast termination of the Henderson Gneiss and bounding Tumblebug Creek thrust, possibly the tail end of a regional scale sheath fold. The Sugarloaf Mountain thrust dies out between section lines A-A' and B-B'. The Mill Spring thrust forms a klippe (projected into the section) and is folded with the footwall into a synform by an F_4 fold. The truncation of the Dysartsville orthogneiss body by the Mill Spring thrust indicates emplacement occurred prior to faulting. Like the Sugarloaf Mountain thrust, the Mill Spring thrust cut up section to the southwest. The Brindle Creek thrust placed the Tallulah Falls Formation on top of the Poor Mountain Formation. Displacement on the Brindle Creek thrust was originally interpreted to be < 5 km (Giorgis, 1999), but due to stratigraphic and

isotopic contrasts across changes in the hanging wall, displacement is probably much greater (Bream *et al.*, 2001).

Section C-C'

Section line C-C' is located in Dysartsville, Benn Knob and Casar quadrangles and illustrates the major structural differences between the hanging wall and footwall of the Brindle Creek thrust. Isoclinal reclined folds (F_{2b}) in the footwall have been refolded by open, upright F_4 folds. Interference patterns and sheath folds complicate the structural geometry in the hanging wall of the Brindle Creek thrust. Boudinage during F_2 has segmented the F_1 regional scale antiform. Sheath folds are represented by the hook-shaped ellipses of the middle and lower Tallulah Falls members. The isolated occurrence of the Walker Top orthogneiss enclosed by the middle and lower Tallulah Falls members may also represent a sheath fold. The Toluca Granite and the Walker Top orthogneiss are consistently associated with the aluminous schist member of the Tallulah Falls Formation. This relationship encourages further study to determine if the Toluca Granite and the Walker Top orthogneiss may be the products of large-scale migmatization.

Section D-D'

Section line D-D' is located in the Boiling Springs and Shelby quadrangles and illustrates the dominance of sheath folds (F_{2b}) in the central and eastern Inner Piedmont.

DEFORMATIONAL SYNTHESIS AND TECTONIC SUMMARY

Due to the rare evidence of D_1, because of the penetrative nature of later deformational episodes, it must have occurred early, probably during the Taconic orogenic event. D_2 is interpreted to be a result of the Acadian orogeny since it represents peak metamorphic conditions.

D_3 structures resulted from either late Acadian deformation or during the Alleghanian orogeny. Because of its brittle and overprinting nature, D_4 is likely a result of Alleghanian deformation. D_5 structures resulted from extension long after the orogenic events in the southern Appalachians.

Several tectonic models have been proposed for the Inner Piedmont and the crystalline southern Appalachians including regional scale nappes (Hatcher, 1972; Griffin, 1974), stockwork tectonics and tectonic slides (Griffin, 1971, 1974), and oblique convergence (Davis, 1993; Hill, 1999). Portions of each of these models are applicable to the compiled portion of the Inner Piedmont, North Carolina.

In South Carolina, Griffin (1971) described the Inner Piedmont as an infrastructure in his stockwork tectonics model. He recognized two major nappes (the Six Mile nappe and the Walhalla nappe) and a deep synformal structure (the non-migmatitic belt) in the Inner Piedmont of South Carolina. Griffin (1974) recognized several types of folds in the Inner Piedmont, but attributed them to only two deformational events. The change in outcrop pattern and structural style between the non-migmatitic belt (western Inner Piedmont) and the Walhalla and Six Mile nappes (central Inner Piedmont) is evidence of a tectonic slide boundary (Griffin, 1974). In his model, the infrastructure is the Inner Piedmont, the Carolina slate belt (Carolina terrane) is the suprastructure, and the non-migmatitic belt represents an infolded abscherung or detachment zone, using the concepts of Wegmann (1935) and Haller (1956).

Hatcher (1972, 1978) recognized the nappe-like structures in the Inner Piedmont were part of D_2 deformation. Hatcher (1978) stated that structures in the Inner Piedmont did not form in a single deformational episode as Griffin's (1971) stockwork-tectonics model suggests. The boundary between the Chauga belt (non-migmatitic belt) and the Inner Piedmont was originally thought to be a fault (Hatcher, 1969; Griffin, 1971). Hatcher (1972) recognized that it was a metamorphic gradient involving an antiform synform pair, rather than a tectonic boundary or

detachment zone, but more recently realized that it in part faulted, as indicated by Nelson *et al.* (1998).

In the Columbus Promontory, Davis (1993) recognized a change in displacement direction within the western Inner Piedmont from W-directed in the core of the Inner Piedmont to SW-directed in the western Inner Piedmont. The variations in structural orientations could be the result of polyphase deformation, partitioning of deformation during a single event, or ductile flow. The progressive change of orientations and similar metamorphic assemblages and textures across the western Inner Piedmont suggest that the structures formed from a single deformation event during amphibolite facies metamorphic conditions (Davis, 1993). Davis (1993) argued that the E-W and NE-SW structures resulted from orogen-oblique to orogen-normal displacement in the central Inner Piedmont that became orogen-parallel in the Brevard fault zone and the Chauga belt. The pervasive nature of S_2 and its control on D_2 and D_3 structures in the western Inner Piedmont suggests that the western Inner Piedmont represents a crustal-scale shear zone (Davis, 1993). "The S_2 mylonitic foliation was the common decollement that linked SW-directed transcurrent movement along the primordial Brevard fault zone with E-W contractional movement of Inner Piedmont thrust sheets" (Davis, 1993). Hatcher (1998) expanded on this crustal flow model by recognizing the NW-directed transport in the eastern Inner Piedmont in addition to W- and SW-directed transport in the central and western Inner Piedmont. Oblique collision and buttressing of the ductile Inner Piedmont against the primordial Brevard fault zone caused this change in transport direction (Davis, 1993; Hatcher, 1998; Hill, 1999)

Hill (1999) proposed that a two-stage oblique collisional event during the Acadian orogeny produced the map patterns and kinematic indicators in the Inner Piedmont of North Carolina. Mineral stretching lineations and significant ductile extension subparallel to cylindrical and sheath fold axes and the orogen length in the footwall are associated with first-phase structures, while the second phase starts with underthrusting towards the foreland (Ellis and

Watkinson, 1987). "First-phase structures develop parallel to the orogen and later deformation in the hanging wall reflects isostatically driven emergence normal to the orogen" (Hill, 1999). First -phase structures in the study area include mineral stretching lineations, sheath fold axes, and isoclinal folds, all part of D_2. The stack of westward-vergent thrust sheets (D_{2b} and D_3) characteristic of the Inner Piedmont in both South Carolina and North Carolina can be thought of as the imbricating blocks of the Ellis and Watkinson (1987) model. The map pattern in the eastern portion of the study area is complicated and disharmonic (Plate 5), indicative of progressively disharmonic deformation of the hanging wall during the second phase.

The detailed geologic map compiled in this study illustrates map patterns that support portions of the above tectonic models. The Mill Spring and Brindle Creek thrust sheets resemble nappes similar to the Walhalla nappe and Six Mile nappe recognized by Griffin (1974) in South Carolina, but Griffin (1974) failed to recognize multiple deformational episodes. The lineation trend (NE-SW, E-W, and NW-SE) and sheath fold axes support Davis' (1993) and Hatcher's (1998) crustal flow model for the Inner Piedmont. Evidence of disharmonic deformation in the hanging wall of the Brindle Creek thrust support Hill's (1999) two-stage oblique collisional event.

Macroscopic evidence of a polyphase deformation includes the truncation of F_1 and F_2 folds by the Sugarloaf Mountain thrust, the Mill Spring thrust, and the Brindle Creek thrust. Mineral stretching lineations and sheath fold axes support a crustal flow model (Davis, 1993; Hatcher, 1998), whereas map patterns provide additional support for Hill's (1999) two-stage oblique collisional model. Therefore, this portion of the Inner Piedmont experienced a polyphase deformational history that included crustal flow during oblique collision.

CHAPTER 6

CONCLUSIONS

This thesis and compilation of other data completes a transverse from the Brevard fault zone across most of the Inner Piedmont in North Carolina.

1. A portion of the stratigraphic sequence (the middle and upper members of the Tallulah Falls Formation) found in the western Inner Piedmont is recognized in the study area and extends into the southeastern Inner Piedmont. The middle aluminous schist member of the Tallulah Falls Formation thickens dramatically in the central Inner Piedmont.

2. The Walker Top orthogneiss is granitic to granodioritic in composition and is present as isolated pods in the northwestern portion of the study area. Disseminated pods of the Toluca Granite occur throughout the study area and are concordant with regional structures.

3. Crystallization ages, preliminary U-Pb zircon ages, mineral assemblages, petrographic textures, garnet chemical zoning profiles, and temperature and pressure estimates from rocks in and around the study area suggest a single prograde metamorphic event that occurred as a result of the Acadian orogeny. Metamorphic conditions estimated from electron microprobe data range from 610 to 645 °C and from 3.5 ± 0.8 to 5.8 ± 0.8 kbar.

4. Five deformational events are recognized in the Inner Piedmont of North Carolina. D_1 folds and foliation are attributed to the Taconic orogeny. D_2 foliation, lineations, tight to isoclinal, reclined to recumbent folds, sheath folds, and Type-F thrust faults represent the early part of the Acadian orogenic event. D_3 folds and Type-C thrust faults probably constitute the latter portion

of ductile Acadian deformation. D_4 open folds are brittle structures resulting from the Alleghanian orogeny. D_5 fractures are a result of Mesozoic uplift and extension.

5. Due to differences in lithology, map patterns, and isotopic data, the Brindle Creek thrust may represent a terrane boundary. Support of this hypothesis requires further structural, petrologic, and geochemical study.

REFERENCES CITED

Berman, B. R., 1990, Mixing properties of Ca-Mg-Fe-Mn garnets: American Mineralogist, v.75, p. 328-344.

Bream, B. R., 1999, Structural and stratigraphic relationships of ortho- and paragneisses southwest of Marion, North Carolina [unpublished M.S. thesis]: Knoxville, University of Tennessee, 155 p.

Bream, B. R., Hatcher, R. D., Jr., Miller, C. G., and Fullagar, P. D., 2001, Geochemistry and provenance of Inner Pidmont paragneisses, NC and SC: Evidence for an internal terrane boundary: Geological Society of America Abstracts with Programs, v. 33, no. 2, p. A65.

Butler, J. R., 1991, Metamorphism, *in* Horton, J. W., Jr., and Zullo, V. A., eds., The geology of the Carolinas, Carolina Geological Society Fiftieth Anniversary Volume: Knoxville, University of Tennessee Press, p. 127-142.

Carrigan, C. W., Bream, B. R., Miller, C. G., and Hatcher, R. D., Jr., 2001, Ion microprobe analysis of zircon rims from the eastern Blue Ridge and Inner Piedmont, NC-SC-GA: Implications for the timing of Paleozoic metamorphism in the southern Appalachians: Geological Society of America Abstracts with Programs, v. 33, no. 2, p. A7.

Chatterjee, N. D., and Johannes, W., 1974, Thermal stability and standard thermodynamic properties of synthetic 2M1 muscovite, $KAl_2AlSi_3O_{10}(OH)_2$: Contributions to Mineralogy and Petrology, v. 48, p. 89-114.

Conley, J. F., and Drummond, K. M., 1975, The geology of Polk County, North Carolina: North Carolina Geological Survey unpublished map, scale 1:125,000.

Curl, D. C., 1998, Stratigraphy and structure of Wellford and Reidville quadrangles in part of the eastern Inner Piedmont, near Spartanburg, South Carolina [unpublished M.S. thesis]: Knoxville, University of Tennessee, 129 p.

Davis, T. L., 1993, Lithostratigraphy, structure, and metamorphism of a crystalline thrust terrane, western Inner Piedmont, North Carolina [unpublished Ph.D. dissertation]: Knoxville, University of Tennessee, 245 p.

Davis, T. L., Hatcher, R. D., Jr., Liu, A., and Tabor, J. R., 1991, Structural development of a progressively deformed crustal-scale shear zone, southern Appalachian Inner Piedmont, U. S. A.: The geometry of deformed rocks: Geological Society of America Abstracts with Programs, v. 23, p. A138.

Dennis, A. J., and Wright, J. E., 1997, Middle and late Paleozoic monazite U-Pb ages, Inner Piedmont, South Carolina: Geological Society of America Abstracts with Programs, v. 29, no. 3, p. 12.

Ellis, M., and Watkinson, A. J., 1987, Orogen-parallel extension and oblique tectonics: The relation between stretching lineations and relative plate motions: Geology, v. 15, p. 1022-1026.

Ferry, J. M., and Spear, F. S., 1978, Experimental calibration of Fe and Mg partitioning between biotite and garnet: Contributions to Mineralogy and Petrology, v. 66, p. 113-117.

Garihan, J. E., Preddy, M. S., and Ranson, W. A., 1993, Summary of Mid-Mesozoic brittle faulting in the Inner Piedmont and nearby Charlotte belt of the Carolinas, *in* Hatcher, R. D., Jr., and Davis, T. L., eds., Studies of the Inner Piedmont geology with a focus on the Columbus Promontory: Carolina Geological Society Guidebook, p. 55–65.

Ghent, E. D., and Stout, M. Z., 1981, Geobarometry and geothermometry of plagioclase-biotite-garnet-muscovite assemblages: Contributions to Mineralogy and Petrology, v. 76, p. 92-97.

Giorgis, S. D., 1999, Geology of the northwestern South Mountains near Morganton, North Carolina [unpublished M.S. thesis]: Knoxville, University of Tennessee, 186 p.

Goldsmith, R., Milton, D. J., and Horton, J. W., Jr., 1988, Geology of the Charlotte 1° x 2° quadrangle, North Carolina and South Carolina: U.S. Geological Survey Map I–1251–E, scale 1:250,000.

Griffin, V. S., Jr., 1971, The Inner Piedmont belt of the southern crystalline Appalachians: Geological Society of America Bulletin, v. 82, p. 1885-1898.

Griffin, V. S., Jr., 1974, Analysis of the Piedmont in northwest South Carolina: Geological Society of America Bulletin, v. 85, p. 1123-1138.

Griffitts, W. C., and Overstreet, W. C., 1952, Granitic rocks of the western Carolina Piedmont: American Journal of Science, v. 250, p. 777-789.

Griffitts, W. C. and Overstreet, W. C., 1962, Preliminary geologic map of the southeast quarter of the Shelby quadrangle, Cleveland County, North Carolina, Field Studies Map MF 250, scale 1:24,000.

Griffitts, W. C., Yates, R. G., Overstreet, W. C., 1962, Preliminary geologic map of the southwest quarter of the Shelby quadrangle, Cleveland and Rutherford Counties, North Carolina, Field Studies Map MF 252, scale 1:24,000.

Haller, J., 1956, Problee der tiefentectonik: Bauformen in Migmatit-Stockwerk der ostgronlandischen Kaledoniden: Geologische Rundschau, v. 45, p. 159-167.

Harper, S. B., and Fullagar, P. D., 1981, Rb-Sr ages of granitic gneisses of the Inner Piedmont belt of northwestern North Carolina and southwestern South Carolina: Geological Society of America Bulletin, v. 92, p. 864-872.

Hatcher, R. D., Jr., 1969, Stratigraphy, petrology, and structure of the low rank belt and part of the Blue Ridge of northwesternmost South Carolina: South Carolina Division of Geology, Geologic Notes, v. 13, p. 105-141.

Hatcher, R. D., Jr., 1970, Stratigraphy of the Brevard zone and Poor Mountain area, northwestern South Carolina: Geological Society of America Bulletin, v. 81, p. 933-940.

Hatcher, R. D., Jr., 1971, The geology of Rabun and Habersham Counties, Georgia: A reconnaissance study: Geological Survey of Georgia, Department of Mines, Mining, and Geology Bulletin 83, 48 p.

Hatcher, R. D., Jr., 1972, Developmental model for the southern Appalachians: Geological Society of America Bulletin, v. 83, p. 2735-2760.

Hatcher, R. D., Jr., 1978, Tectonics of the western Piedmont and Blue Ridge: Review and speculation: American Journal of Science, v. 278, p. 276-304.

Hatcher, R. D., Jr., 1987, Tectonics of the southern and cen tral Appalachian internides: Annual Review Earth Planetary Science, v. 15, p. 337-362.

Hatcher, R. D., Jr., 1989, Tectonic synthesis of the U.S. Appalachians, Chapter 14, *in* Hatcher, R. D., Jr., Thomas, W. A., and Viele, G. W., eds., The Appalachian–Ouachita orogen in the United States: Boulder, Colorado, Geological Society of America, The Geology of North America, v. F–2, p. 511–535.

Hatcher, R. D., Jr., 1993, Perspective on the tectonics of the Inner Piedmont, southern Appalachians, *in* Hatcher, R. D., Jr., and Davis, T. L., eds., Studies of Inner Piedmont geology with a focus on the Columbus Promontory: Carolina Geological Society Guidebook (North Carolina Geological Survey), p. 1-16.

Hatcher, R. D., Jr., 1998, Structure of the Appalachian Inner Piedmont: Geological Society of America Abstracts with Programs, v. 30, p. 17.

Hatcher, R. D., Jr. and Goldberg, S. A., 1991, Blue Ridge geologic province, *in* Horton, J. W., Jr., and Zullo, V. A., eds., The Geology of the Carolinas, Carolina Geological Society Fiftieth Anniversary Volume: Knoxville, University of Tennesssee Press, p. 11-35.

Hatcher, R. D., Jr., Osberg, P. H., Drake, A. A., Jr., Robinson, P., and Thomas, W. A., 1990, Tectonic map of U.S. Appalachians, *in* Hatcher, R. D., Jr., Thomas, W. A., and Viele, G. W., eds., The Appalachian-Ouachita orogen in the United States: Boulder, Colorado, Geological Society of America, The Geology of North America, v. F-2, Plate 1, scale 1:2,000,000.

Hatcher, R. D., Jr., and Hooper, R. J., 1992, Evolution of crystalline thrust sheets in the internal parts of mountain chains, *in* McClay, K. R., ed., Thrust tectonics: London, Chapman and Hall, p. 217–234.

Hatcher, R. D., Jr., Bream, B. R., Hill, J. C., Giorgis, S. D., and Williams, S. T., 1999, Transect through the Acadian orogen in the Carolinas and NE Georgia: Geological Society of America Abstracts with Programs, v. 31, p. A-19.

Hill, J. C., 1999, Stratigraphy, structure, and tectonics of part of the southern Appalachian Inner Piedmont, near Marion, North Carolina [unpublished M.S. thesis]: Knoxville, University of Tennessee, 188 p.

Holdaway, M. J., 1971, Stability of andalusite and the aluminum silicate phase diagram: American Journal of Science, v. 271, p. 97-131.

Hopson, J. L., and Hatcher, R. D., Jr., 1988, Structural and stratigraphic setting of the Alto allochthon, northeast Georgia: Geological Society of America Bulletin, v. 100, p. 339-350.

Keith, A., and Sterrett, D. B., 1931, Description of the Gaffney and Kings Mountain quadrangles, S. C.-N. C.: U. S. Geological Survey Folio 222, 18 p.

Kish, S. A., 1983, A geochronological study of deformation and metamorphism in the Blue Ridge and Piedmont of the Carolinas [unpublished Ph.D. dissertation]: Chapel Hill, University of North Carolina, 220 p.

Koziol, A. M., 1995, Recalibration of the garnet-plagioclase-Al_2SiO_5-quartz (GASP) geobarometer and applications for natural parageneses: EOS, v. 70, p. 493.

Lemmon, R. E., 1973, Geology of the Bat Cave and Fruitland quadrangles and the origin of the Henderson Gneiss, western North Carolina [unpublished Ph.D. dissertation]: Chapel Hill, University of North Carolina, 145 p.

Lemmon, R. E., 1982, Evidence for an Acadian tectonic event in the western Inner Piedmont, North Carolina: Geological Society of America Abstracts with Programs, v. 14, p. 34.

McSween, H. Y., Speer, J. A., and Fullagar, P. D., 1991, Plutonic rocks, *in* Horton, J. W., Jr., and Zullo, V. A., eds., The geology of the Carolinas: Carolina Geological Society 50th anniversary volume: Knoxville, University of Tennessee Press, p. 109-126.

Mirante, D. C. and Patino-Douce, Melting and migmatization in the southern Appalachian Inner Piedmont of northwest Georgia: The Athens Gneiss, Geological Society of America Abstracts with Programs, v. 32, p. A297.

Nelson, A. E., Horton, J. W., Jr., and Clarke, J. W., 1998, Geologic map of the Greenville 1° x 2° quadrangle, Georgia, South Carolina, and North Carolina: U.S. Geological Survey Miscellaneous Investigations Series Map I–2175, scale 1:250,000.

Odom, A. L., and Fullagar, P. D., 1973, Geochronological and tectonic relationship between the Inner Piedmont, Brevard zone, and Blue Ridge belts, North Carolina, American Journal of Science, v. 273-A, p. 143-149.

Odom, A. L., and Russell, G. S., 1975, The timing of regional metamorphism of the Inner Piedmont, N. C., and Smith River allochthon: Inference from whole-rock ages: Geological Society of America Abstracts with Programs, v. 7, , p. 522-523.

Overstreet, W. C., Whitlow, J.W., White, A. W., and Griffits, W. R., 1963a, Geologic map of the southern part of the Casar quadrangle, Cleveland, Lincoln, and Burke Counties, North Carolina: United States Geological Survey Field Studies Map MF-252, scale 1:24,000.

Overstreet, W. C., Yates, R. G., Griffits, W. R., 1963b, Geologic map of the Shelby 15-minute quadrangle, North Carolina: United States Geological Survey Miscellaneous Geologic Investigations Map 1-384, scale 1:62,500.

Passchier, C. W., and Trouw, R. A. J., 1996, Microtectonics: Springer, Berlin, 289 p.

Pearce, J. A., Harris, N. B., and Tindle, A. G., 1984, Trace element discrimination diagrams for the tectonic interpretation of granitic rocks: Journal of Petrology, v. 25, p. 956-983.

Raymond, L. A., 1995, Petrology: The study of igneous, sedimentary, and metamorphic rocks: Dubuque, W. C. Brown, 742 p.

Reed, J. C. Jr., and Bryant, B., 1964, Evidence for strike-slip faulting along the Brevard zone in North Carolina: Geological Society of America Bulletin, v. 75, p. 1177-1195.

Roper, P. J., and Dunn, D. E., 1973, Superposed deformation and polymetamorphism, Brevard zone, South Carolina: Geological Society of America Bulletin, v. 84, p. 3373-3386.

Shufflebarger, T. E., 1961, Notes on relationships of Piedmont sedimentary rocks with emphasis on the Poor Mountain-Chauga River area, Oconee County, South Carolina: South Carolina Division of Geology, Geologic Notes, v. 5, p. 31-38.

Sinha, A. K., Hund, E. A., and Hogan, J. P., 1989, Paleozoic accretionary history of the North American plate margin (central and southern Appalachians): Constraints from the age, origin, and distribution of granitic rocks, *in* Hillhouse, J., ed., Deep structure and past kinematics of accreted terranes: American Geophysical Union Monograph Series, p. 219-238.

Sobolev, V. N., McCammon, C. A., Taylor, L. A., Snyder, G. A., and Sobolev, N. V., 1999, Precise Mossbauer millliprobe determination of ferric iron in rock-forming minerals and limitations of electron microprobe analysis: American Mineralogist, v. 84, p. 78-85.

Snipes, D. S., 1980, Ground water in the Piedmont of northwestern South Carolina: Geological Society of America Programs, v. 12, no. 4, p. 209.

Snipes, D. S., 1981, Fracture zones in metamorphic and igneous rocks in northwestern South Carolina: Geological Society of America Abstracts with Programs, v.13, no. 1, p. 35.

Spear, F. S., 1993, Metamorphic phase equilibria and pressure-temperature-time paths: Mineralogical Society of America Monograph Series: Book Crafters, Inc., 799 p.

Streckeisen, A. L., 1976, To each plutonic rock its proper name: Earth Science Reviews, v. 12, p. 1-33.

Thompson, A. B., 1982, Dehydration melting of pelitic rocks and the generations of H_2O undersaturated liquids: American Journal of Science, v. 282, p. 1567-1595.

Van der Plas, L., and Tobi, A. C., 1965, A chart for judging the reliability of point counting results: American Journal of Science, v. 263, p. 87-90.

Verseput, T. D., 1980, Structure of the South Mountain State Park area, Burke County, North Carolina [unpublished M.S. theisis]: Carbondale, Southern Illinois University, 61 p.

Vinson, S. B., 1999, Ion probe geochronology of granitoid gneisses of the Inner Piedmont, North Carolina and South Carolina [unpublished M.S. thesis]: Nashville, Tennessee, Vanderbilt University, 84 p.

Wegmann, C. E., 1935, Zur Deutung der Migmatite: Geologische Rundschau, v. 26, p. 303-350.

Werner, C. D., 1987, Saxonian granulites–Igneous or lithogenous. A contribution to the geochemical diagnosis of the original rocks in high-metamorphic complexes, *in* Gerstenberger, H., ed., Contributions to the geology of the Saxonian granulite massif: Leipzig, Akademie der Wissenschaften der DDR Zentralinstitut für Isotopen- und Strahlenforschung, p. 221-250.

Whisnant, J. S., 1975, Geology of the southeast quarter of the Marion 15-minute quadrangle, North Carolina [unpublished M.S. thesis]: Chapel Hill, University of North Carolina, 50 p.

Whitten, E. H. T., 1966, Structural geology of folded rocks: Rand McNally and Company, Chicago, 663 p.

Williams, S. T., 2000, Geology, structure, and migmatization in the Inner Piedmont near Morganton, North Carolina [unpublished M.S. thesis]: Knoxville, University of Tennessee,
111 p.

Yanagihara, G. M., 1994, Structure, stratigraphy, and metamorphism of a part of the Columbus Promontory, western Inner Piedmont, North Carolina [unpublished M.S. thesis]: Knoxville, University of Tennessee, 214 p.

Yates, R. G., 1963, Preliminary geologic map of the northwest quarter of the Shelby quadrangle, Cleveland and Rutherford Counties, North Carolina: United States Geological Survey Field Studies Map MF 258, scale 1:24,000.

Yates, R. G. and Overstreet, W. C., 1962, Preliminary geolgogic map of the northeast quarter of the Shelby quadrangle, Cleveland County, North Carolina: United States Geological Survey Field Studies Map MF 249, scale 1:24,000.

APPENDICES

APPENDIX A

MODAL ANALYSES: METHODOLOGY

Rock samples from each unit were collected along traverses in the field. Samples chosen for thin sections were cut perpendicular to the foliation and dominant lineation (where present). Thin sections were made by Spectrum Petrographics, Incorporated.

Major minerals in the Tallulah Falls Formation (metagraywacke-schist and sillimanite schist) and the Toluca Granite range from 0.2 to 4 mm. Step sizes were chosen to be half (0.1 mm) of the smallest grain size (0.2 mm). The steps were taken perpendicular to foliation. Over 2000 counts were done for each section, which covered half of a 270 x 460 mm section. The error is less than 2.2 percent for plagioclase, quartz, biotite, sillimanite, garnet, microcline, tourmaline, and kyanite (Fig. A-1; Van der Plas and Tobi, 1965).

The Walker Top orthogneiss is a megacrystic granite to granodiorite. The microcline megacrysts range from 3-5 mm, while the majority of minerals in the matrix are between 0.5 and 1.5 mm. The point counting method of modal analyses had to be modified to accommodate the bimodal grain size of the Walker Top orthogneiss. First, the percentage of megacrysts of each sample was determined. Slabs (8-20 cm long by 5-10 cm wide) were scanned. Outlines of the entire slab and the megacrysts were traced in Adobe Illustrator 8.0. CAD Tools were used to determine area of the relative proportions of megacrysts to matrix. The matrix was then point counted using 0.1 mm steps (over 2000) perpendicular to foliation.

Grain sizes of zircon, apatite, monazite, and opaque minerals were less than 0.2 mm; therefore, the point counting methodology used in this study did not favor accurate modes of these trace minerals.

The Michel-Levy method was used to determine anorthite content of plagioclase grains.

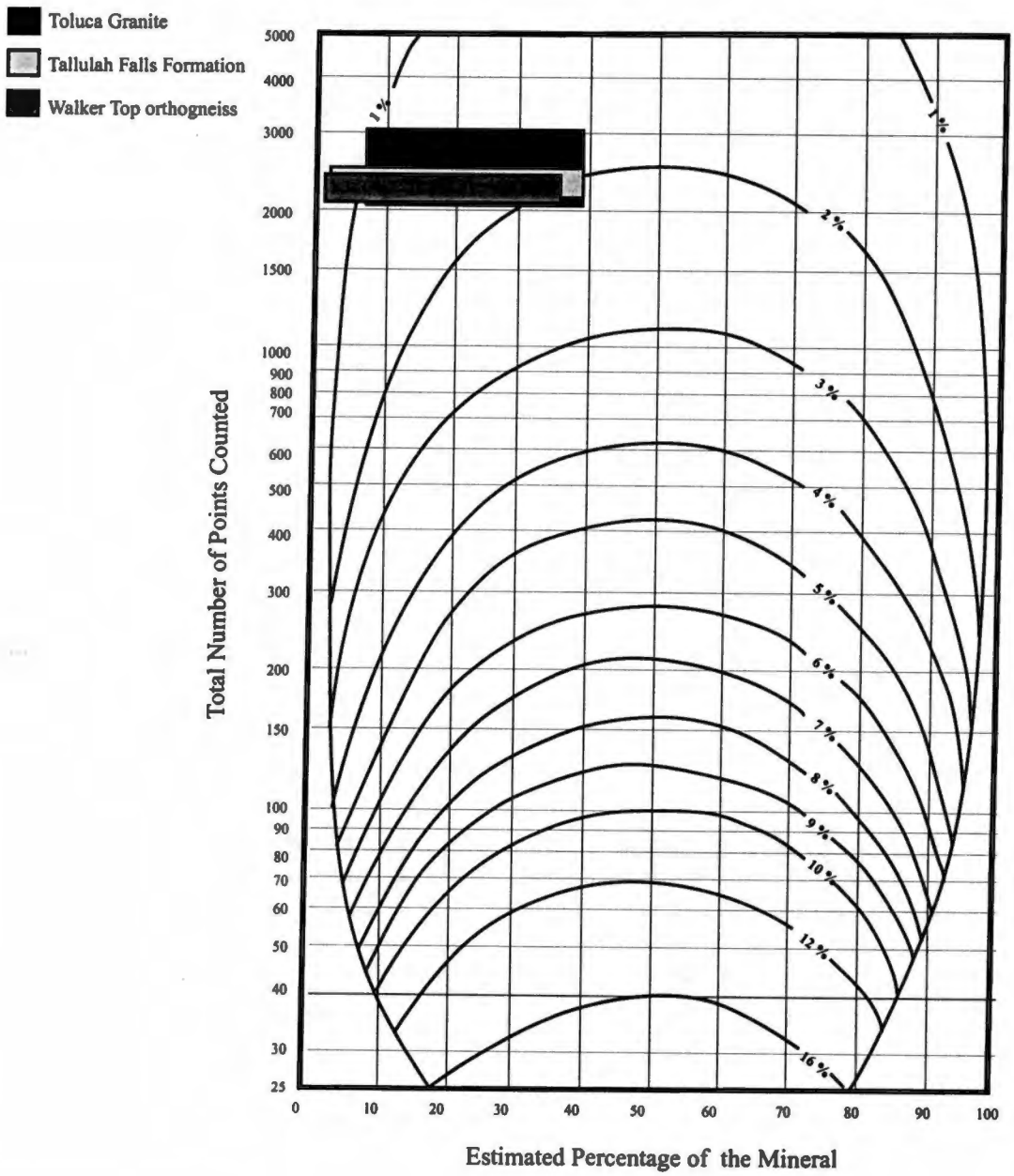


Figure A-1. Chart for judging the reliability of point-counting results (modified from Van der Plas and Tobi, 1965). The curves represent 2σ. Shaded areas represent the range of error for the major minerals of the Toluca Granite, the Tallulah Falls Formation, and the Walker Top gneiss (Tables 2-1, 2-2, and 2-4).

APPENDIX B

XRF ANALYSES:

METHODOLOGY AND ACCURACY AND PRECISION OF RESULTS

METHODOLOGY

NOTE: The following is a summary of the methods used in this study to prepare and analyze pellets (briquettes) on the energy-dispersive EG&G ORTEC TEFA III at the University of Tennessee–Knoxville (modified from Bream, 1999). These instructions are not intended as a replacement for the direct instruction on the equipment involved in the process. Most of the steps in this process are taken directly from the instructions provided in the geochemical analysis course offered at UTK.

Samples were selected for analysis based on their representative nature and the absence of weathering or alteration.

1. Crush the material into pea-sized particles (approximately 3 to 4 mm in diameter). The amount of material that needs to be crushed depends on the grain size and homogeneity of the sample (coarse and/or inhomogeneous material requires a larger volume).

   The method employed in this study involved cutting the rocks into thin (1.5 cm) slabs. The slabs were then broken into small (3-4 mm in diameter) pieces.

2. Grind material into a fine-grained powder.

   A tungsten carbide grinding mill was used in this study. Grinding mills made of ceramic, steel, and other materials are also available.

   a) Dry the sample at 110 °C for at least one hour. Make sure the grinding mill is clean and dry.

   b) Load the sample material into the case assembly, putting approximately half of the material between the disk and outer wall and half between the puck and disk.

   c) Add about three drops of freon to the material and replace grinding mill, O-ring, and lid.

d) Lower shatterbox arm and tighten locking mechanism (a rubber band can be placed around the lock and arm to prevent slipping).

e) Lower shatterbox cover.

f) Turn switch to "on" position and push timer button. The timer should be set for three minutes. After the first three minutes, check inside and tighten the arm if necessary, and repeat.

g) When timer is finished remove grinding mill and place on clean surface.

h) Contents of the grinding mill should be brushed away (using the paint brush for your rock type) and collected (computer or photocopy paper works fine as a collection surface).

i) Dry the material again at 110 °C for at least 1 hour.

j) Clean the grinding mill assembly with hot water and scouring pads, making sure not to use soap. If a residue remains, run quartz sand through the mill and repeat cleaning. The mill must be completely dry before another sample can be run.

3. Make a pressed powder pellet.

Two pellets were made for each sample in this study.

a) Place the base of the pellet die with the lower die plate (polished surface up) on a flat surface and carefully lower the top of the base plate over both.

b) Insert the sample-forming cylinder.

c) Place half of the sample material (~5 grams) into the cylinder, insert the packing piston, and compress the sample with hand pressure.

d) Carefully raise the sample forming cylinder and packing piston.

e) Make sure the sample material is intact and centered. Place 5 grams (~a plastic spoonful) of boric acid on top of the sample.

f) Place the upper die plate into the housing.

g) Place the pressure piston into the housing above the die plate.

h) Place the entire housing assembly into the hydraulic press.

i) Take the press pressure to 10,000 psi for 30 seconds then raise the pressure to 30,000 psi for one minute.

j) Release the pressure, insert the extractor spacer, and invert the assembly within the press.

k) Apply moderate pressure with the press while holding the assembly with your hand so the housing does not drop.

l) Carefully remove the pellet from the assembly, label, and place in a desiccator.

m) Clean all parts with warm water. Avoid scratching or denting the polished surfaces. All parts must be completely dry before the next pellet is pressed.

4. Run samples on XRF machine with appropriate protocol. The machine used in this study was replaced prior to the completion of this thesis.

   The SIAL protocol was recalibrated and used for all samples in this study. All samples were run four or more times.

PRECISION AND ACCURACY OF ANALYSES

The SIAL protocol was used due to the high silica and aluminum contents of both the Walker Top orthogneiss and the Toluca Granite. Table B-1 lists the standards used for the SIAL

protocol; and the range of values, interelement corrections, standards dropped, and the standard error of calibration (SEC) for each of the elements analyzed. The standard error of calibration represents the precision of the machine based on the difference between the certificate value and the value measured. The conditions used in the SIAL protocol are presented in Table B-2.

In Tables B-3 and B-4, analyses of Toluca Granite and Walker Top orthogneiss samples (respectively) are presented, as well as the standard deviation and the standard error of calibration (SEC). The only major minerals whose standard deviations are greater than the error of the machine are MnO, Al_2O_3, and SiO_2, and P_2O_5. Trace minerals with standard deviations greater than the error of the machine include Nb, Rb, Sr, and Zr.Analyses of standards and the standard deviations are presented in Table B-5. The certificate values of the standard are listed to determine accuracy of the machine. The lack of accuracy may be due to the age of the machine, the age of the standards, as well as the standard errors of calibration.

Analyses totals using the SIAL protocol were over 100 percent (Tables B-3 and B-4). The total standard error of calibration for all elements analyzed is 2.07 percent. Recognizing that error, the values were still high, especially considering the amount of volatiles that were not analyzed. The high totals are likely due to the poor quality of the standards and the age of the machine.

In order to determine the amount of volatiles, loss on ignition was determined. A sample from the type locality of the Toluca Granite was sent to Actlabs for analysis. Loss on ignition was reported to be 0.26 percent.

A representative samples of both the Walker Top orthogneiss and the Toluca granite were crushed to a powder (using the methodology described previously). The samples were weighed in porcelain crucibles using an analytical balance. The samples in the porcelain crucibles were heated to 1000 °C for 45 minutes. They were then allowed to cool for 1-2 hours and weighed again. The difference in weights was divided by the weight before heating and multiplied by 100

Table B-1. SIAL protocol used for bulk chemical analyses.

SIAL PROTOCOL

Recalibrated February 2000

The following standards were used to recalibrate the SIAL protocol.

BCS395	Potash Feldspar	SARM2	Syenite
BCS376a*	Bauxite	SDC1	Mica schist
BCR1	Basalt	SI	Silica
FK	Feldspathic Sandstone	SO1	Soil
G2	Granite	SO2	Soil
GNA	Griesen	SO4	Soil
GSP1	Granodiorite	SRM97B	Flint Clay
RGM1	Rhyolite	SRM99A	Soda Feldspar
SARM1	Granite	TB	Slate

*not recommended for use as unknown

Element/ Oxide	Range	SEC	Corrected for:	Standards used (no.)	Standards dropped
Na_2O	0.066-6.20	0.22	MgO, SiO_2, CaO, Fe_2O_3, K_2O, Al_2O_3	17	
MgO	0.020-3.83	0.19	Na_2O, SiO_2, CaO, Fe_2O_3, K_2O, Al_2O_3	16	SDC1
Al_2O_3	6.18-52.4	0.46	MgO, SiO_2, CaO, Fe_2O_3, K_2O, Na_2O	15	GNA, SDC1
SiO_2	1.24-99.995	0.57	Na_2O, MgO, CaO, Fe_2O_3, K_2O	13	SDC1, G2, SRM99A, BCS376a, SRM97B
P_2O_5	0.01-0.69	0.0300	MgO, SiO_2, CaO, Na_2O, K_2O	15	
S	0.01-0.07	0.0057	SiO_2, CaO, Fe_2O_3, Al_2O_3	11	TB
K_2O	0.620-15.4	0.13	MgO, SiO_2, CaO, Na_2O, Al_2O_3	12	SDC1, FK, BCS376. RGM1
CaO	0.034-6.92	0.12	SiO_2, MgO, Fe_2O_3, K_2O	17	
Cu	0.0005-0.0061	0.0013	Co, Ni, Zn	14	
TiO_2	0.0100-2.39	0.0674	CaO, Fe_2O_3, MgO	16	
V	0.0002-0.0399	0.0032	CaO, TiO_2, Cr	13	
Cr	0.0004-0.0230	0.0037	Fe_2O_3, V, SiO_2	14	
MnO	0.0020-0.1800	0.0242	CaO, Fe_2O_3, Cr, Ni	15	
Fe_2O_3	0.0650-13.4	0.22	MnO, TiO_2, Cr, Ni	16	BCS395
Co	0.0007-0.0038	0.0006	Fe_2O_3	14	
Ni	0.0004-0.0094	0.0012	Fe_2O_3, MgO	13	
Zn	0.0005-0.00145	0.0021	SiO_2, Fe_2O_3, Ni, Cu	15	
Pb	0.0005-0.0061	0.0011	Cu, Zn	14	
Rb	0.0033-0.2000	0.0016	CaO, K_2O	14	SARM2
Sr	0.0010-0.0480	0.0021	Fe_2O_3, Rb	15	
Y	0.0011-0.0145	0.001	Rb, Sr, Zr	13	
Zr	0.0033-0.0790	0.0044	Sr, Nb, Y, Mo	14	
Nb	0.0004-0.0090	0.0002	Zr, Fe_2O_3, Nb	11	
Mo	0.0001-0.0100	0.001	Zr, Nb	8	
Ba	0.0047-0.2400	0.0159	CaO, K_2O	16	

Recalibration performed by S. Bier, B. Bream, and O. Kopp.

Table B-2. SIAL conditions of X-ray fluorescence.
Instrument used: EG&G ORTEC X-ray fluorescence spectrometer with an energy dispersive SiLi detector (EDS)

	1	2	3	4
Elements analyzed:	Na, Mg, Al, Si, P, S, K, Ca, Cu	Ti, V, Cr, Mn, Fe, Co, Ni, Zn	Pb, Rb, Sr, Y, Zr, Nb, Mo	Ba
Spectral region of interest (kV):	0.97-8.15	4.37-8.74	10.40-17.65	31.90-32.36
Accelerating voltage (kV):	10	35	45	45
Current (nA):	150	125	150	175
Counting time (sec):	400	400	400	400
Filter:	Open	Copper	Indium	Indium
Anode:	Rh	W	W	W

Table B-3. XRF analyses of the Toluca Granite. The number in parentheses represents 1σ of the least digit cited.

Sample number	BK 238	BK 372	BK 431	BK 529	BK 955	BK 1052	BK 1079	BK 1357	BK 1365	CA 40	CA 63	CA-ARI	SEC
Number of replicate analyses	9	9	9	9	4	4	4	4	4	4	4	4	
Oxides-weight percent													
SiO_2	74.4 (8)	69.0 (8)	76.7 (8)	76.3 (8)	74.9 (9)	77.1 (12)	72.3 (9)	77.8 (12)	74.9 (8)	75.7 (8)	70.6 (8)	76.7 (22)	0.57
TiO_2	0.32 (1)	0.49 (1)	0.10 (1)	0.11 (1)	nd	0.03 (2)	0.27 (1)	0.06 (0)	0.08 (1)	0.01 (2)	0.39 (1)	0.12 (1)	0.07
Al_2O_3	14.3 (3)	16.5 (2)	16.4 (3)	15.4 (2)	17.5 (3)	16.4 (2)	15.4 (3)	16.1 (3)	16.9 (3)	15.9 (3)	17.3 (2)	16.4 (3)	0.46
Fe_2O_3	2.08 (3)	3.37 (10)	1.02 (3)	1.00 (2)	0.74 (2)	0.88 (21)	2.38 (3)	1.23 (2)	0.70 (2)	0.88 (1)	2.91 (18)	2.13 (6)	0.22
MnO	0.01 (0)	0.02 (0)	0.01 (0)	0.01 (0)	0.03 (0)	0.01 (0)	0.02 (0)	nd	nd	nd	0.03 (0)	0.02 (0)	0.02
MgO	0.96 (3)	1.82 (3)	0.46 (8)	0.46 (8)	0.23 (12)	0.49 (8)	1.26 (1)	0.49 (6)	0.64 (7)	0.43 (8)	0.86 (7)	0.79 (8)	0.19
CaO	1.21 (0)	2.27 (1)	0.58 (1)	0.91 (1)	0.53 (1)	0.43 (1)	1.32 (0)	0.28 (1)	1.86 (2)	0.57 (6)	0.50 (1)	2.08 (1)	0.12
Na_2O	2.10 (5)	3.32 (10)	3.22 (14)	3.05 (13)	3.50 (9)	2.81 (19)	2.06 (12)	4.03 (8)	3.97 (4)	2.57 (4)	1.49 (9)	3.37 (9)	0.22
K_2O	1.21 (0)	3.82 (7)	5.84 (13)	6.28 (9)	6.06 (10)	5.40 (8)	7.18 (12)	4.43 (7)	4.16 (6)	5.62 (8)	7.63 (1)	3.92 (14)	0.13
P_2O_5	0.01 (0)	0.18 (2)	0.06 (4)	0.10 (3)	0.12 (3)	0.17 (2)	0.20 (0)	0.10 (2)	0.07 (0)	0.19 (1)	0.26 (1)	0.09 (2)	0.03
Oxide-Total	96.6	101	104	104	104	104	102	105	103	102	102	106	
Trace elements-ppm													
Ba	682 (17)	614 (46)	561 (42)	797 (32)	482 (22)	204 (91)	961 (75)	274 (94)	499 (81)	770 (64)	462 (97)	823 (64)	159
Co	5 (0)	6 (0)	3 (0)	3 (0)	26 (0)	3 (0)	5 (0)	3 (0)	3 (0)	3 (0)	5 (0)	4 (0)	6
Cr	nd	15 (2)	nd	nd	64 (6)	nd	nd	nd	nd	nd	12 (5)	nd	37
Cu	nd	11 (3)	3 (0)	2 (4)	3 (6)	nd	2 (2)	nd	nd	nd	6 (10)	nd	13
Mo	5 (1)	5 (1)	8 (1)	10 (1)	9 (1)	12 (1)	6 (0)	9 (1)	8 (3)	12 (0)	5 (0)	6 (1)	10
Nb	9 (0)	11 (1)	8 (0)	11 (0)	4 (1)	15 (1)	9 (0)	16 (2)	7 (1)	13 (0)	14 (0)	7 (1)	2
Ni	8 (2)	19 (2)	6 (2)	3 (2)	3 (2)	3 (2)	8 (1)	3 (1)	5 (3)	1 (2)	12 (7)	5 (1)	12
Pb	31 (2)	26 (2)	45 (3)	39 (3)	89 (5)	37 (4)	32 (2)	42 (3)	35 (2)	40 (3)	39 (4)	28 (1)	11
Rb	155 (3)	217 (3)	166 (1)	197 (2)	215 (3)	297 (4)	255 (3)	130 (3)	130 (2)	376 (3)	346 (3)	142 (5)	16
S	75 (7)	42 (1)	47 (1)	73 (7)	363 (14)	12 (8)	136 (4)	69 (18)	136 (15)	6 (9)	113 (5)	nd (8)	57
Sr	151 (1)	62 (1)	215 (2)	62 (1)	306 (4)	42 (2)	191 (1)	129 (2)	232 (5)	41 (1)	72 (1)	194 (2)	21
V	16 (1)	30 (1)	10 (1)	10 (1)	15 (21)	6 (7)	17 (0)	6 (5)	9 (9)	5 (1)	21 (3)	14 (1)	32
Y	18 (1)	36 (1)	23 (1)	37 (1)	18 (1)	31 (1)	27 (2)	23 (9)	10 (5)	34 (1)	39 (0)	15 (0)	10
Zn	48 (2)	70 (4)	41 (2)	36 (4)	36 (3)	42 (3)	39 (3)	42 (2)	43 (5)	43 (4)	56 (8)	44 (1)	21
Zr	176 (4)	115 (24)	124 (2)	115 (2)	49 (0)	53 (2)	147 (3)	50 (7)	111 (4)	54 (1)	288 (4)	134 (1)	44

nd = not detected

Table B-4. XRF analyses for the Walker Top orthogneiss. The number in parentheses represents 1σ of the least digit cited.

Sample number Number of replicate analyses	BK 501 10	BK 408 10	BK 396 10	BK 409 9	BK 301 9	SEC
Oxides-weight percent						
SiO_2	68.1 (9)	68.7 (7)	70.7 (8)	75.2 (8)	74.2 (9)	0.57
TiO_2	0.56 (0)	0.58 (1)	0.65 (0)	0.21 (1)	0.45 (1)	0.07
Al_2O_3	17.4 (12)	17.0 (3)	15.4 (2)	15.5 (3)	15.3 (2)	0.46
Fe_2O_3	3.57 (1)	3.40 (15)	3.62 (15)	1.35 (4)	2.48 (7)	0.22
MnO	0.03 (0)	0.04 (1)	0.04 (1)	0.01 (0)	0.02 (6)	0.02
MgO	1.36 (1)	1.38 (7)	1.12 (6)	0.77 (7)	1.20 (11)	0.19
CaO	2.31 (0)	2.12 (1)	1.13 (1)	1.11 (1)	1.73 (1)	0.12
Na_2O	3.37 (20)	2.64 (11)	2.42 (9)	2.23 (9)	2.56 (15)	0.22
K_2O	4.17 (10)	4.64 (7)	5.95 (11)	6.84 (10)	4.96 (10)	0.13
P_2O_5	0.17 (0)	0.20 (4)	0.20 (3)	0.13 (4)	0.14 (3)	0.03
Oxide-Total	101	101	101	103	103	
Trace elements-ppm						
Ba	666 (50)	871 (42)	56 (30)	1160 (20)	1147 (36)	159
Co	7 (0)	6 (0)	64 (0)	34 (0)	49 (1)	6
Cr	20 (5)	13 (5)	16 (4)	nd (1)	3 (3)	37
Cu	14 (4)	7 (4)	10 (4)	2 (4)	5 (5)	13
Mo	3 (1)	2 (1)	2 (1)	6 (1)	5 (2)	10
Nb	15 (4)	13 (1)	14 (7)	7 (0)	10 (5)	2
Ni	18 (2)	12 (2)	12 (3)	5 (2)	8 (5)	12
Pb	33 (2)	22 (2)	30 (2)	32 (2)	25 (8)	11
Rb	171 (38)	220 (7)	222 (5)	239 (5)	144 (2)	16
S	74 (11)	25 (11)	82 (7)	72 (12)	53 (9)	57
Sr	197 (36)	177 (13)	117 (2)	171 (2)	201 (3)	21
V	35 (2)	32 (2)	30 (10)	15 (5)	25 (1)	32
Y	27 (1)	21 (1)	41 (3)	22 (9)	15 (1)	10
Zn	79 (5)	56 (2)	55 (3)	32 (2)	49 (3)	21
Zr	300 (17)	334 (8)	360 (10)	362 (53)	202 (4)	44

nd = not detected

Table B-5. XRF analyses and certificate values of standards. The number in parentheses represents 1σ of the least digit cited.

Sample number	GSP-1B		RGM-1A		SRM99A		SARM1		BCS376		SEC
	Calculated Value	Certificate Value	Calculated Value	Certificate Value	Calculated Value	Certificate Value	Calculated Value	Certificate Value	Calculated Value	Certificate Value	
Oxides-weight percent											
SiO_2	68.7 (6)	69.1	74.9 (9)	73.2	58.9 (7)	65.2	75.5 (9)	75.7	63.9 (8)	67.1	0.57
TiO_2	0.65 (1)	0.67	0.26 (1)	0.29	0.09 (1)	0.01	0.05 (1)		nd		0.07
Al_2O_3	15.5 (3)	16.8	14.5 (3)	13.9	22.7 (42)	20.5	12.6 (2)	12.1	18.2 (3)	17.7	0.46
Fe_2O_3	4.33 (16)	5.98	1.76 (5)	1.95	0.04 (3)	0.06	2.03 (4)	2.00	0.06 (0)	0.06	0.22
MnO	0.04 (1)	0.06	0.02 (0)	0.08	nd		0.01 (4)	0.00	nd		0.02
MgO	1.35 (6)	1.50	0.46 (11)		0.12 (12)	0.02	0.09 (7)		0.09 (4)		0.19
CaO	1.79 (0)	1.40	1.16 (1)	1.24	2.14 (9)	2.14	0.78 (1)	0.78	0.72 (1)	0.54	0.12
Na_2O	2.72 (13)	0.43	4.42 (6)	3.92	6.22 (7)	6.2	3.44 (13)	3.36	2.88 (10)	2.83	0.22
K_2O	5.47 (6)	5.07	3.95 (5)	4.21	5.22 (7)	5.2	5.00 (7)	4.99	10.58 (17)	11.2	0.13
P_2O_5	0.28 (3)	0.85	0.10 (1)		0.04 (3)	0.02	0.08 (2)		0.07 (2)	0.05	0.03
Oxide-Total	101	102	102	98.8	95.5	99.4	99.6	98.9	96.5	99.5	
Trace elements-ppm											
Ba	1104 (19)	1163	772 (27)		2583 (65)	2328	293 (26)		433 (22)		159
Co	8 (0)	7	4 (0)		2 (0)		42 (0)		2 (0)		6
Cr	102 (189)	12	5 (2)		20 (2)		nd		nd		37
Cu	26 (2)	46	16 (4)		nd		5 (4)		nd		13
Mo	nd	1	7 (1)		2 (1)		15 (1)		7 (1)		10
Nb	27 (1)	21	12 (1)		nd		54 (1)	53	3 (1)		2
Ni	25 (2)	7	20 (28)		nd		2 (2)		nd		12
Pb	33 (13)	68	31 (11)		46 (3)		38 (3)		54 (2)		11
Rb	254 (3)		171 (2)	154	134 (2)		354 (4)	325	368 (3)	368	16
S	285 (8)		59 (9)		nd		140 (5)		146 (5)		57
Sr	220 (3)	318	102 (1)	116	433 (4)	1523	7 (1)	49	49 (1)	55	21
V	59 (3)	73	18 (1)		14 (1)		12 (1)		4 (0)		32
Y	37 (1)	31	36 (1)		433 (4)		141 (2)	147	37 (1)		10
Zn	88 (2)	89	54 (2)		34 (1)		41 (2)		21 (1)		21
Zr	523 (14)	352	245 (5)	211	59 (1)		257 (11)	300	24 (1)		44

nd = not detected

to determine loss on ignition. The total loss on ignition of the Toluca Granite was 1.74 percent, and the loss on ignition of the Walker Top orthogneiss was 1.11 percent.

APPENDIX C

STRUCTURAL DATA FOR PORTIONS OF THE BENN KNOB AND CASAR QUADRANGLES

NOTE: The letters preceding station numbers refer to the quadrangle in which they were collected. BK - Benn Knob. CA - Casar. Plate 2 contains the locations of the stations.

Station	Foliation		Lineation		Fold Axis		Axial Plane		Fold	Joint	
	Strike	Dip	Trend	Plunge	Trend	Plunge	Strike	Dip	Verg.	Strike	Dip
BK 1	273	16 S									
BK 2	274	18 S									
BK 3	279	16 S									
BK 4	273	24 S									
BK 5	011	20 SE									
BK 6	026	25 SE									
BK 7	022	32 SE									
BK 8	078	04 S									
BK 9										272	80 N
BK 10	022	14 SE									
BK 11	039	19 SE								054	84 SE
BK 12	310	26 SW								271	82 S
BK 13	058	14 SE									
BK 14											
BK 15	011	66 E									
BK 16	359	49 W								029	89 NW
	323	56 SW									
BK 17	272	49 N									
BK 18	321	18 SW								068	66 NW
										306	81 NE
BK 19	304	31 N								059	86 NW
BK 20	049	26 SE									
BK 21	294	06 S									
BK 22	044	25 SE	289	06						041	74 NW
	324	11 NE								303	71 S
										049	82 SE
BK 23	087	06 NW	100	03						026	86 SE
										052	81 NW
BK 24	323	21 NE								054	81 NW
										306	51 SW
BK 25	274	21 NE								356	76 E
BK 26	346	22 NE								271	81 S
BK 27	001	31 E								301	69 S
BK 28	086	26 N									
BK 29	334	28 SW									
BK 30	081	29 SE									
BK 31	308	43 SW									
BK 32	071	14 SE									
BK 33	332	66 SW									
BK 34										063	34 NW
BK 35	337	54 SW									
BK 36	082	38 SE									
BK 37	332	09 SW									
BK 38	318	21 SW									
BK 39	003	13 SE									
BK 40	064	25 SE									
BK 41	286	36 NE	126	21							
BK 42	342	33 NE									
BK 43	358	24 NE									
BK 44	304	24 SW									
BK 45	354	25 W									
BK 46	282	14 SW									
BK 47	297	57 SW									
BK 48	347	49 SW								079	68 NE
BK 49											
BK 50	337	36 SW								256	82 NW
BK 51	326	51 SW								304	75 N
	326	63 SW									
BK 52	347	36 SW								052	67 NE
BK 53	324	22 SW								074	82 NE
	313	39 SW								046	88 SW
BK 54	281	18 S									
BK 55	329	22 SW	028	143						052	85 SE
BK 56	321	28 SW									
BK 57	067	23 SE									
BK 58	084	14 SE								061	71 NW
BK 59	004	21 E								063	74 NW
BK 60	293	25 SW									
BK 61	284	19 S									
BK 62	301	28 SW									
BK 63	284	46 SW									
BK 64	073	36 SE									
BK 65	273	22 S									
BK 66	274	28 S									
BK 67	356	26 W									
BK 68	317	14 SW									

Station	Foliation		Lineation		Fold Axis		Axial Plane		Fold	Joint	
	Strike	Dip	Trend	Plunge	Trend	Plunge	Strike	Dip	Verg.	Strike	Dip
BK 69	318	11 SW									
BK 70	316	24 SW								054	84 NW
BK 71	076	33 SE									
BK 72	358	25 E									
BK 73	320	84 NE									
BK 74	318	72 NE									
BK 75	318	48 NE									
BK 76	291	41 NE									
BK 77	013	14 NW									
BK 78	347	27 SW									
BK 79	293	36 SW									
BK 80	078	09 SE									
BK 81	324	12 SW									
BK 82	352	34 NE									
BK 83	341	26 NE									
BK 84	326	16 NE									
BK 85	317	31 NE									
BK 86	284	16 N									
BK 87	324	30 NE									
BK 88	072	37 SE								076	41 N
BK 89	046	23 SE									
BK 90	313	31 NW									
BK 91	048	17 SE									
BK 92	028	21 SE								274	84 S
	008	22 W									
BK 93	049	28 SE									
BK 94	051	21 SE									
BK 95	058	15 SE									
BK 96	032	14 SE									
BK 97	074	18 SE									
BK 98	322	26 NE									
BK 99	319	17 SW									
BK 100	296	26 SW									
BK 101	280	27 SW									
BK 102	312	26 SW								354	64 W
BK 103	309	24 SW									
BK 104	321	34 NE									
BK 105	319	33 NE									
BK 106	314	13 SW									
BK 107	297	15 SW									
BK 108	352	19 W									
BK 109	033	21 NW									
BK 110	339	16 NE									
BK 111	334	13 SW									
BK 112	296	36 SW									
BK 113	034	24 E									
BK 114	283	24 NE									
BK 115	064	14 SE									
BK 116	058	12 SE									
BK 117	057	27 SE									
BK 118	074	14 NE									
BK 119	066	29 SE									
BK 120	063	28 SE									
BK 121	304	18 NW									
BK 122	008	32 E									
BK 123	073	26 SE									
BK 124	062	16 NW			239	21	056	76 NW	SE		
BK 125	044	30 SE									
BK 126	319	24 NE									
BK 127	323	10 NE									
BK 128	356	16 E									
BK 129	357	18 E									
BK 130	344	08 NE									
BK 131	075	15 NW									
BK 132	314	06 NE								051	88 SE
BK 133	316	16 NE								084	71 S
BK 134	320	14 NE			356	05	354	62 E	E		
BK 135	317	16 NE								057	76 SE
BK 136	325	33 NE								058	76 NE
BK 137	315	25 NE									
BK 138	309	20 NE									
BK 139	334	09 NE								077	74 NW
BK 140	320	25 NE								073	81 SE
BK 141	038	31 NW									
BK 142	062	09 NW								269	84 S
BK 143	284	09 S								014	86 NW

Station	Foliation		Lineation		Fold Axis		Axial Plane		Fold	Joint	
	Strike	Dip	Trend	Plunge	Trend	Plunge	Strike	Dip	Verg.	Strike	Dip
BK 144	298	08 NE									
BK 145	287	07 NE								090	64 S
BK 146	292	16 NE								004	72 W
BK 147	296	07 NE									
BK 148	332	13 NE									
BK 149	335	29 NE									
	084	66 W									
BK 150	332	36 NE									
BK 151	319	09 NE									
BK 152	322	11 NE									
BK 153	346	34 NE									
BK 154	017	26 SE								066	68 NW
BK 155											
BK 156	352	29 SW									
BK 157	314	27 SW									
BK 158	324	62 SW								034	60 SE
	317	25 SW								039	66 SE
BK 159	334	09 NE			330	16	331	26 SW	SW		
BK 160	065	08 NW								035	70 SE
										076	84 SE
BK 161	316	14 NE									
BK 162	038	25 SE									
BK 163	311	42 NE								030	70 NW
BK 164	348	38 W									
BK 165	332	31 SW									
BK 166	328	14 SW									
BK 167	049	22 SE									
BK 168	009	11 E									
	003	13 E									
BK 169	064	33 SE									
BK 170	343	22 NE									
BK 171											
BK 172	326	17 NE									
BK 173	336	22 NE									
BK 174	356	22 NE									
BK 175	354	39 NE									
BK 176	356	07 E									
BK 177	008	29 E									
BK 178	346	30 NE	083	32							
BK 179	309	26 NE								047	71 SE
BK 180	338	33 NE									
BK 181	338	09 NE									
BK 182	304	24 SW									
BK 183	326	31 NE									
BK 184	073	30 NW									
BK 185	303	24 SW									
BK 186	318	10 SW									
	313	10 SW									
BK 187	065	12 NW									
BK 188	068	48 SE									
BK 189											
BK 190	356	14 E									
BK 191	352	25 E									
BK 192	343	34 NE									
BK 193	346	26 NE									
BK 194	343	14 NE									
BK 195	353	26 NE			140	21	323	34 NE			
BK 196	344	14 NE									
BK 197	324	21 NE									
BK 198	353	12 NE									
BK 199	346	23 NE									
BK 200	340	41 NE									
BK 201	321	12 NE									
BK 202	324	10 NE									
BK 203	348	14 NE									
BK 204	328	21 NE									
BK 205	325	30 NE									
BK 206	028	26 SE			021	54	054	084	NW		
BK 207	354	19 NE									
BK 208	324	23 NE									
BK 209	352	17 NE									
BK 210	074	26 SE									
BK 211	078	51 SE									
BK 212	327	74 SW									
BK 213	354	36 SW									
BK 214	064	13 NW									

Station	Foliation		Lineation		Fold Axis		Axial Plane		Fold	Joint	
	Strike	Dip	Trend	Plunge	Trend	Plunge	Strike	Dip	Verg.	Strike	Dip
BK 215	324	50 NE									
BK 216	328	34 NE									
BK 217	016	29 SE									
BK 218	032	07 SE									
BK 219	034	29 SE									
BK 220	329	26 NE									
BK 221	283	10 SW									
BK 222	035	33 SE									
BK 223	052	27 SE									
BK 224	014	11 SE									
BK 225	007	24 SE									
BK 226	003	17 SE									
BK 227	328	21 NE									
BK 228	341	33 SW									
BK 229	344	34 NE								014	72 SE
BK 230	296	20 NE			046	13	313	28 NE	NE		
BK 231	323	27 NE									
BK 232	317	25 NE									
BK 233	317	41 NE								074	090
BK 234	297	14 NE									
BK 235	314	16 NE									
BK 236	284	13 NE									
BK 237	316	20 NE								276	71 NE
BK 238	356	29 E									
BK 239	336	21 NE									
BK 240	348	22 NE								014	61 NW
										074	80 SE
BK 241	341	29 NE								059	75 SE
BK 242	314	32 NE									
BK 243	356	44 NE									
BK 244	329	32 NE									
BK 245	303	37 NE									
BK 246	306	22 NE									
BK 247	314	21 NE									
BK 248	349	18 NE								037	81 NW
BK 249	019	32 NW									
BK 250	310	37 SW								019	71 SE
BK 251	311	39 NE								032	79 SE
BK 252	087	34 S								027	81 NW
BK 253	292	24 NE								008	79 NW
BK 254	067	07 NW									
BK 255	054	06 SE									
BK 256	276	09 NE									
BK 257	314	03 NE								347	72 NE
BK 258	081	54 SE									
BK 259	044	18 SE									
BK 260	314	22 SW									
BK 261	314	16 NE									
BK 262	053	11 SE									
BK 263	343	34 SW									
BK 264	346	46 NE									
BK 265	046	18 SE									
BK 266	023	24 SE									
BK 267	347	29 SW									
BK 268	310	24 SW									
BK 269	013	31 SE									
BK 270	309	11 SW									
BK 271	013	18 E									
BK 272	072	16 NW									
BK 273	352	23 NE									
BK 274	326	14 NE									
BK 275	314	25 NE									
BK 276	343	36 NE									
BK 277	018	27 SE									
BK 278	052	18 SE								333	86 SW
										068	76 NW
BK 279	058	19 SE									
BK 280	021	37 SE									
BK 281	344	22 NE									
BK 282	337	18 NE									
BK 283	340	19 SW									
BK 284	322	38 SW									
BK 285	339	21 NE									
BK 286	344	21 NE								046	74 SE
BK 287	354	13 E	084	22						316	73 NE
BK 288	071	26 SE									

Station	Foliation		Lineation		Fold Axis		Axial Plane		Fold	Joint	
	Strike	Dip	Trend	Plunge	Trend	Plunge	Strike	Dip	Verg.	Strike	Dip
BK 289	067	11 SE									
BK 290	033	42 SE									
BK 291	291	04 NE									
BK 292	292	22 SW									
BK 293	041	31 SE									
BK 294	352	16 E									
BK 295	335	19 NE									
BK 296	312	21 SW									
BK 297	336	38 NE									
BK 298	296	16 SW									
BK 299	317	23 NE									
BK 300	293	10 SW									
BK 301	347	16 NE									
BK 302	338	14 NE									
BK 303	319	25 NE								326	58 SW
BK 304	313	10 NE									
BK 305	026	37 SE								068	79 SE
										004	58 W
BK 306	320	26 NE									
BK 307	349	27 NE									
BK 308	316	25 NE									
BK 309	337	31 NE	078	34							
BK 310	044	30 SE									
BK 311	046	24 SE									
BK 312	042	19 SE	108	17							
BK 313	033	19 SE									
BK 314	319	23 NE									
BK 315	044	36 SE								279	88 S
										057	59 NW
BK 316	318	26 NE									
BK 317	336	32 SW									
BK 318	321	29 SW									
BK 319	323	29 NE									
BK 320	044	18 SE									
BK 321	304	16 NE									
BK 322	057	27 SE								332	74 NE
BK 323	291	19 NE								314	64 SW
										067	61 SE
BK 324	341	33 NE									
BK 325	043	21 NW									
BK 326	319	25 NE								076	80 SE
										323	68 SW
BK 327	346	18 NE									
BK 328	311	26 NE									
BK 329	064	18 SE								268	57 NE
										325	86 NE
BK 330	286	07 NW									
BK 331	344	14 W									
BK 332	012	17 SE									
BK 333	069	9 NW									
BK 334	319	20 NE								069	85 SE
BK 335	341	08 NE									
BK 336	334	28 NE									
BK 337	323	11 NE									
BK 337	342	24 NE									
BK 339	331	19 NE									
BK 340	291	41 NE									
BK 341	287	24 NE									
BK 342	308	16 NE								074	85 NW
										294	56 SW
BK 343	334	19 NE									
BK 344	017	20 SE									
BK 345	053	12 SE								036	78 NW
BK 346	071	28 SE	176	24							
BK 347	038	36 SE									
BK 348	023	17 SE									
BK 349	072	26 SE									
BK 350	062	18 NW									
BK 351	064	14 SE									
BK 352	062	16 SE									
BK 353	056	19 SE									
BK 354	026	19 SE									
BK 355	069	40 SE									
BK 356	034	26 SE									
BK 357	055	26 SE									
BK 358	041	37 SE									

Station	Foliation		Lineation		Fold Axis		Axial Plane		Fold	Joint	
	Strike	Dip	Trend	Plunge	Trend	Plunge	Strike	Dip	Verg.	Strike	Dip
BK 359	062	30 SE									
BK 360	074	16 SE	133	15							
BK 361	306	23 SW									
BK 362	286	33 NE									
BK 363	063	25 SE									
BK 364	013	14 SE									
BK 365	348	22 NE									
BK 366	048	12 SE									
BK 367	031	40 SE	132	36							
BK 368	024	36 SE									
BK 369	012	30 SE	146	17							
BK 370	032	07 SE									
BK 371	056	24 NE									
	074	83 NW									
BK 372	356	34 E									
BK 373	334	16 NE									
BK 374	332	18 NE									
BK 375	316	09 NE									
BK 376	324	13 NE			032	09	346	19 NE	NW		
BK 377	314	17 NE									
BK 378	354	31 NE									
BK 379	064	39 NW									
BK 380	324	31 NE	102	16						073	88 SE
BK 381	333	27 NE									
BK 382	349	23 NE									
BK 383	065	14 SE									
BK 384	041	14 SE								057	88 SE
BK 385	337	32 NE								087	090
BK 386	321	19 NE									
BK 387	064	16 SE									
BK 388	011	23 SE									
BK 389	002	14 E									
BK 390	003	11 E									
BK 391	059	41 SE									
BK 392	287	08 NE								074	87 SE
										008	090
BK 393	020	19 NW									
BK 394	341	16 NE									
BK 395	059	47 SE									
BK 396	309	29 SW									
BK 397	066	11 SE									
BK 398	069	14 SE									
BK 399	348	23 SW									
BK 400	303	27 NE									
BK 401	082	20 NW									
BK 402	312	17 NE									
BK 403	347	14 NE									
BK 404	333	37 NE									
BK 405	352	11 NE									
BK 406	323	14 NE									
BK 407	345	21 NE									
BK 408	348	14 NE								072	86 NE
BK 409	302	26 SW									
BK 410	344	34 SW									
BK 411	020	17 SE									
BK 412	307	27 SW	266	16						339	68 SW
BK 413	312	24 NE								322	76 NE
BK 414	318	14 NE									
BK 415	277	26 S									
BK 416	015	32 E									
BK 417	058	37 SE									
BK 418	057	14 SE	119	07							
BK 419	059	19 SE									
BK 420	054	34 SE									
BK 421	023	27 NW									
BK 422	319	15 NE									
BK 423	294	33 NE								084	89 NW
BK 424	317	18 NE									
BK 425	312	21 NE									
BK 426	297	16 NE									
BK 427	342	19 NE									
BK 428	353	33 NW									
BK 429	317	30 NE									
BK 430	348	46 NE									
BK 431											
BK 432	316	22 NE									

Station	Foliation		Lineation		Fold Axis		Axial Plane		Fold	Joint	
	Strike	Dip	Trend	Plunge	Trend	Plunge	Strike	Dip	Verg.	Strike	Dip
BK 433	321	14 SW									
BK 434	346	13 SW									
BK 435	334	35 NE									
BK 436	338	40 NE									
BK 437	346	19 NE									
BK 438	014	22 SE	119	13						077	090
BK 439	358	27 E									
BK 440	016	25 SE									
BK 441	019	24 SE									
BK 442	352	27 E									
BK 443	337	26 NE									
BK 444	024	46 NW									
BK 445	284	29 NE								057	76 SE
BK 446	337	13 NE								025	81 NW
BK 447	280	24 N									
BK 448											
BK 449	034	16 NW									
BK 450	342	23 SW									
BK 451	353	14 W									
BK 452	276	25 N									
BK 453	071	14 N									
BK 454	051	49 SE								306	68 NW
BK 455	017	14 W									
BK 456	286	21 SW								078	090
BK 457	047	13 SE									
BK 458	012	26 SE									
BK 459	329	49 NE									
BK 460	329	16 NE								048	71 NW
BK 461	041	39 SE									
BK 462	312	24 SW								074	87 SE
BK 463	056	29 SE								061	81 SE
BK 464	018	12 SE								332	89 SW
										075	80 SE
BK 465	086	24 S									
BK 466	082	14 S			282	06	290	78 NE	SW		
BK 467	314	13 SW								068	76 NW
	047	40 SE									
BK 468	067	30 SE									
BK 469	310	31 SW								044	81 SE
BK 470	315	47 SW								044	76 SE
BK 471	317	36 SW								284	66 NE
BK 472	015	31 SE									
BK 473	060	19 NE								340	76 NE
BK 474	042	23 NW			294	12	305	56 NW	NE		
BK 475	062	24 NW								035	85 NW
										297	77 NE
BK 476	042	23 NW									
BK 477	304	14 NE									
BK 478	348	15 W								042	86 SE
BK 479	032	28 SE			046	16	039	33 NW	W		
BK 480	328	04 NE									
BK 481	019	39 SE									
BK 482	016	14 SE	174	14							
BK 483	018	19 SE									
BK 484	081	27 NW									
BK 485	029	21 SW								064	87 NW
BK 486	046	17 NW									
BK 487	059	21 SE			081	11	017	12 SE	SE		
BK 488	328	14 NE									
BK 489	079	14 NW								011	70 W
BK 490	009	38 E								311	51 SW
BK 491	005	23 E									
BK 492	278	23 SW								336	67 NE
										063	78 SE
BK 493	279	11 S									
BK 494	286	12 SW									
BK 495	076	08 N								051	82 SE
BK 496	341	14 NE								322	83 NE
BK 497	342	08 E									
BK 498	330	14 NE									
BK 499	013	10 SE								312	82 NE
BK 500	347	24 NE								018	84 SE
BK 501	039	14 NW			216	05	346	09 SW	NW		
BK 502	342	14 NE								047	89 SW
BK 503	348	13 SW									
BK 504	355	28 NE									

Station	Foliation		Lineation		Fold Axis		Axial Plane		Fold	Joint	
	Strike	Dip	Trend	Plunge	Trend	Plunge	Strike	Dip	Verg.	Strike	Dip
BK 505	023	25 SE								071	81 NW
										354	52 SW
BK 506	024	19 SE									
BK 507	022	13 SE								303	85 SW
BK 508	081	67 S									
BK 509	080	10 NW									
BK 510	292	18 SW									
BK 511	276	12 N									
BK 512	053	30 NW								066	59 NW
										286	74 NE
BK 513	344	32 NE								072	86 NW
	276	19 NE									
BK 514	311	19 NE									
BK 515	312	10 NE									
BK 516	316	43 NE									
BK 517	313	31 NE	122	20							
BK 518	312	17 NE									
BK 519	321	30 NE	079	14							
BK 520	319	21 NE								064	87 NW
	325	33 NE									
BK 521	309	19 NE									
BK 522	323	27 NE									
BK 523	334	29 NE									
BK 524	320	31 NE			082	13	331	36 NE	N		
BK 525	326	19 NE								064	68 SW
										336	61 NE
BK 526	335	35 NE									
BK 527	338	22 NE									
BK 528	299	17 NE								033	89 NW
BK 529	288	13 NE									
BK 530	307	14 NE									
BK 531	303	26 NE	108	14							
BK 532	326	11 NE								061	80 SE
BK 533	322	17 NE									
BK 534	328	20 NE									
BK 535	082	57 N									
BK 536	316	14 NE									
BK 537	346	31 NE									
BK 538	327	8 NE								064	70 SE
										036	74 SE
BK 539	278	04 SW									
BK 540	322	12 NE									
BK 541	287	12 SW									
BK 542	283	12 NE									
BK 543	004	10 E									
BK 544	352	5 W									
BK 545	030	19 SE									
BK 546	324	36 NE									
BK 547	308	7 NE									
BK 548	068	14 NW								322	73 NE
BK 549	062	29 NW									
BK 550	036	19 SE									
BK 551	319	27 SW			236	10	049	36 SE	SE	032	81 SW
BK 552	352	36 E								004	84 W
BK 553	349	22 E									
BK 554	346	25 NE									
BK 555	088	59 S									
BK 556	084	21 N									
BK 557	321	18 NE									
BK 558	292	25 SW									
BK 559	335	16 SW								071	87 SE
BK 560	319	13 SW									
BK 561	349	10 SW									
BK 562	293	24 NE	096	19							
BK 563	046	37 NW									
BK 564	291	46 SW									
BK 565	341	21 NE									
BK 566	358	27 SE									
BK 567	026	28 SE									
BK 568	356	17 NE									
BK 569	036	29 SE									
BK 570	293	17 NE									
BK 571	346	38 NE								277	89 S
BK 572	343	44 NE									
BK 573	017	09 SE									
BK 574	356	48 N									

Station	Foliation		Lineation		Fold Axis		Axial Plane		Fold	Joint	
	Strike	Dip	Trend	Plunge	Trend	Plunge	Strike	Dip	Verg.	Strike	Dip
BK 575	312	19 NE									
BK 576	085	11 S									
BK 577	354	26 NE									
BK 578	316	23 SW									
BK 579	357	19 SW	291	16							
BK 580	064	21 SE									
BK 581	313	18 NE									
BK 582	302	23 NE									
BK 583	308	17 NE									
BK 584	342	16 NE									
BK 585	086	10 S									
BK 586	304	24 NE									
BK 587	322	31 NE									
BK 588	017	19 SE									
BK 589	042	36 SE									
BK 590	292	32 SW									
BK 591	058	37 SE									
BK 592	018	27 SE									
BK 593	064	18 SE								066	81 NW
BK 594	021	20 SE									
BK 595	341	04 SW									
BK 596	006	59 SE									
BK 597	292	11SW									
BK 598	297	14 SW									
BK 599	314	16 NE									
BK 600	332	13 NE									
BK 601	302	11 NE									
BK 602	343	26 NE	131	36						022	84 NW
BK 603	299	35 SW									
BK 604	316	17 SW									
BK 605	303	22 NE									
BK 606	301	21 NE									
BK 607	293	23 NE									
BK 608	300	22 NE									
BK 609	291	24 NE									
BK 610	318	27 NE									
BK 611	316	24 NE								026	79 NW
BK 612	311	26 NE									
BK 613	348	19 NE									
BK 614	344	16 NE									
BK 615	348	11 NE									
BK 616	347	19 NE									
BK 617	346	18 NE								048	89 SE
BK 618	329	17 NE									
BK 619	336	26 NE								023	70 NW
BK 620	341	10 NE									
BK 621	336	24 NE									
BK 622	331	16 NE									
BK 623	341	28 NE									
BK 624	334	30 NE									
BK 625	056	34 SE									
BK 626	296	14 SW									
BK 627	014	31 SE									
BK 628	071	22 SE									
BK 629	342	26 SW									
BK 630	079	16 SE									
BK 631	074	19 SE									
BK 632	082	23 SE									
BK 633	351	7 NE									
BK 634										064	72 SE
BK 635	084	41 SE									
BK 636	036	19 SE									
BK 637	066	57 SE									
BK 638	076	38 SE									
BK 639	042	36 SE									
BK 640	318	29 SW									
BK 641	334	11 SW									
BK 642	318	7 NE									
BK 643	321	26 NE									
BK 644	317	19 SW								276	59 N
BK 645	334	19 SW									
BK 646	334	19 NE								276	84 N
BK 647	309	11 NE									
BK 648	291	16 NE								051	86 NW
BK 649	342	16 NE									
BK 650	004	46 E									

Station	Foliation		Lineation		Fold Axis		Axial Plane		Fold	Joint	
	Strike	Dip	Trend	Plunge	Trend	Plunge	Strike	Dip	Verg.	Strike	Dip
BK 651	284	15 NE									
BK 652	289	17 NE									
BK 653	064	23 SE									
BK 654	053	13 SE									
BK 655	028	26 SE	134	16							
BK 656	032	26 SE									
BK 657	024	26 SE									
BK 658	017	37 SE									
BK 659	021	36 SE									
BK 660	032	24 SE									
BK 661	074	36 SE									
BK 662	029	24 SE									
BK 663	043	27 SE									
BK 664	012	23 SE									
BK 665	032	18 SE									
BK 666	008	17 SE									
BK 667	341	26 NE									
BK 668	028	46 SE									
BK 669	312	28 SW									
BK 670	023	27 SE									
BK 671	354	14 NE									
BK 672	345	29 NE									
BK 673	024	19 SE									
BK 674	292	34 SW									
BK 675	034	24 SE									
BK 676	321	34 NE									
BK 677	006	29 E									
BK 678	329	17 NE									
BK 679	028	26 SE									
BK 680	334	28 NE									
BK 681	322	22 NE									
BK 682	334	19 NE									
BK 683	321	19 SW									
BK 684	044	22 SE									
BK 685	034	29 SE									
BK 686	316	09 SW									
BK 687	034	36 SE									
BK 688	324	34 SW									
BK 689	331	36 NE									
BK 690	328	26 NE									
BK 691	323	18 NE									
BK 692	302	29 SW									
BK 693	324	21 NE									
BK 694	346	21 NE									
BK 695	326	25 NE									
BK 696	036	29 SE									
BK 697	008	34 E									
BK 698	052	27 SE									
BK 699	337	18 NE									
BK 700	339	16 NE									
BK 701	342	17 NE									
BK 702	312	39 NE									
BK 703	319	36 NE									
BK 704	018	40 SE									
BK 705	023	25 SE									
BK 706	352	24 E									
BK 707	047	17 SE									
BK 708	328	19 NE									
BK 709	349	06 NE									
BK 710	042	27 SE									
BK 711	346	28 SW									
BK 712	303	16 NE									
BK 713	034	25 SE									
BK 714	053	14 SE									
BK 715	034	25 SE									
BK 716	026	51 SE									
BK 718	032	21 SE									
BK 719	323	25 NE									
BK 720	341	29 NE									
BK 721	034	29 SE									
BK 722	342	27 NE								054	82 NW
BK 723	324	16 SW									
BK 724										078	79 N
BK 725	334	16 SW									
BK 726	354	29 NE									
BK 727	316	17 NE									

Station	Foliation		Lineation		Fold Axis		Axial Plane		Fold	Joint	
	Strike	Dip	Trend	Plunge	Trend	Plunge	Strike	Dip	Verg.	Strike	Dip
BK 728	339	29 NE									
BK 729	034	25 SE									
BK 730	023	22 SE									
BK 731	038	26 SE									
BK 732	033	17 SE									
BK 733	024	27 SE									
BK 734	035	29 SE									
BK 735	026	35 SE									
BK 736	019	27 SE									
BK 737	352	35 E									
BK 738	064	25 SE									
BK 739	063	29 SE									
BK740	054	11 SE									
BK 741	069	24 SE									
BK 742	066	17 SE									
BK 743	057	24 SE									
BK 744	026	25 SE									
BK 745	033	17 SE									
BK 746	084	12 S									
BK 747	032	24 SE									
BK 748	044	16 SE									
BK 749	336	42 NE									
BK 750	018	37 SE									
BK 751	006	51 E									
BK 752	026	25 SE									
BK 753	313	30 NE									
BK 754	343	36 NE									
BK 755	328	17 NE									
BK 756	306	18 NE			036	22	038	66 NW	SW		
BK 757	339	15 NE									
BK 758	334	17 NE									
BK 759	321	26 NE									
BK 760	344	32 NE								054	78 SE
										067	88 SE
BK 761	326	24 NE									
BK 762	329	24 NE									
BK 763	351	22 NE									
BK 764	023	27 SE									
BK 765	016	28 SE									
BK 766	023	24 SE									
BK 767	024	22 SE									
BK 768	023	12 SE									
BK 769	011	27 SE									
BK 770	344	28 E									
BK 771	021	12 SE									
BK 772	054	19 SE									
BK 773	018	9 SE									
BK 774	039	24 SE									
BK 775	036	25 SE									
BK 776	027	19 SE									
BK 777	006	19 E									
BK 778	343	16 NE									
BK 779	049	33 SE									
BK 780	014	36 SE									
BK 781	351	37 E									
BK 782	324	32 NE									
BK 783	322	27 NE									
BK 784	343	26 NE									
BK 785	343	21 NE									
BK 786	334	36 NE									
BK 787	336	21 NE									
BK 788	342	28 NE									
BK 789	356	26 E									
BK 790	011	33 SE									
BK 791	356	16 E									
BK 792	357	39 E									
BK 793	347	27 NE									
BK 794	027	31 SE									
BK 795	008	27 E									
BK 796	356	24 NE									
BK 797	349	28 NE									
BK 798	321	28 NE									
BK 799	008	19 SE									
BK 800	326	32 NE									
BK 801	354	19 E									
BK 802	352	35 E									

Station	Foliation		Lineation		Fold Axis		Axial Plane		Fold	Joint	
	Strike	Dip	Trend	Plunge	Trend	Plunge	Strike	Dip	Verg.	Strike	Dip
BK 803	306	14 NE									
BK 804	334	24 NE									
BK 805	342	26 NE									
BK 806	013	30 SE									
BK 807	349	13 NE									
BK 808	352	16 E									
BK 809	338	31 NE									
BK 810	342	26 NE									
BK 811	337	21 NE									
BK 812	338	17 NE									
BK 813	014	15 SE									
BK 814	029	19 SE									
BK 815	019	05 SE									
BK 816	298	26 SW									
BK 817	296	17 NE									
BK 818	302	26 SW									
BK 819	328	23 NE									
BK 820	297	11 NE									
BK 821	326	21 SW									
BK 822	351	34 W									
BK 823	018	20 NW									
BK 824	359	11 W									
BK 825	328	17 E									
BK 826	319	21 NE									
BK 827	042	28 SE									
BK 828	348	10 W									
BK 829	016	25 NW									
BK 830	076	24 S									
BK 831	312	36 NE									
BK 832	316	31 NE									
BK 833	334	23 SW									
BK 834	353	33 W									
BK 835	336	26 NE									
BK 836	064	26 NW									
BK 837	302	23 NE									
BK 838	334	19 NE									
BK 839	326	24 NE									
BK 840	046	18 SE									
BK 841	346	20 NE									
BK 842	336	24 NE									
BK 843	332	14 NE									
BK 844	309	11 NE									
BK 845	332	12 NE									
BK 846	279	14 S									
BK 847	319	14 SW									
BK 848	296	24 NE									
BK 849	318	20 NE									
BK 850	039	26 SE									
BK 851	313	9 SW									
BK 852	308	20 NE									
BK 853	309	19 SW									
BK 854	306	39 SW									
BK 855	324	19 SW									
BK 856	305	29 SW									
BK 857	066	19 NW									
BK 858	336	17 SW									
BK 859	074	26 SE									
BK 860	317	32 SW									
BK 861	084	11 N									
BK 862	007	20 E									
BK 863	042	11 SE									
BK 864	306	33 NE									
BK 865	023	27 SE									
BK 866	032	23 SE									
BK 867	036	34 SE									
BK 868	043	39 SE									
BK 869	028	33 SE									
BK 870	026	16 SE									
BK 871	026	29 SE									
BK 872	016	48 SE									
BK 873	024	30 SE									
BK 874	014	46 SE									
BK 875	026	19 SE									
BK 876	035	38 SE									
BK 877	032	37 SE									
BK 878	045	36 SE									

Station	Foliation		Lineation		Fold Axis		Axial Plane		Fold	Joint	
	Strike	Dip	Trend	Plunge	Trend	Plunge	Strike	Dip	Verg.	Strike	Dip
BK 879	056	29 SE									
BK 880	032	40 SE									
BK 881	046	29 SE									
BK 882	034	34 SE									
BK 883	044	20 SE									
BK 884	292	36 SW									
BK 885	311	34 NE									
BK 886	077	24 SE									
BK 887	324	23 NE									
BK 888	068	16 SE									
BK 889	063	22 SE									
BK 890	312	35 SW									
BK 891	073	26 SE									
BK 892	072	16 SE									
BK 893	054	26 SE									
BK 894	038	29 SW									
BK 895	332	16 NE									
BK 896	294	24SW	276	05						074	68 NW
										048	73 SE
BK 897	343	16 NE	078	04							
BK 898	296	21 SW									
BK 899	088	28 S								053	22 SW
BK 900	306	29 SW			134	27	286	83 NE	SW		
BK 901	083	16 S									
BK 902	304	16 SW									
BK 903	039	13 SE								071	66 SE
BK 904	286	33 NE									
BK 905	324	20 NE									
BK 906	332	26 SW									
BK 907	032	06 SE									
BK 908	292	37 SW									
BK 909	304	21 SW									
BK 910	032	21 SE									
BK 911	354	23 SW									
BK 912	282	44 S									
BK 913	036	20 SE									
BK 914	296	44 SW									
BK 915	039	22 SE			156	16	349	69 SW	W		
BK 916	316	21 SW									
BK 917	033	17 SE									
BK 918	036	17 SE									
BK 919	027	12 SE									
BK 920	034	08 SE									
BK 921	346	26 NE									
BK 922	338	17 NE									
BK 923	341	13 NE									
BK 924	352	21 NE			308	30	304	54 E	NE		
BK 925	003	17 E									
BK 926	017	16 E	072	14							
BK 927	308	32 NE									
BK 928	339	30 NE									
BK 929	346	21 NE	176	03							
BK 930	076	21 SE									
BK 931	077	28 SE									
BK 932	012	21 E									
BK 933	339	22 NE									
BK 934	354	23 NE									
BK 935	346	19 NE								064	86 NW
BK 936	347	20 NE									
BK 937	352	24 NE									
BK 938	343	16 NE									
BK 939	348	23 NE									
BK 940	352	34 NE									
BK 941	339	18 NE									
BK 942	358	17 NE			165	09	014	16 SE	NW		
BK 943	024	15 SE									
BK 944	349	19 NE									
BK 945	026	24 SE									
BK 946	306	19 SW									
BK 947	332	10 NE									
BK 948	304	04 SW									
BK 949	036	27 SE			025	05	012	60 SW	SE		
BK 950	029	7 SE									
BK 951	023	30 SE									
BK 952	299	07 SW									
BK 953	032	17 SE									

Station	Foliation		Lineation		Fold Axis		Axial Plane		Fold	Joint	
	Strike	Dip	Trend	Plunge	Trend	Plunge	Strike	Dip	Verg.	Strike	Dip
BK 954	337	14 NE									
BK 955	340	30 NE									
BK 956	331	16 NE									
BK 957	323	20 NE									
BK 958	342	18 NE									
BK 959	084	19 S									
	024	17 NW									
BK 960	317	26 SW									
BK 961	327	11 NE									
BK 962	333	12 SW									
BK 963	330	18 SW									
BK 964	284	14 SE									
BK 965	319	48 NE									
BK 966	347	21 SW									
BK 967	062	14 NW									
BK 968	299	14 NE									
BK 969	054	20 SE			313	22	046	32 SE	W		
BK 970	084	46 S									
BK 971	330	56 SW									
BK 972	022	17 NW									
BK 973	333	35 NE									
BK 974	312	11 NE									
BK 975	324	11 NE									
BK 976	317	09 NE									
	038	24 NW									
BK 977	063	23 SE									
BK 978	332	35 NE									
BK 979	302	21 SW									
BK 980	008	14 E									
BK 981	333	39 NE									
BK 982	283	23 NE									
BK 983	026	12 SE									
BK 984	298	09 NE									
BK 985	356	26 E									
BK 986	319	17 NE									
BK 987	313	25 NE									
BK 988	293	21 NE									
BK 989	308	14 NE								010	89 N
BK 990											
BK 991	069	25 SE									
BK 992	318	08 NE								311	69 NE
BK 993	012	23 SE			328	04	339	19 SW	SW		
BK 994	291	14 SW									
BK 995	283	19 NE			319	19	018	02 NW	NE		
					281	09	007	04 E	S		
BK 996	328	25 NE									
BK 997	296	88 NW									
BK 998	080	43 S									
BK 999	336	08 NE									
BK 1000	320	24 NE									
BK 1001	318	31 NE									
BK 1002	326	36 NE									
BK 1003	064	17 SE									
BK 1004	352	6 NE									
BK 1005	286	9 NE									
BK 1006	286	4 NE									
BK 1007	311	16 NE									
BK 1008	301	33 NE									
BK 1009	330	06 NE									
BK 1010	329	16 SW									
BK 1011	024	20 SE									
BK 1012	044	16 SE									
BK 1013	336	06 SW									
BK 1014	338	21 SW	356	18							
BK 1015	304	21 SW									
BK 1016	309	14 SW									
BK 1017	011	4 S									
BK 1018	044	32 SE									
BK 1019	053	23 SE									
BK 1020	031	50 SE									
BK 1021	031	15 SE									
BK 1022	064	27 SE									
BK 1023	028	30 SE									
BK 1024	328	20 SW									
BK 1025	303	10 SW									
BK 1026	331	18 NE									

Station	Foliation		Lineation		Fold Axis		Axial Plane		Fold	Joint	
	Strike	Dip	Trend	Plunge	Trend	Plunge	Strike	Dip	Verg.	Strike	Dip
BK 1027	009	16 SE									
BK 1028	036	26 SE									
BK 1029	048	24 SE									
BK 1030	035	06 NW									
BK 1031	066	15 SE									
BK 1032	341	27 NE									
BK 1033	079	21 S									
BK 1034	051	23 SE									
BK 1035	031	29 SE									
BK 1036	341	21 NE									
BK 1037	318	45 SW									
BK 1038	316	65 NE									
BK 1039	339	06 SW									
BK 1040	328	11 NE									
BK 1041	071	36 SE									
BK 1042	012	13 SE									
BK 1043	042	11 SE									
BK 1044	011	33 SE									
BK 1045	298	28 SW									
BK 1046	323	22 SW									
BK 1047	306	16 NE									
BK 1048	316	21 NE								063	78 SE
										314	87 SW
BK 1049	338	27 NE			330	13	060	16 NW	SW		
BK 1050	323	6 NE									
BK 1051	334	26 SW									
BK 1052	011	32 SE									
BK 1053	288	13 NE									
BK 1054	324	29 SW									
BK 1055	061	30 SE									
	332	13 NE									
BK 1056	324	25 NE									
BK 1057	003	32 E									
BK 1058	045	22 SE									
BK 1059	056	26 SE									
BK 1060	089	24 S									
BK 1061	006	25 SE									
BK 1062	052	86 SE									
BK 1063	284	14 SW									
BK 1064	306	14 NE	056	04							
BK 1065	312	36 SW									
BK 1066	016	31 NW									
BK 1067	296	45 SW									
BK 1068	314	36 NE									
BK 1069	296	72 NE									
BK 1070	317	37 SW									
BK 1071	074	16 SE								074	81 SE
BK 1072	306	45 NE									
BK 1073	016	10 SE									
BK 1074	021	11 SE									
BK 1075	012	36 SE									
BK 1076	013	17 SE									
BK 1077	008	19 SE									
BK 1078	306	31 SW	076	24							
BK 1079	034	12 SE			311	03	319	43 SW	NE		
BK 1080	012	19 E									
BK 1081	043	12 SE									
BK 1082	019	08 SE									
BK 1083	356	07 SW									
BK 1084	043	09 SE									
BK 1085	047	22 SE								074	79 NW
BK 1086	281	9 NE									
BK 1087	274	02 N									
BK 1088	358	04 NE								054	87 NW
BK 1089	356	24 NE									
BK 1090	357	18 NE									
BK 1091	354	16 NE									
BK 1092	356	26 NE									
BK 1093	338	20 NE									
BK 1094	032	15 SE									
BK 1095	328	16 NE									
BK 1096	347	16 NE									
BK 1097	328	20 NE									
BK 1098	352	19 NE									
BK 1099	319	19 NE			058	12	074	38 SE	NW		
BK 1100	341	16 NE									

Station	Foliation		Lineation		Fold Axis		Axial Plane		Fold	Joint	
	Strike	Dip	Trend	Plunge	Trend	Plunge	Strike	Dip	Verg.	Strike	Dip
BK 1101	333	11 NE			348	14	288	13 NE	SW		
BK 1102	321	26 NE									
BK 1103	326	26 NE									
BK 1104	323	29 NE									
BK 1105	348	12 NE									
BK 1106	032	24 SE								088	74 NW
BK 1107	019	24 SE								054	78 SE
										334	77 NE
BK 1108	323	23 NE									
BK 1109	324	34 NE									
BK 1110	336	6 NE									
BK 1111	306	15 NE									
BK 1112	341	06 NE									
BK 1113	326	11 NE									
BK 1114	054	24 SE									
BK 1115	048	20 SE									
BK 1116	003	09 NW			356	12	356	18 NE	W		
BK 1117										286	79 SW
BK 1118	285	26 NE									
BK 1119	346	23 NE									
BK 1120	341	22 NE									
BK 1121	009	28 SE								074	86 SE
BK 1122	014	24 SE								309	81 NE
BK 1123	013	22 SE									
BK 1124	011	21 SE									
BK 1125	007	27 E								074	75 SE
BK 1126	016	32 SE									
BK 1127	007	17 SE									
BK 1128	046	16 SE									
BK 1129	341	21 NE									
BK 1130	342	16 NE									
BK 1131	008	29 E									
BK 1132	356	17 E									
BK 1133	334	13 NE									
BK 1134	326	26 NE									
BK 1135	011	31 SE									
BK 1136	012	25 SE									
BK 1137	006	17 E									
BK 1138	024	24 SE									
BK 1139	061	14 SE									
BK 1140	054	15 SE									
BK 1141	302	23 NE	076	13						026	76 SE
BK 1142	299	21 NE									
BK 1143	354	36 NE									
BK 1144	344	11 NE									
BK 1145	296	9 SW									
BK 1146	312	29 NE								033	69 SE
BK 1147	322	32 NE								082	86 NW
BK 1148	331	26 NE									
BK 1149	332	26 NE									
BK 1150	328	28 NE									
BK 1151	323	31 NE									
BK 1152	328	19 NE									
BK 1153	321	21 NE									
BK 1154	324	13 NE									
	294	17 NE									
BK 1155	331	17 NE	108	21							
BK 1156	323	28 NE									
BK 1157	328	14 NE									
BK 1158	334	19 NE									
BK 1159	339	21 NE	103	19							
BK 1160	324	17 NE									
BK 1161	324	17 NE	112	15							
BK 1162	331	18 NE									
BK 1163	079	8 NW								356	82 SW
BK 1164	354	17 NE									
BK 1165	047	19 SE			088	13	074	20 SE	S	356	87 NE
BK 1166	348	10 NE									
BK 1167	087	9 NE									
BK 1168	273	9 N									
BK 1169	278	10 N									
BK 1170	344	10 NE									
BK 1171	348	15 NE									
BK 1172	343	11 NE	097	08							
BK 1173	312	15 NE	121	09							
BK 1174	350	23 NE									

Station	Foliation		Lineation		Fold Axis		Axial Plane		Fold	Joint	
	Strike	Dip	Trend	Plunge	Trend	Plunge	Strike	Dip	Verg.	Strike	Dip
BK 1175	343	11 NE									
BK 1176	300	17 NE									
BK 1177	331	13 NE	131	07						274	89 SW
										043	89 SE
BK 1178	341	8 NE	126	07							
BK 1179	351	22 NE									
BK 1180	331	21 NE								044	78 SE
BK 1181	306	26 NE									
BK 1182	345	22 NE									
BK 1183	350	15 NE									
BK 1184	328	21 NE									
BK 1185	334	18 NE									
BK 1186	333	22 NE									
BK 1187	294	13 NE								048	84 NW
										076	86 NW
BK 1188	291	19 NE									
BK 1189	303	6 NE								068	88 NW
BK 1190	336	7 NE									
BK 1191	314	3 NE									
BK 1192	329	16 NE									
BK 1193	321	9 NE	113	09						034	86 NW
BK 1194	328	7 SW									
BK 1195	331	6 SW									
BK 1196	324	12 SW									
BK 1197	019	29 SE									
BK 1198	286	10 SW									
BK 1199	308	2 NE								274	86 SW
										011	88 SE
BK 1200	323	8 NE									
BK 1201	329	10 NE									
BK 1202	314	10 NE									
BK 1203	331	10 NE	114	11						052	81 SE
BK 1204	319	22 NE	109	10						038	86 SE
BK 1205	296	43 NE									
BK 1206	322	26 NE									
BK 1207	276	26 S									
BK 1208	074	19 N									
BK 1209	336	21 NE									
BK 1210	332	14 NE									
BK 1211	064	11 SE									
BK 1212	317	23 NE									
BK 1213	314	15 NE									
BK 1214	318	20 NE									
BK 1215	324	17 NE									
BK 1216	317	16 NE	108	16							
BK 1217	321	24 NE									
BK 1218	326	26 NE	114	16							
BK 1219	332	22 NE	123	17							
BK 1220	328	15 NE									
BK 1221	330	19 NE									
BK 1222	326	22 NE									
BK 1223	331	13 NE									
BK 1224	327	37 NE									
BK 1225	324	11 NE									
BK 1226	306	25 NE									
BK 1227	314	29 NE									
BK 1228	308	16 NE									
BK 1229	317	15 NE									
BK 1230	318	15 NE									
BK 1231	321	21 NE									
BK 1232	320	20 NE									
BK 1233	314	18 NE									
BK 1234	324	26 NE									
BK 1235	326	24 NE									
BK 1236	341	12 NE									
BK 1237	322	12 NE									
BK 1238	322	14 NE									
BK 1239	341	16 NE									
BK 1240	333	17 NE									
BK 1241	309	19 NE									
BK 1242	339	19 NE									
BK 1243	336	12 NE			080	11	080	54 SE	S		
BK 1244	315	11 NE									
BK 1245	343	19 NE									
BK 1246	316	11 NE									
BK 1247	334	19 NR									

Station	Foliation		Lineation		Fold Axis		Axial Plane		Fold	Joint	
	Strike	Dip	Trend	Plunge	Trend	Plunge	Strike	Dip	Verg.	Strike	Dip
BK 1248	342	21 NE	108	33							
BK 1249	341	14 NE									
BK 1250	343	11 NE								046	88 SE
BK 1251	326	18 NE	118	13							
BK 1252	344	26 NE	117	20							
BK 1253	344	9 NE			352	16	349	11 NE	NE		
BK 1254	337	13 NE									
BK 1255	316	17 NE									
BK 1256	340	17 NE									
BK 1257	347	21 NE									
BK 1258	326	17 NE									
BK 1259	015	17 SE									
BK 1260	333	12 NE									
BK 1261	321	15 NE									
BK 1262	334	17 NE									
BK 1263	319	24 NE									
BK 1264	333	26 NE									
BK 1265	347	26 NE									
BK 1266	312	26 NE	116	16							
BK 1267	312	21 NE									
BK 1268	327	16 NE			338	11	323	14 NE	W		
BK 1269	325	25 NE									
BK 1270	324	21 NE									
BK 1271	321	25 NE									
BK 1272	351	24 E									
BK 1273	349	27 NE									
BK 1274	329	10 NE	115	08							
BK 1275	329	15 NE									
BK 1276	356	17 E	104	11							
BK 1277	350	11 E									
BK 1278	331	28 NE									
BK 1279	324	15 NE									
BK 1280	342	10 NE									
BK 1281	336	27 NE	103	07							
BK 1282	080	25 NE									
BK 1283	337	17 NE									
BK 1284	076	22 NW									
BK 1285	331	10 NE								087	86 N
BK 1286	334	17 NE									
BK 1287	347	11 NE									
BK 1288	333	12 NE									
BK 1289	328	12 NE									
BK 1290	338	19 NE	114	26	334	21	340	29 NE	W	073	79 SE
BK 1291	323	16 NE									
BK 1292	328	22 NE									
BK 1293	324	11 NE									
BK 1294	331	07 SW									
BK 1295	306	15 NE								030	82 SE
BK 1296	321	19 NE								309	79 NE
										053	82 SE
BK 1297	327	27 NE								072	72 SE
BK 1298	333	11 NE									
BK 1299	346	20 NE									
BK 1300	350	15 E									
BK 1301	342	23 NE									
BK 1302	343	16 NE									
BK 1303	333	21 NE	102	07							
BK 1304	318	25 NE									
BK 1305	328	10 NE									
BK 1306	070	15 NW									
BK 1307	010	21 SE									
BK 1308	329	22 NE									
BK 1309	313	22 NE									
BK 1310	344	23 NE								076	81 NW
BK 1311	341	16 NE								074	88 NW
BK 1312	339	17 NE								073	86 NW
BK 1313	338	21 NE									
BK 1314	336	18 NE									
BK 1315	326	22 NE									
BK 1316	343	20 NE									
BK 1317	328	24 NE									
BK 1318	349	30 NE									
BK 1319	021	22 SE									
BK 1320	348	18 NE									
BK 1321	347	09 NE									
BK 1322	335	11 NE									

Station	Foliation		Lineation		Fold Axis		Axial Plane		Fold	Joint	
	Strike	Dip	Trend	Plunge	Trend	Plunge	Strike	Dip	Verg.	Strike	Dip
BK 1323	350	13 NE									
BK 1324	349	20 NE								046	86 NW
BK 1325	346	16 NE									
BK 1326	348	17 NE			331	16	339	17 NE	SW		
BK 1327	354	17 E									
BK 1328	344	21 NE									
BK 1329	342	17 NE									
BK 1330	352	13 NE									
BK 1331	350	4 NE									
BK 1332	334	27 NE									
BK 1333	344	25 NE									
BK 1334	348	16 NE									
BK 1335	333	16 NE									
BK 1336	313	34 NE									
BK 1337	304	20 NE									
BK 1338	333	23 NE									
BK 1339	326	16 NE								044	89 SE
BK 1340	339	15 NE									
BK 1341	335	14 NE			344	14	023	39 SE	W		
BK 1342	324	9 NE									
BK 1343	327	12 NE								064	83 NW
										329	82 NE
BK 1344	012	28 SE									
BK 1345	331	14 NE									
BK 1346	311	20 NE									
BK 1347	326	18 SE									
BK 1348	346	18 NE								044	87 SE
BK 1349	038	15 SE									
BK 1350	322	16 NE									
BK 1351	336	17 NE									
BK 1352	336	22 NE									
BK 1353	326	26 NE								071	78 SE
BK 1354	324	19 NE									
BK 1355	341	23 NE								294	79 SW
BK 1356	344	23 NE									
BK 1357	340	13 NE								081	89 S
BK 1358	333	21 NE	119	20						048	81 NW
BK 1359	327	17 NE									
BK 1360	348	21 NE									
BK 1361	334	19 NE									
BK 1362	335	19 NE									
BK 1363	329	17 NE								054	79 SE
BK 1364	331	18 NE									
BK 1365	324	29 NE									
BK 1366	340	25 NE									
BK 1367	328	22 NE									
BK 1368	336	16 NE			137	08	340	16 NE	SW		
BK 1369	316	9 NE									
BK 1370	338	5 NE			339	12	325	7 NE	SW	084	86 NW
BK 1371	328	15 NE									
BK 1372	339	26 NE									
BK 1373	349	13 NE									
BK 1374	331	17 NE									
BK 1375	328	16 NE			059	14	354	14 NE	N		
					082	13	342	13 NE	S		
					064	13	325	13 NE	N		
BK 1376	328	15 NE			331	07	327	11 NE	W		
BK 1377	341	11 NE									
BK 1378	331	21 NE									
BK 1379	341	17 NE	113	09							
BK 1380	333	19 NE									
BK 1381	323	13 SW									
BK 1382	316	12 SW									
BK 1383	334	10 SW									
BK 1384	032	16 SE									
BK 1385	023	20 SE									
BK 1386	064	15 SE									
BK 1387	341	14 NE								047	74 NW
BK 1388	329	12 NE									
BK 1389	331	12 NE									
BK 1390	324	13 NE									
BK 1391	320	11 NE									
BK 1392	343	13 SW									
BK 1393	339	20 NE									
BK 1394	341	20 NE									
BK 1395	306	49 SW									

	Foliation		Lineation		Fold Axis		Axial Plane		Fold	Joint	
Station	Strike	Dip	Trend	Plunge	Trend	Plunge	Strike	Dip	Verg.	Strike	Dip
BK 1396	328	13 SW									
BK 1397	306	21 SW									
BK 1398	326	26 SW									
BK 1399	041	19 SE									
BK 1400	036	26 SE									
BK 1401	042	14 SE									
BK 1402	326	17 SW									
BK 1403	325	17 SW									
BK 1404	304	15 SW									
BK 1405	333	6 SW									
BK 1406	317	7 SW									
BK 1407	019	15 SE									
BK 1408	049	6 SE									
BK 1409	291	15 SW									
BK 1410	316	13 SW									
BK 1411	323	12 SW									
BK 1412	065	11 SE									
BK 1413	037	17 SE									
BK 1414	073	16 SE									
BK 1415	071	61 NW									
BK 1416	039	6 NW									
BK 1417	037	13 SE									
BK 1418	034	25 NW									
BK 1419	319	18 NE									
BK 1420	323	15 NE									
BK 1421	061	23 SE									
BK 1422	059	17 SE									
BK 1423	053	26 SE									
BK 1424	306	26 SW									
BK 1425	044	27 SE									
BK 1426	061	5 NW			213	03	034	8 SE	W		
BK 1427	039	14 SE									
BK 1428	284	21 NE	074	13							
BK 1429	302	24 NE									
BK 1430	333	41 NE									
BK 1431	354	29 NE									
BK 1432	328	24 NE									
BK 1433	286	17 NE									
	336	23 NE									
BK 1434	016	30 SE									
	333	26 NE									
BK 1435	346	24 NE									
BK 1436	349	14 NE									
	349	29 NE									
BK 1437	014	33 SE			037	11	321	14 NE	SE		
	304	19 NE									
BK 1438	349	19 NE									
BK 1439	349	12 NE									
	304	38 NE									
BK 1440	314	11 NE									
	337	13 NE									
BK 1441	309	34 NE									
BK 1442	328	37 NE									
BK 1443	318	13 NE									
BK 1444	349	25 NE									
BK 1445	349	25 NE	122	12							
BK 1446	323	18 NE									
	334	30 NE									
BK 1447	308	14 NE									
BK 1448	319	22 NE									
BK 1449	314	28 NE									
BK 1450	284	20 NE								064	82 NW
BK 1451	044	19 SE								066	74 SE
BK 1452	311	21 NE									
BK 1453	056	22 SE									
BK 1454	043	14 SE									
BK 1455	057	18 SE								064	81 SE
BK 1456	056	32 SE									
BK 1457	016	8 SE									
BK 1458	288	18 SW									
BK 1459	034	18 SE									
BK 1460	031	24 SE									
BK 1461	033	29 SE									
BK 1462	009	19 SE									
BK 1463	311	5 NE								047	75 NW
BK 1464	026	20 SE									

Station	Foliation		Lineation		Fold Axis		Axial Plane		Fold	Joint	
	Strike	Dip	Trend	Plunge	Trend	Plunge	Strike	Dip	Verg.	Strike	Dip
BK 1465	034	24 SE									
BK 1466	019	16 SE									
BK 1467	023	19 SE									
BK 1468	021	17 SE									
BK 1469	026	17 SE									
BK 1470	022	19 SE									
BK 1471	023	8 SE			227	05	044	5 NW	NW		
BK 1472	014	21 SE									
BK 1473	346	31 NE									
BK 1474	036	21 SE									
BK 1475	020	18 SE									
BK 1476	023	28 SE									
BK 1477	319	14 NE									
BK 1478	318	13 NE	103	14						034	79 SE
										284	82 NE
BK 1479	329	15 NE									
BK 1480	349	23 NE								314	86 NE
										074	71 SE
BK 1481	338	11 NE								084	82 NW
										331	78 SW
BK 1482	324	12 SW									
BK 1483	012	26 SE									
BK 1484	022	11 SE									
BK 1485	352	19 NE									
BK 1486	029	22 SE									
BK 1487	019	23 SE									
BK 1488	066	10 SE									
BK 1489	023	12 SE									
BK 1490	031	11 SE									
BK 1491	023	17 SE									
BK 1492	020	23 SE									
BK 1493	031	12 SE									
BK 1494	021	18 SE									
BK 1495	037	10 SE									
BK 1496	028	24 SE									
BK 1497	011	23 SE									
BK 1498	034	32 SE									
BK 1499	024	22 SE									
BK 1500	018	25 SE									
BK 1501	028	20 SE									
BK 1502	036	14 SE									
BK 1503	013	6 NW									
BK 1504	011	9 SE									
BK 1505	032	11 SE									
BK 1506	008	25 NW									
BK 1507											
BK 1508											
BK 1509	017	11 SE									
BK 1510	012	17 SE									
BK 1511	306	17 NE								034	87 NW
BK 1512	301	18 NE									
BK 1513	012	22 SE									
BK 1514	019	24 SE									
BK 1515	019	14 SE									
BK 1516	348	15 NE									
BK 1517	018	12 SE									
BK 1518	008	16 E									
BK 1519	332	19 NE								036	79 NW
										316	74 NE
BK 1520	016	24 SE									
BK 1521	022	20 SE									
BK 1522	028	25 SE									
BK 1523	007	23 E									
BK 1524	353	14 E	106	18							
BK 1525	011	17 SE									
BK 1526	354	8 W									
BK 1527	333	20 NE								061	82 SE
BK 1528	337	25 NE									
BK 1529	334	6 SW									
BK 1530	326	13 NE									
BK 1531	331	17 SW									
BK 1532	332	11 NE									
BK 1533	346	15 NE									
BK 1534	336	8 NE									
BK 1535	338	24 NE									
BK 1536	322	12 NE									

Station	Foliation		Lineation		Fold Axis		Axial Plane		Fold	Joint	
	Strike	Dip	Trend	Plunge	Trend	Plunge	Strike	Dip	Verg.	Strike	Dip
BK 1537	320	14 NE									
BK 1538	323	15 SW									
BK 1539	338	10 SW									
BK 1540	053	17 NW									
BK 1541	337	22 NE									
BK 1542	016	13 SE									
BK 1543	041	26 SE									
BK 1544	061	21 SE									
BK 1545	324	18 NE									
BK 1546	296	13 NE									
BK 1547	343	9 NE									
BK 1548	320	14 NE									
BK 1549	323	20 NE								063	78 SE
BK 1550	324	17 NE									
BK 1551	341	16 NE								302	79 NE
										062	89 SE
BK 1552	327	18 NE									
BK 1553	341	13 SW									
BK 1554	328	15 NE									
BK 1555	064	25 SE	122	17							
BK 1556	333	16 NE									
BK 1557	046	12 NW									
BK 1558	276	24 N									
BK 1559	283	8 NE									
BK 1560	023	7 NW									
BK 1561	061	8 NW									
BK 1562	058	26 NW									
BK 1563	326	25 NE	116	21							
BK 1564	337	17 NE									
BK 1565	334	14 NE									
BK 1566	324	21 NE									
BK 1567	329	28 NE									
BK 1568	331	30 NE									
BK 1569	324	26 NE									
BK 1570	323	22 NE	098	14							
BK 1571	322	19 NE									
BK 1572	336	21 NE									
BK 1573	328	27 NE									
BK 1574	334	13 NE									
BK 1575	329	14 NE									
BK 1576	333	15 NE									
BK 1577	344	14 NE									
BK 1578	011	19 NW									
BK 1579	326	19 NW									
BK 1580	317	38 NE									
BK 1581	323	8 NE									
BK 1582	330	17 NE									
BK 1583	325	15 NE									
BK 1584	009	26 E									
BK 1585	326	11 NE									
BK 1586	011	18 SE									
BK 1587	341	21 NE									
BK 1588	344	7 NE								048	82 SE
	031	11 SE									
BK 1589	027	19 SE									
BK 1590	012	17 SE									
BK 1591	306	34 SW									
BK 1592	026	33 SE									
BK 1593	044	5 NW									
BK 1594	328	19 NE									
BK 1595	324	29 NE									
BK 1596	334	15 NE									
BK 1597	337	25 NE									
BK 1598	335	12 SE									
BK 1599	333	17 NE									
BK 1600	011	21 SE								281	88 NE
BK 1601	020	12 SE									
BK 1602	306	13 NE									
	026	26 SE									
BK 1603	033	20 SE	129	26							
BK 1604	007	11 SE	106	16							
BK 1605	353	19 NE	119	11							
BK 1606	031	18 SE									
BK 1607	021	15 SE									
BK 1608	011	13 SE									
BK 1609	054	12 SE									

Station	Foliation		Lineation		Fold Axis		Axial Plane		Fold	Joint	
	Strike	Dip	Trend	Plunge	Trend	Plunge	Strike	Dip	Verg.	Strike	Dip
BK 1610	333	13 NE									
BK 1611	324	11 NE									
BK 1612	331	14 NE									
BK 1613	353	11 NE	121	06							
CA 1											
CA 2	312	11 NE									
CA 3	084	07 S									
CA 4	064	29 SE									
CA 5	064	14 SE									
CA 6	294	14 SW									
CA 7	084	24 SE									
CA 8	052	19 SE	146	19							
CA 9	011	14 S									
CA 10	046	10 S									
CA 11	004	29 SE									
CA 12	004	06 W									
CA 13	044	12 SE									
CA 14	352	11 NE									
CA 15	086	34 S									
CA 16	082	14 SE									
CA 17	282	14 NE									
CA 18	004	05 SE									
CA 19	318	06 SW									
CA 20	293	14 NE									
CA 21	296	7 NE									
CA 22	271	8 N									
CA 23	030	7 NW									
CA 24	062	14 SE									
CA 25	017	12 SE									
CA 26	014	14 SE									
CA 27	032	31 SE									
CA 28	048	21 NW									
CA 29	285	18 NE									
CA 30	324	16 NE									
CA 31	314	16 NE									
CA 32	334	09 NE									
CA 33	051	06 NW									
CA 34	333	12 NE									
CA 35	332	29 NE									
CA 36	321	06 NE									
CA 37	032	24 SE									
CA 38	311	22 NE									
CA 39	036	28 SE									
CA 40	319	32 NE									
CA 41	027	13 SE									
CA 42	318	23 NE									
CA 43	019	14 NW									
CA 44	032	19 NW									
CA 45	064	21 SE									
CA 46	316	21 NE									
CA 47	333	23 NE									
CA 48	293	14 SW									
CA 49	324	21 NE									
CA 50	299	06 SW									
CA 51	064	12 SE									
CA 52	049	10 SE									
CA 53	052	11 SE									
CA 54	332	13 NE									
CA 55	340	11 NE									
CA 56	289	17 NE									
CA 57	046	24 SE									
CA 58	019	14 NW									
CA 59	033	16 NW									
CA 60	067	33 SE									
CA 61	066	10 SE									
CA 62	296	16 SW									
CA 63	078	18 SE									
CA 64	336	50 NE									
CA 65	339	37 NE									
CA 66	016	21 SE	291	19							
CA 67	341	14 NE									
CA 68	336	10 NE	110	17							
CA 69	346	19 NE									
CA 70	056	31 SE									
CA 71	316	21 SW									
CA 72	024	24 SE									

Station	Foliation		Lineation		Fold Axis		Axial Plane		Fold	Joint	
	Strike	Dip	Trend	Plunge	Trend	Plunge	Strike	Dip	Verg.	Strike	Dip
CA 73	028	32 SE									
CA 74	011	32 SE									
CA 75	329	26 SW									
CA 76	327	26 SW									
CA 77	288	76 NE									
CA 78	059	24 SE									
CA 79	274	27 SW									
CA 80	318	24 SW									
CA 81	306	29 SW									
CA 82	066	26 NW									
CA 83	296	26 SW									
CA 84	296	12 NE									
CA 85	296	14 NE									
CA 86	313	15 NE									
CA 87	319	15 NE									
CA 88	334	29 SW									
CA 89	322	26 NE									
CA 90	300	40 SW									
CA 91	313	34 SW									
CA 92	316	14 SE									
CA 93	344	34 SW									
CA 94	337	10 NE									
CA 95	329	9 NE									
CA 96	334	12 NE									
CA 97	082	41 S									
CA 98	286	34 SW									
CA 99	072	15 SE									
CA 100	083	17 S									

APPENDIX D

COMPILED STRUCTURAL DATA FOR THE CASAR, LAWNDALE, SHELBY, AND BOILING SPRINGS QUADRANGLES

NOTE: The letters preceding station numbers refer to the quadrangle in which they were collected. CA – Casar. BS – Boiling Springs. SH – Shelby. PV – Polkville. LD – Lawndale. Plate 4 contains the locations of the stations.

	Foliation		Lineation		Fold Axis			Foliation		Lineation		Fold Axis	
Station	Strike	Dip	Trend	Plunge	Trend	Plunge	Station	Strike	Dip	Trend	Plunge	Trend	Plunge
CA 1	N 47 W	30 SW					CA 80	N 65 W	55 SW				
CA 2	N 69 W	60 SW					CA 81	N 59 W	10 NE				
CA 3	N 75 W	35 SW					CA 82	N 30 W	10 NE				
CA 4	N 62 W	15 NE					CA 83	N 58 W	20 NE				
CA 5	N 82 W	10 NE					CA 84	N 40 W	40 SW				
CA 6	N 47 W	80 NE					CA 85	N 70 W	45 SW				
CA 7	N 86 E	10 SE					CA 86	N 84 W	30 SW				
CA 8	N 88 E	10 SE					CA 87	N 83 E	25 SE				
CA 9	N 63 W	15 SW					CA 88	N 88 W	30 SW				
CA 10	N 83 E	50 SE					CA 89	N 86 E	25 SE				
CA 11	N 71 E	50 SE					CA 90	N 87 E	35 SE				
CA 12	N 55 W	30 SW					CA 91	N 20 W	30 NE				
CA 13	N 67 E	10 SE					CA 92	N 12 W	60 NE				
CA 14	N 49 W	15 SW					CA 93	N 30 E	20 NW				
CA 15	N 47 W	20 NE	141	10			CA 94	N 50 E	60 SE				
CA 16	N 89 E	15 SE					CA 95	N 89 E	35 SE				
CA 17	N 61 E	30 SE					CA 96	N 38 W	30 SW				
CA 18	N 38 W	30 NE					CA 97	N 68 W	40 NE				
CA 19	N 16 W	55 NE					CA 98	N 44 E	35 NE				
CA 20	N 42 W	50 SW					CA 99	N 75 W	75 SW				
CA 21	N 89 W	50 SW					CA 100	N 45 E	20 SE				
CA 22	N 74 W	30 SW					CA 101	N 40 E	40 SE				
CA 23	N 81 E	25 NW					CA 102	N 08 E	15 SE				
CA 24	N 89 W	20 SW					CA 103	N 85 W	40 SW				
CA 25	N 75 W	25 SW					CA 104	N 24 E	30 SE				
CA 26	N 50 W	16 SW					CA 105	N 50 E	30 SE				
CA 27	N 88 E	20 SE					CA 106	N 18 W	50 SW				
CA 28	N 74 W	60 SW					CA 107	N 38 E	15 SE				
CA 29	N 11 W	10 NE					CA 108	N 37 E	25 SE				
CA 30	N 63 W	75 NE					CA 109	N 20 W	25 SW				
CA 31	N 75 W	20 SW					CA 110	N 46 E	25 SE				
CA 32	N 44 W	55 NE					CA 111	N 87 E	40 SE				
CA 33	N 18 W	30 NE					CA 112	N 51 E	15 SE				
CA 34	N 84 E	30 SE					CA 113	N 86 E	75 SE				
CA 35	N 29 W	45 SW					CA 114	N 85 E	40 SE				
CA 36	N 75 E	35 SE					CA 115	N 76 W	65 SW				
CA 37	N 33 W	20 SW	104	10			CA 116	N 89 W	15 SW				
CA 38					96	10	CA 117	N 64 E	40 SE				
CA 39	N 75 W	10 SW					CA 118	N 76 E	60 SE				
CA 40			126	10			CA 119	N 77 E	30 SE				
CA 41					295	10	CA 120	N 76 W	15 SW				
CA 42	N 53 W	10 SW					CA 121	N 32 E	10 SE				
CA 43	N 35 W	35 NE					CA 122	N 24 E	55 SE				
CA 44	N 40 W	25 NE					CA 123	N 47 W	50 NE				
CA 45	N 41 W	15 NE					CA 124	N 40 W	35 SW				
CA 46	N 53 W	40 SW					CA 125	N 52 W	30 NE				
CA 47	N 77 W	70 SW					CA 126	N 49 W	20 NE				
CA 48					246	10	CA 127	N 78 E	50 SE				
CA 49	N 87 E	30 SE					CA 128	N 44 E	20 SE				
CA 50	N 37 W	50 SW					CA 129	N 64 E	45 SE				
CA 51	N 33 W	70 SW					CA 130	N 34 E	25 NW				
CA 52	N 41 W	15 SW					CA 131	N 80 W	15 SW				
CA 53	N 08 E	75 NW					CA 132	N 85 E	15 NE				
CA 54	N 66 W	20 SW					CA 133	N 22 W	20 SW				
CA 55	N 81 W	15 NE					CA 134	N 02 E	20 NW				
CA 56	N 56 W	70 SW					CA 135	N 78 W	25 SW				
CA 57					305	15	CA 136	N 56 W	25 NE	331	5		
CA 58	N 69 W	40 SW					CA 137	N 36 E	25 SE				
CA 59			137	20			CA 138	N 07 W	20 SW				
CA 60	N 37 W	40 NE					CA 139	N 05 W	25 SW				
CA 61	N 74 W	30 NE					CA 140	N 07 W	25 NE				
CA 62	N 51 E	30 SE					CA 141	N 39 W	45 SW				
CA 63	N 68 W	40 SW					CA 142	N 56 W	20 SW				
CA 64	N 17 E	10 SE					CA 143	N 50 W	20 SW				
CA 65	N 71 W	80 SW					CA 144	N 06 E	35 SE				
CA 66	N 30 W	20 NE					CA 145	N 89 W	15 SW				
CA 67	N 07 W	25 NE					CA 146	N 22 E	25 SE				
CA 68	N 20 E	15 SE					CA 147	N 33 W	30 NE				
CA 69	N 15 E	80 SE					CA 148	N 39 W	45 SW				
CA 70	N 52 E	60 SE					CA 149	N 32 E	15 SE				
CA 71	N 23 W	20 SW					CA 150	N 74 E	20 SE				
CA 72	N 88 E	40 SE					CA 151	N 36 E	20 NW				
CA 73	N 78 W	30 SW					CA 152	N 34 E	40 SE				
CA 74	N 35 E	40 SE					CA 153	N 08 E	15 NW				
CA 75	N 51 W	50 SW					CA 154	N 78 E	45 SE				
CA 76	N 39 W	50 NE					CA 155	N 46 E	15 NW				
CA 77	N 60 E	35 NW					CA 156	N 79 W	15 NE	332	10		
CA 78	N 46 W	65 SW	128	20			CA 157	N 33 E	45 SE				
CA 79	N 64 E	25 SW					CA 158	N 41 W	20 NE				
CA 159	N 26 E	40 SE					CA 238	N 56 W	70 SW				
CA 160	N 38 W	20 NE					CA 239	N 19 W	80 NE				
CA 161	N 19 E	40 SE					CA 240	N 30 E	55 SE				
CA 162	N 36 W	25 NE					CA 241	N 73 W	70 NE				
CA 163	N 55 W	15 SW					CA 242	N 81 W	65 SW				
CA 164	N 35 W	40 NE					CA 243	N 86 W	75 SW				
CA 165	N 61 W	45 NE					CA 244	N 46 W	70 NE				
CA 166	N 25 W	45 NE					CA 245	N 56 W	65 NE				
CA 167	N 08 E	15 NW					CA 246	N 34 W	60 SW	296	30		
CA 168	N 68 W	35 SW					CA 247	N 61 W	70 SW				
CA 169	N 87 W	50 SW					CA 248	N 29 W	25 SW				
CA 170	N 65 E	35 SE					CA 249	N 60 E	25 SE				

	Foliation		Lineation		Fold Axis			Foliation		Lineation		Fold Axis	
Station	Strike	Dip	Trend	Plunge	Trend	Plunge	Station	Strike	Dip	Trend	Plunge	Trend	Plunge
CA 171	N 23 W	10 NE					CA 250	N 14 W	25 NE				
CA 172	N 05 W	10 NE					CA 251	N 84 W	40 SW				
CA 173	N 72 W	20 SW					CA 252	N 82 E	40 NW				
CA 174	N 50 W	20 SW					CA 253	N 86 E	40 SE				
CA 175	N 29 W	15 NE					CA 254	N 43 W	75 SW				
CA 176	N 25 E	35 SE					CA 255	N 56 W	70 SW				
CA 177	N 27 W	30 SW					CA 256	N 60 W	40 SW				
CA 178	N 40 E	15 NW					CA 257	N 89 E	40 SE				
CA 179	N 72 W	30 NE					CA 258	N 66 E	45 SE				
CA 180	N 73 W	25 NE					CA 259	N 49 W	70 SW				
CA 181	N 47 W	30 NE					CA 260	N 51 W	45 SW				
CA 182	N 07 W	40 NE	154	25			CA 261	N 37 W	45 SW				
CA 183	N 09 W	30 NE					CA 262	N 52 W	65 SW				
CA 184	N 09 W	30 NE					CA 263	N 84 W	35 SW				
CA 185	N 14 E	35 SE					CA 264	N 88 E	80 SE				
CA 186	N 15 W	40 NE					CA 265	N 79 W	50 SW				
CA 187	N 57 W	15 NE					CA 266	N 45 W	30 SW				
CA 188	N 83 E	15 SE					CA 267	N 85 W	60 SW				
CA 189	N 30 W	45 SW					CA 268	N 84 E	50 SE				
CA 190	N 87 E	70 SE					CA 269	N 54 W	35 NE				
CA 191	N 06 W	70 NE					CA 270	N 57 W	60 NE				
CA 192	N 60 W	65 SW					CA 271	N 48 E	20 SE				
CA 193	N 31 W	30 NE					CA 272	N 35 E	35 SE				
CA 194	N 66 W	50 NE					CA 273	N 47 E	25 SE				
CA 195	N 70 W	55 SW					CA 274	N 28 E	60 SE				
CA 196	N 50 W	30 SW					CA 275	N 63 W	60 SW				
CA 197	N 43 W	35 SW					CA 276	N 29 W	40 SW				
CA 198	N 59 W	75 SW					CA 277	N 87 E	15 SE				
CA 199	N 88 E	25 SE	143	15			CA 278	N 44 E	35 SE				
CA 200	N 74 E	30 SE					CA 279	N 68 E	10 SE				
CA 201	N 33 W	40 NE					CA 280	N 36 W	40 SW				
CA 202	N 61 W	55 SW					CA 281	N 58 E	50 SW				
CA 203	N 35 W	40 NE					CA 282	N 34 W	45 SW				
CA 204	N 62 W	35 NE					CA 283	N 37 W	65 SW				
CA 205	N 85 W	30 NE					CA 284	N 31 W	45 SW				
CA 206	N 39 W	80 NE					CA 285	N 23 W	75 SW				
CA 207	N 85 W	10 SW					CA 286	N 39 W	85 NE				
CA 208	N 45 W	65 SW					CA 287	N 62 W	55 NE				
CA 209	N 89 W	65 SW					CA 288	N 42 W	65 NE				
CA 210	N 61 W	75 SW					CA 289	N 26 W	65 NE				
CA 211	N 47 W	15 SW					CA 290	N 49 W	40 SW				
CA 212	N 89 W	65 SW					CA 291	N 44 W	55 SW				
CA 213	N 41 W	80 SW					CA 292	N 65 W	75 SW				
CA 214	N 86 W	15 SW					CA 293	N 65 W	55 SW				
CA 215	N 29 W	15 NE					CA 294	N 26 W	85 SW				
CA 216	N 65 W	65 SW					CA 295	N 60 W	55 SW				
CA 217	N 66 W	50 SW					CA 296	N 70 W	60 SW				
CA 218	N 56 W	65 SW					CA 297	N 52 W	70 NE				
CA 219	N 66 W	85 SW					CA 298	N 63 W	55 SW				
CA 220	N 85 W	50 SW					CA 299	N 75 E	15 SE				
CA 221	N 18 W	30 NE					CA 300	N 53 W	35 SW				
CA 222	N 83 W	10 NE					CA 301	N 63 W	50 SW				
CA 223	N 13 E	35 SE					CA 302	N 03 W	25 SW				
CA 224	N 04 E	35 SE					CA 303	N 47 E	25 SE				
CA 225	N 54 E	45 SE					CA 304	N 52 W	25 SW				
CA 226	N 38 W	25 SW					CA 305	N 28 W	55 SW				
CA 227	N 21 E	55 SE					CA 306	N 49 W	70 SW				
CA 228	N 06 E	15 SE					CA 307	N 51 W	55 SW				
CA 229	N 40 W	15 NE					CA 308	N 34 W	75 SW				
CA 230	N 40 E	10 SE					CA 309	N 89 W	35 SW				
CA 231	N 85 W	80 NE					CA 310	N 38 W	60 SW				
CA 232	N 84 W	70 SW					CA 311	N 51 E	20 SE				
CA 233	N 13 E	35 SE					CA 312	N 34 W	40 SW				
CA 234	N 75 W	20 SW					CA 313	N 89 W	25 SW				
CA 235	N 55 W	75 NE					CA 314	N 51 W	60 SW				
CA 236	N 73 E	20 SE					CA 315	N 34 W	70 SW				
CA 237	N 59 W	50 NE					CA 316	N 49 W	55 SW				
CA 317	N 88 E	30 SE					CA 396	N 20 W	20 NE				
CA 318	N 85 W	20 SW					CA 397	N 41 W	25 NE				
CA 319	N 49 W	55 SW					CA 398	N 30 E	20 NW				
CA 320	N 88 W	50 SW					CA 399	N 08 E	35 NW				
CA 321	N 56 W	50 SW					CA 400	N 28 E	25 SE				
CA 322	N 40 W	50 SW					CA 401	N 42 W	20 SW				
CA 323	N 89 E	55 SE					CA 402	N 49 W	50 SW				
CA 324	N 74 W	45 SW					CA 403	N 40 W	45 SW				
CA 325	N 40 W	60 SW					CA 404	N 11 W	35 SW				
CA 326	N 37 W	65 NE					CA 405	N 27 E	45 SE				
CA 327	N 53 W	65 NE					CA 406	N 57 E	55 SE				
CA 328	N 36 W	45 SW					CA 407	N 88 E	35 SE				
CA 329	N 43 W	60 SW					CA 408	N 40 W	15 NE				
CA 330	N 56 W	25 SW					CA 409	N 40 W	20 NE				
CA 331	N 19 W	60 SW					CA 410	N 45 W	20 NE				
CA 332	N 32 W	50 SW					CA 411	N 03 E	20 SE				
CA 333	N 42 W	35 SW					CA 412	N 36 E	65 SE				
CA 334	N 50 W	45 SW					CA 413	N 14 W	20 NE				
CA 335	N 51 W	65 SW					CA 414	N 76 W	30 NE				
CA 336	N 30 W	60 SW					CA 415	N 68 E	26 NW				
CA 337	N 42 W	40 SW					CA 416	N 08 W	10 SW				
CA 338	N 67 W	55 SW					CA 417	N 40 W	30 NE				
CA 339	N 52 W	50 SW					CA 418	N 24 W	20 NE	89	15		
CA 340	N 67 W	40 SW					CA 419	N 58 W	35 NE				

	Foliation		Lineation		Fold Axis			Foliation		Lineation		Fold Axis	
Station	Strike	Dip	Trend	Plunge	Trend	Plunge	Station	Strike	Dip	Trend	Plunge	Trend	Plunge
CA 341	N 52 W	50 SW					CA 420	N 50 E	10 SE				
CA 342	N 67 W	40 SW					CA 421	N 22 W	30 NE				
CA 343	N 52 W	60 SW					CA 422	N 15 E	25 NW				
CA 344	N 38 W	60 SW					CA 423	N 28 W	20 SW				
CA 345	N 24 W	80 SW					CA 424	N 18 E	20 SW				
CA 346	N 84 W	80 SW					CA 425	N 30 W	10 NE				
CA 347	N 37 W	45 SW					CA 426	N 36 W	15 SW				
CA 348	N 52 W	45 SW					CA 427	N 06 W	10 SW				
CA 349	N 67 W	25 SW					CA 428	N 66 W	30 NE				
CA 350	N 65 W	50 NE					CA 429	N 46 W	15 NE				
CA 351	N 44 W	50 SW	159	15			CA 430	N 80 W	20 SW				
CA 352	N 33 E	45 SE					CA 431	N 43 W	55 NE				
CA 353	N 51 W	55 SW					CA 432	N 65 W	35 NE				
CA 354	N 32 W	50 SW					CA 433	N 73 E	20 NW				
CA 355	N 69 W	75 SW					CA 434	N 40 W	15 NE				
CA 356	N 76 W	60 NE					CA 435	N 02 W	35 NE				
CA 357	N 33 W	30 NE					CA 436	N 51 E	15 NW				
CA 358	N 60 W	60 SW					CA 437	N 74 W	15 NE				
CA 359	N 29 W	45 SW					CA 438	N 55 E	15 SE				
CA 360	N 59 W	30 SW					CA 439	N 11 E	10 NW	329	15		
CA 361	N 62 W	30 SW					CA 440	N 20 W	55 SW				
CA 362	N 46 W	35 SW					CA 441	N 20 E	35 SE				
CA 363	N 46 W	35 SW					CA 442	N 02 E	35 SE				
CA 364	N 89 W	70 SW					CA 443	N 33 W	30 NE				
CA 365	N 80 W	15 SW					CA 444	N 39 W	25 NE				
CA 366	N 66 E	15 SE					CA 445	N 83 W	25 NE				
CA 367	N 87 E	15 SE					CA 446	N 73 E	40 SE				
CA 368	N 77 W	70 SW					CA 447	N 20 W	15 SW				
CA 369	N 51 E	15 SE					CA 448	N 54 E	25 SE				
CA 370	N 59 E	30 SE	145	30			CA 449	N 23 E	25 SE				
CA 371	N 75 E	20 SE					CA 450	N 22 W	45 NE				
CA 372	N 46 W	50 SW					CA 451	N 72 E	30 SE				
CA 373	N 31 W	30 SW					CA 452	N 56 W	20 SW				
CA 374	N 15 W	30 NE					CA 453	N 37 E	25 SE				
CA 375	N 37 W	20 SW					CA 454	N 18 E	20 SE				
CA 376	N 38 W	20 NE					CA 455	N 89 W	60 NE				
CA 377	N 22 E	50 SE					CA 456	N 69 W	20 NE				
CA 378	N 48 E	20 SE					CA 457	N 06 E	40 SE				
CA 379	N 57 W	80 SW					CA 458	N 16 E	10 NW				
CA 380	N 44 W	15 NE					CA 459	N 04 W	15 SW				
CA 381	N 35 E	20 SE					CA 460	N 16 E	20 SE	319	5		
CA 382	N 70 E	35 SE					CA 461	N 36 W	25 SW				
CA 383	N 08 E	60 SE					CA 462	N 27 W	20NE				
CA 384	N 34 E	40 SE					CA 463	N 86 E	30 SE				
CA 385	N 27 E	40 SE					CA 464	N 21 W	30 SW				
CA 386	N 29 W	30 NE					CA 465	N 88 W	35 SW	131	30		
CA 387	N 45 W	25 SW					CA 466	N 47 W	25 SW				
CA 388	N 25 W	25 NE					CA 467	N 84 W	30 SW				
CA 389	N 42 W	35 SW					CA 468	N 28 W	15 NE				
CA 390	N 34 E	20 SE					CA 469	N 11 E	30 SE				
CA 391	N 63 E	45 SE					CA 470	N 05 W	10 NE				
CA 392	N 88 W	55 SW					CA 471	N 42 E	20 SE				
CA 393	N 24 W	15 NE					CA 472	N 21 E	10 SE				
CA 394	N 40 W	40 SW					CA 473	N 32 E	15 SE				
CA 395	N 08 W	45 NE					CA 474	N 89 W	10 SW				
CA 475	N 32 E	15 NW					CA 554	N 67 W	25 NE				
CA 476	N 89 W	10 SW					CA 555	N 55 E	20 SE				
CA 477	N 39 E	35 SE					CA 556	N 85 E	30 SE				
CA 478	N 08 E	15 SE					CA 557	N 70 E	15 SE				
CA 479	N 89 W	15 NE					CA 558	N 25 E	25 NW				
CA 480	N 72 E	20 SE					CA 559	N 67 E	25 SE				
CA 481	N 68 E	25 SE	148	20			CA 560	N 85 E	30 SE				
CA 482	N 54 E	15 SE					CA 561	N 33 E	15 SE				
CA 483	N 20 E	15 SE					CA 562	N 67 E	10 NW				
CA 484	N 44 E	55 SE					CA 563	N 09 W	15 NE				
CA 485	N 45 E	20 NW					CA 564	N 03 E	15 NW				
CA 486	N 45 W	20 SW					CA 565	N 62 W	65 NE				
CA 487	N 55 E	25 SE	98	20			CA 566	N 06 W	25 NE				
CA 488	N 21 W	30 SW					CA 567	N 62 E	20 SE				
CA 489	N 55 W	20 SW					CA 568	N 03 W	25 SW				
CA 490	N 65 W	30 SW					CA 569	N 56 W	30 NE				
CA 491	N 63 W	60 NE					CA 570	N 78 E	10 SE				
CA 492	N 25 W	10 NE					CA 571	N 38 E	20 SE				
CA 493	N 54 E	10 NW					CA 572	N 24 W	20 NE				
CA 494	N 87 E	20 NW					CA 573	N 46 W	15 SW				
CA 495	N 23 W	30 NE					CA 574	N 34 E	20 SE				
CA 496	N 87 W	20 NE					CA 575	N 13 E	10 SE				
CA 497	N 80 E	25 NW					CA 576	N 10 E	10 NW				
CA 498	N 49 W	20 SW					CA 577	N 59 W	15 NE				
CA 499	N 39 W	5 NE					CA 578	N 85 W	5 SW				
CA 500	N 49 W	10 NE					CA 579	N 84 W	15 NE				
CA 501	N 71 W	20 SW					CA 580	N 87 W	20 NE				
CA 502	N 42 W	35 SW					CA 581	N 10 W	35 NE				
CA 503	N 48 E	75 NW					CA 582	N 89 E	15 SE				
CA 504	N 85 W	45 SW	144	25			CA 583	N 83 E	45 SE				
CA 505	N 65 E	25 SE					CA 584	N 80 E	35 SE				
CA 506	N 71 E	30 SE					CA 585	N 44 W	10 SW				
CA 507	N 20 E	25 SE					CA 586	N 83 E	20 SE				
CA 508	N 08 W	25 NE					CA 587	N 78 W	10 SW				
CA 509	N 67 W	15 NE					CA 588	N 13 W	15 NE				
CA 510	N 38 E	65 SE					CA 589	N 05 E	30 SE				

	Foliation		Lineation		Fold Axis			Foliation		Lineation		Fold Axis	
Station	Strike	Dip	Trend	Plunge	Trend	Plunge	Station	Strike	Dip	Trend	Plunge	Trend	Plunge
CA 511	N 64 E	10 NW					CA 590	N 33 E	10 SE				
CA 512	N 40 W	10 NE					CA 591	N 07 W	15 NE				
CA 513	N 42 W	30 NE					CA 592	N 03 W	20 NE				
CA 514	N 61 W	45 SW					CA 593	N 75 W	10 SE				
CA 515	N 17 E	45 SE					CA 594	N 89 W	10 NE				
CA 516	N 13 E	20 SE					CA 595	N 56 E	10 SE				
CA 517	N 38 W	10 SW					CA 596	N 59 E	15 SE				
CA 518	N 39 E	55 SE					CA 597	N 08 W	20 NE				
CA 519	N 53 E	25 SE					CA 598	N 58 E	15 SE				
CA 520	N 07 W	30 NE					CA 599	N 72 W	15 SW				
CA 521	N 10 E	20 NW					CA 600	N 86 E	15 SE				
CA 522	N 20 W	40 NE					CA 601	N 45 E	15 SE				
CA 523	N 75 E	25 NW					CA 602	N 41 E	10 SE				
CA 524	N 05 W	30 NE					CA 603	N 21 E	15 SE				
CA 525	N 46 E	25 SE					CA 604					29	5
CA 526	N 79 W	15 NE					CA 605	N 61 W	30 SW				
CA 527	N 44 W	10 NE					CA 606	N 56 E	10 SE				
CA 528	N 28 E	20 SE					CA 607	N 02 E	25 SE				
CA 529	N 63 W	20 SW					CA 608	N 56 E	30 SE				
CA 530	N 22 E	10 SE					CA 609	N 51 W	35 NE				
CA 531	N 32 E	20 SE					CA 610	N 73 W	50 SW				
CA 532	N 85 W	10 SW					CA 611	N 05 E	15 SE				
CA 533	N 26 E	10 SE					CA 612	N 04 W	30 SW				
CA 534	N 36 E	25 SE					CA 613	N 51 E	30 SE				
CA 535	N 73 W	20 SW	138	10			CA 614	N 88 E	25 SE				
CA 536	N 38 W	20 SW					CA 615	N 42 W	25 SW				
CA 537	N 03 W	45 SW					CA 616	N 42 W	15 SW				
CA 538	N 23 E	15 NW					CA 617	N 57 W	20 SW				
CA 539	N 51 W	10 SW					CA 618	N 49 E	30 SE				
CA 540	N 80 W	10 SW					CA 619					170	10
CA 541	N 62 W	15 SW					CA 620	N 78 E	15 NW				
CA 542	N 17 W	65 NE					CA 621	N 34 W	15 SW				
CA 543	N 34 E	25 SE					CA 622	N 11 E	30 SE				
CA 544	N 88 W	25 SW					CA 623	N 76 E	30 SE				
CA 545	N 88 E	20 SE					CA 624	N 75 E	20 SE				
CA 546	N 83 W	15 SW					CA 625	N 32 W	35 SW				
CA 547	N 82 W	15 SW					CA 626	N 13 W	30 SW				
CA 548	N 72 W	35 SW					CA 627	N 89 E	30 SE				
CA 549	N 73 E	15 SE					CA 628	N 40 W	10 NE				
CA 550	N 64 E	20 SE					CA 629	N 87 E	30 SE				
CA 551	N 21 W	25 SW					CA 630	N 45 W	20 SW				
CA 552	N 22 E	15 SE					CA 631	N 87 E	30 SE				
CA 553	N 24 W	25 NE					CA 632	N 45 W	20 SW				
CA 633	N 03 W	35 SW	285	15			CA 712	N 21 E	30 SE				
CA 634	N 21 E	20 SE					CA 713	N 07 E	15 SE				
CA 635	N 37 W	50 SW					CA 714					330	15
CA 636	N 52 E	20 NW					CA 715	N 08 W	70 NE				
CA 637	N 83 E	15 SE					CA 716	N 14 W	60 SW				
CA 638	N 71 E	25 SE					CA 717	N 45 W	25 NE				
CA 639	N 10 W	10 NE					CA 718	N 10 W	35 SW				
CA 640	N 41 W	20 NE					CA 719	N 80 E	30 NW				
CA 641	N 87 W	20 NE					CA 720	N 37 W	30 NE				
CA 642	N 33 E	30 SE					CA 721	N 07 E	30 SE				
CA 643	N 17 E	20 SE					CA 722	N 13 W	35 NE				
CA 644	N 06 W	20 NE					CA 723	N 45 W	20 NE				
CA 645	N 34 E	15 NW					CA 724	N 30 E	20 SE				
CA 646	N 47 E	50 SE					CA 725	N 05 E	50 SE				
CA 647	N 43 W	20 NE					CA 726	N 39 W	30 NE				
CA 648	N 04 E	20 SE					CA 727	N 21 E	10 NW				
CA 649	N 37 W	15 SW					CA 728	N 76 W	15 SW				
CA 650	N 46 W	15 SW					CA 729	N 18 E	20 SE				
CA 651	N 82 E	15 SE					CA 730	N 73 W	10 NE				
CA 652	N 46 E	15 NW					CA 731	N 85 W	50 SW				
CA 653	N 39 E	15 SE					CA 732	N 14 E	60 NW				
CA 654	N 88 W	10 SW					CA 733	N 16 W	30 SW				
CA 655	N 10 E	45 SE					CA 734	N 47 E	50 SE				
CA 656	N 29 E	15 SE					CA 735	N 85 W	50 SW				
CA 657	N 27 E	15 SE					CA 736	N 60 W	45 SW				
CA 658	N 83 W	15 SW					CA 737	N 10 E	30 NW				
CA 659	N 43 W	30 NE					CA 738	N 81 W	30 SW				
CA 660	N 24 W	15 NE					CA 739	N 10 W	20 NE				
CA 661	N 80 E	15 NW					CA 740	N 23 W	25 NE				
CA 662	N 37 W	15 SW					CA 741	N 23 E	35 NW				
CA 663	N 37 E	30 NW					CA 742	N 57 E	30 NW				
CA 664	N 24 E	10 NW					CA 743	N 43 W	15 NE				
CA 665	N 64 W	10 SW					CA 744	N 28 W	15 NE				
CA 666	N 59 W	15 NE					CA 745			328	10		
CA 667	N 23 W	40 NE					CA 746	N 41 E	35 SE				
CA 668	N 38 W	20 NE					CA 747	N 18 E	25 SE				
CA 669	N 49 E	20 SE					CA 748	N 17 W	30 NE				
CA 670	N 62 W	20 SW					CA 749	N 31 E	30 SE				
CA 671	N 09 E	40 SE					CA 750	N 42 E	40 SE				
CA 672	N 17 W	20 SW					CA 751	N 83 W	15 NE				
CA 673	N 38 E	20 SE					CA 752	N 39 W	10 NE				
CA 674	N 31 W	20 SW					CA 753	N 88 E	15 SE				
CA 675	N 74 W	15 SW					CA 754	N 80 E	15 SE				
CA 676	N 53 W	20 NE					CA 755	N 06 E	10 NW				
CA 677	N 34 E	25 SE					CA 756	N 08 W	30 NE				
CA 678	N 09 W	15 NE					CA 757	N 65 E	50 SE				
CA 679	N 51 W	15 SW					CA 758	N 53 W	30 NE				
CA 680	N 83 W	15 SW					CA 759	N 40 W	35 NE				

	Foliation		Lineation		Fold Axis			Foliation		Lineation		Fold Axis	
Station	Strike	Dip	Trend	Plunge	Trend	Plunge	Station	Strike	Dip	Trend	Plunge	Trend	Plunge
CA 681	N 21 W	15 SW					CA 760	N 72 E	15 NW				
CA 682	N 81 E	25 SE					CA 761	N 23 E	15 NW				
CA 683	N 66 W	55 SW					CA 762	N 75 W	10 SW				
CA 684	N 36 W	55 SW					CA 763	N 24 W	10 NE				
CA 685	N 39 W	10 NE					CA 764	N 35 E	15 SE				
CA 686					148	5	CA 765	N 56 W	10 NE				
CA 687	N 67 E	10 NW					CA 766	N 49 W	30 SW				
CA 688	N 21 E	15 NW					CA 767	N 60 W	5 NE				
CA 689	N 88 W	10 NE					CA 768	N 88 W	5 NE				
CA 690	N 68 E	45 NW					CA 769	N 71 W	30 NE				
CA 691	N 34 W	10 NE	151	5			CA 770	N 39 E	40 NW				
CA 692	N 35 E	20 SE					CA 771	N 24 W	40 NE				
CA 693	N 89 E	5 NW					CA 772	N 11 W	40 NE				
CA 694	N 07 E	40 SE					CA 773	N 02 E	15 SE				
CA 695			42	5			CA 774	N 36 W	30 NE				
CA 696	N 07 W	5 NE					CA 775					26	10
CA 697	N 07 E	15 NW					CA 776	N 28 E	40 SE				
CA 698	N 28 E	15 NW					CA 777	N 59 E	15 SE				
CA 699	N 16 E	15 NW					CA 778	N 53 W	20 SW				
CA 700	N 17 W	30 NE					CA 779	N 44 W	30 NE				
CA 701	N 48 E	25 SE					CA 780	N 04 E	30 SE				
CA 702	N 40 E	30 NW					CA 781	N 04 W	25 NE				
CA 703	N 32 W	20 NE					CA 782	N 34 W	35 NE				
CA 704	N 05 W	20 NE					CA 783	N 07 E	15 SE				
CA 705	N 06 W	30 NE					CA 784	N 01 E	20 SE				
CA 706	N 29 E	20 NW					CA 785	N 03 E	40 SE				
CA 707	N 16 W	20 NE					CA 786	N 24 W	55 NE				
CA 708	N 36 W	15 SW					CA 787	N 22 W	20 NE				
CA 709	N 13 W	20 NE					CA 788	N 11 W	15 NE				
CA 710	N 06 W	30 NE					CA 789	N 56 E	20 SE				
CA 711	N 10 W	20 NE					CA 790	N 09 W	30 NE				
CA 791	N 04 W	80 NE					CA 870	N 37 E	30 SE				
CA 792	N 09 E	45 SE					CA 871	N 23 E	30 SE				
CA 793	N 05 W	30 NE					CA 872	N 28 W	15 SW				
CA 794	N 05 E	20 SE					CA 873	N 24 E	40 SE				
CA 795	N 23 W	40 NE					CA 874	N 11 W	35 NE				
CA 796	N 69 W	15 NE					CA 875	N 68 E	35 SE				
CA 797	N 25 E	25 SE					CA 876	N 20 W	45 SW				
CA 798	N 77 W	35 NE					CA 877	N 59 W	20 SW				
CA 799	N 56 E	35 SE					CA 878	N 63 W	20 SW				
CA 800	N 41 E	55 SE					CA 879	N 87 E	20 SE				
CA 801	N 69 E	40 SE					CA 880	N 75 E	20 SE				
CA 802	N 78 W	60 SW					CA 881	N 22 E	30 SE				
CA 803	N 89 E	60 SE					CA 882	N 08 W	20 NE				
CA 804	N 17 W	55 NE					CA 883	N 67 W	30 NE				
CA 805	N 35 E	20 SE					CA 884	N 85 W	20 SW				
CA 806	N 36 E	40 SE					CA 885	N 47 W	30 SW				
CA 807	N 20 E	30 SE					CA 886	N 19 W	10 SW				
CA 808	N 62 W	20 NE					CA 887	N 26 E	10 SE				
CA 809	N 05 W	20 NE					CA 888	N 66 E	10 SE				
CA 810	N 70 W	15 NE					CA 889	N 61 E	20 SE				
CA 811	N 66 E	20 SE					CA 890	N 13 E	10 NW				
CA 812	N 62 E	20 SE					CA 891	N 34 W	20 SW				
CA 813	N 84 W	65 SW					CA 892	N 11 W	20 SW				
CA 814	N 61 E	40 SE					CA 893	N 08 E	35 SE				
CA 815	N 06 E	35 SE					CA 894	N 19 E	35 NW				
CA 816	N 13 E	35 SE					CA 895	N 86 W	5 SW				
CA 817	N 16 E	65 SE					CA 896	N 67 W	10 SW				
CA 818	N 60 E	35 SE					CA 897	N 22 W	15 SW				
CA 819	N 42 E	20 SE	152	5			CA 898	N 37 W	20 NE				
CA 820	N 35 E	40 SE					CA 899	N 32 W	50 NE				
CA 821	N 54 W	40 SW					CA 900	N 43 W	25 SW				
CA 822	N 66 W	40 SW					CA 901	N 40 E	15 SE				
CA 823	N 56 W	25 SW					CA 902	N 22 E	15 NW				
CA 824	N 51 E	15 SE					CA 903	N 89 E	5 SE				
CA 825	N 45 W	30 SW					CA 904	N 37 W	20 NE				
CA 826	N 83 E	50 SE					CA 905	N 28 E	15 NW				
CA 827	N 22 E	40 SE					CA 906	N 26 W	15 NE				
CA 828	N 42 E	35 SE					CA 907	N 88 W	15 SW				
CA 829	N 27 E	15 SE					CA 908	N 78 W	25 SW				
CA 830	N 19 E	25 SE					CA 909	N 63 W	15 SW				
CA 831	N 39 E	30 SE					CA 910	N 75 W	25 SW				
CA 832					165	20	CA 911	N 63 W	30 SW				
CA 833	N 04 E	20 SE					CA 912	N 75 W	25 SW				
CA 834	N 35 W	15 NE					CA 913	N 64 W	50 SW				
CA 835	N 35 W	40 SW					CA 914	N 32 W	60 SW				
CA 836	N 55 E	30 SE					CA 915	N 30 W	40 SW				
CA 837	N 56 E	40 SE					CA 916	N 04 E	30 NW				
CA 838	N 41 E	35 SE					CA 917	N 22 W	30 SW				
CA 839	N 04 W	45 NE					CA 918	N 59 W	15 NE				
CA 840	N 56 E	45 SE					CA 919	N 77 W	20 NE				
CA 841	N 64 E	40 SE					CA 920	N 66 W	5 SW				
CA 842	N 40 E	20 SE					CA 921	N 25 W	5 NE				
CA 843	N 14 E	20 SE					CA 922	N 38 W	20 SW				
CA 844	N 42 E	30 SE					CA 923	N 67 W	30 SW				
CA 845	N 31 E	20 SE	128	15			CA 924	N 21 E	30 SE				
CA 846	N 37 E	25 SE					CA 925			133	5		
CA 847	N 07 W	10 NE					CA 926	N 47 W	15 SW				
CA 848	N 28 E	60 SE					CA 927	N 12 W	15 SW				
CA 849					340	10	CA 928	N 10 E	35 SE				
CA 850	N 29 E	35 SE					CA 929					344	10

	Foliation		Lineation		Fold Axis			Foliation		Lineation		Fold Axis	
Station	Strike	Dip	Trend	Plunge	Trend	Plunge	Station	Strike	Dip	Trend	Plunge	Trend	Plunge
CA 851	N 46 E	40 SE					CA 930	N 06 E	20 NW				
CA 852	N 17 E	70 SE					CA 931	N 51 E	25 NW				
CA 853	N 37 E	70 SE					CA 932	N 66 E	30 NW				
CA 854	N 29 W	70 NE					CA 933	N 34 W	25 SW				
CA 855	N 18 W	60 NE					CA 934	N 76 W	15 SW				
CA 856	N 33 W	20 NE					CA 935	N 36 W	30 SW				
CA 857	N 31 E	30 SE					CA 936	N 09 W	25 SW				
CA 858	N 37 W	20 SW					CA 937	N 37 W	20 SW				
CA 859	N 44 E	15 SE					CA 938	N 37 W	15 SW				
CA 860	N 64 E	35 SE					CA 939					163	5
CA 861	N 08 W	40 NE					CA 940	N 84 W	30 SW				
CA 862	N 28 W	80 NE					CA 941	N 79 E	15 SE	153	10		
CA 863	N 18 W	30 NE					CA 942	N 49 W	25 SW				
CA 864	N 20 W	20 NE					CA 943	N 54 E	15 SE				
CA 865	N 33 E	50 SE					CA 944	N 60 W	30 SW				
CA 866	N 12 E	15 SE					CA 945	N 28 E	15 SE				
CA 867	N 25 E	60 SE					CA 946	N 13 W	15 SW				
CA 868	N 25 E	60 SE					CA 947	N 82 E	20 SE				
CA 869	N 53 E	40 SE					CA 948	N 42 E	30 SE				
CA 949	N 86 W	30 SW					CA 1028	N 32 W	20 SW				
CA 950	N 46 W	25 SW					CA 1029	N 05 E	30 NW				
CA 951	N 16 W	15 SW					CA 1030	N 39 E	40 SE				
CA 952					93	5	CA 1031	N 56 W	15 SW				
CA 953	N 61 E	5 SE					CA 1032	N 03 E	40 SE				
CA 954	N 22 E	15 SE					CA 1033	N 21 W	50 NE				
CA 955	N 22 E	15 SE					CA 1034	N 27 E	15 SE				
CA 956	N 05 W	45 NE					CA 1035	N 14 W	10 NE				
CA 957	N 80 W	10 NE					CA 1036	N 23 E	15 NW				
CA 958	N 42 E	20 SE					CA 1037	N 88 E	10 SE				
CA 959	N 47 W	10 NE					BS 1	N 88 E	70 SE				
CA 960	N 34 E	5 SE					BS 2	N 33 W	15 SW				
CA 961	N 79 W	25 NE					BS 3	N 86 W	5 NE				
CA 962	N 54 E	10 SE					BS 4	N 58 W	60 SW				
CA 963	N 20 E	30 NW					BS 5	N 47 W	50 SW				
CA 964	N 26 W	20 NE					BS 6	N 47 W	50 SW				
CA 965	N 24 W	20 NE					BS 7	N 64 W	85 SW				
CA 966	N 89 E	10 NW					BS 8	N 60 W	60 SW				
CA 967	N 30 W	25 NE					BS 9	N 55 E	30 NW				
CA 968	N 32 W	25 NE					BS 10	N 47 W	40 SW				
CA 969	N 16 W	50 NE					BS 11	N 79 E	50 SE				
CA 970	N 27 E	65 NW					BS 12	N 66 E	45 SE				
CA 971	N 80 E	20 SE					BS 13	N 89 W	60 SW				
CA 972	N 13 E	70 NW					BS 14	N 71 W	40 SW				
CA 973	N 18 E	30 SE					BS 15	N 22 W	20 NE				
CA 974	N 14 W	20 SW					BS 16	N 61 W	80 SW				
CA 975	N 22 W	35 SW					BS 17	N 64 W	15 SW				
CA 976	N 44 W	20 SW					BS 18	N 67 W	45 SW				
CA 977	N 09 E	40 NW					BS 19	N 56 W	20 SW				
CA 978	N 58 E	30 SE					BS 20	N 67 W	80 SW				
CA 979	N 67 W	20 NE					BS 21	N 56 W	20 SW				
CA 980	N 31 W	45 NE					BS 22	N 74 W	30 SW				
CA 981	N 42 W	20 NE	103	10			BS 23	N 73 W	70 SW				
CA 982	N 08 E	15 SE	127	10			BS 24					292	10
CA 983	N 04 E	30 NW					BS 25					112	5
CA 984	N 46 W	25 NE					BS 26	N 69 E	60 SE				
CA 985	N 37 E	10 NW	311	10			BS 27	N 83 E	50 NW				
CA 986	N 59 W	40 NE					BS 28	N 76 E	60 NW				
CA 987	N 84 W	15 NE					BS 29	N 22 E	60 SE				
CA 988	N 10 E	15 SE					BS 30	N 24 W	60 SW				
CA 989	N 15 W	20 SW					BS 31	N 31 W	50 SW				
CA 990	N 48 W	15 NE					BS 32	N 31 W	50 SW				
CA 991	N 22 W	15 NE					BS 33	N 85 E	20 SE				
CA 992	N 24 E	60 NW					BS 34	N 46 E	45 NW				
CA 993					224	10	BS 35	N 27 E	45 NW				
CA 994	N 70 E	25 SE					BS 36	N 14 E	45 NW				
CA 995	N 30 E	20 SE					BS 37	N 21 E	40 NW				
CA 996	N 41 E	15 SE	99	10			BS 38	N 86 W	30 NE				
CA 997	N 87 W	10 NE					BS 39	N 81 W	65 NE				
CA 998	N 20 W	15 NE					BS 40	B 81 W	20 NE				
CA 999	N 46 E	50 SE					BS 41	B 23 E	30 NW				
CA 1000	N 30 W	20 SW					BS 42	N 35 E	40 NW				
CA 1001	N 22 E	20 NW	304	20			BS 43	N 63 E	35 NW				
CA 1002	N 58 W	15 SW	265	10			BS 44	N 58 E	50 NW				
CA 1003	N 26 W	20 NE					BS 45	N 49 W	30 NE				
CA 1004	N 11 E	40 SE					BS 46	N 56 E	30 NW				
CA 1005	N 24 E	20 SE	141	15			BS 47	N 44 E	45 NW				
CA 1006	N 17 E	40 SE					BS 48	N 36 E	20 NW				
CA 1007	N 39 W	30 NE					BS 49	N 20 E	35 NW				
CA 1008	N 47 W	20 NE					BS 50	N 40 E	30 NW				
CA 1009	N 29 W	25 NE					BS 51	N 69 E	35 NW				
CA 1010	N 24 W	20 NE	87	20			BS 52	N 12 W	30 SW				
CA 1011	N 69 W	10 SW					BS 53	N 8 E	30 NW				
CA 1012	N 52 W	25 SW					BS 54	N 56 E	30 NW				
CA 1013	N 42 E	20 NW					BS 55	N 14 W	20 SW				
CA 1014	N 63 W	20 SW					BS 56	N 82 W	15 NE				
CA 1015	N 51 W	40 SW					BS 57	N 35 E	30 SE				
CA 1016	N 35 E	40 SE					BS 58	N 3 W	30 NE				
CA 1017	N 87 E	15 SE					BS 59	N 37 E	20 SE				
CA 1018	N 42 W	20 SW					BS 60	N 60 E	30 SE				
CA 1019	N 23 W	40 SW					BS 61	N 9 W	20 NE				
CA 1020	N 12 W	15 NE					BS 62	N 69 W	40 NE				

	Foliation		Lineation		Fold Axis			Foliation		Lineation		Fold Axis	
Station	Strike	Dip	Trend	Plunge	Trend	Plunge	Station	Strike	Dip	Trend	Plunge	Trend	Plunge
CA 1021	N 63 E	20 NE					BS 63	N 30 W	30 SW				
CA 1022	N 23 W	20 SW					BS 64	N 40 W	45 NE				
CA 1023	N 56 W	15 SW					BS 65	N 60 W	30 SW				
CA 1024	N 44 W	10 NE					BS 66	N 60 W	30 SW				
CA 1025	N 39 W	35 SW					BS 67	N 11 E	30 NW				
CA 1026	N 51 W	25 NE					BS 68	N 67 W	40 NE				
CA 1027	N 30 E	15 SE					BS 69	N 83 W	45 NE				
BS 70	N 61 W	20 NE					BS 149	N 25 W	30 SW				
BS 71	N 73 W	45 NE					BS 150	N 32 E	35 SE				
BS 72	N 70 W	70 NE					BS 151	N 50 W	35 SW				
BS 73	N 67 W	60 NE					BS 152	N 74 W	20 SW				
BS 74	N 58 W	85 SW					BS 153	N 31 E	20 SE				
BS 75	N 43 W	60 NE					BS 154	N 54 E	30 SE				
BS 76	N 51 W	75 SW					BS 155	N 67 E	50 SE				
BS 77	N 59 W	80 SW					BS 156	N 76 E	25 SE				
BS 78	N 78 W	80 NE					BS 157	N 46 E	45 SE				
BS 79	N 53 W	60 NE					BS 158	N 47 E	60 SE				
BS 80	N 62 W	15 NE					BS 159	N 48 W	25 SW				
BS 81	N 44 E	50 NW					BS 160	N 42 W	60 SW				
BS 82	N 15 E	45 NW					BS 161	N 31 W	25 SW				
BS 83	N 52 E	80 NW					BS 162	N 88 W	30 SW				
BS 84	N 29 W	75 SW					BS 163	N 29 E	30 SE				
BS 85	N 17 E	20 SE					BS 164	N 29 E	30 SE				
BS 86	N 30 E	25 NW					BS 165	N 28 E	30 SE				
BS 87	N 61 E	35 NW					BS 166	N 43 E	45 SE				
BS 88	N 45 W	35 SW					BS 167	N 8 W	30 NE				
BS 89	N 9 W	45 SW					BS 168	N 85 E	70 SE				
BS 90	N 33 E	45 NW					BS 169	N 71 E	45 SE				
BS 91	N 43 W	45 SW					BS 170	N 16 E	50 SE				
BS 92					298	10	BS 171	N 70 E	60 SE				
BS 93	N 15 W	10 SW					BS 172	N 32 E	60 SE				
BS 94	N 22 W	15 SW					BS 173	N 18 E	35 SE				
BS 95	N 87 E	30 SE					BS 174	N 37 E	25 SE				
BS 96	N 31 W	30 SW					BS 175	N 18 W	45 NE				
BS 97	N 47 W	30 NE					BS 176	N 19 E	45 SE				
BS 98	N 41 W	20 NE					BS 177	N 80 E	45 SE				
BS 99	N 44 W	60 SW					BS 178	N 60 W	50 SW				
BS 100	N 33 W	20 SW					BS 179	N 32 E	60 SE				
BS 101	N 60 W	45 SW					BS 180	N 39 W	60 NE				
BS 102	N 28 W	25 NE					BS 181	N 28 E	60 SE				
BS 103	N 28 W	25 NE					BS 182					348	10
BS 104	N 30 E	30 SE					BS 183	N 86 W	45 SW				
BS 105	N 61 W	20 NE					BS 184	N 87 W	70 SW				
BS 106	N 37 W	30 SW					BS 185	N 69 W	45 SW				
BS 107	N 11 E	45 SE					BS 186	N 79 E	70 SE				
BS 108	N 8 W	60 SW					BS 187	N 57 E	10 SE				
BS 109	N 24 E	20 SE					BS 188	N 33 E	60 SE				
BS 110	N 26 E	20 SE					BS 189	N 75 E	60 SE				
BS 111	N 46 E	15 SE					BS 190	N 50 E	45 SE				
BS 112	N 6 E	10 SE					BS 191	N 45 E	60 SE				
BS 113	N 33 E	30 SE					BS 192	N 49 E	65 SE				
BS 114	N 72 W	20 SW					BS 193	N 40 E	50 SE				
BS 115	N 26 E	20 SE					BS 194	N 41 E	45 SE				
BS 116	N 9 W	80 NE					BS 195	N 76 E	45 SE				
BS 117	N 6 W	70 NE					BS 196	N 76 E	45 SE				
BS 118	N 74 E	45 SE					BS 197	N 47 E	85 SE				
BS 119	N 56 E	45 SE					BS 198	N 63 E	85 SE				
BS 120	N 57 E	35 SE					BS 199	N 49 E	30 NW				
BS 121	N 30 E	45 NW					BS 200	N 43 W	30 SW				
BS 122	N 45 E	50 SE					BS 201	N 55 E	45 SE				
BS 123	N 53 E	45 SE					BS 202	N 38 E	70 SE				
BS 124	N 88 E	20 NW					BS 203	N 43 E	50 SE				
BS 125	N 74 W	40 SW					BS 204	N 10 E	50 NW				
BS 126	N 6 E	45 SE					BS 205	N 46 E	10 SE				
BS 127	N 8 E	50 SE					BS 206	N 69 E	15 SE				
BS 128	N 19 E	30 SE					BS 207	N 23 E	60 SE				
BS 129	N 20 E	30 SE					BS 208	N 18 E	75 SE				
BS 130	N 39 E	60 SE					BS 209	N 13 W	15 NE				
BS 131	N 32 E	30 SE					BS 210	N 10 W	30 NE				
BS 132	N 57 W	15 SW					BS 211	N 75 E	45 SE				
BS 133	N 41 W	20 SW					BS 212	N 69 E	45 SE				
BS 134	N 45 E	45 NW					BS 213	N 44 E	40 SE				
BS 135					148	10	BS 214	N 88 W	60 SW				
BS 136	N 39 W	50 SW					BS 215	N 84 W	40 SW				
BS 137	N 65 W	50 SW					BS 216	N 72 W	60 SW				
BS 138	N 48 E	80 SE					BS 217	N 55 E	45 SE				
BS 139	N 26 E	30 SE					BS 218	N 16 E	75 SE				
BS 140	N 13 E	30 SE					BS 219	N 56 E	60 NW				
BS 141	N 62 E	30 SE					BS 220	N 20 W	75 NE				
BS 142	N 68 E	30 SE					BS 221	N 75 W	45 SE				
BS 143	N 85 W	60 SW					BS 222	N 73 W	75 SW				
BS 144	N 40 E	30 SE					BS 223	N 9 E	60 SE				
BS 145	N 51 W	45 SW					BS 224	N 75 E	45 SE				
BS 146	N 25 W	30 SW					BS 225	N 5 E	60 SE				
BS 147	N 19 W	25 SW					BS 226	N 30 E	60 SE				
BS 148	N 32 E	30 NW					BS 227	N 8 W	15 NE				
BS 228	N 20 E	45 SE					BS 307	N 55 W	30 NE				
BS 229	N N 25 W	75 NE					BS 308	N 20 W	45 NE				
BS 230	N 25 E	60 SE					BS 309	N 58 W	75 SW				
BS 231	N 87 W	80 SW					BS 310	N 84 E	15 SE				
BS 232	N 26 E	45 SE					BS 311	N 72 W	30 NE				

	Foliation		Lineation		Fold Axis			Foliation		Lineation		Fold Axis	
Station	Strike	Dip	Trend	Plunge	Trend	Plunge	Station	Strike	Dip	Trend	Plunge	Trend	Plunge
BS 233	N 24 E	45 SE					BS 312					272	20
BS 234	N 65 W	40 SW					BS 313	N 47 E	60 NW				
BS 235	N 30 E	40 SE					BS 314	N 83 E	45 SE				
BS 236	N 88 W	15 SW					BS 315	N 61 E	45 SE				
BS 237	N 36 E	45 SE					BS 316	N 71 W	50 SW				
BS 238	N 86 W	30 NW					BS 317	N 40 W	60 SW				
BS 239	N 41 W	40 NE					BS 318	N 86 E	60 SE				
BS 240	N 37 W	30 NE					BS 319	N 89 E	50 SE				
BS 241	N 35 W	15 NE					BS 320	N 87 W	70 SW				
BS 242	N 20 W	45 NE					BS 321	N 69 E	60 SE				
BS 243	N 28 W	30 NE					BS 322	N 41 W	45 SW				
BS 244	N 47 W	10 SW					BS 323	N 67 W	20 SW				
BS 245	N 30 W	45 NE					BS 324					155	10
BS 246	N 28 W	50 NE					BS 325	N 76 W	75 SW				
BS 247	N 56 W	30 NE					BS 326	N 44 W	30 SW				
BS 248	N 38 W	30 NE					BS 327	N 65 W	30 SW				
BS 249	N 23 W	50 NE					BS 328	N 88 W	25 SW				
BS 250	N 83 W	35 NE					BS 329	N 84 W	30 SW				
BS 251	N 53 W	30 NE					BS 330	N 66 W	30 SW				
BS 252	N 69 W	75 SW					BS 331	N 32 W	40 NE				
BS 253	N 64 W	70 NE					BS 332	N 54 W	20 NE				
BS 254	N 37 W	30 NE					BS 333	N 53 W	60 SW				
BS 255	N 35 W	45 NE					BS 334	N 31 W	30 SW				
BS 256	N 38 W	20 NE					BS 335	N 39 W	30 NE				
BS 257	N 5 E	10 SE					BS 336	N 85 W	45 SW				
BS 258	N 87 E	75 SE					BS 337	N 66 W	60 SW				
BS 259	N 25 W	40 NE					BS 338	N 32 W	40 NE				
BS 260	N 39 W	30 NE					BS 339	N 34 W	20 NE				
BS 261	N 51 W	30 NE					BS 340	N 14 W	20 SW				
BS 262	N 31 W	30 NE					BS 341	N 87 W	75 SW				
BS 263	N 17 W	20 NE					BS 342	N 66 W	30 SW				
BS 264	N 31 E	20 SE					BS 343	N 78 W	70 SW				
BS 265	N 25 E	30 SE					BS 344	N 61 W	70 SW				
BS 266	N 25 E	30 SE					BS 345	N 86 W	75 SW				
BS 267	N 11 W	45 NE					BS 346	N 72 W	60 SW				
BS 268	N 17 W	20 NE					BS 347	N 81 W	45 SW				
BS 269	N 23 W	40 NE					BS 348	N 81 W	80 SW				
BS 270	N 34 W	30 NE					BS 349	N 72 E	30 SE				
BS 271	N 89 E	25 NW					BS 350	N 88 W	45 SW				
BS 272	N 70 W	40 NE					BS 351	N 12 E	45 SE				
BS 273	N 55 W	30 NE					BS 352	N 80 W	70 SW				
BS 274	N 33 W	30 NE					BS 353	N 72 E	65 SE				
BS 275	N 35 W	30 NE					BS 354	N 38 E	65 SE				
BS 276	N 23 W	30 NE					BS 355	N 86 E	20 NW				
BS 277	N 56 W	30 NE					BS 356	N 85 W	20 SW				
BS 278	N 84 W	30 NE					BS 357	N 44 W	20 SW				
BS 279	N 37 W	35 NE					BS 358	N 81 W	45 NE				
BS 280	N 63 E	70 SE					BS 359	N 76 W	30 SW				
BS 281	N 69 W	75 SW					BS 360	N 53 W	45 SW				
BS 282	N 56 E	15 NW					BS 361	N 89 W	30 NE				
BS 283	N 51 E	50 NW					BS 362	N 76 W	20 NW				
BS 284	N 62 E	40 NW					BS 363	N 76 E	20 NW				
BS 285	N 71 W	45 NE					BS 364	N 58 E	20 NW				
BS 286	N 59 W	30 NE					BS 365	N 74 E	45 NW				
BS 287	N 32 W	20 NE					BS 366	N 89 E	10 SE				
BS 288	N 58 E	25 SE					BS 367	N 73 W	50 SW				
BS 289	N 69 E	20 NW					BS 368	N 2 E	30 SE				
BS 290	N 40 W	50 SW					BS 369	N 40 W	30 NE				
BS 291	N 54 W	40 NE					BS 370	N 58 W	40 NE				
BS 292	N 50 W	45 NE					BS 371	N 40 W	60 NE				
BS 293	N 42 W	30 NE					BS 372	N 58 W	40 NE				
BS 294	N 82 E	50 NW					BS 373	N 89 E	45 NW				
BS 295	N 37 E	60 NW					BS 374	N 51 W	50 NE				
BS 296	N 66 W	45 NE					BS 375	N 40 E	30 SE				
BS 297	N 19 W	30 NE					BS 376	N 43 W	40 NE				
BS 298	N 59 W	45 NE					BS 377	N 51 W	50 NE				
BS 299	N 48 E	30 NW					BS 378	N 37 W	40 NE				
BS 300					123	10	BS 379	N 35 W	30 NE				
BS 301	N 72 W	40 NE					BS 380	N 25 W	45 NE				
BS 302	N 59 W	60 NE					BS 381	N 42 W	40 NE				
BS 303	N 53 E	30 SE					BS 382	N 47 W	40 NE				
BS 304	N 26 W	25 SW					BS 383	N 47 W	40 NE				
BS 305	N 57 E	20 NW					BS 384	N 29 W	20 NE				
BS 306	N 76 E	30 NW					BS 385	N 35 W	30 NE				
BS 386	N 53 W	50 NE					BS 465	N 32 W	70 SW				
BS 387	N 12 W	45 NE					BS 466	N 39 E	60 SE				
BS 388	N 27 W	30 NE					BS 467	N 38 E	60 SE				
BS 389	N 27 W	30 NE					BS 468	N 49 E	60 SE				
BS 390	N 40 W	55 NE					BS 469	N 56 E	45 SE				
BS 391	N 8 W	30 NE					BS 470	N 47 E	45 SE				
BS 392	N 22 W	30 NE					BS 471	N 47 W	60 NE				
BS 393	N 85 W	40 NE					BS 472					149	10
BS 394	N 53 W	30 NE					BS 473	N 2 W	70 NE				
BS 395	N 34 W	30 NE					BS 474	N 45 E	45 SE				
BS 396	N 24 W	30 NE					BS 475	N 40 E	85 SE				
BS 397	N 26 W	45 NE					BS 476	N 41 W	40 SW				
BS 398	N 33 W	80 NE					BS 477	N 45 W	50 SW				
BS 399	N 6 W	20 NE					BS 478	N 24 E	60 SE				
BS 400	N 25 E	45 SE					BS 479	N 21 E	60 SE				
BS 401	N 55 W	80 NE					BS 480	N 64 E	40 SE				
BS 402	N 27 W	45 NE					BS 481	N 64 E	70 SE				

	Foliation		Lineation		Fold Axis			Foliation		Lineation		Fold Axis	
Station	Strike	Dip	Trend	Plunge	Trend	Plunge	Station	Strike	Dip	Trend	Plunge	Trend	Plunge
BS 403	N 11 E	60 SE					BS 482	N 63 E	60 SE				
BS 404	N 21 W	65 NE					BS 483	N 32 E	45 SE				
BS 405	N 9 W	60 NE					BS 484	N 65 E	35 SE				
BS 406	N 16 W	45 NE					BS 485	N 18 E	50 SE				
BS 407	N 38 W	60 NE					BS 486	N 75 E	30 SE				
BS 408	N 5 W	10 NE					BS 487	N 40 E	45 SE				
BS 409	N 27 W	35 NE					BS 488	N 29 E	15 SE				
BS 410	N 18 W	70 SW					BS 489	N 31 E	45 SE				
BS 411	N 26 W	50 NE					BS 490	N 38 E	60 SE				
BS 412	N 13 W	60 NE					BS 491	N 21 W	65 NE				
BS 413	N 16 W	60 NE					BS 492	N 11 W	45 NE				
BS 414	N 39 W	70 NE					BS 493	N 38 W	45 NE				
BS 415	N 26 W	50 NE					BS 494	N 35 W	60 NE				
BS 416	N 47 W	45 NE					BS 495	N 42 W	45 NE				
BS 417	N 22 W	30 NE					BS 496	N 29 E	40 SE				
BS 418	N 44 W	45 NE					BS 497	N 32 E	45 SE				
BS 419	N 49 W	30 SE					BS 498	N 24 E	45 SE				
BS 420	N 49 W	20 NE					BS 499	N 15 W	60 NE				
BS 421	N 1 E	30 SE					BS 500	N 1 E	30 SE				
BS 422	N 48 W	70 NE					BS 501	N 1 W	60 NE				
BS 423	N 64 W	20 SW					BS 502	N 19 W	70 NE				
BS 424	N 44 W	45 NE					BS 503	N 55 W	70 NE				
BS 425	N 12 E	30 SE					BS 504	N 48 W	30 NE				
BS 426	N 11 E	45 SE					BS 505	N 68 E	55 SE				
BS 427	N 14 E	45 SE					BS 506	N 46 E	30 SE				
BS 428	N 44 W	30 NE					BS 507	N 44 E	45 SE				
BS 429	N 25 W	40 NE					BS 508	N 24 E	40 SE				
BS 430	N 50 W	45 NE					BS 509	N 20 W	30 NE				
BS 431	N 22 E	60 SE					BS 510					132	10
BS 432	N 24 W	30 NE					BS 511	N 15 E	30 SE				
BS 433	N 27 W	45 NE					BS 512	N 50 E	50 SE				
BS 434	N 32 E	20 SE					BS 513	N 39 E	25 SE				
BS 435	N 7 W	20 NE					BS 514	N 77 E	50 SE				
BS 436	N 46 W	25 NE					BS 515	N 38 E	45 SE				
BS 437	N 6 W	45 NE					BS 516	N 3 E	60 SE				
BS 438	N 6 W	45 NE					BS 517	N 15 W	80 NE				
BS 439	N 1 W	60 NE					BS 518	N 8 E	45 SE				
BS 440	N 11 W	45 NE					BS 519	N 87 E	15 SE				
BS 441	N 40 E	40 SE					BS 520	N 45 W	20 NE				
BS 442	N 7 E	15 SE					BS 521	N 35 E	25 SE				
BS 443	N 46 W	25 NE					BS 522	N 38 E	20 SE				
BS 444	N 6 W	35 NE					BS 523	N 76 W	30 NE				
BS 445	N 1 W	60 NE					BS 524	N 51 E	30 SE				
BS 446	N 11 W	45 NE					BS 525	N 89 W	25 SW				
BS 447	N 40 E	40 SE					BS 526	N 54 E	20 SE				
BS 448	N 7 E	15 SE					BS 527	N 89 W	25 SW				
BS 449	N 17 W	50 NE					BS 528	N 54 E	20 SE				
BS 450	N 16 W	30 NE					BS 529	N 84 E	45 SE				
BS 451	N 46 E	70 SE					BS 530	N 13 W	70 NE				
BS 452	N 17 E	70 SE					BS 531	N 17 E	20 SE				
BS 453	N 26 E	45 SE					BS 532	N 19 E	40 SE				
BS 454	N 38 E	30 SE					BS 533	N 83 E	40 SE				
BS 455	N 29 W	40 NE					BS 534	N 33 E	60 SE				
BS 456	N 5 E	20 SE					BS 535	N 32 E	30 SE				
BS 457	N 15 W	50 NE					BS 536	N 3 W	30 NE				
BS 458	N 29 W	40 NE					BS 537	N 18 W	60 NE				
BS 459	N 5 E	20 SE					BS 538	N 11 E	35 SE				
BS 460	N 15 W	50 NE					BS 539	N 26 E	30 SE				
BS 461	N 28 E	20 SE					BS 540	N 29 E	40 SE				
BS 462	N 43 E	30 SE					BS 541	N 8 E	25 SE				
BS 463	N 18 E	60 SE					BS 542	N 27 E	30 SE				
BS 464	N 66 E	25 SE					BS 543	N 3 E	20 SE				
BS 544	N 21 E	30 SE					BS 623	N 13 E	45 SE				
BS 545	N 14 E	30 SE					BS 624	N 18 W	40 NE				
BS 546	N 15 E	50 SE					BS 625	N 21 W	20 SW				
BS 547	N 27 E	50 SE					BS 626	N 13 W	35 NE				
BS 548	N 20 E	80 SE					BS 627	N 30 W	45 NE				
BS 549	N 32 W	45 NE					BS 628	N 10 E	40 SE				
BS 550	N 4 E	40 SE					BS 629	N 9 E	60 SE				
BS 551	N 12 E	40 SE					BS 630	N 6 E	40 NW				
BS 552	N 14 W	40 NE					BS 631	N 72 E	45 SE				
BS 553	N 53 W	20 SW					BS 632	N 8 W	45 NE				
BS 554	N 87 W	80 SW					BS 633	N 20 W	45 NE				
BS 555	N 49 W	45 SW					BS 634	N 39 E	35 SE				
BS 556	N 46 W	40 SW					BS 635	N 68 E	20 SE				
BS 557	N 22 W	40 SW					BS 636	N 25 W	75 NE				
BS 558	N 41 E	30 SE					BS 637	N 11 W	45 NE				
BS 559	N 16 E	30 SE					BS 638	N 4 E	60 SE				
BS 560	N 26 E	20 SE					BS 639	N 29 E	60 SE				
BS 561	N 38 E	35 SE					BS 640	N 15 W	60 NE				
BS 562	N 13 E	22 SE					BS 641	N 26 W	30 NE				
BS 563	N 3 W	30 NE					BS 642	N 74 W	45 SW				
BS 564	N 59 W	20 SW					BS 643	N 7 E	45 SE				
BS 565	N 10 W	20 SW					BS 644	N 32 W	30 NE				
BS 566	N 35 E	45 SE					BS 645	N 13 W	45 NE				
BS 567	N 23 E	45 SE					BS 646	N 14 E	60 SE				
BS 568	N 27 W	30 SW					BS 647	N 46 W	70 NE				
BS 569					149	10	BS 648	N 30 E	30 SE				
BS 570	N 32 W	45 SW					BS 649	N 49 E	30 SE				
BS 571	N 21 E	40 SE					BS 650	N 15 W	40 NE				
BS 572	N 14 E	45 SE					BS 651	N 48 E	30 SE				

	Foliation		Lineation		Fold Axis			Foliation		Lineation		Fold Axis	
Station	Strike	Dip	Trend	Plunge	Trend	Plunge	Station	Strike	Dip	Trend	Plunge	Trend	Plunge
BS 573	N 21 E	35 SE					BS 652	N 51 E	30 SE				
BS 574	N 14 E	45 SE					BS 653	N 43 E	30 NW				
BS 575	N 27 E	30 SE					BS 654	N 46 W	20 NE				
BS 576	N 78 E	30 SE					BS 655	N 27 W	30 NE				
BS 577	N 33 E	30 SE					BS 656	N 61 W	60 SW				
BS 578	N 53 E	30 SE					BS 657	N 53 W	45 SW				
BS 579	N 42 W	60 SW					BS 658	N 88 W	75 SW				
BS 580	N 19 E	60 SE					BS 659	N 35 E	60 SE				
BS 581	N 89 E	30 SE					BS 660	N 39 E	35 SE				
BS 582	N 36 E	30 NW					BS 661	N 20 W	40 NE				
BS 583	N 25 E	45 SE					BS 662	N 23 W	40 SW				
BS 584	N 32 E	45 SE					BS 663	N 59 E	30 SE				
BS 585	N 3 W	25 NW					BS 664	N 43 W	30 NE				
BS 586	N 17 E	60 SE					BS 665	N 50 W	30 NE				
BS 587	N 30 E	75 SE					BS 666	N 48 W	30 NE				
BS 588	N 36 E	30 NW					BS 667	N 21 W	40 NE				
BS 589	N 27 E	60 SE					BS 668					137	10
BS 590	N 24 W	60 NE					BS 669	N 89 E	45 SE				
BS 591	N 19 E	70 SE					BS 670	N 37 E	45 SE				
BS 592	N 68 E	45 SE					BS 671	N 6 E	50 SE				
BS 593	N 7 E	40 SE					BS 672					123	10
BS 594	N 10 W	45 NW					BS 673	N 52 W	35 NE				
BS 595	N 25 E	10 SE					BS 674					153	10
BS 596	N 48 E	45 SE					BS 675					124	10
BS 597	N 31 E	45 NW					BS 676	N 19 E	30 NW				
BS 598	N 11 E	80 SE					BS 677	N 23 W	30 NE				
BS 599	N 2 E	70 SE					BS 678	N 8 W	20 NE				
BS 600	N 34 E	30 SE					BS 679	N 16 E	40 NW				
BS 601	N 46 E	55 SE					BS 680	N 37 E	30 NW				
BS 602	N 78 E						BS 681	N 7 E	40 NW				
BS 603	N 31 E	75 SE					BS 682	N 69 W	70 SW				
BS 604	N 19 E	40 SE					BS 683	N 37 W	75 SW				
BS 605	N 24 E	45 SE					BS 684	N 7 E	40 NW				
BS 606	N 31 E	35 SE					BS 685	N 69 W	70 SW				
BS 607	N 19 W	20 NE					BS 686	N 61 W	60 NE				
BS 608	N 24 W	40 NE					BS 687	N 34 W	30 SW				
BS 609	N 88 W	20 SW					BS 688	N 39 E	20 NW				
BS 610	N 34 E	70 NW					BS 689	N 25 W	45 NE				
BS 611	N 45 E	45 SE					BS 690	N 45 W	30 NE				
BS 612	N 36 E	45 SE					BS 691	N 30 E	30 SE				
BS 613	N 34 E	30 SE					BS 692	N 19 E	20 SE				
BS 614	N 7 W	30 NE					BS 693	N 26 E	30 SE				
BS 615	N 68 W	60 SW					BS 694	N 47 W	40 SW				
BS 616	N 60 W	30 SW					BS 695	N 6 E	30 SE				
BS 617	N 12 W	40 NE					BS 696	N 50 W	60 NE				
BS 618	N 10 E	45 SE					BS 697	N 27 W	40 NE				
BS 619	N 59 E	40 SE					BS 698	N 46 W	80 NE				
BS 620	N 6 E	60 SE					BS 699	N 49 W	45 SW				
BS 621	N 8 E	20 SE					BS 700	N 80 W	60 NE				
BS 622	N 27 E	20 SE					BS 701	N 55 W	20 NE				
BS 702	N 5 E	35 SE					BS 781	N 81 W	20 SW				
BS 703	N 55 E	40 SE					BS 782	N 39 W	30 NE				
BS 704	N 14 W	60 NE					BS 783	N 39 W	45 NE				
BS 705	N 46 W	20 NE					BS 784	N 30 W	20 SW				
BS 706	N 39 W	30 SW					BS 785	N 40 W	30 SW				
BS 707	N 52 W	40 SW					BS 786	N 37 W	70 NE				
BS 708	N 62 W	45 SW					BS 787	N 49 W	70 NE				
BS 709	N 65 W	30 SW					BS 788	N 55 W	40 SW				
BS 710	N 82 W	70 SW					BS 789	N 25 W	45 SW				
BS 711	N 57 W	45 SW					BS 790	N 79 W	25 SW				
BS 712	N 62 W	45 SW					BS 791	N 68 W	45 SW				
BS 713	N 65 W	35 SW					BS 792	N 68 W	80 SW				
BS 714	N 82 W	70 SW					BS 793	N 73 W	20 SW				
BS 715	N 57 W	45 SW					BS 794	N 45 W	70 SW				
BS 716	N 24 W	40 SW					BS 795	N 83 W	40 SW				
BS 717	N 48 W	80 SW					BS 796	N 74 W	45 SW				
BS 718	N 51 W	75 SW					BS 797	N 63 W	20 SW				
BS 719	N 34 W	20 NE					BS 798	N 37 E	50 SE				
BS 720	N 85 E	40 SE					BS 799	N 2 W	60 NE				
BS 721	N 34 W	20 NE					BS 800	N 42 W	45 NE				
BS 722	N 85 E	40 SE					BS 801	N 55 E	45 SE				
BS 723	N 38 W	45 SE					BS 802	N 37 E	45 SE				
BS 724	N 88 W	30 SE					BS 803	N 31 EE	50 SE				
BS 725	N 78 W	30 NE					BS 804	N 19 W	60 NE				
BS 726	N 26 W	20 NE					BS 805	N 21 W	45 NE				
BS 727	N 43 W	15 NE					BS 806	N 29 W	40 NE				
BS 728	N 46 W	45 SW					BS 807	N 17 W	45 SW				
BS 729	N 60 E	20 NW					BS 808	N 23 W	45 NE				
BS 730	N 77 W	30 NE					BS 809	N 48 W	50 SW				
BS 731	N 89 E	10 NW					BS 810	N 6 E	10 SE				
BS 732	N 67 W	70 SW					BS 811	N 24 E	45 SE				
BS 733	N 39 W	60 NE					BS 812	N 89 E	20 SE				
BS 734	N 15 E	30 SE					BS 813	N 11 E	60 SE				
BS 735	N 18 W	20 NE					BS 814	N 12 E	45 SE				
BS 736	N 14 W	15 NE					BS 815	N 36 E	50 SE				
BS 737	N 71 W	45 NE					BS 816	N 27 E	40 SE				
BS 738	N 51 W	45 NE					BS 817	N 44 E	45 SE				
BS 739	N 54 W	40 NE					BS 818	N 22 E	40 SE				
BS 740	N 89 E	10 NW					BS 819	N 11 E	60 SE				
BS 741	N 41 W	30 NE					BS 820	N 4 E	25 SE				
BS 742	N 64 E	40 NW					BS 821	N 10 E	25 SE				

	Foliation		Lineation		Fold Axis			Foliation		Lineation		Fold Axis	
Station	Strike	Dip	Trend	Plunge	Trend	Plunge	Station	Strike	Dip	Trend	Plunge	Trend	Plunge
BS 743	N 55 E	30 NW					BS 822	N 17 E	45 SE				
BS 744	N 53 W	30 NE					BS 823	N 64 E	20 NW				
BS 745	N 34 E	20 NW					BS 824	N 70 W	15 SW				
BS 746	N 87 W	30 NE					BS 825	N 52 E	70 SE				
BS 747	N 6 E	60 SE					BS 826	N 22 W	20 SW				
BS 748	N 6 E	25 NW					BS 827	N 12 W	30 NE				
BS 749	N 38 W	30 SW					BS 828	N 20 W	20 SW				
BS 750	N 48 W	25 NE					BS 829	N 24 W	60 SW				
BS 751	N 10 W	30 NE					BS 830	N 21 W	80 SW				
BS 752	N 41 W	30 NE					BS 831	N 23 E	20 SE				
BS 753	N 71 W	20 SW					BS 832	N 27 E	30 SE				
BS 754	N 59 W	45 SW					BS 833	N 20 E	20 NW				
BS 755	N 42 W	45 SW					BS 834	N 39 E	40 NW				
BS 756	N 29 W	45 SW					BS 835	N 5 E	25 NW				
BS 757	N 49 W	60 NE					BS 836	N 24 W	30 SW				
BS 758	N 47 W	60 NE					BS 837	N 61 W	35 SW				
BS 759	N 49 W	65 SW					BS 838	N 21 W	20 NE				
BS 760	N 44 W	70 SW					BS 839	N 86 W	50 NE				
BS 761	N 57 W	30 SW					BS 840	N 34 W	40 NE				
BS 762	N 23 W	60 NE					BS 841	N 18 W	15 SW				
BS 763	N 24 W	45 SW					BS 842	N 27 W	30 SW				
BS 764	N 75 W	60 SW					BS 843	N 23 W	40 NE				
BS 765	N 25 W	30 SW					BS 844	N 47 E	60 SE				
BS 766					118	20	BS 845	N 51 E	50 NW				
BS 767	N 62 W	30 SW					BS 846	N 38 E	30 SE				
BS 768	N 22 W	25 NE					BS 847	N 52 E	30 SE				
BS 769	N 20 W	40 NE					BS 848	N 25 E	30 SE				
BS 770	N 14 E	20 SE					BS 849	N 34 E	15 SE				
BS 771	N 33 W	30 NE					BS 850	N 9 W	25 SW				
BS 772	N 40 W	35 SW					BS 851	N 4 E	30 SE				
BS 773	N 15 E	30 SE					BS 852	N 68 W	40 SW				
BS 774	N 5 W	60 NE					BS 853	N 35 W	15 SW				
BS 775	N 60 W	75 NE					BS 854	N 16 W	30 SW				
BS 776	N 81 W	30 SW					BS 855	N 7 E	20 NW				
BS 777	N 50 W	30 NE					BS 856	N 54 E	10 SE				
BS 778	N 75 W	45 SW					BS 857	N 13 W	15 SW				
BS 779	N 81 W	30 SW					BS 858	N 3 W	25 SW				
BS 780	N 81 W	60 SW					BS 859	N 21 E	30 NW				
BS 860	N 25 W	30 SW					BS 939	N 38 W	30 SW				
BS 861	N 30 E	25 SE					BS 940	N 67 W	40 SW				
BS 862	N 65 W	35 SW					BS 941	N 7 W	70 SW				
BS 863	N 12 E	60 SE					BS 942	N 17 E	60 SW				
BS 864	N 18 E	45 NW					BS 943	N 1 E	30 SE				
BS 865	N 27 E	45 NW					BS 944	N 20 E	40 SE				
BS 866	N 24 E	45 NW					BS 945	N 30 E	40 SE				
BS 867	N 85 W	30 NE					BS 946	N 55 W	45 SW				
BS 868	N 2 E	30 NW					BS 947	N 87 E	5 SE				
BS 869	N 60 W	20 NE					BS 948	N 49 W	35 NE				
BS 870	N 57 W	50 SW					BS 949	N 9 W	60 NE				
BS 871	N 15 W	60 SW					BS 950	N 2 W	30 NE				
BS 872	N 15 E	50 SE					BS 951	N 64 W	40 SW				
BS 873	N 43 W	30 SW					BS 952	N 36 E	45 SE				
BS 874	N 16 W	45 SW					BS 953	N 3 W	45 NE				
BS 875	N 18 E	30 NW					BS 954	N 27 W	30 NE				
BS 876	N 27 E	45 NW					BS 955	N 22 W	30 NE				
BS 877	N 24 E	45 NW					BS 956	N 19 W	15 NE				
BS 878	N 12 W	45 SW					BS 957	N 22 W	40 SW				
BS 879	N 16 W	30 SW					BS 958	N 17 W	30 SW				
BS 880	N 5 E	60 NW					BS 959	N 21 W	60 NE				
BS 881	N 1 W	25 NE					BS 960	N 52 E	50 SE				
BS 882	N 2 W	30 SW					BS 961	N 38 W	30 SW				
BS 883	N 17 W	20 SW					BS 962	N 45 W	30 SW				
BS 884	N 15 W	30 SW					BS 963	N 28 W	20 SW				
BS 885	N 5 W	20 SW					BS 964	N 87 E	20 SE				
BS 886	N 46 E	45 SE					BS 965	N 11 E	50 NW				
BS 887	N 21 W	20 SW					BS 966	N 26 W	20 SW				
BS 888	N 31 W	40 SW					BS 967	N 31 W	30 NE				
BS 889	N 36 W	30 NE					BS 968	N 59 W	30 SW				
BS 890	N 10 E	45 NW					BS 969	N 20 W	30 SW				
BS 891	N 16 W	60 SW					BS 970	N 58 W	30 SW				
BS 892	N 3 E	45 SE					BS 971	N 40 W	30 NE				
BS 893	N 2 W	60 NE					BS 972	N 23 W	65 NE				
BS 894	N 25 E	30 SE					BS 973	N 27 W	60 NE				
BS 895	N 19 W	15 SW					BS 974	N 23 W	70 NE				
BS 896	N 34 W	30 SW					BS 975	N 60 W	60 NE				
BS 897	N 41 E	20 SE					BS 976	N 39 W	45 NE				
BS 898	N 74 E	40 NW					BS 977	N 39 W	30 NE				
BS 899	N 88 W	20 NE					BS 978	N 43 W	30 NE				
BS 900	N 57 E	15 NW					BS 979	N 57 W	70 SW				
BS 901	N 21 W	45 SW					BS 980	N 22 W	60 NE				
BS 902	N 20 E	25 SE					BS 981	N 69 W	30 SW				
BS 903	N 68 W	15 SW					BS 982	N 35 W	70 NE				
BS 904					240	20	BS 983	N 13 W	70 NE				
BS 905	N 20 W	30 NE					BS 984	N 35 W	70 NE				
BS 906	N 17 E	15 SE					BS 985	N 13 W	70 NE				
BS 907	N 80 W	20 NE					BS 986	N 2 E	70 SE				
BS 908	N 14 W	70 NE					BS 987	N 59 W	30 SW				
BS 909	N 3 E	20 NW					BS 988	N 78 W	30 SW				
BS 910	N 12 W	80 NE					BS 989	N 41 W	45 SW				
BS 911	N 10 E	45 SE					BS 990	N 53 E	10 SE				
BS 912	N 15 E	50 SE					BS 991	N 44 W	60 NE				

	Foliation		Lineation		Fold Axis			Foliation		Lineation		Fold Axis	
Station	Strike	Dip	Trend	Plunge	Trend	Plunge	Station	Strike	Dip	Trend	Plunge	Trend	Plunge
BS 913	N 21 W	35 SW					BS 992	N 9 W	60 NE				
BS 914	N 11 W	45 NE					BS 993	N 49 W	60 NE				
BS 915	N 71 E	25 SE					BS 994	N 60 W	30 NE				
BS 916	N 81 W	15 SE					BS 995	N 63 W	40 SW				
BS 917	N 77 W	20 SW					BS 996	N 37 W	60 SW				
BS 918	N 20 W	70 SW					BS 997	N 30 W	60 SW				
BS 919	N 12 W	60 SW					BS 998	N 79 W	40 SW				
BS 920	N 31 W	20 SW					BS 999	N 24 W	40 SW				
BS 921	N 7 W	30 NE					BS 1000	N 40 W	30 SW				
BS 922	N 8 W	30 NE					BS 1001	N 61 W	40 SW				
BS 923	N 4 W	45 NE					BS 1002	N 14 E	30 SE				
BS 924	N 6 W	35 NE					BS 1003	N 46 W	45 NE				
BS 925	N 11 W	50 NE					BS 1004	N 54 W	40 NE				
BS 926	N 4 W	30 NE					BS 1005	N 56 W	40 NE				
BS 927	N 17 W	25 SW					BS 1006	N 40 W	40 SW				
BS 928	N 41 W	30 SW					BS 1007	N 63 W	30 SW				
BS 929	N 34 E	30 NW					BS 1008	N 34 W	30 NE				
BS 930	N 22 W	30 SW					BS 1009	N 39 W	80 NE				
BS 931	N 52 W	30 SW					BS 1010	N 22 W	50 SW				
BS 932					152	20	BS 1011	N 37 W	40 NE				
BS 933	N 72 W	30 SW					BS 1012	N 78 E	25 SE				
BS 934	N 43 W	30 SW					BS 1013	N 65 W	25 SW				
BS 935	N 34 W	30 SW					BS 1014	N 38 W	20 NE				
BS 936	N 23 W	45 SW					BS 1015	N 55 W	35 SW				
BS 937	N 11 W	60 NE					BS 1016	N 41 E	20 SE				
BS 938	N 48 W	30 SW					BS 1017	N 35 E	60 SE				
BS 1018	N 23 W	30 SW					BS 1097	N 23 W	31 SW				
BS 1019	N 20 W	30 NE					BS 1098	N 7 W	40 SW				
BS 1020	N 8 E	30 SE					BS 1099	N 81 W	30 SW				
BS 1021	N 38 W	40 SW					BS 1100	N 15 W	50 SW				
BS 1022	N 26 W	15 SW					BS 1101	N 49 W	40 NE				
BS 1023	N 30 W	45 SW					BS 1102	N 27 W	20 SW				
BS 1024	N 7 E	45 SE					BS 1103	N 37 W	40 SW				
BS 1025	N 27 W	60 NE					BS 1104	N 61 W	20 NE				
BS 1026	N 27 W	75 NE					BS 1105	N 29 W	60 SW				
BS 1027					143	10	BS 1106	N 72 W	20 SW				
BS 1028	N 45 W	45 NE					BS 1107	N 64 W	70 SW				
BS 1029	N 45 W	20 NW					BS 1108	N 37 W	65 SW				
BS 1030	N 86 W	30 SW					BS 1109	N 40 E	30 NW				
BS 1031	N 29 W	45 SW					BS 1110	N 18 W	60 SW				
BS 1032	N 29 W	30 SW					BS 1111	N 52 W	55 SW				
BS 1033	N 49 W	45 SW					BS 1112	N 45 W	40 SW				
BS 1034	N 38 W	45 SW					BS 1113	N 31 W	45 SW				
BS 1035	N 16 W	45 SW					BS 1114	N 23 W	40 SW				
BS 1036					151	10	BS 1115	N 51 W	60 SW				
BS 1037	N 28 W	75 SW					BS 1116	N 37 W	60 SW				
BS 1038	N 42 W	20 NE					BS 1117	N 28 W	25 SW				
BS 1039	N 45 E	60 SE					BS 1118	N 28 W	20 SW				
BS 1040	N 29 W	45 SW					BS 1119	N 29 W	60 SW				
BS 1041	N 19 W	40 SW					BS 1120	N 43 W	30 SW				
BS 1042					149	10	BS 1121	N 13 W	60 NE				
BS 1043	N 41 W	20 NE					BS 1122	N 17 E	30 NW				
BS 1044	N 50 W	60 SW					BS 1123	N 25 W	20 SW				
BS 1045	N 17 W	60 SW					BS 1124	N 31 W	20 SW				
BS 1046	N 59 W	20 SW					BS 1125	N 37 W	45 SW				
BS 1047	N 42 W	70 SW					BS 1126	N 20 W	20 SW				
BS 1048	N 25 W	20 SW					BS 1127	N 29 W	60 SW				
BS 1049	N 41 W	45 NE					BS 1128	N 7 W	40 SW				
BS 1050	N 28 W	30 NE					BS 1129	N 54 W	45 SW				
BS 1051	N 16 W	30 NE					BS 1130	N 40 W	50 SW				
BS 1052	N 29 W	30 SW					BS 1131	N 34 W	45 SW				
BS 1053	N 42 W	45 NE					BS 1132	N 35 W	50 SW				
BS 1054	N 22 W	45 NE					BS 1133	N 15 W	45 SW				
BS 1055	N 29 W	45 SW					BS 1134	N 44 W	30 SW				
BS 1056	N 19 W	60 NE					BS 1135	N 36 W	30 SW				
BS 1057	N 24 W	60 NE					BS 1136	N 47 W	25 SW				
BS 1058	N 19 W	60 NE					BS 1137	N 26 W	50 SW				
BS 1059	N 24 W	60 NE					BS 1138	N 54 W	70 SW				
BS 1060	N 43 W	75 SW					BS 1139	N 82 E	15 SE				
BS 1061	N 66 E	30 SE					BS 1140	N 12 E	40 SE				
BS 1062	N 52 W	30 SW					BS 1141	N 13 W	10 SW				
BS 1063	N 54 E	20 NW					BS 1142	N 24 W	25 SW				
BS 1064	N 35 E	35 SE					BS 1143	N 52 E	35 NW				
BS 1065	N 49 E	45 SE					BS 1144	N 14 W	50 NE				
BS 1066	N 42 W	60 SW					BS 1145	N 19 W	50 SW				
BS 1067	N 47 W	45 SW					BS 1146	N 7 W	40 SW				
BS 1068	N 23 W	30 NE					BS 1147	N 10 E	50 NW				
BS 1069	N 28 W	30 NE					BS 1148	N 48 W	35 SW				
BS 1070	N 28 W	30 NE					BS 1149	N 37 W	30 SW				
BS 1071	N 28 W	20 SW					BS 1150	N 48 W	60 NE				
BS 1072	N 39 W	30 SW					BS 1151	N 5 E	25 NW				
BS 1073	N 31 W	75 NE					BS 1152	N 68 E	30 NW				
BS 1074	N 18 W	30 SW					BS 1153	N 16 W	30 SW				
BS 1075	N 4 E	75 NW					BS 1154	N 79 W	30 SW				
BS 1076	N 25 W	75 SW					BS 1155	N 61 E	35 NW				
BS 1077	N 28 W	40 NE					BS 1156	N 31 W	40 SW				
BS 1078	N 34 W	45 NE					BS 1157	N 24 W	35 SW				
BS 1079	N 38 W	60 SW					BS 1158	N 17 W	30 NE				
BS 1080	N 2 W	30 SW					BS 1159	N 39 W	45 SW				
BS 1081	N 44 W	35 SW					BS 1160	N 15 E	10 SE				
BS 1082	N 16 W	60 SW					BS 1161	N 73 W	20 SW				

	Foliation		Lineation		Fold Axis			Foliation		Lineation		Fold Axis	
Station	Strike	Dip	Trend	Plunge	Trend	Plunge	Station	Strike	Dip	Trend	Plunge	Trend	Plunge
BS 1083	N 6 W	85 SW					BS 1162	N 20 W	30 NE				
BS 1084					121	15	BS 1163	N 20 W	50 NE				
BS 1085	N 22 W	20 SW					BS 1164	N 34 W	20 NE				
BS 1086	N 25 W	25 SW					BS 1165	N 24 E	30 NW				
BS 1087	N 14 W	60 SW					BS 1166	N 27 W	45 NE				
BS 1088	N 19 E	60 NE					BS 1167	N 36 W	20 SW				
BS 1089	N 77 E	30 SE					BS 1168	N 11 W	30 SW				
BS 1090	N 34 E	30 SE					BS 1169	N 14 E	60 SE				
BS 1091	N 72 W	30 NE					BS 1170	N 43 W	40 NE				
BS 1092	N 45 W	60 SW					BS 1171	N 9 E	20 SW				
BS 1093	N 66 W	55 SW					BS 1172	N 30 E	45 NW				
BS 1094	N 78 E	45 SE					BS 1173	N 40 E	20 NW				
BS 1095	N 66 W	45 SW					BS 1174	N 49 W	40 NE				
BS 1096	N 85 E	40 SE					BS 1175	N 21 W	45 SW				
BS 1176	N 25 E	20 NW					SH 46	N 32 E	35 SE				
BS 1177	N 43 W	30 NE					SH 47	N 40 W	35 NE				
BS 1178	N 11 E	60 SE					SH 48	N 8 W	20 SW				
BS 1179	N 13 W	20 SW					SH 49	N 2 E	45 SE				
BS 1180	N 45 E	30 NW					SH 50			147	5		
BS 1181	N 26 W	20 SW					SH 51	N 35 W	40 NE				
BS 1182	N 32 E	20 SE					SH 52	N 40 E	20 NE				
BS 1183	N 18 E	45 NW					SH 53	N 5 W	15 NE				
BS 1184	N 8 W	40 SW					SH 54			153	5		
BS 1185	N 46 E	30 NW					SH 55	N 15 E	10 NW				
BS 1186	N 27 W	20 SW					SH 56	N 20 E	10 NW				
BS 1187	N 33 W	10 SW					SH 57	N 16 W	40 NE				
BS 1188	N 4 E	25 NW					SH 58	N 35 W	30 NE				
BS 1189	N 34 E	40 NW					SH 59	N 57 E	25 NW				
BS 1190	N 19 W	30 SW					SH 60	N 22 E	20 NW				
BS 1191	N 16 W	30 NE					SH 61	N 21 W	40 SW				
BS 1192	N 48 E	50 SE					SH 62	N 11 W	40 SW				
BS 1193	N 20 W	30 SW					SH 63	N 26 W	40 SW				
BS 1194	N 9 W	50 NE					SH 64	N 44 W	30 SW				
BS 1195					297	40	SH 65	N 59 W	20 SW				
BS 1196	N 51 W	45 SW					SH 66	N 2 E	60 SE				
BS 1197	N 9 E	40 NW					SH 67	N 46 W	45 SW				
BS 1198	N 5 W	40 SW					SH 68	N 25 E	15 SE				
BS 1199	N 12 E	55 NW					SH 69	N 6 W	45 SW				
BS 1200	N 52 E	50 SE					SH 70	N 32 E	30 SE				
BS 1201	N 62 E	30 SE					SH 71	N 38 W	20 SW				
BS 1202	N 61 W	50 SW					SH 72	N 13 W	15 SW				
BS 1203	N 33 W	20 NE					SH 73	N 57 W	30 SW				
BS 1204	N 25 W	40 SW					SH 74	N 36 E	30 SE				
BS 1205	N 21 W	20 NE					SH 75	N 5 E	50 SE				
BS 1206	N 36 W	30 NE					SH 76	N 52 W	20 SW				
BS 1207	N 14 W	50 SW					SH 77	N 40 E	20 SE				
BS 1208	N 40 W	30 SW					SH 78	N 43 W	30 SW				
BS 1209	N 30 W	30 NE					SH 79	N 35 W	35 SW				
SH 1	N 46 W	65 NE					SH 80	N 18 W	40 NE				
SH 2	N 32 W	60 SW					SH 81	N 89 E	45 NW				
SH 3	N 10 W	55 SW					SH 82	N 25 E	50 SE				
SH 4	N 23 W	40 SW					SH 83	N 53 E	20 SE				
SH 5	N 6 W	30 SW					SH 84	N 23 E	30 SE				
SH 6	N 42 W	45 SW					SH 85	N 87 E	50 SE				
SH 7	N 30 E	30 NW					SH 86	N 18 W	40 NE				
SH 8	N 5 W	40 SW					SH 87	N 21 W	70 SW				
SH 9	N 3 E	45 NW					SH 88	N 13 W	40 SW				
SH 10	N 22 W	65 SW					SH 89	N 18 W	25 NE				
SH 11	N 2 E	55 SE					SH 90	N 26 E	50 NW				
SH 12	N 35 W	70 SW					SH 91	N 43 E	30 SE				
SH 13	N 16 W	40 SW					SH 92	N 27 E	60 SE				
SH 14	N 26 E	50 SE					SH 93	N 73 E	35 SE				
SH 15	N 12 W	45 SW			323	25	SH 94	N 16 E	30 SE				
SH 16	N 14 W	35 SW					SH 95	N 27 W	60 NE				
SH 17	N 10 E	25 NW					SH 96	N 3 W	45 SW				
SH 18	N 18 W	80 NE					SH 97	N 78 W	45 SE				
SH 19	N 4 W	30 SW					SH 98	N 78 E	45 SE				
SH 20	N 5 W	15 SW					SH 99	N 32 E	45 SE				
SH 21	N 47 W	20 NE					SH 100	N 45 E	45 SE				
SH 22	N 14 W	20 SW					SH 101	N 16 E	20 SE				
SH 23	N 22 E	40 NW					SH 102	N 44 E	35 SE				
SH 24	N 3 W	65 NE					SH 103	N 41 E	35 SE				
SH 25	N 20 E	25 SE					SH 104	N 31 E	35 SE				
SH 26	N 25 W	20 NE					SH 105	N 81 E	40 SE				
SH 27	N 2 W	20 SW					SH 106	N 42 E	75 SE				
SH 28	N 2 W	20 NE					SH 107	N 24 E	60 SE				
SH 29	N 14 E	35 SE					SH 108	N 50 E	45 SE				
SH 30	N 21 E	70 SE					SH 109	N 69 E	25 SE				
SH 31	N 2 W	20 SW					SH 110	N 25 E	25 SE				
SH 32	N 2 W	30 NE					SH 111	N 15 E	65 SE				
SH 33	N 32 W	30 SW					SH 112	N 47 E	25 SE				
SH 34	N 38 W	20 SW					SH 113	N 61 E	25 SE				
SH 35	N 50 E	20 SE					SH 114	N 45 E	30 SE				
SH 36					206	10	SH 115	N 50 E	40 SE				
SH 37	N 84 W	70 SW					SH 116	N 17 E	45 SE				
SH 38	N 17 W	20 NE					SH 117	N 2 W	40 SW				
SH 39	N 31 W	45 NE					SH 118	N 58 E	50 SE				
SH 40	N 71 W	10 SW					SH 119	N 33 E	30 SE				
SH 41	N 20 E	15 SE					SH 120	N 37 E	25 SE				
SH 42	N 12 E	20 NW					SH 121	N 77 W	10 NE				
SH 43	N 79 E	20 SW					SH 122	N 65 E	35 SE				

	Foliation		Lineation		Fold Axis			Foliation		Lineation		Fold Axis	
Station	Strike	Dip	Trend	Plunge	Trend	Plunge	Station	Strike	Dip	Trend	Plunge	Trend	Plunge
SH 44	N 17 E	70 NW					SH 123	N 42 E	30 SE				
SH 45	N 30 E	40 SE					SH 124	N 47 W	30 SW				
SH 125	N 73 W	30 SW					SH 204	N 5 E	15 SE				
SH 126	N 31 E	40 SE					SH 205	N 35 E	40 SE				
SH 127	N 53 E	30 SE					SH 206	N 37 E	45 SE				
SH 128	N 46 E	30 SE					SH 207	N 37 E	15 SE				
SH 129	N 82 W	20 SW					SH 208	N 4 W	15 NE				
SH 130	N 79 W	20 SW					SH 209	N 48 E	10 SE				
SH 131	N 42 E	20 SE					SH 210	N 57 E	60 SE				
SH 132	N 79 W	20 SW					SH 211	N 8 W	15 SW				
SH 133	N 42 E	30 SE					SH 212	N 20 E	15 SE				
SH 134	N 21 E	60 SE					SH 213	N 19 E	20 NW				
SH 135	N 71 E	45 SE					SH 214	N 60 E	30 SE				
SH 136	N 45 E	45 SE					SH 215	N 32 E	30 SE				
SH 137	N 82 E	20 SE					SH 216	N 42 E	30 SE				
SH 138	N 34 E	40 SE					SH 217	N 35 E	25 SE				
SH 139	N 48 E	30 SE					SH 218					192	20
SH 140	N 70 E	30 SE					SH 219	N 20 E	15 SE	170	5		
SH 141					89	10	SH 220	N 45 W	15 NE				
SH 142	N 31 W	30 SW					SH 221	N 48 E	10 SE				
SH 143	N 66 W	40 SW					SH 222	N 31 E	25 SE				
SH 144	N 39 W	50 SW					SH 223	N 82 W	10 SW				
SH 145	N 77 E	50 SE					SH 224	N 49 E	25 SE				
SH 146	N 74 E	40 SE					SH 225	N 82 W	10 SW				
SH 147	N 56 E	50 SE					SH 226	N 56 E	20 SE				
SH 148	N 43 E	50 SE					SH 227	N 54 E	15 SE				
SH 149	N 37 E	65 SE					SH 228	N 77 E	20 SE				
SH 150	N 37 E	25 SE					SH 229					169	10
SH 151	N 42 E	30 SE					SH 230	N 28 E	40 SE				
SH 152	N 34 E	50 SE					SH 231	N 22 E	20 SE				
SH 153	N 10 E	15 SE					SH 232	N 37 E	60 SE				
SH 154	N 9 E	35 SE					SH 233	N 40 E	35 SE				
SH 155	N 39 E	10 SE					SH 234	N 57 E	30 SE				
SH 156	N 23 E	55 SE					SH 235	N 34 E	50 SE				
SH 157	N 37 E	30 SE					SH 236	N 37 E	45 SE				
SH 158	N 13 E	40 SE					SH 237	N 49 E	55 SE				
SH 159	N 20 E	45 SE					SH 238	N 61 E	30 SE				
SH 160	N 18 E	65 SE					SH 239	N 35 E	40 SE				
SH 161	N 26 E	45 SE					SH 240	N 37 E	15 SE				
SH 162	N 42 E	25 SE					SH 241	N 51 E	15 SE				
SH 163	N 58 E	50 SE					SH 242	N 34 E	20 SE				
SH 164			193	15			SH 243	N 38 E	10 SE				
SH 165	N 55 E	30 SE					SH 244	N 56 E	30 SE				
SH 166	N 46 E	25 SE					SH 245	N 35 E	50 SE				
SH 167	N 42 E	20 SE					SH 246	N 13 E	30 SE				
SH 168	N 61 E	25 SE					SH 247	N 19 E	30 SE				
SH 169	N 57 E	20 SE					SH 248	N 12 W	25 SW				
SH 170	N 49 E	10 SE					SH 249	N 38 E	36 SE				
SH 171	N 41 E	30 SE					SH 250	N 21 E	40 SE				
SH 172	N 39 E	30 SE					SH 251	N 35 E	20 SE				
SH 173	N 24 E	30 SE					SH 252	N 23 E	20 SE				
SH 174	N 12 E	50 SE					SH 253	N 33 E	60 SE				
SH 175	N 14 E	25 SE					SH 254	N 44 E	40 SE				
SH 176	N 45 E	65 SE					SH 255	N 43 E	50 SE				
SH 177	N 35 E	55 SE					SH 256	N 65 E	50 SE				
SH 178	N 35 E	35 SE					SH 257	N 40 E	15 SE				
SH 179	N 41 E	25 SE					SH 258	N 57 E	60 SE				
SH 180	N 20 E	60 SE					SH 259	N 24 E	70 SE				
SH 181	N 63 E	80 SE					SH 260	N 45 E	30 SE				
SH 182	N 47 E	30 SE					SH 261	N 31 E	75 SE				
SH 183	N 67 E	25 SE					SH 262	N 44 E	65 SE				
SH 184	N 61 E	20 SE					SH 263	N 36 E	60 SE				
SH 185	N 71 E	20 SE					SH 264	N 41 E	40 SE				
SH 186	N 89 E	10 SE					SH 265	N 45 E	45 SE				
SH 187	N 49 E	45 SE					SH 266	N 55 E	35 SE				
SH 188	N 58 E	15 SE					SH 267	N 58 E	35 SE				
SH 189	N 66 E	25 SE					SH 268	N 57 E	40 SE				
SH 190	N 74 E	15 SE					SH 269	N 59 E	70 SE				
SH 191	N 33 E	35 SE					SH 270	N 52 E	50 SE				
SH 192	N 30 E	30 SE					SH 271	N 32 E	45 SE				
SH 193	N 29 E	30 SE					SH 272	N 58 E	55 SE				
SH 194	N 29 E	45 SE					SH 273	N 21 E	70 SE				
SH 195	N 28 E	25 SE					SH 274	N 61 E	40 SE				
SH 196	N 19 E	45 SE					SH 275	N 36 E	20 SE				
SH 197	N 40 E	50 SE					SH 276	N 26 E	20 SE				
SH 198	N 52 E	55 SE					SH 277	N 53 E	50 SE				
SH 199	N 29 E	45 SE					SH 278	N 29 E	30 SE				
SH 200	N 26 E	55 SE					SH 279	N 33 E	50 SE				
SH 201	N 32 E	35 SE					SH 280	N 58 E	20 SE				
SH 202	N 21 E	30 SE					SH 281	N 76 E	10 NW				
SH 203	N 5 E	40 SE					SH 282	N 63 W	30 NW				
SH 283	N 35 E	65 SE					SH 362	N 12 W	25 NE				
SH 284	N 17 E	35 SE					SH 363	N 35 E	50 NW				
SH 285	N 27 E	25 SE					SH 364	N 6 W	45 NE				
SH 286	N 87 E	40 SE					SH 365	N 20 W	20 SW				
SH 287	N 28 E	50 SE					SH 366					236	25
SH 288	N 9 E	40 SE					SH 367	N 12 E	70 SE				
SH 289	N 35 E	25 SE					SH 368	N 26 E	70 SE				
SH 290	N 64 E	55 SE					SH 369	N 1 E	55 SE				
SH 291	N 34 E	20 SE					SH 370	N 26 E	45 SE				
SH 292	N 49 E	25 SE					SH 371	N 14 E	30 NW				

	Foliation		Lineation		Fold Axis			Foliation		Lineation		Fold Axis	
Station	Strike	Dip	Trend	Plunge	Trend	Plunge	Station	Strike	Dip	Trend	Plunge	Trend	Plunge
SH 293	N 61 E	5 SE					SH 372	N 33 W	30 SW				
SH 294	N 42 E	30 SE					SH 373	N 10 W	40 NE				
SH 295	N 26 E	20 SE					SH 374	N 26 W	40 NE				
SH 296	N 44 E	30 SE					SH 375	N 23 E	30 SE				
SH 297	N 78 E	20 SE					SH 376	N 16 W	35 NE				
SH 298	N 47 E	30 SE					SH 377	N 68 W	10 NE				
SH 299	N 59 E	45 SE					SH 378	N 84 W	15 SW				
SH 300	N 20 E	20 SE					SH 379	N 69 W	15 SW				
SH 301	N 48 E	35 SE					SH 380	N 8 E	25 SE				
SH 302	N 74 E	35 SE					SH 381	N 4 E	50 SE				
SH 303	N 28 E	30 SE					SH 382	N 22 E	20 NW				
SH 304	N 71 E	40 SE					SH 383	N 28 W	15 NE				
SH 305	N 39 E	35 SE					SH 384	N 9 E	35 SE				
SH 306	N 53 E	40 SE					SH 385	N 30 W	10 SW				
SH 307	N 32 E	70 SE					SH 386	N 18 W	30 SW				
SH 308	N 58 E	50 SE					SH 387	N 43 W	45 SW				
SH 309	N 47 E	60 SE					SH 388	N 39 W	25 NE				
SH 310	N 22 E	40 SE					SH 389	N 51 W	35 SW				
SH 311	N 73 E	55 SE					SH 390	N 18 W	60 NE				
SH 312	N 84 E	60 NW					SH 391	N 40 W	40 SW				
SH 313	N 50 E	25 SE					SH 392	N 39 W	40 SW				
SH 314	N 38 E	35 SE					SH 393	N 51 W	35 SW				
SH 315	N 24 E	30 SE					SH 394	N 4 E	40 NW				
SH 316	N 39 E	40 SE					SH 395	N 30 W	25 SW				
SH 317	N 9 E	25 SE					SH 396	N 24 W	10 SW				
SH 318	N 22 E	20 SE					SH 397	N 20 E	15 SE	122	15		
SH 319	N 38 E	30 SE					SH 398	N 15 W	20 NE				
SH 320	N 24 E	30 SE					SH 399	N 4 W	25 SW			270	5
SH 321	N 39 E	40 SE					SH 400	N 36 E	20 NW				
SH 322	N 19 E	25 SE					SH 401	N 23 E	20 SW				
SH 323	N 22 E	20 SE					SH 402	N 7 E	45 SE				
SH 324	N 44 E	45 SE					SH 403	N 70 W	25 NE				
SH 325	N 18 E	15 SE					SH 404	N 16 W	45 NE				
SH 326	N 53 E	20 SE					SH 405	N 45 E	25 NW				
SH 327	N 38 E	50 SE					SH 406	N 28 E	20 NW				
SH 328	N 70 E	60 SE					SH 407	N 53 W	55 SW				
SH 329	N 28 E	15 SE					SH 408	N 21 W	40 NE				
SH 330	N 33 E	50 SE					SH 409	N 32 W	75 NE				
SH 331	N 40 E	35 SE					SH 410	N 20 W	80 SW				
SH 332	N 38 E	15 SE					SH 411	N 15 E	30 NW				
SH 333	N 50 E	50 SE					SH 412	N 19 W	85 SW				
SH 334	N 50 E	70 SE					SH 413	N 85 E	40 NW				
SH 335	N 22 E	45 SE					SH 414	N 40 W	70 SW				
SH 336	N 18 E	30 SE					SH 415	N 30 W	30 NE				
SH 337	N 47 E	20 SE					SH 416	N 22 W	75 SW				
SH 338	N 26 E	30 SE					SH 417	N 3 W	15 SW				
SH 339	N 77 W	25 SW					SH 418	N 40 W	60 NE				
SH 340	N 57 E	60 SE					SH 419	N 30 W	30 NE				
SH 341	N 41 E	35 SE					SH 420	N 22 W	75 SW				
SH 342	N 28 E	70 SE					SH 421	N 3 W	15 SW				
SH 343	N 62 W	40 SW					SH 422	N 40 W	60 NE				
SH 344	N 50 E	55 SE					SH 423	N 28 W	30 NE				
SH 345					359	5	SH 424	N 2 E	60 NW				
SH 346	N 22 E	25 SE					SH 425	N 66 W	15 NE				
SH 347	N 32 E	20 SE					SH 426	N 33 W	50 NE				
SH 348	N 13 E	30 SE					SH 427	N 87 W	50 NE				
SH 349	N 61 E	35 SE					SH 428	N 51 W	40 NE				
SH 350	N 23 E	30 SE					SH 429	N 53 W	25 NE				
SH 351	N 5 E	15 SE					SH 430	N 49 W	40 SW				
SH 352	N 23 E	15 SE					SH 431	N 30 W	30 NE				
SH 353	N 7 E	15 SE					SH 432	N 63 E	45 NW				
SH 354	N 30 E	40 SE					SH 433					16	30
SH 355	N 39 E	45 SE					SH 434	N 17 W	30 NE				
SH 356	N 17 E	20 SE					SH 435	N 31 W	60 NE				
SH 357	N 8 E	15 SE					SH 436	N 68 W	35 SW				
SH 358	N 50 W	15 SW					SH 437	N 18 W	30 NE				
SH 359	N 5 E	10 SE					SH 438	N 38 W	15 NE				
SH 360	N 19 E	60 SE					SH 439	N 28 E	50 NW				
SH 361	N 3 W	20 NE	33	15			SH 440	N 38 E	40 SE				
SH 441	N 33 E	35 SE					SH 520	N 56 E	25 SE				
SH 442	N 33 E	35 SE					SH 521	N 25 E	60 SE				
SH 443	N 27 W	30 SW					SH 522	N 55 E	50 SE				
SH 444	N 32 W	35 SW					SH 523	N 21 E	45 SE				
SH 445	N 37 W	20 SW					SH 524	N 28 E	20 NW				
SH 446	N 4 E	50 SE					SH 525	N 13 E	65 SE				
SH 447	N 44 W	45 NE					SH 526	N 24 E	35 SE				
SH 448	N 60 E	50 NW					SH 527	N 21 E	60 NW				
SH 449	N 55 E	55 SE					SH 528	N 4 E	50 SE				
SH 450	N 24 E	35 SE					SH 529	N 58 E	75 SE				
SH 451					326	45	SH 530	N 4 E	50 SE				
SH 452	N 41 E	35 SE					SH 531	N 58 E	75 SE				
SH 453	N 27 E	20 NW					SH 532	N 42 E	55 SE				
SH 454	N 24 E	50 SE					SH 533	N 25 E	60 SE				
SH 455	N 44 W	30 NE					SH 534	N 25 E	20 SE				
SH 456	N 55 W	70 NE					SH 535	N 32 E	35 SE				
SH 457	N 6 W	20 NE					SH 536	N 46 E	45 SE				
SH 458	N 27 E	35 SE					SH 537	N 38 E	40 SE				
SH 459	N 62 W	25 SW					SH 538	N 37 E	45 SE				
SH 460	N 34 E	30 SE					SH 539	N 39 E	30 SE				
SH 461	N 11 E	35 SE					SH 540	N 21 E	45 SE				
SH 462	N 33 W	30 SW					SH 541	N 27 E	35 SE				

	Foliation		Lineation		Fold Axis	
Station	Strike	Dip	Trend	Plunge	Trend	Plunge
SH 463	N 35 W	45 SW				
SH 464	N 84 E	25 NW				
SH 465	N 36 W	30 NE				
SH 466	N 25 W	50 NE				
SH 467	N 14 W	50 NE				
SH 468	N 24 W	50 NE				
SH 469	N 23 E	45 SE				
SH 470	N 13 E	15 SE				
SH 471	N 65 E	45 SE				
SH 472	N 7 E	40 SE				
SH 473	N 15 E	15 SE				
SH 474	N 21 W	60 NE				
SH 475	N 60 W	30 NE				
SH 476	N 48 W	40 NE				
SH 477	N 5 W	15 NE				
SH 478	N 7 E	70 SE				
SH 479	N 33 E	50 NW				
SH 480	N 33 W	40 NE				
SH 481	N 3 W	45 NE				
SH 482	N 22 E	50 SE				
SH 483	N 2 E	35 SE				
SH 484	N 19 W	30 NE				
SH 485	N 32 E	35 SE				
SH 486	N 2 E	15 SE				
SH 487	N 33 E	15 SE				
SH 488	N 55 E	35 SE				
SH 489	N 7 E	20 SE				
SH 490	N 21 E	60 SE				
SH 491	N 37 E	40 SE				
SH 492	N 15 E	35 SE				
SH 493	N 64 E	50 SE				
SH 494	N 8 E	15 SE				
SH 495	N 12 E	65 SE				
SH 496	N 59 E	50 SE				
SH 497	N 26 E	35 SE				
SH 498	N 19 E	75 SE				
SH 499	N 37 E	40 SE				
SH 500	N 35 E	20 SE				
SH 501	N 46 E	25 SE				
SH 502	N 66 E	30 SE				
SH 503	N 17 E	55 SE				
SH 504	N 21 E	35 SE				
SH 505	N 3 E	50 SE				
SH 506	N 17 E	55 SE				
SH 507	N 14 E	70 SE				
SH 508	N 66 E	55 SE				
SH 509	N 42 E	65 SE				
SH 510	N 5 E	50 SE				
SH 511	N 48 E	40 SE				
SH 512	N 48 E	40 SE				
SH 513	N 11 E	55 SE				
SH 514	N 7 E	50 SE				
SH 515	N 11 E	70 SE				
SH 516	N 7 E	60 SE				
SH 517	N 8 E	70 SE				
SH 518	N 83 E	60 SE				
SH 519	N 40 E	60 SE				
SH 599	N 52 E	20 SE				
SH 600	N 25 E	15 SE				
SH 601	N 28 E	60 SE				
SH 602	N 25 E	30 SE				
SH 603	N 46 E	20 SE				
SH 604	N 36 E	15 SE				
SH 605	N 24 E	45 SE				
SH 606	N 76 E	15 SE				
SH 607	N 31 E	25 SE				
SH 608	N 39 E	15 SE				
SH 609	N 24 E	50 SE				
SH 610	N 21 E	30 SE				
SH 611	N 35 E	20 SE				
SH 612	N 59 E	15 SE				
SH 613	N 44 E	20 SE				
SH 614	N 40 E	20 SE				
SH 615	N 23 E	15 SE				
SH 616	N 60 E	15 SE				
SH 617	N 74 E	20 SE				
SH 618	N 31 E	60 SE				
SH 619	N 16 E	20 SE				
SH 620	N 4 W	40 NE				
SH 621	N 66 E	20 SE				
SH 622	N 40 E	25 SE				
SH 623	N 78 E	40 SE				
SH 624	N 63 E	20 SE				
SH 625	N 58 E	20 SE				
SH 626	N 24 E	25 SE				
SH 627	N 15 E	25 NW				
SH 628	N 4 E	20 NW				
SH 629	N 77 W	20 SW				
SH 630	N 12 E	60 SE				
SH 631	N 41 E	25 SE				
SH 632	N 7 E	25 NW				

	Foliation		Lineation		Fold Axis	
Station	Strike	Dip	Trend	Plunge	Trend	Plunge
SH 542	N 43 E	30 SE				
SH 543	N 23 E	30 SE				
SH 544	N 24 E	60 SE				
SH 545	N 54 E	65 SE				
SH 546	N 68 E	35 SE				
SH 547	N 48 E	50 SE				
SH 548	N 34 E	45 SE				
SH 549	N 61 E	45 SE				
SH 550	N 35 E	50 SE				
SH 551	N 30 E	30 SE				
SH 552	N 39 E	45 SE				
SH 553	N 33 E	20 SE				
SH 554	N 26 E	60 SE				
SH 555	N 32 E	40 SE				
SH 556	N 24 E	15 SE				
SH 557	N 22 E	25 SE				
SH 558	N 17 E	70 SE				
SH 559	N 66 E	60 SE				
SH 560	N 51 E	25 SE				
SH 561	N 35 E	25 SE				
SH 562	N 49 E	65 SE				
SH 563			177	15		
SH 564	N 54 E	40 SE				
SH 565	N 51 E	12 SE				
SH 566	N 52 E	15 SE				
SH 567	N 29 E	20 SE				
SH 568	N 30 E	20 SE				
SH 569	N 32 E	60 SE				
SH 570	N 20 W	40 NE				
SH 571	N 49 W	30 SW				
SH 572	N 30 E	35 SE				
SH 573	N 25 W	25 NE				
SH 574	N 48 E	20 SE				
SH 575	N 18 E	45 SE				
SH 576	N 61 W	30 SW				
SH 577	N 18 E	20 SE				
SH 578	N 23 E	25 SE				
SH 579	N 19 E	55 SE				
SH 580	N 16 E	55 SE				
SH 581	N 35 E	25 SE				
SH 582	N 25 E	30 SE				
SH 583	N 28 E	35 SE				
SH 584	N 70 E	25 SE				
SH 585	N 63 E	15 SE				
SH 586	N 37 E	10 SE				
SH 587	N 83 E	20 SE				
SH 588	N 13 E	70 SE				
SH 589	N 25 E	30 SE				
SH 590	N 28 E	25 SE				
SH 591	N 29 E	30 SE				
SH 592	N 38 E	50 SE				
SH 593	N 81 E	30 SE				
SH 594	N 36 W	25 SW				
SH 595	N 34 E	25 SE				
SH 596	N 37 E	20 SE				
SH 597	N 27 E	25 SE				
SH 598	N 22 E	25 SE				
SH 678	N 66 E	30 SE				
SH 679	N 62 E	15 NW				
SH 680	N 68 W	15 SW				
SH 681	N 25 E	20 SE				
SH 682	N 27 E	20 SE				
SH 683	N 27 E	50 SE				
SH 684	N 32 E	30 SE				
SH 685	N 30 E	25 SE				
SH 686	N 10 E	15 SE				
SH 687	N 14 E	20 SE				
SH 688	N 20 E	10 SE				
SH 689	N 22 E	15 SE				
SH 690	N 61 E	20 SE				
SH 691	N 67 E	10 SE				
SH 692	N 44 E	70 SE				
SH 693	N 6 E	20 SE				
SH 694	N 35 E	30 SE				
SH 695	N 24 E	25 SE				
SH 696	N 16 W	25 NE				
SH 697	N 23 E	40 SE				
SH 698	N 51 E	20 SE				
SH 699	N 14 E	10 SE				
SH 700	N 49 E	40 SE				
SH 701	N 20 E	35 SE				
SH 702	N 34 E	25 SE				
SH 703	N 14 E	50 SE				
SH 704	N 23 E	20 SE				
SH 705	N 36 E	15 SE				
SH 706	N 54 W	10 SW				
SH 707	N 27 E	35 SE				
SH 708	N 21 E	20 SE				
SH 709	N 23 E	25 SE				
SH 710	N 83 E	25 SE				
SH 711	N 25 E	30 SE				

	Foliation		Lineation		Fold Axis			Foliation		Lineation		Fold Axis	
Station	Strike	Dip	Trend	Plunge	Trend	Plunge	Station	Strike	Dip	Trend	Plunge	Trend	Plunge
SH 633	N 6 E	45 SE					SH 712	N 5 E	25 SE				
SH 634	N 5 W	70 NE					SH 713	N 21 E	20 SE				
SH 635	N 24 W	45 NE					SH 714	N 8 E	10 SE				
SH 636	N 29 W	45 SW					SH 715	N 26 E	15 SE				
SH 637	N 78 E	30 SE					SH 716	N 35 E	15 SE				
SH 638	N 5 E	45 NW					SH 717	N 87 E	10 SE				
SH 639	N 5 E	55 SE					SH 718	N 40 E	25 SE				
SH 640	N 19 E	40 NW					SH 719	N 49 E	50 SE				
SH 641	N 22 E	25 SE					SH 720	N 49 E	50 SE				
SH 642	N 71 W	70 NE					SH 721	N 45 E	30 SE				
SH 643	N 13 E	50 SE					SH 722	N 23 E	25 SE				
SH 644	N 33 E	60 SE					SH 723	N 17 E	15 SE				
SH 645	N 28 W	20 NE					SH 724					118	10
SH 646	N 34 E	30 SE					SH 725	N 21 E	10 SE				
SH 647	N 23 E	40 NW					SH 726	N 43 E	30 SE				
SH 648	N 9 E	70 SE					SH 727	N 35 E	25 SE				
SH 649	N 31 E	40 NW					SH 728	N 23 E	40 SE				
SH 650	N 35 E	20 SE					SH 729	N 19 E	40 SE				
SH 651	N 48 W	25 NE					SH 730	N 31 E	30 SE				
SH 652	N 25 W	40 NE					SH 731	N 24 E	10 SE				
SH 653	N 11 E	10 SE					SH 732	N 41 E	25 SE				
SH 654	N 48 W	50 NE					SH 733	N 41 E	20 SE				
SH 655	N 61 E	30 NW					SH 734	N 35 E	25 SE				
SH 656			23	20			SH 735	N 39 E	15 SE				
SH 657	N 11 E	10 SE					SH 736	N 25 E	35 SE				
SH 658	N 11 E	30 SE					SH 737	N 59 E	35 SE				
SH 659	N 82 E	30 SE					SH 738	N 49 E	45 SE				
SH 660	N 48 E	15 NW					SH 739	N 68 E	15 SE				
SH 661	N 17 E	25 SE					SH 740	N 20 E	40 SE				
SH 662	N 9 W	15 NE					SH 741	N 27 E	45 SE				
SH 663	N 9 E	15 SE					SH 742	N 31 E	20 SE				
SH 664	N 34 E	25 SE					SH 743	N 43 E	25 SE				
SH 665	N 16 E	50 SE					SH 744	N 40 E	30 SE				
SH 666	N 42 E	20 SE					SH 745	N 26 E	20 SE				
SH 667	N 40 E	10 SE					SH 746	N 39 E	40 SE				
SH 668	N 42 E	15 SE					SH 747	N 56 E	30 SE				
SH 669	N 49 E	20 SE					SH 748	N 72 E	50 SE				
SH 670	N 18 E	15 SE					SH 749	N 59 E	30 SE				
SH 671	N 14 E	20 NW					SH 750	N 48 E	45 SE				
SH 672	N 65 E	75 SE					SH 751	N 32 E	45 SE				
SH 673	N 68 E	10 SE					SH 752	N 31 E	45 SE				
SH 674	N 72 E	25 SE					SH 753	N 11 W	30 NE				
SH 675					196	15	SH 754	N 67 E	10 SE				
SH 676	N 4 E	45 NW					SH 755	N 32 E	25 SE				
SH 677	N 52 E	15 SE					SH 756	N 71 E	35 SE				
SH 757	N 19 E	20 SE					SH 836	N 44 W	30 NE				
SH 758	N 53 E	40 SE					SH 837	N 49 E	50 SE				
SH 759	N 48 E	20 SE					SH 838	N 43 E	10 SE				
SH 760	N 49 E	50 SE					SH 839	N 49 E	20 SE				
SH 761	N 2 W	35 SW					SH 840	N 31 W	20 NE				
SH 762	N 6 E	15 SE					SH 841	N 36 W	20 NE				
SH 763	N 31 E	45 SE					SH 842	N 54 E	25 SE				
SH 764	N 26 E	20 SE					SH 843	N 21 W	40 NE				
SH 765	N 18 E	40 SE					SH 844	N 45 W	20 SW				
SH 766	N 14 W	20 NE					SH 845	N 64 W	20 SW				
SH 767	N 30 E	70 SE					SH 846	N 42 E	20 SE				
SH 768	N 57 E	25 SE					SH 847	N 64 W	20 SW				
SH 769	N 32 E	30 SE					SH 848	N 31 E	20 NW				
SH 770	N 41 E	30 SE					SH 849	N 21 W	50 NE				
SH 771	N 20 E	50 SE					SH 850	N 43 W	10 SW				
SH 772	N 39 E	50 SE					SH 851	N 51 E	15 NE				
SH 773	N 31 E	55 SE					SH 852	N 64 W	40 NE				
SH 774	N 46 E	55 SE					SH 853	N 4 W	30 NE				
SH 775	N 28 E	40 SE					SH 854	N 45 W	20 NE				
SH 776	N 59 E	20 SE					SH 855	N 60 W	25 NE				
SH 777	N 49 E	45 SE					SH 856	N 13 E	20 SE				
SH 778	N 16 E	55 SE					SH 857	N 56 W	25 NE				
SH 779	N 33 E	25 SE					SH 858	N 48 E	20 NW				
SH 780	N 41 E	45 SE					SH 859	N 36 W	20 NE				
SH 781	N 43 E	60 SE					SH 860	N 27 W	30 NE				
SH 782	N 20 E	60 SE					SH 861	N 34 W	20 NE				
SH 783	N 10 E	70 SE					SH 862	N 19 W	20 NE				
SH 784	N 16 W	45 NE					SH 863	N 14 W	20 NE				
SH 785	N 8 W	30 NE					SH 864	N 40 E	25 NW				
SH 786	N 26 W	45 NE					SH 865	N 54 W	45 NE				
SH 787	N 10 E	35 SE	142	5			SH 866	N 45 W	20 NE				
SH 788	N 36 E	35 SE					SH 867	N 45 W	20 NE				
SH 789	N 37 E	50 SE					SH 868	N 9 E	45 SE				
SH 790	N 47 E	25 SE					SH 869	N 23 W	40 SW				
SH 791	N 40 W	40 NE	87	35			SH 870	N 2 W	40 NE				
SH 792	N 21 E	35 SE					SH 871	N 8 W	45 NE				
SH 793	N 12 W	45 NE					SH 872	N 84 W	50 NE				
SH 794	N 45 W	30 NE					SH 873	N 16 W	45 SW				
SH 795	N 19 E	50 SE					SH 874	N 14 W	40 NE				
SH 796	N 31 E	50 SE					SH 875	N 53 W	40 NE				
SH 797	N 19 W	20 NE					SH 876	N 38 E	40 SE				
SH 798	N 7 W	55 NE					SH 877	N 13 W	30 NE				
SH 799	N 7 E	50 SE					SH 878	N 60 W	20 SW				
SH 800	N 17 E	15 SE					SH 879	N 23 W	30 SW				
SH 801	N 5 E	55 SE					SH 880					36	5
SH 802					152	15	SH 881	N 61 E	25 SE				

	Foliation		Lineation		Fold Axis			Foliation		Lineation		Fold Axis	
Station	Strike	Dip	Trend	Plunge	Trend	Plunge	Station	Strike	Dip	Trend	Plunge	Trend	Plunge
SH 803					149	20	SH 882	N 29 W	25 SW				
SH 804					174	20	SH 883	N 34 W	20 SW				
SH 805	N 8 W	65 NE					SH 884	N 25 W	40 SW				
SH 806	N 45 W	65 NE					SH 885	N 38 E	25 SE				
SH 807	N 25 E	50 SE					SH 886	N 29 E	10 NW				
SH 808	N 9 E	40 SE					SH 887	N 33 E	15 NW				
SH 809	N 11 E	60 SE					SH 888					37	5
SH 810	N 19 E	5 SE					SH 889	N 38 W	40 NE				
SH 811	N 43 E	40 SE					SH 890	N 16 W	40 NE				
SH 812	N 22 W	15 SW					SH 891	N 30 E	40 SE				
SH 813	N 27 E	45 SE					SH 892	N 51 E	50 NW				
SH 814	N 24 E	45 SE					SH 893	N 47 E	15 SE				
SH 815	N 54 W	25 SW					SH 894	N 26 E	10 SE				
SH 816					125	10	SH 895	N 9 E	20 SE				
SH 817	N 18 E	15 SE					SH 896	N 51 E	10 SE				
SH 818	N 26 E	20 SE					SH 897	N 42 E	10 SE				
SH 819	N 19 W	5 NE					SH 898	N 27 E	40 SE				
SH 820					186	10	SH 899	N 87 W	40 SW				
SH 821	N 9 E	20 SE					SH 900	N 49 E	20 SE				
SH 822	N 42 W	45 NE					SH 901					179	15
SH 823	N 29 W	45 NE					SH 902	N 25 W	30 NE				
SH 824	N 21 W	35 SW					SH 903	N 76 E	10 SE				
SH 825	N 9 E	25 SE					SH 904	N 82 E	10 SE				
SH 826					124	10	SH 905	N 50 W	10 SW				
SH 827					64	20	SH 906	N 37 E	30 SE				
SH 828	N 69 W	15 NE					SH 907	N 27 W	10 NE				
SH 829	N 19 W	15 NE					SH 908	N 60 E	25 SE				
SH 830	N 24 E	45 SE					SH 909	N 51 E	30 NW				
SH 831	N 71 W	40 NE					SH 910	N 28 W	20 SW				
SH 832	N 89 W	45 NE					SH 911	N 16 E	25 SE				
SH 833	N 60 W	30 NE					SH 912	N 33 E	45 SE				
SH 834	N 34 W	30 NE					SH 913	N 31 E	65 SE				
SH 835	N 26 W	50 NE					SH 914	N 55 W	20 SW				
SH 915	N 6 E	30 SE					SH 994	N 57 W	20 SW				
SH 916	N 52 W	25 SW					SH 995	N 62 W	30 SW	175	5		
SH 917	N 23 E	35 SE					SH 996	N 86 W	40 SW				
SH 918	N 64 W	10 SW					SH 997	N 8 W	40 NE				
SH 919	N 19 W	10 SW					SH 998	N 57 W	10 SW				
SH 920	N 44 E	30 SE					SH 999	N 50 W	40 SW				
SH 921	N 25 E	10 NW					SH 1000	N 60 W	20 SW				
SH 922	N 25 W	30 NE					SH 1001	N 46 E	25 SE				
SH 923	N 60 E	30 SE					SH 1002	N 45 E	20 SE				
SH 924	N 80 E	30 SE					SH 1003	N 36 E	45 SE				
SH 925	N 38 E	20 SE					SH 1004	N 76 W	15 SW				
SH 926	N 3 E	25 SE					SH 1005	N 52 W	15 SW				
SH 927	N 15 E	35 SE					SH 1006	N 24 E	20 SE				
SH 928	N 5 E	25 SE					SH 1007	N 30 E	30 SE				
SH 929	N 46 W	15 NE					SH 1008	N 30 W	15 SW				
SH 930	N 16 E	40 SE					SH 1009	N 9 E	40 SE				
SH 931	N 35 E	30 SE					SH 1010	N 24 E	20 SE				
SH 932	N 13 E	15 SE					SH 1011	N 12 E	15 SE				
SH 933	N 25 E	30 SE					SH 1012	N 42 E	25 SE				
SH 934	N 41 E	20 SE					SH 1013	N 24 E	20 SE				
SH 935	N 41 E	20 SE					SH 1014	N 37 E	20 SE				
SH 936	N 18 W	40 NE					SH 1015	N 38 E	20 SE				
SH 937	N 37 E	60 SE					SH 1016	N 14 E	20 SE				
SH 938	N 29 E	10 SE					SH 1017	N 36 E	25 SE				
SH 939	N 22 E	15 SE					SH 1018	N 58 E	15 SE				
SH 940	N 35 W	40 SW					SH 1019	N 10 E	20 SE				
SH 941	N 25 E	30 SE					SH 1020	N 24 E	20 SE				
SH 942	N 13 E	25 SE					SH 1021	N 52 E	20 SE				
SH 943	N 25 E	30 SE					SH 1022	N 25 E	70 SE				
SH 944	N 27 E	15 SE					SH 1023	N 36 E	15 SE				
SH 945	N 65 E	15 SE					SH 1024	N 42 E	15 SE				
SH 946	N 36 E	10 NW					SH 1025	N 88 E	50 SE				
SH 947	N 14 E	20 SE					SH 1026	N 68 E	35 SE				
SH 948	N 89 W	20 SW			126	20	SH 1027	N 14 E	30 SE				
SH 949	N 20 E	60 SE					SH 1028	N 10 E	30 SE				
SH 950	N 88 W	50 SW					SH 1029	N 35 E	15 SE				
SH 951	N 43 E	40 SE					SH 1030	N 6 W	45 NW				
SH 952	N 19 E	25 SE					SH 1031	N 32 E	15 SE				
SH 953	N 21 E	45 SE					SH 1032	N 40 E	20 SE				
SH 954	N 19 E	50 SE					SH 1033	N 15 E	10 SE				
SH 955	N 34 E	50 SE					SH 1034	N 12 W	45 NE				
SH 956	N 50 E	60 SE					SH 1035	N 36 E	15 SE				
SH 957	N 47 E	35 SE					SH 1036	N 36 E	15 SE				
SH 958	N 49 E	60 SE					SH 1037	N 41 E	20 SE				
SH 959	N 53 E	20 SE					SH 1038	N 16 E	15 SE				
SH 960	N 33 E	25 SE					SH 1039	N 31 E	10 SE				
SH 961	N 8 E	20 SE					SH 1040	N 41 E	20 SE				
SH 962	N 51 E	10 SE					SH 1041	N 15 E	15 SE				
SH 963	N 56 E	10 SE					SH 1042	N 51 E	15 SE				
SH 964	N 24 E	20 SE					SH 1043	N 22 W	40 SW				
SH 965	N 25 E	30 SE					SH 1044	N 49 E	15 SE	168	15		
SH 966	N 24 E	70 SE					SH 1045	N 41 E	15 SE				
SH 967	N 8 E	70 SE					SH 1046	N 32 E	10 SE				
SH 968	N 9 E	10 SE					SH 1047	N 18 W	20 NE				
SH 969	N 5 E	35 SE					SH 1048	N 58 E	10 SE				
SH 970	N 6 W	25 NE					SH 1049	N 37 E	50 SE				
SH 971	N 41 E	40 SE					SH 1050	N 53 E	25 SE				
SH 972	N 37 E	20 SE					SH 1051	N 27 EE	50 SE				

	Foliation		Lineation		Fold Axis			Foliation		Lineation		Fold Axis	
Station	Strike	Dip	Trend	Plunge	Trend	Plunge	Station	Strike	Dip	Trend	Plunge	Trend	Plunge
SH 973	N 54 E	25 SE					SH 1052	N 30 E	40 SE				
SH 974	N 64 E	35 SE					SH 1053	N 11 E	25 SE				
SH 975	N 50 E	15 SE					SH 1054	N 33 E	30 SE				
SH 976	N 11 E	15 SE					SH 1055	N 23 E	45 SE				
SH 977	N 27 E	30 SE					SH 1056	N 24 E	40 SE				
SH 978	N 27 E	30 SE					SH 1057	N 12 E	45 SE				
SH 979	N 82 E	10 SE					SH 1058	N 26 E	50 SE				
SH 980	N 79 E	20 SE					SH 1059	N 18 E	30 SE				
SH 981	N 68 E	30 SE					SH 1060	N 7 W	15 NE				
SH 982	N 61 E	10 SE					SH 1061	N 31 E	70 SE				
SH 983	N 38 E	20 SE					SH 1062	N 45 E	45 SE				
SH 984	N 19 E	20 SE					SH 1063	N 31 W	10 NE				
SH 985	N 77 E	10 SE					SH 1064	N 41 E	45 SE				
SH 986	N 48 E	20 SE					SH 1065	N 3 E	30 SE				
SH 987	N 84 E	15 SE					SH 1066	N 66 E	15 SE				
SH 988	N 70 E	15 SE					SH 1067	N 31 E	10 SE				
SH 989	N 70 W	10 NE					SH 1068	N 30 E	15 SE				
SH 990	N 79 E	10 SE					SH 1069	N 10 E	15 SE				
SH 991	N 89 W	10 SW					SH 1070	N 25 E	10 SE				
SH 992	N 5 W	15 SW					SH 1071	N 31 E	30 SE				
SH 993	N 75 W	15 SW					SH 1072	N 14 E	10 SE				
SH 1073	N 20 E	20 SE					SH 1152	N 11 E	35 SE				
SH 1074	N 25 E	10 SE					SH 1153	N 14 E	35 SE				
SH 1075					189	5	SH 1154	N 20 E	30 SE				
SH 1076	N 5 W	15 NE					SH 1155	N 82 W	30 SW				
SH 1077	N 5 E	45 SE					SH 1156					187	10
SH 1078	N 27 W	20 SW					SH 1157	N 14 W	30 SW				
SH 1079	N 12 E	30 SE					SH 1158	N 14 E	15 NW				
SH 1080	N 15 E	75 NW					SH 1159	N 25 E	25 SE				
SH 1081	N 33 E	15 SE					SH 1160					17	15
SH 1082	N 12 E	50 SE					SH 1161	N 18 E	25 SE				
SH 1083	N 43 E	25 SE					SH 1162	N 9 E	10 SE				
SH 1084	N 37 E	25 SE					SH 1163	N 81 E	30 NW				
SH 1085	N 68 E	15 SE					SH 1164	N 22 E	30 NW				
SH 1086	N 32 E	25 SE					SH 1165	N 16 E	25 SE				
SH 1087	N 14 E	50 SE					SH 1166	N 17 E	10 SE				
SH 1088	N 16 E	10 SE					SH 1167	N 45 E	30 NW				
SH 1089	N 13 E	40 NW					SH 1168	N 18 E	10 NW				
SH 1090	N 25 E	70 SE					SH 1169	N 21 E	35 SE				
SH 1091	N 18 E	25 SE					SH 1170	N 15 E	10 SE				
SH 1092	N 9 E	20 SE					SH 1171	N 29 E	70 SE				
SH 1093	N 6 E	60 SE					SH 1172	N 28 W	25 SW				
SH 1094	N 42 E	20 SE					SH 1173	N 59 E	50 NW				
SH 1095	N 39 E	10 SE					SH 1174	N 86 W	15 SW				
SH 1096	N 11 E	30 SE					SH 1175	N 10 E	15 NW				
SH 1097	N 21 E	40 SE					SH 1176	N 18 E	20 SE				
SH 1098	N 26 E	40 SE					SH 1177	N 66 E	10 SE				
SH 1099	N 26 E	25 SE					SH 1178	N 49 E	10 SE				
SH 1100	N 14 E	30 SE					SH 1179	N 13 E	30 SE				
SH 1101	N 3 E	10 NW					SH 1180	N 13 E	25 SE				
SH 1102					170	10	SH 1181					174	10
SH 1103	N 8 W	25 NE					SH 1182	N 1 W	20 NE				
SH 1104	N 77 W	20 SW					SH 1183	N 5 E	40 SE				
SH 1105	N 34 E	15 SE					SH 1184	N 11 E	30 SE				
SH 1106	N 43 W	25 NE					SH 1185	N 23 E	25 SE				
SH 1107	N 28 W	15 NE					SH 1186	N 10 E	40 SE				
SH 1108	N 58 W	40 NE					SH 1187	N 10 E	20 SE				
SH 1109	N 31 E	25 SE					SH 1188	N 7 E	25 SE				
SH 1110					201	20	SH 1189	N 18 E	20 SE				
SH 1111	N 46 W	15 SW					SH 1190	N 2 E	15 SE				
SH 1112	N 3 W	15 SW					SH 1191	N 70 W	20 SW				
SH 1113	N 5 E	30 SE					SH 1192	N 23 W	10 SW				
SH 1114	N 15 E	30 SE					SH 1193	N 19 W	30 SW				
SH 1115	N 10 E	25 SE					SH 1194	N 33 E	10 SE				
SH 1116	N 40 E	10 SE					SH 1195	N 41 W	20 SW				
SH 1117	N 12 E	25 SE					SH 1196	N 27 E	55 SE				
SH 1118	N 46 E	30 SE					SH 1197	N 37 E	20 SE				
SH 1119	N 24 E	20 SE					SH 1198	N 4 E	10 SE				
SH 1120	N 30 E	10 SE					SH 1199	N 78 E	15 SE				
SH 1121	N 10 E	20 SE					SH 1200	N 60 E	20 SE				
SH 1122	N 27 E	30 SE					SH 1201	N 79 E	25 SE				
SH 1123	N 49 E	50 SE					SH 1202	N 63 E	30 SE				
SH 1124					18	10	SH 1203	N 36 W	15 SW				
SH 1125	N 19 E	30 SE					SH 1204	N 59 E	15 SE				
SH 1126	N 16 E	45 SE					SH 1205	N 21 E	35 SE				
SH 1127	N 22 E	35 SE					SH 1206	N 32 E	20 SE				
SH 1128	N 5 E	50 SE					SH 1207					183	10
SH 1129	N 28 E	50 SE					SH 1208	N 49 W	30 NE				
SH 1130	N 21 E	10 SE					SH 1209					172	10
SH 1131	N 23 E	30 SE					SH 1210	N 9 E	15 SE				
SH 1132	N 10 E	30 SE					SH 1211	N 16 W	35 SW				
SH 1133	N 10 E	25 SE					SH 1212	N 61 W	65 SW				
SH 1134	N 38 E	25 SE					SH 1213	N 20 E	25 SE				
SH 1135	N 25 E	30 SE					SH 1214	N 33 W	30 NE				
SH 1136	N 56 E	20 SE					SH 1215	N 26 E	45 SE				
SH 1137	N 29 E	35 SE					SH 1216	N 86 E	20 SE				
SH 1138	N 19 E	25 SE					SH 1217	N 28 E	25 SE				
SH 1139	N 61 E	10 SE					SH 1218	N 89 W	15 SW				
SH 1140	N 20 E	50 SE					SH 1219	N 66 E	55 SE				
SH 1141	N 31 E	10 SE					SH 1220	N 56 E	25 SE				
SH 1142	N 12 E	15 NW					SH 1221	N 61 W	20 SW				

	Foliation		Lineation		Fold Axis			Foliation		Lineation		Fold Axis	
Station	Strike	Dip	Trend	Plunge	Trend	Plunge	Station	Strike	Dip	Trend	Plunge	Trend	Plunge
SH 1143	N 33 E	40 SE					SH 1222	N 48 E	40 SE				
SH 1144	N 21 E	70 SE					SH 1223	N 27 E	50 NW				
SH 1145	N 25 E	70 SE					SH 1224	N 22 W	15 SW				
SH 1146	N 12 E	30 SE					SH 1225	N 33 W	25 SW				
SH 1147	N 26 E	50 NW					SH 1226	N 29 W	25 SW				
SH 1148	N 29 E	20 SE					SH 1227	N 69 W	10 SW				
SH 1149	N 12 E	65 SE					SH 1228	N 88 W	20 SW				
SH 1150	N 11 E	50 SE					SH 1229	N 54 W	10 SW				
SH 1151					24	10	SH 1230	N 86 W	20 SW				
SH 1231	N 85 E	30 SE					SH 1310	N 54 E	15 SE				
SH 1232	N 78 W	10 SW					SH 1311	N 28 E	25 SE				
SH 1233	N 51 E	10 SE					SH 1312	N 16 E	15 SE				
SH 1234	N 45 E	20 SE					SH 1313	N 40 E	15 SE				
SH 1235	N 44 W	15 NE					SH 1314	N 61 E	20 SE				
SH 1236	N 54 W	30 SW					SH 1315	N 10 E	20 SE				
SH 1237	N 86 W	20 SW					SH 1316	N 43 E	35 SE				
SH 1238	N 85 E	30 SE					SH 1317	N 18 E	55 SE				
SH 1239	N 78 W	20 SW					SH 1318	N 22 W	25 SW				
SH 1240	N 51 E	20 SE					SH 1319	N 61 E	55 SE				
SH 1241	N 52 E	25 SE					SH 1320	N 32 E	10 SE				
SH 1242	N 5 E	10 SE					SH 1321	N 26 E	40 SE				
SH 1243	N 86 W	15 SW					SH 1322	N 57 E	30 SE				
SH 1244	N 58 E	15 SE					SH 1323	N 16 W	30 NE				
SH 1245	N 89 E	30 SE					SH 1324	N 54 E	55 SE				
SH 1246	N 89 W	30 SW					SH 1325	N 48 E	20 SE				
SH 1247	N 77 W	15 SW					SH 1326	N 64 E	30 SE				
SH 1248	N 58 E	10 SE					SH 1327	N 14 E	15 SE				
SH 1249	N 45 W	10 SW					SH 1328	N 23 E	10 SE				
SH 1250	N 82 E	25 SE					SH 1329	N 20 E	45 SE				
SH 1251	N 82 W	10 SW					SH 1330			103	23		
SH 1252	N 71 E	30 SE					SH 1331	N 43 W	20 SW				
SH 1253	N 35 E	25 SE					SH 1332	N 41 E	40 SE				
SH 1254	N 23 E	20 SE					SH 1333	N 67 W	50 SW				
SH 1255	N 43 E	30 SE					SH 1334	N 19 E	55 SE				
SH 1256	N 28 E	25 SE					SH 1335	N 67 E	25 SE				
SH 1257	N 49 E	15 SE					SH 1336	N 58 E	20 SE				
SH 1258	N 77 E	10 SE					SH 1337			110	40		
SH 1259					163	10	SH 1338	N 62 E	10 NW				
SH 1260	N 22 E	35 SE					SH 1339	N 15 E	20 SE				
SH 1261	N 48 E	30 SE					SH 1340	N 12 E	55 SE				
SH 1262	N 68 E	35 SE					SH 1341	N 69 W	20 SW				
SH 1263	N 42 E	20 SE					SH 1342	N 46 W	20 SW				
SH 1264	N 61 E	20 SE					SH 1343	N 43 W	25 SW				
SH 1265	N 80 E	25 SE					SH 1344	N 78 W	25 SW				
SH 1266	N 37 E	55 SE					SH 1345	N 88 W	20 SW				
SH 1267	N 31 E	40 SE					SH 1346	N 24 W	20 SW				
SH 1268	N 74 E	25 SE					SH 1345	N 30 E	20 SW				
SH 1269	N 36 E	15 SE					SH 1348	N 12 E	30 SE				
SH 1270	N 28 E	40 SE					SH 1349	N 57 W	15 SW				
SH 1271	N 33 E	25 SE					SH 1350	N 14 E	35 SE				
SH 1272	N 51 E	25 SE					SH 1351	N 80 E	10 SE				
SH 1273	N 66 E	15 SE					SH 1352	N 63 E	25 SE				
SH 1274	N 83 W	20 SW					SH 1353	N 67 E	5 SE				
SH 1275	N 78 W	20 SW					SH 1354	N 21 W	15 NE				
SH 1276	N 72 E	20 SE					SH 1355	N 19 W	30 NE				
SH 1277	N 31 W	35 SW					SH 1356	N 26 W	20 NE				
SH 1278	N 88 W	20 SW					SH 1357	N 27 W	10 NE				
SH 1279	N 37 E	40 SE					SH 1358	N 55 E	15 SE				
SH 1280	N 45 E	20 SE					SH 1359	N 31 E	10 SE				
SH 1281	N 32 W	35 SW					SH 1360	N 44 E	20 SE				
SH 1282	N 29 E	20 SE					SH 1361	N 61 W	15 NE				
SH 1283	N 34 E	20 SE					SH 1362	N 39 W	20 NE				
SH 1284	N 7 E	70 SE					SH 1363	N 14 E	10 NW				
SH 1285	N 47 E	20 SE					SH 1364	N 39 E	10 NW				
SH 1286	N 32 E	15 SE					SH 1365	N 43 W	25 NE				
SH 1287	N 21 E	20 SE					SH 1366	N 33 E	30 NW				
SH 1288	N 89 E	15 SE					SH 1367	N 27 E	20 SE				
SH 1289	N 62 E	10 SE					SH 1368	N 36 W	30 NE				
SH 1290	N 28 E	20 SE					SH 1369	N 44 W	25 NE				
SH 1291	N 49 E	25 SE					SH 1370	N 13 E	20 SE				
SH 1292	N 56 W	25 SW					SH 1371	M 21 W	30 SW				
SH 1293	N 35 E	15 SE					SH 1372					332	30
SH 1294	N 28 E	35 SE					SH 1373					321	30
SH 1295	N 30 W	25 SW					SH 1374					314	50
SH 1296	N 75 E	75 SE					SH 1375					261	25
SH 1297	N 64 E	10 SE					SH 1376	N 45 E	20 NW				
SH 1298	N 75 E	10 SE					SH 1377	N 57 W	10 NE				
SH 1299	N 64 E	10 SE					SH 1378	N 22 E	15 NW				
SH 1300	N 46 E	35 SE					SH 1379	N 3 E	2 NW				
SH 1301	N 31 E	45 SE					SH 1380	N 32 E	15 NW				
SH 1302	N 68 E	55 SE					SH 1381	N 33 W	50 NE				
SH 1303	N 22 E	50 SE					SH 1382	N 42 W	35 NE				
SH 1304	N 58 E	20 SE					SH 1383	N 35 E	25 NW				
SH 1305	N 42 E	40 SE					SH 1384	N 17 W	10 NE				
SH 1306	N 21 E	30 SE					SH 1385	N 42 W	15 NE				
SH 1307	N 45 E	20 SE					SH 1386	N 31 W	20 NE				
SH 1308	N 43 E	20 SE					SH 1387	N 64 W	20 NE				
SH 1309	N 46 E	20 NW					SH 1388	N 22 E	10 SE				
SH 1389	N 51 E	10 NW					SH 1468	N 53 W	10 SW				
SH 1390	N 25 E	20 NW					SH 1469	N 40 W	5 SW				
SH 1391	N 23 W	60 SW					SH 1470	N 42 W	20 SW				

	Foliation		Lineation		Fold Axis			Foliation		Lineation		Fold Axis	
Station	Strike	Dip	Trend	Plunge	Trend	Plunge	Station	Strike	Dip	Trend	Plunge	Trend	Plunge
SH 1392	N 17 W	25 NE					SH 1471					220	5
SH 1393	N 47 W	45 NE					SH 1472	N 17 W	30 SW				
SH 1394	N 42 E	45 SE					SH 1473	N 17 W	30 SW				
SH 1395	N 62 W	20 NE					SH 1474	N 26 W	30 SW				
SH 1396	N 57 W	20 NE					SH 1475	N 22 W	15 SW				
SH 1397	N 48 W	10 NE					SH 1476	N 15 W	80 SW				
SH 1398	N 38 W	40 NE					SH 1477	N 43 E	20 NE				
SH 1399	N 82 E	15 SE					SH 1478	N 42 E	20 SE				
SH 1400	N 25 W	10 NE					SH 1479	N 38 E	50 SE				
SH 1401	N 6 W	20 NE					SH 1480	N 16 W	5 NE				
SH 1402	N 13 W	15 NE					SH 1481	N 56 E	20 SE				
SH 1403	N 43 E	10 NW					SH 1482	N 39 E	55 SE				
SH 1404	N 58 E	10 NW					SH 1483	N 64 E	40 SE				
SH 1405	N 54 W	40 SW					SH 1484	N 9 W	15 NE				
SH 1406	N 2 E	10 SE					SH 1485	N 27 W	15 NE				
SH 1407	N 36 E	10 SE					SH 1486	N 13 E	35 SE				
SH 1408	N 25 W	25 NE					SH 1487	N 78 W	25 SW				
SH 1409	N 44 W	30 NE					SH 1488	N 55 W	25 SW				
SH 1410	N 89 W	30 NE					SH 1489	N 42 W	30 SW				
SH 1411	N 39 W	35 NE					SH 1490	N 57 E	25 NW				
SH 1412	N 42 E	15 SE					SH 1491	N 2 E	30 NW				
SH 1413	N 23 E	10 NW					SH 1492	N 27 E	25 NW				
SH 1414	N 39 E	15 SE					SH 1493	N 4 W	25 NE				
SH 1415	N 42 E	15 SE					SH 1494	N 77 E	20 SE				
SH 1416	N 23 E	10 NW					SH 1495	N 68 E	10 SE				
SH 1417	N 39 E	15 SE					SH 1496	N 66 E	10 SE				
SH 1418	N 36 W	20 NE					SH 1497	N 9 E	50 SE				
SH 1419	N 60 W	25 NE					SH 1498	N 18 E	50 NW				
SH 1420					172	5	SH 1499	N 6 E	30 NW				
SH 1421	N 18 E	25 SE					SH 1500	N 3 E	10 NW				
SH 1422	N 9 E	25 SE					SH 1501	N 71 W	5 SW				
SH 1423	N 20 E	15 SE					SH 1502	N 80 W	10 SW				
SH 1424	N 61 E	50 SE					SH 1503	N 32 W	15 SW				
SH 1425	N 27 E	15 SE					SH 1504	N 46 W	5 SW				
SH 1426	N 9 E	15 SE					SH 1505	N 5 W	30 SW				
SH 1427	N 17 E	15 SE					SH 1506	N 39 W	30 SW				
SH 1428	N 23 E	10 SE					SH 1507	N 25 W	30 SW				
SH 1429	N 16 E	25 SE					SH 1508	N 27 E	20 SE				
SH 1430	N 6 W	25 NE					SH 1509	N 38 W	15 SW				
SH 1431	N 11 E	10 NW					SH 1510	N 60 W	15 SW				
SH 1432	N 5 W	10 NE					SH 1511	N 65 W	20 SW				
SH 1433	N 23 E	10 NW					SH 1512	N 82 W	15 SW				
SH 1434	N 35 E	20 NW					SH 1513	N 74 W	35 SW				
SH 1435	N 19 W	45 SW					SH 1514	N 47 W	20 SW				
SH 1436	N 13 E	45 NW					SH 1515	N 68 W	20 SW				
SH 1437	N 52 E	10 NW					SH 1516	N 65 W	20 SW				
SH 1438	N 13 E	10 NW					SH 1517	N 82 W	15 SW				
SH 1439	N 10 E	15 SE					SH 1518	N 89 E	10 SE				
SH 1440	N 5 W	20 SW					SH 1519	N 76 E	15 SE				
SH 1441	N 54 W	30 NE					SH 1520	N 84 W	15 SW				
SH 1442	N 19 E	45 NW					SH 1521	N 55 W	25 SW				
SH 1443	N 7 E	15 NW					SH 1522	N 50 W	20 SW				
SH 1444	N 25 E	45 NW					SH 1523	N 39 W	25 SW				
SH 1445	N 7 E	15 NW					SH 1524	N 26 W	25 SW				
SH 1446	N 11 E	10 NW					SH 1525	N 22 E	15 SE				
SH 1447					198	10	SH 1526	N 34 E	35 SE				
SH 1448	N 39 W	50 NE					SH 1527	N 2 E	30 SE				
SH 1449	N 9 W	20 SW					SH 1528	N 43 W	20 SW				
SH 1450	N 16 W	30 SW					SH 1529	N 31 W	40 SW				
SH 1451	N 25 E	60 SE					SH 1530	N 37 W	25 SW				
SH 1452	N 8 E	20 SE					SH 1531	N 22 W	15 SW				
SH 1453	N 46 E	35 SE					SH 1532	N 55 E	30 SE				
SH 1454	N 10 E	30 SE					SH 1533	N 20 W	25 SW				
SH 1455	N 9 W	20 NE					SH 1534	N 11 E	15 SE				
SH 1456	N 34 E	85 SE					SH 1535	N 35 E	40 SE				
SH 1457	N 69 E	10 SE					SH 1536	N 30 E	20 NW				
SH 1458	N 17 E	15 SE					SH 1537	N 48 W	20 SW				
SH 1459	N 7 E	20 SE					SH 1538			166	10		
SH 1460	N 47 W	15 NE					SH 1539	N 25 E	20 SE				
SH 1461	N 59 E	15 SE					SH 1540	N 29 E	25 SW				
SH 1462	N 35 E	10 SE					SH 1541	N 38 E	20 SE				
SH 1463	N 41 E	10 SE					SH 1542	N 27 E	20 SE				
SH 1464	N 28 E	20 SE					SH 1543	N 31 E	30 SE				
SH 1465	N 12 W	20 SW					SH 1544	N 35 E	25 SE				
SH 1466	N 25 E	50 SE					SH 1545	N 35 E	50 SE				
SH 1467	N 39 E	50 SE					SH 1546	N 45 E	55 SE				
SH 1547	N 14 W	35 NE					SH 1626	N 24 E	45 SE				
SH 1548	N 38 E	20 SE					SH 1627	N 32 E	15 SE				
SH 1549	N 8 E	10 SE					SH 1628	N 39 E	25 SE				
SH 1550					13	10	SH 1629	N 24 E	45 SE				
SH 1551	N 8 E	50 NW					SH 1630	N 34 E	10 SE				
SH 1552	N 10 E	20 NW					SH 1631	N 48 E	15 SE				
SH 1553	N 43 E	20 SE					SH 1632	N 15 E	45 SE				
SH 1554	N 28 E	5 NW					SH 1633					17	5
SH 1555	N 52 E	25 SE					SH 1634					170	15
SH 1556	N 15 E	85 SE					SH 1635					175	15
SH 1557	N 8 E	45 NW					SH 1636	N 20 E	50 SE				
SH 1558	N 31 W	10 SW					SH 1637	N 26 E	10 NW				
SH 1559	N 45 E	50 SE					SH 1638	N 22 E	40 SE				
SH 1560					22	10	SH 1639	N 17 E	60 SE				
SH 1561	N 34 E	15 NW					SH 1640	N 53 E	35 SW				

	Foliation		Lineation		Fold Axis			Foliation		Lineation		Fold Axis	
Station	Strike	Dip	Trend	Plunge	Trend	Plunge	Station	Strike	Dip	Trend	Plunge	Trend	Plunge
SH 1562	N 3 E	10 SE					SH 1641	N 11 E	35 SE				
SH 1563	N 14 E	50 SE					SH 1642	N 8 E	25 SE				
SH 1564	N 13 E	20 SE					SH 1643	N 9 E	25 SE				
SH 1565					187	10	SH 1644						
SH 1566	N 46 E	15 SE					SH 1645	N 54 E	30 SE				
SH 1567	N 11 E	60 SE					SH 1646	N 46 W	25 SW				
SH 1568	N 40 E	10 SE					SH 1647	N 20 W	30 NE				
SH 1569	N 54 W	10 SW					SH 1648	N 17 W	40 NE				
SH 1570	N 7 W	20 SW					SH 1649	N 8 W	50 NE				
SH 1571	N 4 W	65 NE					SH 1650	N 25 E	20 SE				
SH 1572	N 8 E	40 SE					SH 1651	N 4 E	20 NW				
SH 1573	N 70 E	10 SE					SH 1652	N 36 W	15 NE				
SH 1574	N 46 E	40 SE					SH 1653	N 24 E	20 SE				
SH 1575	N 32 E	45 SE					SH 1654	N 19 W	10 NE				
SH 1576	N 38 E	25 SE					SH 1655	N 62 E	25 NW				
SH 1577	N 19 W	20 SW					SH 1656	N 26 W	20 SW				
SH 1578	N 89 E	25 SE					SH 1657	N 6 E	10 NW				
SH 1579	N 33 W	20 SW					SH 1658	N 6 E	40 SE				
SH 1580					177	10	SH 1659	N 17 E	35 NW				
SH 1581	N 23 E	25 SE					SH 1660	N 13 E	70 SE				
SH 1582	N 5 W	20 NE					SH 1661	N 68 W	20 NE				
SH 1583	N 53 E	25 SE					SH 1662	N 7 E	40 SE				
SH 1584	N 19 E	40 SE					SH 1663	N 6 W	70 NE				
SH 1585	N 17 E	15 SE					SH 1664	N 51 E	15 SE				
SH 1586	N 4 W	40 SW					SH 1665	N 65 E	40 NW				
SH 1587	N 18 E	55 SE					SH 1666	N 29 E	60 NW				
SH 1588	N 21 E	20 SE					SH 1667	N 9 E	15 NW				
SH 1589	N 8 E	25 SE					SH 1668	N 18 E	20 NW				
SH 1590	N 27 E	40 SE					SH 1669	N 31 E	15 NW				
SH 1591	N 17 E	30 SE					SH 1670	N 10 E	35 SW				
SH 1592					23	15	SH 1671	N 23 E	35 SE				
SH 1593					10	15	SH 1672	N 12 W	15 NE				
SH 1594	N 54 E	35 SE					SH 1673			190	15		
SH 1595	N 55 E	25 SE					SH 1674	N 23 E	40 SE				
SH 1596	N 16 W	10 SW					SH 1675	N 37 E	15 SE				
SH 1597					14	15	SH 1676	N 14 E	50 NW				
SH 1598	N 12 E	25 SE					SH 1677	N 12 E	15 NW				
SH 1599	N 40 W	10 SW					SH 1678	N 7 E	20 NW				
SH 1600	N 17 E	15 SE					SH 1679					19	20
SH 1601	N 13 E	35 SE					SH 1680	N 23 E	20 SE				
SH 1602	N 41 E	30 SE					SH 1681	N 38 E	25 SE				
SH 1603	N 19 E	15 SE					SH 1682	N 32 E	40 SE				
SH 1604	N 5 W	15 NE					SH 1683	N 46 E	35 SE				
SH 1605	N 13 E	45 SE					SH 1684	N 24 E	20 SE				
SH 1606	N 18 E	20 NW					SH 1685	N 11 E	15 SE				
SH 1607	N 26 E	30 NW					SH 1686	N 35 W	10 SW				
SH 1608	N 15 E	60 SE					SH 1687	N 13 E	20 SE				
SH 1609	N 62 W	10 NE					SH 1688	N 15 W	20 NE				
SH 1610	N 4 W	20 NE					SH 1689	N 46 E	25 SE				
SH 1611	N 4 W	10 NE					SH 1690	N 11 E	20 SE				
SH 1612	N 24 W	30 NE					SH 1691	N 34 E	25 SE				
SH 1613	N 28 E	15 SE					SH 1692	N 58 E	10 SE				
SH 1614	N 66 E	40 SE					SH 1693	N 44 E	20 SE				
SH 1615	N 4 E	30 SE					SH 1694	N 34 E	15 SE				
SH 1616	N 49 E	20 SE					SH 1695					218	10
SH 1617	N 5 E	45 SE					SH 1696	N 8 E	60 NW				
SH 1618	N 5 E	25 SE					SH 1697	N 27 E	20 SE				
SH 1619	N 11 W	45 NE					SH 1698	N 10 W	35 SW				
SH 1620	N 43 E	40 SE					SH 1699	N 23 E	25 SE				
SH 1621	N 27 E	35 SE					SH 1700	N 35 E	15 SE				
SH 1622	N 6 E	50 SE					SH 1701	N 37 E	30 SE				
SH 1623	N 35 E	20 SE					SH 1702	N 10 E	30 SE				
SH 1624	N 16 E	35 SE					SH 1703	N 25 E	40 SE				
SH 1625	N 16 E	25 SE					SH 1704	N 24 E	20 SE				
SH 1705	N 8 E	20 NW					SH 1784	N 79 W	20 NE				
SH 1706	N 3 E	40 SE					SH 1785					14	15
SH 1707	N 15 E	30 SE					SH 1786	N 11 E	20 SE				
SH 1708	N 32 E	20 SE					SH 1787					199	15
SH 1709	N 25 E	20 NW					SH 1788	N 10 E	30 SE				
SH 1710					189	15	SH 1789	N 7 E	60 SE				
SH 1711	N 50 E	35 SE					SH 1790	N 16 E	25 NW				
SH 1712	N 22 E	10 SE					SH 1791					22	15
SH 1713	N 18 E	45 SE					SH 1792	N 22 E	30 SE				
SH 1714	N 27 E	70 SE					SH 1793	N 28 E	40 SE				
SH 1715	N 22 E	50 SE					SH 1794	N 14 E	50 SE				
SH 1716	N 5 E	15 SE					SH 1795	N 43 E	25 SE				
SH 1717	N 33 E	60 SE					SH 1796	N 12 E	25 NW				
SH 1718	N 5 E	10 SE					SH 1797	N 85 E	15 NW				
SH 1719	N 5 W	25 NE					SH 1798	N 1 E	10 NW				
SH 1720	N 14 E	35 SE					SH 1799	N 14 E	15 NW				
SH 1721	N 47 E	60 NW					SH 1800	N 12 E	60 SE				
SH 1722	N 27 W	15 NE					SH 1801	N 4 E	15 SE				
SH 1723	N 18 E	25 NW					SH 1802	N 20 E	60 SE				
SH 1724	N 24 E	35 NW					SH 1803	N 24 E	20 NW				
SH 1725			18	10			SH 1804	N 13 E	20 NW				
SH 1726	N 18 E	40 NW					SH 1805	N 16 W	25 NE				
SH 1727			4	20			SH 1806	N 9 W	30 NE				
SH 1728	N 23 E	15 NW					SH 1807	N 13 W	20 SW				
SH 1729	N 12 E	10 NW					SH 1808	N 12 W	45 NE				
SH 1730	N 39 W	10 NE					SH 1809	N 14 E	60 SE				
SH 1731	N 9 E	70 NW					SH 1810	N 37 W	20 SW				

	Foliation		Lineation		Fold Axis			Foliation		Lineation		Fold Axis	
Station	Strike	Dip	Trend	Plunge	Trend	Plunge	Station	Strike	Dip	Trend	Plunge	Trend	Plunge
SH 1732	N 4 E	15 NW					SH 1811	N 17 E	45 SE				
SH 1733	N 22 E	15 NW					SH 1812	N 5 E	30 SE				
SH 1734	N 53 E	10 NW					SH 1813	N 30 W	15 NE				
SH 1735	N 16 E	10 NW					SH 1814	N 69 W	15 NE				
SH 1736							SH 1815	N 19 E	15 SE				
SH 1737	N 14 E	45 NW					SH 1816	N 27 W	15 SW				
SH 1738	N 7 E	30 SE					SH 1817	N 60 W	15 SW				
SH 1739	N 75 E	20 NW					SH 1818	N 37 E	10 SE				
SH 1740	N 13 E	10 NW					SH 1819	N 47 E	20 SE				
SH 1741	N 4 E	10 NW					SH 1820	N 41 E	20 SE				
SH 1742	N 11 E	15 NW					SH 1821	N 66 E	15 SE				
SH 1743	N 35 W	25 NE					SH 1822	N 51 E	30 SE				
SH 1744	N 21 E	20 NW					SH 1823	N 36 E	25 SE				
SH 1745					11	5	SH 1824	N 35 E	40 SE				
SH 1746	N 31 E	35 SE					SH 1825	N 15 E	70 SE				
SH 1747					198	15	SH 1826	N 324 E	20 SE				
SH 1748	N 28 E	20 SE					SH 1827	N 33 E	40 SE				
SH 1749	N 22 E	60 NW					SH 1828	N 34 E	25 SE				
SH 1750	N 13 E	10 SE					SH 1829	N 27 E	40 SE				
SH 1751	N 11 E	25 NW					SH 1830	N 54 E	15 SE				
SH 1752	N 11 E	20 NW					SH 1831	N 15 E	60 NW				
SH 1753	N 24 E	60 NW					SH 1832	N 43 E	40 NW				
SH 1754	N 8 W	70 SW					SH 1833	N 21 E	60 SE				
SH 1755	N 23 E	70 NW					SH 1834	N 19 E	30 SE				
SH 1756	N 5 W	25 SW					SH 1835	N 22 E	45 SE				
SH 1757	N 32 W	15 NE					SH 1836	N 54 E	20 SE				
SH 1758	N 35 W	25 NE					SH 1837	N 31 E	15 SE				
SH 1759	N 43 E	35 NW					SH 1838	N 29 W	20 SW				
SH 1760	N 31 E	5 SE					SH 1839	N 56 E	25 SE				
SH 1761					16	5	SH 1840	N 58 E	20 SE				
SH 1762	N 42 E	15 SE					SH 1841	N 14 E	25 SE				
SH 1763	N 17 W	15 SW					SH 1842	N 38 E	20 SE				
SH 1764	N 5 W	40 NE					SH 1843	N 12 E	20 SE				
SH 1765	N 7 E	20 SE					SH 1844	N 60 E	65 SE				
SH 1766	N 42 W	50 NE					SH 1845	N 74 W	25 SW				
SH 1767	N 88 E	50 SE					SH 1846	N 57 E	15 SE				
SH 1768	N 25 E	50 NW					SH 1847	N 29 E	25 SE				
SH 1769	N 21 E	40 NW					SH 1848					179	10
SH 1770	N 51 E	20 NW					SH 1849	N 24 E	10 SE				
SH 1771			181	10			SH 1850	N 71 E	15 SE				
SH 1772			184	10			SH 1851					170	5
SH 1773	N 20 E	20 SE					SH 1852	N 61 E	50 SE				
SH 1774	N 64 E	20 NW					SH 1853	N 46 E	25 SE				
SH 1775	N 3 E	30 SE					SH 1854	N 23 E	30 SE				
SH 1776	N 10 W	20 NE					SH 1855	N 35 E	20 SE				
SH 1777	N 11 E	15 NW					SH 1856	N 19 E	30 SE				
SH 1778	N 20 W	20 NE					SH 1857	N 27 W	15 SW				
SH 1779	N 19 E	10 SE					SH 1858	N 39 E	15 SE				
SH 1780	N 14 E	5 NW					SH 1859	N 15 W	10 NE				
SH 1781	N 27 W	20 NE					SH 1860	N 16 W	10 NE				
SH 1782	N 86 W	20 NE					SH 1861	N 14 E	40 NW				
SH 1783	N 76 E	15 SE					SH 1862	N 36 E	45 SE				
SH 1863	N 17 W	25 SW					SH 1942	N 57 E	10 SE				
SH 1864	N 86 W	10 SW					SH 1943	N 37 E	10 SE				
SH 1865	N 11 W	30 SW					SH 1944	N 66 W	15 SW				
SH 1866	N 53 E	15 SE					SH 1945	N 74 E	80 SE				
SH 1867	N 6 E	45 SE					SH 1946	N 45 W	30 SW				
SH 1868	N 17 W	10 SW					SH 1947	N 19 W	30 SW				
SH 1869	N 32 W	25 SW					SH 1948	N 43 W	10 SW				
SH 1870	N 7 E	20 SE					SH 1949	N 89 E	30 SE				
SH 1871	N 29 W	25 SW					SH 1950					182	5
SH 1872	N 72 E	25 SE					SH 1951	N 41 E	45 NW				
SH 1873	N 42 W	15 SW					SH 1952	N 21 W	15 SW				
SH 1874	N 67 E	20 SE					SH 1953	N 30 W	10 SW				
SH 1875	N 50 E	25 SE					SH 1954	N 62 W	60 SW				
SH 1876	N 17 E	30 SE					SH 1955	N 27 W	10 SW				
SH 1877	N 82 E	5 SE					SH 1956	N 19 W	30 NE				
SH 1878	N 17 E	50 SE					SH 1957	N 29 E	15 SE				
SH 1879	N 37 E	35 SE					SH 1958	N 11 E	10 NW				
SH 1880	N 15 E	60 SE					SH 1959	N 65 W	15 SW				
SH 1881	N 73 W	30 SW					SH 1960	N 25 W	30 SW				
SH 1882	N 65 E	20 SE					SH 1961	N 43 E	10 SE				
SH 1883	N 54 W	40 SW					SH 1962					179	5
SH 1884					183	10	SH 1963	N 36 W	15 SW				
SH 1885	N 55 E	20 SE					SH 1964	N 54 E	20 NW				
SH 1886	N 25 E	15 SE					SH 1965						
SH 1887	N 49 W	25 SW					SH 1966						
SH 1888	N 86 W	30 SW					SH 1967					9	5
SH 1889	N 63 W	25 SW					SH 1968					173	10
SH 1890	N 40 W	70 SW					SH 1969	N 23 W	20 SW				
SH 1891	N 48 W	20 SW					SH 1970	N 8 W	10 SW				
SH 1892	N 75 E	25 NW					SH 1971	N 23 W	30 SW				
SH 1893	N 7 E	25 NW					SH 1972	N 15 E	20 NW				
SH 1894	N 6 E	20 SE					SH 1973	N 11 W	35 SW				
SH 1895	N 10 W	50 SW					SH 1974	N 2 E	40 NW				
SH 1896	N 23 E	30 NW					SH 1975	N 63 E	10 SE				
SH 1897	N 3 E	30 NW					SH 1976	N 44 W	15 SW				
SH 1898	N 11 W	20 SW					SH 1977	N 18 W	50 SW				
SH 1899	N 34 W	15 SW					SH 1978	N 16 E	15 NW				
SH 1900	N 68 E	10 SE					SH 1979	N 28 W	15 NE				
SH 1901					186	5	SH 1980	N 11 E	15 NW				

	Foliation		Lineation		Fold Axis			Foliation		Lineation		Fold Axis	
Station	Strike	Dip	Trend	Plunge	Trend	Plunge	Station	Strike	Dip	Trend	Plunge	Trend	Plunge
SH 1902	N 83 E	10 SE					SH 1981	N 39 E	15 NW				
SH 1903	N 48 W	10 SW					SH 1982	N 27 E	30 NW				
SH 1904	N 48 W	15 SW					SH 1983	N 55 E	30 NW				
SH 1905	N 72 E	10 SE					SH 1984					353	15
SH 1906	N 74 W	15 SW					SH 1985					98	5
SH 1907	N 53 E	5 SE					SH 1986	N 21 W	20 NE				
SH 1908	N 27 E	15 SE					SH 1987	N 27 E	25 NW				
SH 1909	N 40 E	25 SE					SH 1988	N 41 E	30 NW				
SH 1910	N 29 W	20 SW					SH 1989	N 19 W	15 NE				
SH 1911	N 42 E	20 SE					SH 1990	N 16 W	25 SW				
SH 1912	N 21 E	20 SE					SH 1991	N 15 W	30 SW				
SH 1913	N 71 E	15 SE					SH 1992					183	5
SH 1914	N 88 E	10 SE					SH 1993	N 6 W	30 SW				
SH 1915	N 82 E	15 SE					SH 1994	N 51 E	10 SE				
SH 1916	N 18 E	10 SE					SH 1995	N 44 W	25 SW				
SH 1917	N 23 W	40 SW					SH 1996	N 34 W	50 SW				
SH 1918	N 46 W	15 SW					SH 1997	N 70 E	10 SE				
SH 1919	N 34 E	30 SE					SH 1998	N 67 W	40 SW				
SH 1920	N 8 W	20 SW					SH 1999	N 24 W	20 SW				
SH 1921	N 35 W	10 SW					SH 2000	N 23 E	25 SE				
SH 1922	N 75 E	45 SE					SH 2001	N 14 E	35 NW				
SH 1923	N 31 E	10 SE					SH 2002	N 70 W	5 NE				
SH 1924					175	10	SH 2003	N 25 W	35 SW				
SH 1925					190	10	SH 2004					95	10
SH 1926	N 85 W	15 SW					SH 2005	N 56 W	50 SW				
SH 1927	N 12 E	10 SE					SH 2006	N 16 E	40 NW				
SH 1928	N 17 W	20 SW					SH 2007	N 13 E	30 NW				
SH 1929	N 7 W	25 NE					SH 2008	N 76 W	10 NE				
SH 1930	N 81 E	30 SE					SH 2009	N 5 E	30 NW				
SH 1931	N 73 E	15 SE					SH 2010	N 19 W	20 NE				
SH 1932	N 52 E	15 NW					SH 2011	N 15 W	20 NE				
SH 1933	N 8 W	20 SW					SH 2012	N 16 W	25 NE				
SH 1934	N 20 W	30 SW					SH 2013	N 7 W	15 SW				
SH 1935	N 5 E	50 SE					SH 2014	N 24 W	10 SW				
SH 1936	N 22 E	20 SE					SH 2015	N 32 W	15 NE				
SH 1937	N 15 E	30 SE					SH 2016	N 18 E	10 SE				
SH 1938	N 28 W	50 SW					SH 2017	N 72 W	25 SW				
SH 1939	N 18 W	35 SW					SH 2018	N 19 W	45 SW				
SH 1940	N 2 E	45 SE					SH 2019	N 57 W	40 SW				
SH 1941	N 74 W	45 SW					SH 2020	N 66 W	30 SW				
SH 2021	N 30 W	15 SW					SH 2100	N 7 E	10 NW				
SH 2022	N 20 E	50 NW					SH 2101	N 26 W	15 NE				
SH 2023	N 53 E	20 SE					SH 2102	N 19 W	15 NE				
SH 2024	N 9 E	10 NW					SH 2103	N 14 W	10 NE				
SH 2025	N 8 E	15 NW					SH 2104	N 27 W	20 NE				
SH 2026	N 27 W	15 SW					SH 2105	N 22 W	30 NE				
SH 2027	N 15 W	15 NE					SH 2106	N 25 W	40 NE				
SH 2028	N 7 E	70 NW					SH 2107	N 15 W	15 NE				
SH 2029	N 43 E	10 NW					SH 2108	N 63 E	15 NW				
SH 2030	N 18 E	10 SE					SH 2109	N 36 W	15 SW				
SH 2031	N 43 E	10 NW					SH 2110	N 30 W	10 NE				
SH 2032	N 18 E	10 SE					SH 2111	N 9 E	15 SE				
SH 2033	N 43 E	40 NW					SH 2112	N 10 E	35 SE				
SH 2034	N 53 E	25 NW					SH 2113	N 47 W	30 NE				
SH 2035	N 43 E	20 NW					SH 2114	N 24 W	25 SW				
SH 2036	N 16 E	15 NW					SH 2115	N 17 E	25 SW				
SH 2037					354	10	SH 2116	N 35 W	30 NE				
SH 2038					353	5	SH 2117	N 44 W	20 NE				
SH 2039	N 57 W	30 SW					SH 2118	N 45 W	20 NE				
SH 2040	N 48 E	15 NW					SH 2119					353	20
SH 2041	N 19 W	35 SW					SH 2120	N 31 W	25 SW				
SH 2042	N 61 E	25 SE					SH 2121	N 27 W	15 SW				
SH 2043	N 43 E	25 NW					SH 2122	N 26 E	15 SE				
SH 2044	N 19 W	35 SW					SH 2123	N 37 W	15 SW				
SH 2045	N 61 E	25 SE					SH 2124					354	10
SH 2046	N 6 E	16 SE					SH 2125	N 12 W	20 NE				
SH 2047	N 27 E	15 SE					SH 2126					353	15
SH 2048	N 41 E	15 SE					SH 2127	N 23 W	15 SW				
SH 2049					169	20	SH 2128	N 51 W	25 NE				
SH 2050					171	5	SH 2129	N 8 W	15 NE				
SH 2051	N 24 E	10 SE					SH 2130	N 11 E	15 SE				
SH 2052					264	10	SH 2131	N 13 E	25 SE				
SH 2053	N 16 W	20 SW					SH 2132	N 28 E	10 NW				
SH 2054	N 57 W	50 SW					SH 2133	N 74 E	20 SE				
SH 2055	N 16 E	15 NW					SH 2134	N 74 E	20 SE				
SH 2056					163	10	SH 2135	N 20 E	20 SE				
SH 2057	N 27 W	20 NE					SH 2136	N 24 E	30 SE				
SH 2058					179	10	SH 2137	N 8 W	10 SW				
SH 2059	N 11 E	15 NW					SH 2138	N 12 W	15 NE				
SH 2060	N 22 E	25 NW					SH 2139	N 35 W	30 NE				
SH 2061	N 42 E	30 NW					SH 2140	N 30 W	15 SW				
SH 2062	N 36 E	20 NW					SH 2141	N 16 E	25 SE				
SH 2063	N 53 W	15 NE					SH 2142	N 45 W	20 NE				
SH 2064	N 70 E	20 NW					SH 2143	N 66 W	10 NE				
SH 2065	N 9 E	50 NW					SH 2144	N 86 W	20 SW				
SH 2066	N 9 E	50 NW					SH 2145	N 70 W	10 NE				
SH 2067	N 19 W	10 NE					SH 2146	N 84 W	25 NE				
SH 2068	N 30 W	10 NE					SH 2147	N 20 E	45 SE				
SH 2069	N 28 W	15 SW					SH 2148	N 34 W	10 NE				
SH 2070	N 33 W	15 SW					SH 2149	N 35 E	15 SE				
SH 2071					253	10	SH 2150	N 42 W	20 NE				

	Foliation		Lineation		Fold Axis			Foliation		Lineation		Fold Axis	
Station	Strike	Dip	Trend	Plunge	Trend	Plunge	Station	Strike	Dip	Trend	Plunge	Trend	Plunge
SH 2072	N 42 E	30 NW					LD 1	N 37 E	25 SE				
SH 2073	N 26 E	25 NW					LD 2	N 24 W	30 SW				
SH 2074	N 40 E	25 NW					LD 3	N 36 W	60 SW				
SH 2075					5	5	LD 4	N 40 W	30 SW				
SH 2076	N 15 E	25 NW					LD 5	N 41 W	35 NE				
SH 2077	N 30 E	25 NW					LD 6	N 64 E	65 SE				
SH 2078	N 50 E	15 NW					LD 7	N 36 E	15 SE				
SH 2079	N 44 E	35 NW					LD 8					44	15 SE
SH 2080	N 67 E	30 NW					LD 9	N 81 W	15 SW				
SH 2081	N 22 E	25 SE					LD 10	N 28 E	15 SE				
SH 2082	N 16 E	20 SE					LD 11	N 20 W	15 SW				
SH 2083	N 15 E	25 SE					LD 12	N 18 W	10 SW				
SH 2084	N 24 E	25 NW					LD 13	N 79 E	60 NW				
SH 2085	N 47 W	25 NE					LD 14	N 16 W	10 SW				
SH 2086	N 54 E	40 SE					LD 15	N 88 E	20 SE				
SH 2087	N 45 W	15 NE					LD 16	N 46 W	60 NE				
SH 2088	N 41 E	30 NW					LD 17	N 83 W	10 NE				
SH 2089	N 35 W	10 SW					LD 18	N 24 W	35 NE				
SH 2090					2	10	LD 19	N 51 W	10 NE				
SH 2091	N 4 E	30 SE					LD 20	N 48 W	20 SW				
SH 2092	N 33 E	20 NW					LD 21	N 29 W	45 NE				
SH 2093	N 73 E	60 SE					LD 22	N 18 W	30 NE				
SH 2094	N 43 E	15 NW					LD 23	N 24 E	15 SE				
SH 2095	N 11 W	35 SW					LD 24	N 20 E	10 SE				
SH 2096	N 58 E	30 NW					LD 25	N 58 W	75 SW				
SH 2097	N 49 E	25 NW					LD 26	N 48 W	40 SW				
SH 2098	N 79 E	30 NW					LD 27	N 67 E	5 SE				
SH 2099	N 16 W	30 NE					LD 28	N 39 E	15 NW				
LD 29	N 14 W	10 SW					LD 108	N 33 W	20 SW				
LD 30	N 79 W	5 NE					LD 109	N 59 E	30 SE				
LD 31	N 42 W	30 NE					LD 110	N 47 E	15 SE				
LD 32	N 8 E	15 SE					LD 111	N 51 E	15 SE				
LD 33	N 37 W	40 NW					LD 112	N 55 W	40 NE				
LD 34	N 33 W	60 NE					LD 113	N 43 W	40 SW				
LD 35	N 41 W	25 SW					LD 114	N 67 E	20 SE				
LD 36	N 43 E	20 SE					LD 115	N 15 E	20 SE				
LD 37	N 11 W	20 NE					LD 116	N 70 E	10 SE				
LD 38	N 37 W	30 SW					LD 117	N 62 E	30 SE				
LD 39	N 23 W	30 SW					LD 118	N 7 W	15 NE				
LD 40	N 28 W	15 NE					LD 119	N 17 W	20 NE				
LD 41	N 64 W	30 SW					LD 120	N 24 W	40 SW				
LD 42	N 18 W	15 NE					LD 121	N 65 W	30 SW				
LD 43	N 36 W	45 SW					LD 122	N 18 E	20 SE				
LD 44	N 35 W	20 NE					LD 123	N 48 E	10 SE				
LD 45	N 8 W	25 SW					LD 124	N 19 E	15 SE				
LD 46	N 53 W	20 SW					LD 125	N 37 W	15 NE				
LD 47	N 25 W	20 NE					LD 126	N 43 E	20 SE				
LD 48	N 19 W	20 SW					LD 127	N 86 E	20 SE				
LD 49	N 24 W	40 NE					LD 128	N 88 E	20SE				
LD 50	N 31 W	20 SW					LD 129	N 45 W	40 NE				
LD 51	N 85 W	15 SW					LD 130	N 24 W	15 SW				
LD 52	N 24 W	20 NE					LD 131	N 75 W	45 NE				
LD 53	N 25 E	20 SE					LD 132	N 29 W	10 SW				
LD 54	N 16 W	75 NE					LD 133	N 21 W	30 NE				
LD 55	N 23 W	45 NE					LD 134	N 26 W	30 NE				
LD 56	N 40 E	15 SE					LD 135	N 13 W	20 SW				
LD 57	N 78 E	25 SE					LD 136	N 16 W	30 SW				
LD 58	N 74 E	40 SE					LD 137	N 32 W	30 SW				
LD 59	N 69 W	40 SW					LD 138	N 58 W	30 NE				
LD 60	N 25 E	30 SE					LD 139	N 44 W	30 NE				
LD 61	N 43 W	15 SW					LD 140	N 18 W	20 NE				
LD 62	N 30 W	45 NE					LD 141	N 32 W	25 NE				
LD 63	N 41 W	45 NE					LD 142	N 3 E	15 SE				
LD 64	N 38 W	30 NE					LD 143	N 21 W	30 NE				
LD 65	N 29 W	30 NE					LD 144	N 27 W	45 NE				
LD 66	N 30 W	30 NE					LD 145	N 14 W	30 NE				
LD 67	N 22 W	30 NE					LD 146	N 15 W	30 NE				
LD 68	N 26 W	20 NE					LD 147	N 23 E	20 SW				
LD 69	N 48 W	20 NE					LD 148	N 6 W	20 NE				
LD 70	N 30 E	20 SE					LD 149	N 6 E	30 NW				
LD 71	N 18 W	15 NE					LD 150	N 66 W	20 NE				
LD 72	N 33 W	20 NE					LD 151	N 27 W	20 SW				
LD 73	N 27 W	30 NE					LD 152	N 32 W	60 NE				
LD 74	N 28 E	40 SE					LD 153	N 49 W	20 NE				
LD 75	N 18 W	30 NE					LD 154	N 44 W	45 NE				
LD 76	N 28 E	30 SE					LD 155	N 47 W	30 NE				
LD 77	N 25 W	30 SW					LD 156	N 37 W	30 NE				
LD 78	N 28 W	45 NE					LD 157	N 30 W	15 SW				
LD 79	N 29 W	45 NE					LD 158	N 8 W	15 NE				
LD 80	N 29 W	60 NE					LD 159	N 3 E	60 SE				
LD 81	N 52 E	20 SE					LD 160	N 38 W	45 NE				
LD 82	N 22 E	15 SE					LD 161	N 58 E	30 SE				
LD 83	N 26 W	40 NE					LD 162	N 62 W	10 NE				
LD 84	N 44 E	40 SE					LD 163	N 40 W	20 NE				
LD 85	N 51 E	20 SE					LD 164	N 24 W	60 NE				
LD 86	N 45 E	30 SE					LD 165	N 33 W	30 NE				
LD 87	N 38 E	15 SE					LD 166	N 84 W	40 NE				
LD 88	N 34 E	20 SE					LD 167	N 66 W	10 NE				
LD 89	N 27 E	20 SE					LD 168	N 3 W	15 NE				
LD 90	N 7 E	20 SE					LD 169	N 60 W	30 SW				
LD 91	N 68 E	40 SE					LD 170	N 5 E	15 SE				

	Foliation		Lineation		Fold Axis			Foliation		Lineation		Fold Axis	
Station	Strike	Dip	Trend	Plunge	Trend	Plunge	Station	Strike	Dip	Trend	Plunge	Trend	Plunge
LD 92	N 78 E	35 SE					LD 171	N 48 W	30 NE				
LD 93	N 74 W	15 NE					LD 172	N 24 W	15 NE				
LD 94	N 12 E	30 SE					LD 173	N 39 W	30 NE				
LD 95	N 85 E	20 SE					LD 174					147	5
LD 96	N 59 E	15 SE					LD 175	N 60 W	35 NE				
LD 97	N 2 W	15 NE					LD 176	N 2 W	25 NE				
LD 98	N 82 W	20 NE					LD 177	N 83 W	30 NE				
LD 99	N 12 W	30 NE					LD 178	N 71 W	30 NE				
LD 100	N 40 E	30 SE					LD 179	N 12 W	45 NE				
LD 101	N 10 E	30 SE					LD 180	N 60 W	30 SW				
LD 102	N 21 E	30 SE					LD 181	N 34 E	30 NW				
LD 103	N 41 E	20 SE					LD 182	N 21 W	15 SW				
LD 104	N 20 W	30 NE					LD 183	N 17 W	70 SW				
LD 105	N 41 W	30 SW					LD 184	N 58 E	30 SE				
LD 106	N 87 W	15 SW					LD 185	N 16 W	35 SW				
LD 107	N 31 W	35 SW					LD 186	N 34 W	35 NE				
LD 187	N 7 W	30 NE					LD 266	N 2 W	15 NE				
LD 188					211	5	LD 267	N 27 W	20 NE				
LD 189	N 34 W	30 NE					LD 268	N 28 W	35 NE				
LD 190	N 18 W	40 SW					LD 269	N 56 W	10 NE				
LD 191	N 35 W	30 NE					LD 270	N 49 W	15 SW				
LD 192	N 49 W	40 NE					LD 271	N 3 E	10 NW				
LD 193	N 56 E	30 NW					LD 272	N 10 W	40 NE				
LD 194	N 58 W	40 NE					LD 273	N 8 W	35 NE				
LD 195	N 8 E	40 SE					LD 274	N 14 W	10 NE				
LD 196	N 48 E	30 NW					LD 275	N 5 E	10 SE				
LD 197	N 37 E	35NW					LD 276	N 42 E	30 SE				
LD 198	N 37 E	70 NW					LD 277	N 17 W	45 SW				
LD 199	N 57 E	35 NW					LD 278	N 43 W	10 NE				
LD 200	N 42 E	15 NW					LD 279	N 9 E	20 SE				
LD 201	N 31 W	50 NE					LD 280	N 20 W	10 NE				
LD 202	N 12 W	15 SW					LD 281	N 18 E	60 SE				
LD 203	N 27 E	30 NW					LD 282	N 72 W	15 SW				
LD 204	N 65 E	60 NW					LD 283	N 74 W	45 SW				
LD 205	N 42 E	45 NW					LD 284	N 20 E	15 SE				
LD 206	N 41 E	40 NW					LD 285	N 6 W	15 NE				
LD 207	N 24 E	30 SE					LD 286	N 31 E	30 SE				
LD 208	N 47 E	35 NW					LD 287	N 44 W	10 NE				
LD 209	N 63 E	20 NW					LD 288	N 48 W	35 NE				
LD 210	N 49 W	20 NE					LD 289	N 89 W	75 SW				
LD 211	N 61 W	15 NE					LD 290	N 73 W	15 SW				
LD 212	N 30 W	20 NE					LD 291	N 79 E	25 SE				
LD 213	N 10 W	15 SW					LD 292	N 33 W	30 NE				
LD 214	N 37 W	50 NE					LD 293	N 39 E	15 SE				
LD 215	N 27 W	25 NE					LD 294	N 52 E	230 SE				
LD 216	N 36 W	15 NE					LD 295			350	15		
LD 217	N 31 W	30 SW					LD 296	N 22 W	30 NE				
LD 218	N 25 W	50 NE					LD 297	N 41 W	10 NE				
LD 219	N 77 E	20 NW					LD 298	N 75 E	20 SEV				
LD 220	N 65 W	35 NE					LD 299	N 89 E	5 SE				
LD 221	N 68 W	40 NE					LD 300	N 24 E	20 SE				
LD 222	N 53 W	35 NE					LD 301	N 2 E	10 SE				
LD 223	N 47 E	20 NW					LD 302	N 19 E	25 SE				
LD 224							LD 303	N 13 E	15 SE				
LD 225	N 83 W	30 NE			201	10	LD 304	N 22 E	5 SE				
LD 226	N 65 E	45 SE					LD 305	N 19 W	30 NE				
LD 227	N 55 W	35 NE					LD 306	N 34 W	60 NE				
LD 228	N 55 W	25 NE					LD 307	N 23 W	10 NE				
LD 229	N 13 W	40 SW					LD 308	N 38 E	20 SE				
LD 230	N 43 E	30 SE					LD 309	N 81 W	10 SW				
LD 231	N 9 W	30 NE					LD 310	N 55 E	15 SE				
LD 232	N 45 W	20 NE					LD 311	N 28 E	10 SE				
LD 233	N 2 E	10 NW					LD 312	N 20 W	60 NE				
LD 234	N 18 E	15 SE					LD 313	N 74 E	20 SE				
LD 235	N 27 E	20 NW					LD 314	N 20 E	15 SE				
LD 236	N 40 E	15 SE					LD 315	N 36 E	20 SE				
LD 237	N 57 W	5 SW					LD 316	N 7 E	5 NE				
LD 238	N 47 W	10 SW					LD 317	N 21 W	15 NE				
LD 239	N 16 W	15 NE					LD 318	N 9 W	15 NE				
LD 240	N 37 W	20 NE					LD 319	N 22 W	45 SW				
LD 241	N 43 W	30 NE					LD 320	N 20 E	25 SW				
LD 242	N 8 W	30 SW					LD 321	N 20 W	30 NE				
LD 243	N 28 W	30 SW					LD 322	N 19 E	5 SE				
LD 244	N 83 W	10 SW					LD 323	N 25 E	15 SE				
LD 245	N 77 W	10 NE					LD 324	N 22 E	10 SE				
LD 248	N 30 E	30 SE					LD 325					152	10
LD 247	N 28 W	15 SW					LD 326	N 10 W	45 NE				
LD 248	N 42 W	20 SW					LD 327	N 10 W	30 NE				
LD 249	N 9 W	10 NE					LD 328	N 17 W	30 NE				
LD 250	N 78 W	30 NE					LD 329	N 42 W	20 NE				
LD 251	N 36 E	30 SE					LD 330	N 20 E	60 NW				
LD 252	N 23 W	30 NE					LD 331	N 18 W	15 SW				
LD 253	N 38 W	60 SW					LD 332	N 48 W	25 NE				
LD 254	N 10 E	30 SE					LD 333	N 15 E	25 SE				
LD 255	N 18 E	20 NW					LD 334	N 18 E	10 SE				
LD 256	N 35 E	15 NW					LD 335	N 15 E	20 SE				
LD 257	N 15 E	20 SE					LD 336	N 24 E	10 SE				
LD 258	N 57 W	45 NE					LD 337	N 68 W	10 SW				
LD 259	N 8 E	20 SE					LD 338	N 5 W	20 NE				
LD 260	N 7 E	20 SE					LD 339	N 15 E	15 SE				
LD 261	N 30 W	20 SW					LD 340	N 30 E	20 SE				

	Foliation		Lineation		Fold Axis			Foliation		Lineation		Fold Axis	
Station	Strike	Dip	Trend	Plunge	Trend	Plunge	Station	Strike	Dip	Trend	Plunge	Trend	Plunge
LD 262	N 18 W	10 SW					LD 341	N 18 E	10 SE				
LD 263	N 24 W	30 SW					LD 342	N 39 E	45 SE				
LD 264	N 3 W	35 NE					LD 343	N 3 E	45 NE				
LD 265	N 5 W	10 NE					LD 344	N 6 W	15 SW				
LD 345	N 72 W	70 SW					LD 424	N 41 W	20 NE				
LD 346	N 16 E	40 SE					LD 425	N 17 W	30 SW				
LD 347	N 6 E	20 SE					LD 426	N 48 W	10 SW				
LD 348	N 38 W	65 SW					LD 427	N 53 E	50 SE				
LD 349	N 36 E	15 SE					LD 428	N 43 E	25 SE				
LD 350	N 21 E	10 SE					LD 429	N 17 E	45 SE				
LD 351	N 41 W	20 NE					LD 430	N 75 E	50 SE				
LD 352	N 40 W	25 NE					LD 431	N 34 W	30 SW				
LD 353	N 65 E	10 NW					LD 432	N 58 E	30 SE				
LD 354	N 50 E	15 SE					LD 433	N 48 W	20 SW				
LD 355	N 48 E	20 SE					LD 434	N 86 W	20 SW				
LD 356	N 67 W	30 SW					LD 435	N 47 W	20 SW				
LD 357	N 55 W	10 SW					LD 436	N 34 W	70 NE				
LD 358	N 58 W	15 SW					LD 437	N 76 W	10 SW				
LD 359	N 17 E	25 NW					LD 438	N 77 E	10 SE				
LD 360	N 22 W	15 NE					LD 439	N 5 E	10 NW				
LD 361	N 21 W	30 NE					LD 440	N 14 W	20 SW				
LD 362	N 49 W	45 SW					LD 441	N 19 W	10 SW				
LD 363	N 27 E	30 SE					LD 442	N 62 E	10 SE				
LD 364	N 40 E	50 SE					LD 443	N 56 E	10 SE				
LD 365	N 39 E	30 SE					LD 444	N 23 W	10 NE				
LD 366	N 44 W	20 SW					LD 445	N 38 E	10 NW				
LD 367	N 3 W	45 NE					LD 446	N 21 E	10 SE				
LD 368	N 60 W	20 SW					LD 447	N 39 E	45 SE				
LD 369	N 26 E	20 SE					LD 448	N 55 E	55 SE				
LD 370	N 4 E	45 SE					LD 449	N 71 E	30 SE				
LD 371	N 42 E	30 NW					LD 450	N 37 E	20 SE				
LD 372	N 38 W	40 SW					LD 451	N 72 W	20 SW				
LD 373	N 89 E	30 SE					LD 452	N 73 E	15 SE				
LD 374	N 88 E	20 SE					LD 453	N 85 W	20 SW				
LD 375	N 55 E	20 SE					LD 454	N 81 W	15 SW				
LD 376	N 45 E	50 SE					LD 455	N 78 W	25 SW				
LD 377	N 37 W	15 SW					LD 456	N 67 W	60 SW				
LD 378	N 81 E	50 SE					LD 457	N 74 W	35 SW				
LD 379	N 21 E	50 SE					LD 458	N 47 E	20 SE				
LD 380	N 34 W	20 SW					LD 459	N 89 W	20 NE				
LD 381	N 68 W	45 SW					LD 460	N 55 W	15 NE				
LD 382	N 69 W	45 SW					LD 461	N 44 W	5 NE				
LD 383	N 50 W	50 SW					LD 462	N 29 W	20 SW				
LD 384	N 73 W	30 SW					LD 463	N 45 W	25 SW				
LD 385	N 63 W	75 SW					LD 464	N 44 W	25 SW				
LD 386	N 80 W	20 SW					LD 465	N 45 E	25 SE				
LD 387	N 35 E	50 SE					LD 466	N 54 E	15 SW				
LD 388	N 46 E	30 SE					LD 467	N 42 W	25 SW				
LD 389	N 30 E	40 SE					LD 468	N 40 W	20 NE				
LD 390	N 31 E	40 SE					LD 469	N 43 W	10 SW				
LD 391	N 21 W	10 NE					LD 470	N 29 E	20 SE				
LD 392	N 50 W	25 NE					LD 471	N 17 E	25 SE				
LD 393	N 64 W	80 SW					LD 472	N 57 W	20 SW				
LD 394	N 60 W	40 SW					LD 473	N 65 W	20 SW				
LD 395	N 81 W	35 SW					LD 474	N 48 W	20 SW				
LD 396	N 26 W	75 SW					LD 475	N 41 W	20 NE				
LD 397	N 64 W	30 NE					LD 476	N 42 E	30 SE				
LD 398	N 50 W	25 SW					LD 477	N 45 E	45 NW				
LD 399	N 46 W	75 SW					LD 478	N 68 W	20 SW				
LD 400	N 77 W	30 NE					LD 479	N 76 E	25 SE				
LD 401	N 61 W	30 NE					LD 480	N 62 E	5 SE				
LD 402	N 87 W	10 NE					LD 481	N 54 W	20 SW				
LD 403	N 69 E	75 SW					LD 482	N 52 W	50 SW				
LD 404	N 42 W	70 NW					LD 483	N 68 W	20 SW				
LD 405	N 37 W	35 NE					LD 484	N 28 W	25 SW				
LD 406	N 38 W	45 NE					LD 485	N 73 E	20 NW				
LD 407	N 21 W	65 NE					LD 486	N 9 W	70 NE				
LD 408	N 48 W	60 SW					LD 487	N 22 E	20 SEV				
LD 409	N 28 W	45 SW					LD 488	N 5 E	20 SE				
LD 410	N 58 W	30 SE					LD 489	N 19 W	10 NE				
LD 411	N 89 E	75 SE					LD 490	N 40 W	20 NE				
LD 412	N 56 W	25 NE					LD 491	N 53 E	20 NW				
LD 413	N 63 W	65 SW					LD 492	N 13 W	30 SW				
LD 414	N 71 W	70 NE					LD 493	N 27 W	10 SW				
LD 415	N 32 W	75 SW					LD 494	N 27 E	10 SE				
LD 416	N 25 W	35 SW					LD 495	N 43 W	20 NE				
LD 417	N 18 W	65 NE					LD 496	N 70 E	40 SE				
LD 418	N 74 W	20 SW					LD 497	N 86 W	5 NE				
LD 419	N 85 W	80 SW					LD 498	N 51 W	15 SW				
LD 420	N 25 E	20 NW					LD 499	N 62 W	15 NE				
LD 421	N 78 W	20 SW					LD 500	N 74 E	30 SE				
LD 422	N 37 W	35 NE					LD 501	N 78 W	30 NE				
LD 423	N 64 W	40 SW					LD 502	N 10 W	15 NE				
LD 503	N 88 W	25 NE					LD 582	N 85 W	5 SW				
LD 504	N 47 W	20 NE					LD 583	N 33 E	30 NW				
LD 505	N 20 W	25 NE					LD 584	N 25 W	35 NE				
LD 506	N 31 E	20 NW					LD 585	N 55 W	35 NE				
LD 507	N 22 E	70 NE					LD 586	N 7 W	40 NE				
LD 508	N 87 E	10 NW					LD 587	N 21 W	55 NE				
LD 509	N 36 W	70 SW					LD 588	N 50 E	60 NW				
LD 510	N 15 W	20 NE					LD 589	N 71 W	35 NE				

	Foliation		Lineation		Fold Axis			Foliation		Lineation		Fold Axis	
Station	Strike	Dip	Trend	Plunge	Trend	Plunge	Station	Strike	Dip	Trend	Plunge	Trend	Plunge
LD 511	N 18 W	25 NE					LD 590	N 60 W	20 NE				
LD 512	N 21 W	20 NE					LD 591	N 72 W	50 SW				
LD 513	N 72 W	15 NE					LD 592	N 40 W	40 NE				
LD 514	N 16 W	15 NE					LD 593	N 27 W	15 NE				
LD 515	N 9 W	60 NE					LD 594	N 44 W	15 NE				
LD 516	N 29 W	15 NE					LD 595	N 74 W	30 NE				
LD 517	N 46 W	15 NE					LD 596	N 85 W	35 NE				
LD 518	N 41 W	20 NE					LD 597	N 33 W	35 NE				
LD 519	N 84 E	25 NE					LD 598	N 29 W	35 NE				
LD 520	N 53 E	20 NW					LD 599	N 34 W	30 NE				
LD 521	N 56 E	15 NW					LD 600	N 57 W	20 NE				
LD 522					41	10	LD 601	N 28 W	20 NE				
LD 523					195	13	LD 602	N 25 W	20 NE				
LD 524	N 3 W	10 SW					LD 603	N 29 W	35 NE				
LD 525	N 44 E	40 NW					LD 604	N 16 W	30 NE				
LD 526	N 34 E	10 NW					LD 605	N 26 W	15 NE				
LD 527	N 13 E	30 NW					LD 606	N 29 W	30 NE				
LD 528	N 8 E	30 NW					LD 607					337	15
LD 529	N 19 E	45 SE					LD 608					289	5
LD 530	N 62 E	25 SE					LD 609	N 45 W	60 SW				
LD 531	N 63 W	40 NE					LD 610	N 31 W	15 NE				
LD 532	N 28 W	20 NE					LD 611	N 41 E	50 NW				
LD 533	N 13 W	20 NE					LD 612	N 54 E	15 NW				
LD 534	N 55 W	20 NE					LD 613					24	10
LD 535	N 37 W	15 NE					LD 614	N 16 W	20 NE				
LD 536	N 8 W	15 NE					LD 615	N 48 W	65 NE				
LD 537	N 44 W	45 NE					LD 616	N 19 E	10 NW				
LD 538	N 21 W	30 NE					LD 617	N 65 E	20 NW				
LD 539	N 64 E	20 NW					LD 618	N 41 W	10 SW				
LD 540					64	10	LD 619	N 16 W	35 NE				
LD 541	N 57 W	30 NE					LD 620	N 12 W	15 NE				
LD 542	N 9 E	45 SE					LD 621	N 54 W	30 NE				
LD 543	N 36 E	20 SE					LD 622	N 55 W	30 NE				
LD 544	N 11 W	20 NE					LD 623	N 26 W	15 NE				
LD 545	N 5 E	15 SE					LD 624	N 65 E	15 NW				
LD 546	N 64 E	15 NW					LD 625	N 67 E	15 NW				
LD 547	N 48 W	15 NE					LD 626	N 42 W	35 NE				
LD 548	N 56 W	45 NE					LD 627	N 18 W	20 NE				
LD 549					321	20	LD 628	N 47 W	20 NE				
LD 550	N 13 W	45 NE					LD 629	N 52 E	20 NW				
LD 551	N 50 W	10 NE					LD 630	N 50 W	20 NE				
LD 552	N 17 E	10 SE					LD 631	N 6 W	35 NE				
LD 553	N 3 W	15 SW					LD 632	N 20 W	20 NE				
LD 554	N 82 W	25 SW					LD 633	N 8 E	20SE				
LD 555	N 13 E	25 SE					LD 634	N 8 E	20 SE				
LD 556	N 20 W	45 SW					LD 635	N 38 E	10 NW				
LD 557	N 21 E	40 SE					LD 636	N 22 W	20 SW				
LD 558	N 21 W	35 NE					LD 637	N 6 W	20 SW				
LD 559	N 10 W	50 NE					LD 638	N 42 E	20 NW				
LD 560	N 67 W	50 NE					LD 639	N 48 E	15 SE				
LD 561	N 7 W	10 NE					LD 640	N 16 E	15 SE				
LD 562	N 3 E	40 SE					LD 641	N 24 W	30 NE				
LD 563	N 30 W	50 NE					LD 642	N 24 E	20 SE				
LD 564	37	25					LD 643	N 11 E	35 NW				
LD 565	N 35 E	30 NW					LD 644	N 48 W	20 SW				
LD 566	N 30 W	25 NE					LD 645	N 23 W	20 SW				
LD 567	N 24 W	40 NE					LD 646	N 60 E	25 NW				
LD 568	N 23 W	30 NE					LD 647					231	5
LD 569	N 29 W	40 NE					LD 648	N 44 E	20 SE				
LD 570	N 34 W	20 NE					LD 649	N 56 E	50 SE				
LD 571	N 66 W	50 NE					LD 650	N 39 E	10 SE				
LD 572	N 33 W	65 NE					LD 651	N 37 W	10 NE				
LD 573	N 24 W	35 NE					LD 652	N 27 W	25 NE				
LD 574	N 44 W	20 NE					LD 653	N 36 E	15 NW				
LD 575					76	25	LD 654	N 23 E	10 SE				
LD 576	N 71 W	30 SW					LD 655	N 25 W	10 SW				
LD 577	N 43 W	15 NE					LD 656	N 28 E	15 NW				
LD 578	N 25 W	20 SW					LD 657	N 30 E	30 SE				
LD 579	N 55 W	20 NE					LD 658	N 29 W	15 NE				
LD 580	N 21 W	15 NE					LD 659	N 51 W	10 NE				
LD 581	N 51 W	30 NE					LD 660	N 27 W	35 NE				
LD 661	N 36 W	25 NE					LD 740	N 81 W	20 SW				
LD 662	N 63 W	10 NE					LD 741	N 67 W	30 SW				
LD 663	N 55 W	10 NE					LD 742	N 28 W	20 SW				
LD 664	N 23 E	15 SE					LD 743	N 37 E	20 NW				
LD 665	N 46 W	10 NE					LD 744	N 58 W	25 SW				
LD 666	N 32 W	15 NE					LD 745	N 46 W	20 SW				
LD 667	N 38 W	15 NE					LD 746	N 44 W	35 SW				
LD 668	N 9 E	15 SE					LD 747	N 39 W	25 SW				
LD 669	N 21 W	35 NE					LD 748	N 62 W	20 SW				
LD 670	N 43 W	10 NE					LD 749	N 43 E	20 SE				
LD 671	N 55 W	15 NE					LD 750	N 85 W	20 SW				
LD 672	N 51 E	10 SE					LD 751	N 78 W	10 SW				
LD 673	N 56 E	15 SE					LD 752	N 64 W	25 SW				
LD 674	N 24 E	20 SE					LD 753	N 70 W	20 SW				
LD 675	N 18 W	15 NE					LD 754	N 62 W	20 SW				
LD 676	N 30 W	20 NE					LD 755	N 34 E	20 NW				
LD 677	N 74 W	20 NE					LD 756	N 36 E	25 SE				
LD 678	N 67 W	10 NE					LD 757	N 63 W	5 SW				
LD 679	N 69 W	15 NE					LD 758	N 59 E	60 NW				
LD 680	N 89 E	5 SE					LD 759	N 10 E	45 NW				

	Foliation		Lineation		Fold Axis			Foliation		Lineation		Fold Axis	
Station	Strike	Dip	Trend	Plunge	Trend	Plunge	Station	Strike	Dip	Trend	Plunge	Trend	Plunge
LD 681	N 45 W	10 SW					LD 760	N 18 W	10 NE				
LD 682	N 85 E	10 SE					LD 761	N 62 E	15 SE				
LD 683	N 67 E	5 SE					LD 762	N 74 E	15 SE				
LD 684	N 68 W	10 SW					LD 763	N 58 W	10 SW				
LD 685	N 68 E	30 SE					LD 764	N 79 E	25 SE				
LD 686	N 67 W	25 SW					LD 765	N 51 W	15 SW				
LD 687	N 80 E	15 SE					LD 766	N 10 W	50 SW				
LD 688	N 19 W	20 NE					LD 767	N 1 E	10 SE				
LD 689	N 57 E	20 SE					LD 768	N 65 E	20 SE				
LD 690	N 31 E	20 NW					LD 769	N 43 E	20 SE				
LD 691	N 66 W	40 SW					LD 770	N 72 W	15 SW				
LD 692	N 12 W	10 NE					LD 771	N 17 W	15 SW				
LD 693	N 59 E	10 NR					LD 772	N 11 W	10 SW				
LD 694	N 83 W	25 NE					LD 773	N 85 E	15 SE				
LD 695	N 48 W	20 NE					LD 774	N 32 W	20 SW				
LD 696	N 55 W	10 SW					LD 775	N 23 W	20 SW				
LD 697	N 64 W	10 SW					LD 776	N 4 W	15 SW				
LD 698	N 70 W	10 SW					LD 777	N 54 W	15 SW				
LD 699	N 88 W	10 NE					LD 778	N 21 W	20 SW				
LD 700	N 72 E	5 NW					LD 779	N 43 E	15 SE				
LD 701	N 29 E	10 NW					LD 780	N 69 W	50 SW				
LD 702					301	20	LD 781	N 89 E	50 SE				
LD 703	N 6 W	30 NE					LD 782	N 45 E	50 SE				
LD 704	N 30 W	10 SW					LD 783	N 54 W	30 SW				
LD 705	N 21 W	25 SW					LD 784	N 45 E	20 SE				
LD 706	N 29 W	15 SW					LD 785	N 75 W	30 SW				
LD 707	N 39 W	10 SW					LD 786	N 73 W	20 SW				
LD 708	N 72 W	15 SW					LD 787	N 72 W	30 SW				
LD 709	N 71 E	15 SE					LD 788	N 8 E	20 SE				
LD 710	N 37 W	20 SW					LD 789	N 22 W	60 SW				
LD 711	N 58 W	50 SW					LD 790	N 34 R	15 SE				
LD 712	N 16 E	20 NE					LD 791	N 16 E	35 SE				
LD 713	N 81 E	5 SE					LD 792	N 55 E	15 NW				
LD 714	N 63 W	20 SW					LD 793	N 68 E	15 NE				
LD 715	N 66 E	5 SE					LD 794	N 22 W	10 NE				
LD 716	N 60 E	15 SE					LD 795	N 15 E	15SE				
LD 717	N 61 W	10 SW					LD 796	N 15 E	60 SE				
LD 718	N 69 W	15 SW					LD 797	N 15 W	30 NE				
LD 719	N 80 W	5 SW					LD 798	N 6 E	10 SE				
LD 720	N 72 E	5 SE					LD 799	N 36 W	10 NE				
LD 721	N 57 W	20 SW					LD 800	N 22 W	20NE				
LD 722	N 32 W	25 NE					LD 801	N 56 E	15 NW				
LD 723	N 75 E	25 SE					LD 802	N 6 W	15 NE				
LD 724	N 86 E	25 SE					LD 803	N 16 W	20 SW				
LD 725	N 43 W	15 SW					LD 804	N 39 W	20 SW				
LD 726	N 43 W	40 SW					LD 805	N 38 E	65 NW				
LD 727	N 61 W	40 NE					LD 806	N 66W	10 SW				
LD 728	N 42 W	20 SW					LD 807	N 26 W	25 SW				
LD 729	N 62 W	20 SW					LD 808	N 64 W	15 SW				
LD 730	N 89 E	40 SE					LD 809	N 68 W	15 SW				
LD 731	N 81 W	25 SW					LD 810	N 23 W	20 SW				
LD 732	N 87 E	25 NE					LD 811	N 5 W	55 SW				
LD 733	N 69 W	35 SW					LD 812	N 39 E	60 NE				
LD 734	N 66 W	20 SW					LD 813	N 34 W	10 NE				
LD 735	N 35 E	15 SE					LD 814	N 11 W	15 NE				
LD 736	N 36 E	25 NE					LD 815	N 79 E	40 SE				
LD 737	N 27 W	30 NE					LD 816	N 52 W	45 SW				
LD 738	N 37 W	20 NE					LD 817	N 70 W	20 NE				
LD 739	N 42 W	10 NE					LD 818	N 57 E	10 SE				
LD 819	N 34 E	5 NW					LD 898	N 64 E	25 SE				
LD 820	N 49 W	50 NE					LD 899	N 86 W	15 SW				
LD 821	N 24 W	15 SW					LD 900	N 63 E	15 SE				
LD 822	N 69 E	20 SE					LD 901	N 65 E	10 SE				
LD 823	N 46 W	50 SW					LD 902	N 54 W	15 NE				
LD 824	N 61 E	20 SE					LD 903	N 47 W	5 NE				
LD 825	N 79 E	20 SE					LD 904	N 58 W	10 NE				
LD 826	N 29 W	35 SW					LD 905	N 27 W	25 NE				
LD 827	N 43 W	25 SW					LD 906	N 31 W	20 SW				
LD 828	N 56 W	80 SW					LD 907	N 32 W	15 SW				
LD 829	N 49 W	15 SW					LD 908	N 38 W	10 NE				
LD 830	N 78 W	40 SW					LD 909	N 46 W	20 SW				
LD 831	N 13 W	20 NE					LD 910	N 20 W	20 SW				
LD 832					124	10	LD 911	N 31 W	25 NE				
LD 833	N 37 W	25 SW					LD 912	N 9 E	20 NE				
LD 834	N 59 E	10 SE					LD 913	N 69 E	15 SE				
LD 835					58	10	LD 914	N 25 E	40 SE				
LD 836	N 11 E	25 SE					LD 915	N 27 W	10 NE				
LD 837	N 89 E	15 SE					LD 916	N 9 W	40 SW				
LD 838	N 67 E	30 SE					LD 917	N 3 W	10 SW				
LD 839	N 46 E	25 SE					LD 918	N 11 W	25 SW				
LD 840	N 32 W	15 SW					LD 919	N 25 W	25 SW				
LD 841	N 23 W	20 SW					LD 920	N 62 W	30 NE				
LD 842	N 28 W	10 SW					LD 921	N 29 E	40 SE				
LD 843	N 88W	10 SW					LD 922	N 10 E	25 SE				
LD 844	N 66W	55 SW					LD 923	N 66 W	10 NE				
LD 845	N 89 W	35 SW					LD 924	N 46 E	20 NW				
LD 846	N 26 W	30 SW					LD 925	N 44 E	10 SE				
LD 847	N 28 W	15 SW					LD 926	N 66 E	15 SE				
LD 848	N 64 W	20 SW					LD 927	N 26 W	10 NE				
LD 849	N 71 W	20 SW					LD 928	N 45 W	10 NE				
LD 850	N 84 W	25 SW					LD 929	N 9 W	10 NE				

	Foliation		Lineation		Fold Axis			Foliation		Lineation		Fold Axis	
Station	Strike	Dip	Trend	Plunge	Trend	Plunge	Station	Strike	Dip	Trend	Plunge	Trend	Plunge
LD 851	N 51 E	15 SE					LD 930	N 38 E	10 SE				
LD 852	N 29 E	40 SE					LD 931	N 63 W	30 SW				
LD 853	N 18 E	20 SE					LD 932	N 22 E	40 SE				
LD 854	N 65 W	30 NE					LD 933	N 46 W	15 SW				
LD 855	N 25 E	10 SE					LD 934	N 12 E	10 SE				
LD 856	N 32 E	20 SE					LD 935	N 29 W	15 SW				
LD 857	N 39 E	45 SE					LD 936	N 18 E	10 SE				
LD 858	N 56 W	20 SW					LD 937	N 29 W	15 SW				
LD 859	N 5 W	15 NE					LD 938	N 48 W	40 SW				
LD 860	N 70 E	25 SE					LD 939	N 12 E	15 SE				
LD 861	N 20 E	15 SE					LD 940	N 16 W	25 SW				
LD 862	N 8 W	20 NE					LD 941	N 38 W	10 NE				
LD 863	N 45 W	10 SW					LD 942	N 51 E	10 SE				
LD 864	N 60 E	30 SE					LD 943	N 28 E	15 SE				
LD 865					137	15	LD 944	N 20 E	10 NE				
LD 866	N 27 E	40 SE					LD 945	N 36 W	20 NE				
LD 867							LD 946	N 45 W	10 NE				
LD 868	N 61 E	25 SE					LD 947	N 22 W	45 SW				
LD 869	N 24 W	5 NE					LD 948	N 24 W	30 SW				
LD 870	N 67 E	10 SE					LD 949	N 29 W	15 SW				
LD 871	N 32 W	25 SW					LD 950	N 10 W	30 SW				
LD 872	N 82 W	20 SW					LD 951	N 41 W	30 NE				
LD 873	N 58 W	25 SW					LD 952	N 60 W	25 NE				
LD 874	N 31 W	15 SW					LD 953	N 20 W	30 NE				
LD 875	N 79 W	40 SW					LD 954	N 29 W	20 NE				
LD 876	N 51 W	20 SW					LD 955	N 39 W	10 NE				
LD 877	N 43 E	15 SE					LD 956	N 47 W	10 NE				
LD 878	N 74 W	25 SW					LD 957	N 26 W	20 NE				
LD 879	N 8 E	5 SE					LD 958	N 8 E	25 SE				
LD 880	N 80 W	30 SW					LD 959	N 49 W	25 SW				
LD 881	N 62 W	25 SW					LD 960	N 42 W	15 NE				
LD 882	N 11 W	10 NE					LD 961	N 36 W	20 NE				
LD 883	N 11W	10 SW					LD 962	N 11 W	50 NE				
LD 884	N 19 W	15 NE					LD 963	N 25 W	25 NE				
LD 885	N 63 E	20 SE					LD 964	N 2 E	25 SE				
LD 886	N 27 E	25 SE					LD 965	N 22 W	15 NE				
LD 887	N 41 W	20 SW					LD 966	N 20 W	20 NE				
LD 888	N 62 W	25 SW					LD 967	N 12 W	40 NE				
LD 889	N 48 E	5 NW					LD 968	N 67 W	15 NE				
LD 890	N 33 E	35 SE					LD 969	N 82 E	5 NW				
LD 891	N 74 E	10 SE					LD 970	N 54 E	20 SE				
LD 892	N 78 W	20 SW					LD 971	N 31 W	50 NE				
LD 893					316	10	LD 972	N 70 W	30 SW				
LD 894	N 23 W	15 NE					LD 973	N 6 E	15 SE				
LD 895	N 36 W	5 NE					LD 974	N 54 W	15 NE				
LD 896	N 49 W	50 SW					LD 975	N 20 W	15 NE				
LD 897	N 47 W	15 SW					LD 976	N 24 W	20 NE				
LD 977	N 51 W	15 NE					LD 1056	N 52 E	10 SE				
LD 978	N 42 W	15 NE					LD 1057	N 45 E	10 NW				
LD 979	N 66 W	10 NE					LD 1058	N 33 W	25 SW				
LD 980	N 35 W	20 NE					LD 1059	N 24 W	30 SW				
LD 981	N 85 W	10 NE					LD 1060	N 15 W	45 SW				
LD 982	N 66 W	20 NE					LD 1061	N 16 W	10 SW				
LD 983	N 5 W	10 NE					LD 1062	N 36 E	10 NW				
LD 984	N 18 W	20 SW					LD 1063	N 8 W	30 SW				
LD 985	N 55 E	15 NW					LD 1064	N 46 W	25 SW				
LD 986	N 50 W	20 NE					LD 1065	N 25 W	40 SW				
LD 987	N 1 E	20 NE					LD 1066	N 61 E	20 NW				
LD 988	N 68 E	15 NW					LD 1067	N 17 E	60 NW				
LD 989	N 19 W	15 NE					LD 1068	N 20 E	40 NW				
LD 990	N 31 W	15 NE					LD 1069	N 22 E	40 NW				
LD 991	N 26 W	10 NE					LD 1070	N 22E	20 NW				
LD 992	N 23 W	30 NE					LD 1071	N 33 W	20 SW				
LD 993	N 20 W	15 NE					LD 1072	N 38 E	10 NW				
LD 994	N 7 E	30SE					LD 1073	N 32 E	15 NW				
LD 995	N 71 W	15 NE					LD 1074	N 33 E	30 NW				
LD 996	N 65 W	10 NE					LD 1075	N 50 W	20 SW				
LD 997	N 89 E	10 NW					LD 1076	N 9 E	20 NW				
LD 998	N 50 W	5 NE					LD 1077	N 34 E	20 SE				
LD 999	N 40 W	20 NE					LD 1078	N 26 E	30 NW				
LD 1000					6	20	LD 1079	N 69 E	20 NW				
LD 1001					186	10	LD 1080	N 54 E	15 NW				
LD 1002	N 22 E	15 SE					LD 1081	N 61 E	40 NW				
LD 1003	N 23 E	15 SE					LD 1082					30	20
LD 1004	N 17 E	30 NW					LD 1083	N 34 E	30 NW				
LD 1005	N 37 E	40 NW					LD 1084	N 47 E	40 NW				
LD 1006	N 17 W	60 NE					LD 1085	N 19 W	30 SW				
LD 1007	N 66 W	25 NE					LD 1086	N 45 W	20 NE				
LD 1008	N 30 E	40 SE					LD 1087					336	10
LD 1009	N 5 W	15 NE					LD 1088	N 27 W	20 SW				
LD 1010	N 9 W	10 NE					LD 1089	N 36 W	20 SW				
LD 1011	N 11 E	15 SE					LD 1090	N 19 E	10 SE				
LD 1012	N 13 W	30 NE					LD 1091	N 43 W	20 SW				
LD 1013	N 56 W	25 NE					LD 1092	N 68 W	15 SW				
LD 1014	N 9 W	10 NE					LD 1093	N 40 W	45 SW				
LD 1015	N 43 W	5 NE					LD 1094	N 45 E	15 NW				
LD 1016	N 39 W	30 NE					LD 1095	N 33 W	30 SW				
LD 1017	N 35 W	20 SW					LD 1096	N 11 W	15 SW				
LD 1018	N 23 W	20 SE					LD 1097	N 26 W	40 SW				
LD 1019	N 24 E	15 SE					LD 1098	N 88 E	25 NW				
LD 1020	N 36 W	20 NE					LD 1099	N 83 W	20 NE				

	Foliation		Lineation		Fold Axis			Foliation		Lineation		Fold Axis	
Station	Strike	Dip	Trend	Plunge	Trend	Plunge	Station	Strike	Dip	Trend	Plunge	Trend	Plunge
LD 1021	N 28 E	15 NE					LD 1100	N 28 W	15 SW				
LD 1022	N 46 W	10 NE					LD 1101	N 71 W	35 NE				
LD 1023	N 30 W	25 NE					LD 1102	N 42 W	40 NE				
LD 1024	N 21 W	20 NE					LD 1103	N 47 E	40 NW				
LD 1025	N 38 E	20 NW					LD 1104	N 59 E	20 NW				
LD 1026	N 33 E	20 SE					LD 1105					338	10
LD 1027	N 20 W	25 NE					LD 1106					308	15
LD 1028	N 55 W	30 NE					LD 1107	N 18 W	5 NE				
LD 1029	N 44 W	35 NE					LD 1108	N 85 W	15 NE				
LD 1030	N 18 W	10 NE					LD 1109			4	5		
LD 1031	N 37 E	15 NE					LD 1110	N 37 W	25 SW				
LD 1032	N 18 W	20 NE					LD 1111	N 9 W	15 NE				
LD 1033	N 6 W	25 SW					LD 1112	N 5 W	20 SW				
LD 1034	N 6 E	20 SE					LD 1113	N 33 W	30 SW				
LD 1035	N 45 W	15 NE					LD 1114	N 57 W	10 SW				
LD 1036	N 25 W	45 NE					LD 1115	N 16 W	20 NE				
LD 1037	N 46 E	15 NW					LD 1116	N 72 W	50 SW				
LD 1038	N 47 W	20 NE					LD 1117	N 23 W	20 NE				
LD 1039	N 24 W	30 NE					LD 1118	N 6 W	20 NE				
LD 1040	N 78 W	25 NE					LD 1119	N 62 W	10 SW				
LD 1041	N 68 E	10 NW					LD 1120	N 18 E	20 SE				
LD 1042	N 68 E	45 NW					LD 1121	N 34 W	15 SW				
LD 1043	N 23 W	5 NE					LD 1122					329	5
LD 1044	N 86 E	15 NW					LD 1123					38	10
LD 1045	N 18 E	20 SE					LD 1124	N 7 W	20 NE				
LD 1046					149	10	LD 1125	N 3 W	15 NE				
LD 1047	N 14 W	10 NE					LD 1126	N 5 W	15 NE				
LD 1048	N 36 W	20 SW					LD 1127	N 13 W	25 NE				
LD 1049	N 40 W	10 SW					LD 1128					322	5
LD 1050	N 15 W	40 NE					LD 1129			314	5		
LD 1051	N 37 W	10 NE					LD 1130	N 43 W	65 NE				
LD 1052	N 39 E	15 SE					LD 1131	N 34 E	30 NW				
LD 1053	N 39 W	10 NE					LD 1132	N 62 E	40 SE				
LD 1054					332	10	LD 1133	N 46 W	10 NE				
LD 1055	N 12 W	10 NE					LD 1134	N 88 W	10 NE				
LD 1135	N 21 W	30 NE					LD 1214	N 71 W	15 NE				
LD 1136	N 4 W	10 NE					LD 1215					127	15
LD 1137	N 2 E	15 SE					LD 1216	N 34 W	10 NE				
LD 1138	N 55 E	15 SE					LD 1217	N 22 W	25 NE				
LD 1139	N 27 E	15 NW					LD 1218	N 13 E	10 NW				
LD 1140	N 18 E	40 SE					LD 1219	N 49 E	10 NW				
LD 1141	N 57 E	30 SE					LD 1220	N 51 W	10 NE				
LD 1142	N 78 W	30 SW					LD 1221					15	10
LD 1143	N 36 E	50 SE					LD 1222	N 13 E	80 NW				
LD 1144	N 53 E	30 SE					LD 1223					327	10
LD 1145	N 50 E	30 SE					LD 1224	N 70 W	10 NE				
LD 1146	N 42 E	25 SE					LD 1225	N 76 E	40 SE				
LD 1147	N 7 W	5 NE					LD 1226	N 83 E	20 SE				
LD 1148	N 22 W	15 NE					LD 1227	N 72 W	25 NE				
LD 1149	N 8 W	20 NE					LD 1228	N 21 W	20 NE				
LD 1150	N 54 W	25 NE					LD 1229	N 61 E	50 SE				
LD 1151	N 50 E	15 SE					LD 1230	N 38 W	20 SW				
LD 1152	N 19 E	15 NW					LD 1231	N 11 E	35 NW				
LD 1153	N 65 E	35 SE					LD 1232	N 48 E	15 NW				
LD 1154	N 27 E	35 SE					LD 1233	N 24 E	5 NW				
LD 1155					201	10	LD 1234	N 81 E	25 SE				
LD 1156					354	10	LD 1235	N 41 E	10 SE				
LD 1157	N 15 W	10 SW					LD 1236	N 6 W	35 SW				
LD 1158					150	15	LD 1237	N 60 W	40 SW				
LD 1159	N 30 W	40 SW					LD 1238					318	15
LD 1160	N 50 W	20 NE					LD 1239	N 54 E	10 NW				
LD 1161	N 51 W	45 SW					LD 1240	N 48 W	15 NE				
LD 1162	N 65 W	45 SW					LD 1241	N 12 E	40 SE				
LD 1163					145	20	LD 1242	N 57 E	30 SE				
LD 1164	N 18 E	10 SE					LD 1243	N 19 W	20 SW				
LD 1165	N 33 E	20 SE					LD 1244	N 57 E	15 SE				
LD 1166	N 50 E	25 SE					LD 1245	N 88 W	75 NE				
LD 1167	N 66 W	50 SW					LD 1246	N 74 W	50 SW				
LD 1168	N 4 W	20NE					LD 1247	N 77 E	20 NW				
LD 1169	N 50 W	25 SW					LD 1248	N 84 E	20 SE				
LD 1170					171	10	LD 1249	N 13 W	30 NE				
LD 1171	N 62 E	45 SE					LD 1250	N 60 W	10 NE				
LD 1172	N 4 W	60 NE					LD 1251	N 79 E	15 SE				
LD 1173	N 50 W	25 SW					LD 1252	N 52 W	30 SW				
LD 1174	N 58 E	10 SE					LD 1253	N 56 W	15 SW				
LD 1175	N 29 W	70 SW					LD 1254	N 72 W	35 SW				
LD 1176	N 76 E	20 SE					LD 1255	N 67 W	25 SW				
LD 1177	N 37 W	30 SW					LD 1256	N 61 W	10 SW				
LD 1178	N 69 W	75 SW					LD 1257	N 18 W	60 NE				
LD 1179	N 75 W	30 SW					LD 1258					314	10
LD 1180	N 27 E	20 SE					LD 1259	N 18 E	20 SE				
LD 1181	N 39 E	65 SE					LD 1260	N 5 W	40 NE				
LD 1182	N 46 W	40 SW					LD 1261	N 82 W	25 NE				
LD 1183	N 76 W	20 SW					LD 1262	N 66 W	70 NE				
LD 1184	N 39 W	30 SW					LD 1263	N 52 W	40 NE				
LD 1185	N 71 E	40 SE					LD 1264	N 43 W	5 NE				
LD 1186	N 44 E	40 SE					LD 1265	N 50 W	40 NE				
LD 1187	N 69 W	25 SW					LD 1266	N 45 W	10 NE				
LD 1188	N 29 E	20 SE					LD 1267	N 56 W	30 NE				
LD 1189	N 50 E	30 NW					LD 1268	N 40 E	50 SE				
LD 1190	N 36 E	40 SE					LD 1269	N 46 E	45 NW				

	Foliation		Lineation		Fold Axis			Foliation		Lineation		Fold Axis	
Station	Strike	Dip	Trend	Plunge	Trend	Plunge	Station	Strike	Dip	Trend	Plunge	Trend	Plunge
LD 1191	N 88 E	20 SE					LD 1270	N 75 E	10 NW				
LD 1192	N 60 W	30 SW					LD 1271	N 70 E	15 NW				
LD 1193	N 24 E	25 NW					LD 1272	N 75 W	30 NE				
LD 1194	N 67 W	40 NE					LD 1273	N 44 E	20 SE				
LD 1195	N 76 E	20 SE					LD 1274	N 42 E	20 SE				
LD 1196	N 16 E	15 SE					LD 1275	N 18 W	10 SW				
LD 1197	N 31 E	20 SE					LD 1276					140	20
LD 1198	N 20 E	15 SE					LD 1277	N 12 W	20 SW				
LD 1199	N 17 W	20 NE					LD 1278	N 34 W	20 NE				
LD 1200	N 25 W	25 SW					LD 1279	N 50 E	30 NW				
LD 1201	N 68 E	25 SE					LD 1280	N 81 E	5 NW				
LD 1202	N 30 E	30 SE					LD 1281	N 45 W	35 NE				
LD 1203	N 63 E	30 SE					LD 1282	N 78 E	20 NW				
LD 1204	N 60 E	25 SE					LD 1283	N 70 E	10 NW				
LD 1205					215	30	LD 1284	N 39 E	40 NW				
LD 1206	N 70 E	15 SE					LD 1285	N 9 W	30 SW				
LD 1207	N 3 E	30 SE					LD 1286	N 26 W	20 SW				
LD 1208	N 88 E	10 NW					LD 1287	N 10 E	10 NW				
LD 1209	N 49 E	20 NW					LD 1288	N 44 E	15 NW				
LD 1210	N 25 E	20 NW					LD 1289	N 60 E	50 NW				
LD 1211	N 63 W	15 SW					LD 1290	N 38 E	25 NW				
LD 1212	N 39 W	15 NE					LD 1291	N 32 E	40 NW				
LD 1213	N 78 E	10 SE					LD 1292	N 36 W	20 SW				
LD 1293	N 40 E	15 NW					LD 1372	N 42 W	15 NE				
LD 1294	N 31 E	35 NW					LD 1373	N 35 W	20 NE				
LD 1295	N 35 W	50 NW					LD 1374	N 80 W	15 NE				
LD 1296	N 17 E	20 NW					LD 1375	N 40 W	20 NE				
LD 1297	N 25 E	30 NW					LD 1376	N 48 E	25 NW				
LD 1298	N 5 E	50 NW					LD 1377	N 24 W	20 SW				
LD 1299	N 12 E	25 NW					LD 1378	N 29 W	35 NE				
LD 1300	N 25 W	30 SW					LD 1379	N 60 W	45 NE				
LD 1301					339	15	LD 1380	N 53 W	10 NE				
LD 1302	N 20 W	15 SW					LD 1381	N 54 E	25 NW				
LD 1303	N 24 W	30 SW					LD 1382	N 31 E	25 NW				
LD 1304	N 8 E	10 NW					LD 1383	N 36 E	10 SE				
LD 1305	N 9 E	30 NW					LD 1384	N 26 E	10 SE				
LD 1306	N 44 W	15 SW					LD 1385	N 50 E	25 NW				
LD 1307	N 18 W	30 SW					LD 1386					2	10
LD 1308	N 17 W	30 SW					LD 1387	N 63 E	25 NW				
LD 1309					329	5	LD 1388	N 74 W	20 NE				
LD 1310	N 43 W	20 SW					LD 1389	N 16 W	20 SW				
LD 1311	N 31 W	20 SW					LD 1390	N 77 E	15 NE				
LD 1312	N 38 W	55 SW					LD 1391	N 41 W	15 NE				
LD 1313	N 26 W	20 SW					LD 1392	N 67 W	10 NE				
LD 1314	N 12 W	50 SW					LD 1393	N 29 W	10 NE				
LD 1315	N 17 E	15 SE					LD 1394	N 35 W	30 NE				
LD 1316	N 12 W	15 SW					LD 1395	N 32 W	30 SW				
LD 1317	N 18 W	20 SW					LD 1396	N 24 E	25 NW				
LD 1318	N 34 E	15 NW					LD 1397	N 62 W	20 NE				
LD 1319	N 35 W	50 SW					LD 1398	N 29 W	10 NE				
LD 1320	N 30 W	55 SW					LD 1399	N 57 W	20 NE				
LD 1321	N 2 W	30 SW					LD 1400	N 25 E	15 NW				
LD 1322	N 22 E	25 SE					LD 1401	N 71 W	20 NE				
LD 1323	N 13 W	30 SW					LD 1402	N 50 E	15 NW				
LD 1324	N 25 W	65 SW					LD 1403	N 22 E	20 NW				
LD 1325	N 3 W	65 SW					LD 1404					338	10
LD 1326	N 40 E	60 NW					LD 1405	N 39 E	10 NW				
LD 1327	N 14 W	30 SW					LD 1406	N 33E	10 NW				
LD 1328	N 24 W	30 SW					LD 1407	N 67 E	15 NW				
LD 1329	N 17 W	45 SW					LD 1408	N 85 E	25 NW				
LD 1330	N 81 E	60 SE					LD 1409			180	5		
LD 1331	N 8 E	45 SE					LD 1410	N 71 W	20 NE				
LD 1332	N 50 W	25 NE					LD 1411	N 21 W	30 NE				
LD 1333	N 29 W	20 SW					LD 1412	N 10 E	15 NW				
LD 1334	N 10 W	70 SW					LD 1413	N 65 E	15 NW				
LD 1335	N 42 E	25 NW					LD 1414	N 66 E	25 NW				
LD 1336	N 24 W	15 NE					LD 1415	N 61 W	15 NE				
LD 1337	N 5 E	35 NW					LD 1416	N 63 W	10 SW				
LD 1338	N 56 W	15 NE											
LD 1339	N 6 E	20 NW											
LD 1340	N 17 W	30 SW											
LD 1341	N 16 E	40 NW											
LD 1342	N 87 W	25 SW											
LD 1343	N 28 W	15 SW											
LD 1344	N 25 E	15 NW											
LD 1345	N 15 E	10 NW											
LD 1346					341	10							
LD 1347	N 14 W	15 SW											
LD 1348					335	10							
LD 1349	N 24 W	10 NE											
LD 1350	N 13 E	25 NW											
LD 1351	N 17 W	10 NE											
LD 1352	N 34 W	30 NE											
LD 1353	N 54 W	35 NE											
LD 1354	N 40 W	35 NE											
LD 1355	N 43 W	25 NE											
LD 1356	N 37 W	10 NE											
LD 1357	N 26 W	35 NE											
LD 1358	N 23 W	20 NE											
LD 1359	N 21 W	30 NE											
LD 1360	N 16 W	30 NE											

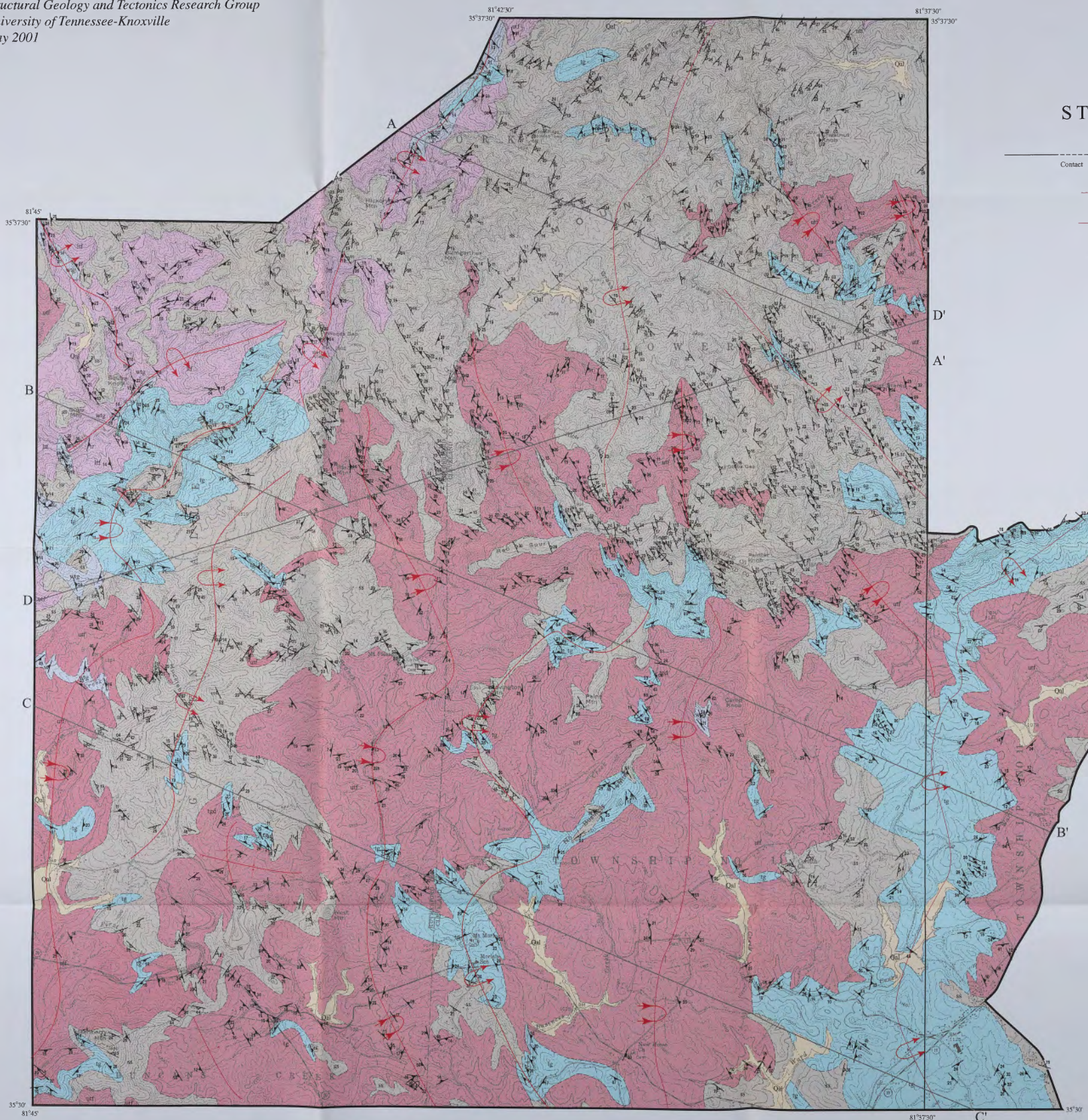
	Foliation		Lineation		Fold Axis			Foliation		Lineation		Fold Axis	
Station	Strike	Dip	Trend	Plunge	Trend	Plunge	Station	Strike	Dip	Trend	Plunge	Trend	Plunge
LD 1361	N 16 W	40 SW											
LD 1362	N 55 E	30 NW											
LD 1363	N 40 W	20 NE											
LD 1364	N 25 W	30 NE											
LD 1365	N 11 E	45 NW											
LD 1366	N 41 E	30 NW											
LD 1367	N 16 E	30 SE											
LD 1368	N 20 W	30 NE											
LD 1369	N 6 W	15 NE											
LD 1370	N 40 W	10 NE											
LD 1371	N 21 E	20 NW											

VITA

Sara Elizabeth Bier was born and raised in the foothills of the Blue Ridge Mountains in Ferrum, Virginia. She played with her three older siblings and fellow creatures in the babbling brooks and magical forests of Hippy Hollow. She began her geologic studies at Juniata College in Huntingdon, Pennsylvania where she was fortunate to find a home at Blue Moon Farm. Sara graduated in 1997 and headed west to the high desert and lava tubes of California, at Lava Beds National Monument. After a year as a park ranger, she headed to field camp in the North Woods of Canada. She returned to the southern Appalachians to attend University of Tennessee-Knoxville in the fall of 1998. During her three years at UT, Sara played in the South Mountains of North Carolina, returned to the North Woods, and went trekking in Nepal. Sara received her Masters degree in August 2001. She is presently in pursuit of a Ph.D. at Pennsylvania State University.

Plate I. Geologic map and cross sections of portions of the Benn Knob and Casar 7.5-minute quadrangles, North Carolina

Sara Bier
Supervised by Robert D. Hatcher, Jr.
Structural Geology and Tectonics Research Group
University of Tennessee-Knoxville
May 2001



STRUCTURE

Contact — *Solid where confident, dashed where approximate and dotted where concealed.*

Trace of axial surface of overturned, recumbent anticline

Trace of axial surface of overturned, recumbent syncline.

Trace of axial surface of open, upright anticline.

Trace of axial surface of open, upright syncline.

Strike and dip of schistosity

Strike and dip of foliation

Trend and plunge of mineral elongation lineation

Trend and plunge of overturned, recumbent antiform

Trend and plunge of overturned, recumbent synform

Trend and plunge of upright, open synform

Trend and plunge of upright, open antiform

BCT *Brindle Creek Thrust*

EXPLANATION

QUATERNARY

Qal
Alluvium
Unconsolidated stream deposits of gravel, sand, silt, and clay.

ORDOVICIAN

tg
Toluca Granite
Granite, gray, gneissic, medium-grained, granoblastic. Major minerals include plagioclase (18-42%, An_{20-30}), microcline (15-44%), quartz (17-25%), muscovite (2-22%), biotite (1-16%), and garnet (<1-4%). Accessory minerals include monazite, zircon, ilmenite, and rutile. Weathers to white and tan saprolite, and contains xenoliths of biotite gneiss (utf).

wtg
Walker Top orthogneiss
Granite to granodiorite, grey, massive, weakly foliated, porphyroblastic. Microcline megacrysts (18-35%) are often rimmed with myrmekite. Matrix is composed dominantly of fine- to medium-grained quartz (14-16%), biotite (13-22%), plagioclase (15-26% An_{25-35}), microcline (5-18%), and minor amounts of muscovite (1-3%). Accessory minerals include garnet, zircon, apatite, and opaques.

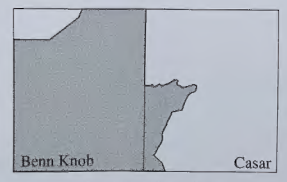
UPPER PRECAMBRIAN (?) or LOWER PALEOZOIC (?)

Tallulah Falls Formation

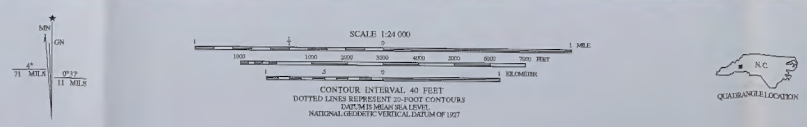
utf
Upper Tallulah Falls Formation
Metagraywacke-schist, light-gray to dark-gray, medium- to fine-grained, massive- to thick-layered, well-foliated, commonly porphyroblastic. Major minerals are quartz (19-40%), plagioclase (16-32%, An_{20-30}), biotite (32-38%), and muscovite (3-9%). Minor constituents are sillimanite, epidote, microcline, chlorite, and opaques. Layer thickness varies from a few millimeters to several meters. Foliation is defined by biotite and muscovite in the gneiss and schist. Biotite schist, granitic gneiss, and calc-silicate occur throughout the unit.Probably derived from feldspathic sandstone.

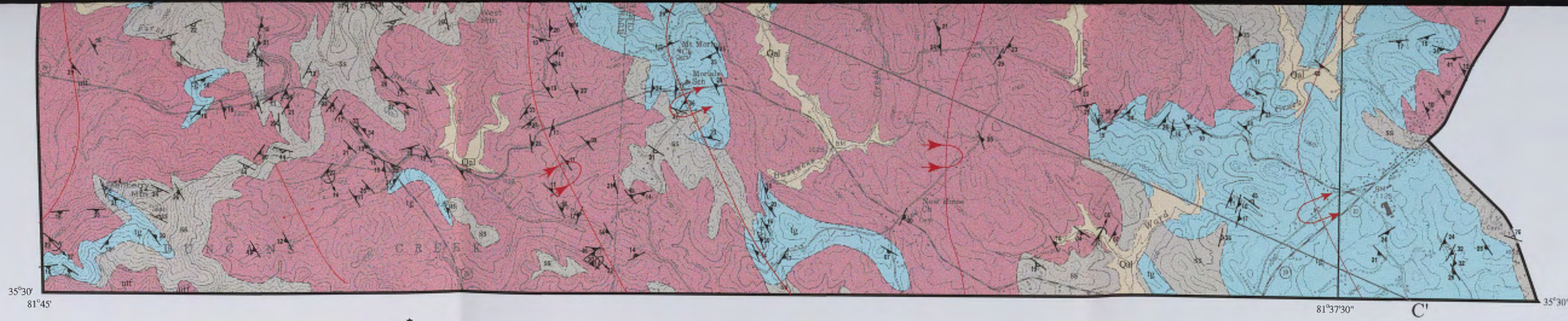
ss
Tallulah Falls aluminous schist
Aluminous schist, light- to dark-silver-gray, inequigranular to porphyroblastic. Minerals include quartz (19-32%), plagioclase (6-15%, An_{20-30}), muscovite (6-41%), sillimanite (16-42%), biotite (2-25%), and garnet (4-13%). Accessory minerals include chlorite, epidote, zircon, and opaques. Subhedral garnet porphyroblasts up to 4 mm in diameter occur in a fine-grained matrix. Weathers to grayish-red-purple saprolite. Probably derived from argillaceous rocks.

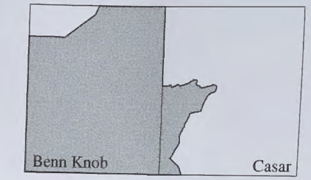
ltf
Lower Tallulah Falls Formation
Metagraywacke-biotite gneiss, light-gray to dark-gray, medium- to fine-grained, massive- to thick-layered, well-foliated, commonly porphyroblastic. Major minerals include quartz (12-45%), plagioclase (22-36%, An_{45-55}), biotite (15-26%), muscovite (1-19%), k-feldspar (<1-19%), and garnet (1-25%). Minor contituents include sillimanite, chlorite, and opaques. Muscovite-biotite schist, granitic gneiss, and amphibolite occur throughout the unit. Probably derived from feldspathic sandstone. (Description from Giorgis, 1999).



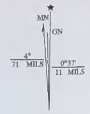
7.5-minute quadrangle index

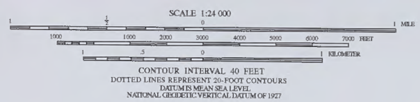




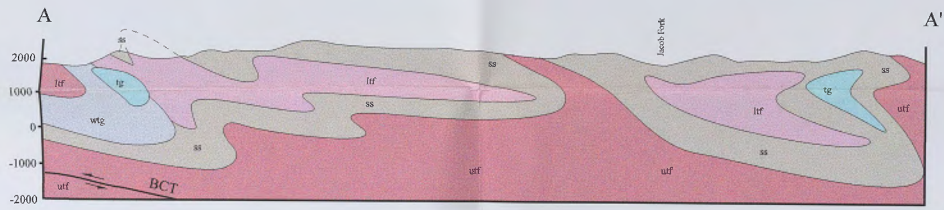


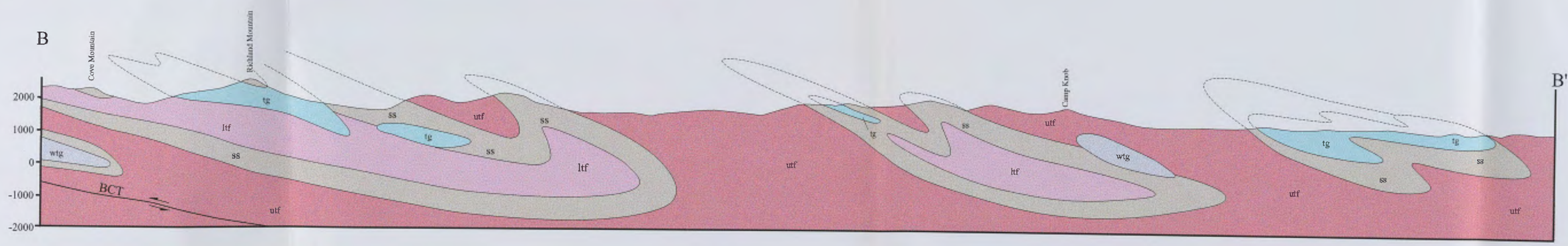
7.5-minute quadrangle index

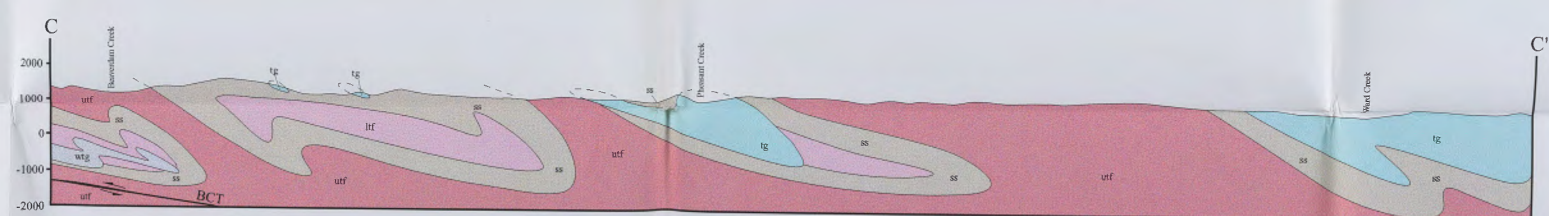


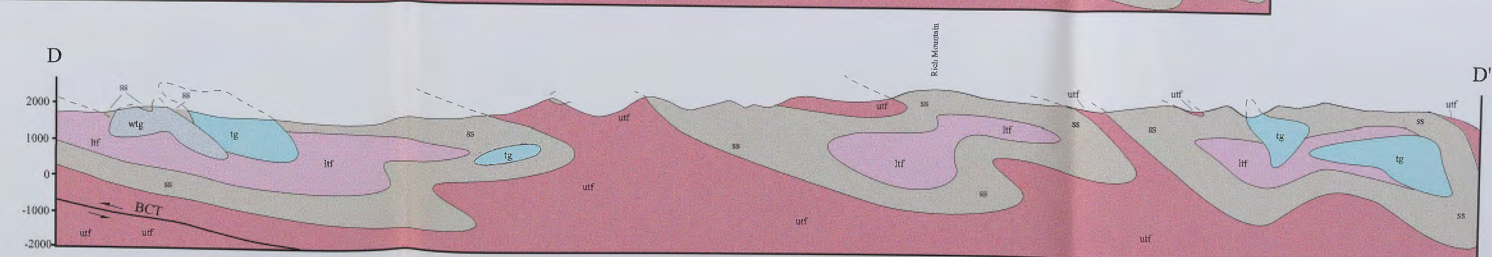








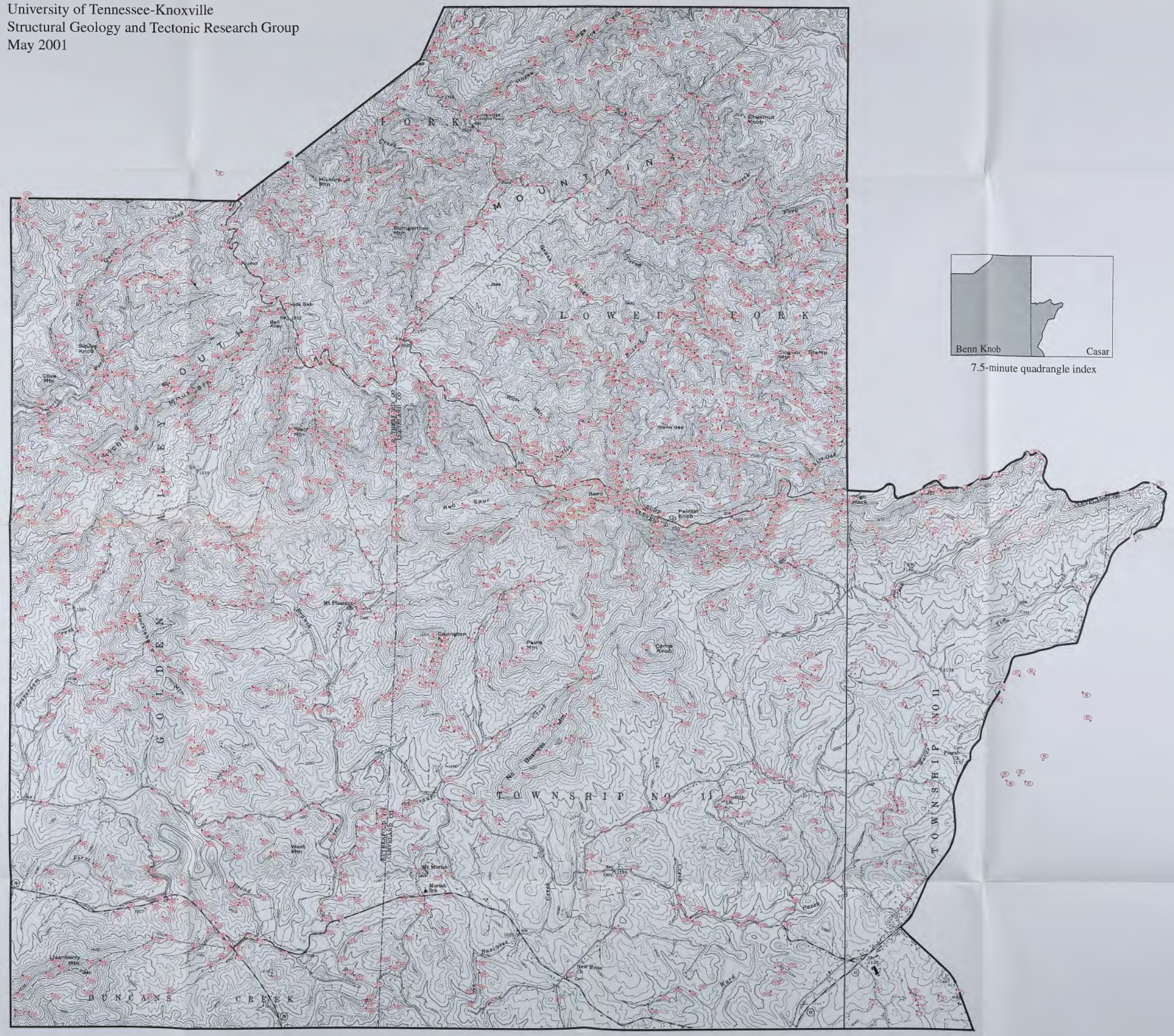




Supported by the National Cooperative
Geologic Mapping Program, EDMAP component,
under Assistance Award No. 00HQAG0035 and
the University of Tennessee Science Alliance Center
of Excellence.

Plate II. Station map of portions of the Benn Knob and Casar 7.5-minute quadrangles, North Carolina

Sara Bier
Supervised by Robert D. Hatcher, Jr.
University of Tennessee-Knoxville
Structural Geology and Tectonic Research Group
May 2001



7.5-minute quadrangle index

SCALE 1:24 000

CONTOUR INTERVAL 40 FEET
DOTTED LINES REPRESENT 20-FOOT CONTOURS
DATUM IS MEAN SEA LEVEL
NATIONAL GEODETIC VERTICAL DATUM OF 1927

QUADRANGLE LOCATION

Plate III. Compiled geologic map of the Casar, Polkville, Lawndale, Boiling Springs, and Shelby 7.5-minute quadrangles, North Carolina

compiled by Sara Bier
supervised by Robert D. Hatcher, Jr.
University of Tennessee-Knoxville
Structural Geology and Tectonic Research Group
May 2001

EXPLANATION

QUATERNARY

Qal

Alluvium

Bedded, poorly sorted in consolidated flood plain deposits consisting of a discontinuous basal layer of white to brown quartz pebble gravel with yellow to gray sandy matrix resting on mainly weathered crystalline rocks, overlain by a layer of gray to black clay, carbonaceous clay or muck, which is overlain by fine-grained red, brown, or gray sand and silt.

ORDOVICIAN

Opm

Microcline-oligoclase-quartz-biotite pegmatite

White, coarse-grained, porphyritic, unzoned, gneissic microcline-oligoclase-quartz-biotite pegmatite of quartz monzonitic composition occurring as large sills, dikes, and irregular masses; accessory apatite, monazite, xenotime, and zircon common, locally contains thin crystals of prismatic brown zircon enclosed in parallel position by stubby crystals of green xenotime.

Otg

Toluca Granite

Gray, gneissic, massive, lineated, medium-grained, equigranular to very rarely and locally porphyritic biotite granite, contains accessory almandine, monazite, zircon, ilmenite, and rutile; bodies are strongly gneissic at marginsbut may be nearly massive a few hundred feet from the contacts; weathers to white, yellow, or red saprolite; uncommon inclusions of biotite schist occur as wispy relicts.

OCh OCp

Hornblende gneiss

Dark-green to black, fine- to coarse-grained equigranular hornblende gneiss consisting mainly of hornblende and andesine with accessory biotite, garnet, quartz, magnetite, and ilmenite; occurs as elongate masses and layers in sillimanite schist and locally in biotite schist, exceptionally exposed as envelopes or partial envelopes around ellipsoidal masses of gabbro; formed by the shearing and metamorphism of bodies of gabbro; commonly deeply weathered dark red, brown, or mustard colored clayey saprolite or granular greenish brown saprolite.

Pyroxenite

Greenish -gray, dark greenish gray, or black, medium- to coarse-grained, inequigranular pyroxenite, norite, and peridotite metamorphosed into hornblende hypersthene, also commonly chloritized, locally sheared into hornlende gneiss; occurs as lenticular to oval masses intruded into the sillimanite schist, and as thin dikes; rare saprolite is dark brown to yellowish green, granular, or clayey, usually exposd as rough-textured, round boulders.

OCg

Gabbro

Dark-gray to black, fine- to coarse- grained, equigranular to inequigranular, massive hornblende gabbro, garnetiferous hornblende gabbro and local hornblendegneiss, occurs as dikes, sills and oval masses in sillimanite schist; weathers to dark red, brown, or mustard-colored saprolite.

UPPER PRECAMBRIAN (?) or LOWER PALEOZOIC (?)

Pzb

Biotite schist and gneiss

Gray to dark-gray, massive to foliated, layered, fine- to coarse-grained, inequigranular biotite schist and gneiss, garnetiferous biotite schist and gneiss, and hornblende biotite schist and gneiss formed by upper amphibolite-grade metamorphism of graywacke, argillite and volcanic rocks; interlayered with sillimanite schist; intruded by the Toluca Granite from which it can be distinguished from by composition and layering; deeply weathered locally to white, dark-red, or brown saprolite, but it is the most resistant rock in the study area to chemical and mechanical weathering; generally lacks sharp plications; thin veins, sills, and pods of monazite-bearing microcline-oligoclase-quartz pegmatite are present but much less common than in the sillimanite schist unit; accessory minerals are very sparse, mainly fine-grained zircon.

Pzs

Sillimanite schist

Light to dull-gray, schistose, layered fine- to coarse-grained, inequigranular sillimanite-biotite schist and gneiss, garnetiferous sillimanite-biotite schist and gneiss, sillimanite-muscovite schist and gneiss, sillimanite-quartz schist, tourmaline-sillimanite schist, and graphite-sillimanite schist, formed by upper amphibolite grade metamorphism of argillite, sandstone, and weathered pyroclastic rocks; mainly consist of sillimanite-biotite schist composed of biotite, quartz, oligoclase, sillimanite, and almandine; interlayered with the biotite schist and biotite gness units into which it grades by decrease in amount of silimanite below 5 percent of the volume of the rock; commonly deeply weathered and generally stained brown and purple by iron and manganese oxides; usually thinly layered and complexly folded, sygmoidal foliation planes common; closely threaded with numerous veins, sills, and pods of monazite-bearing microcline-oligoclase-quartz pegmatite; accesssory monazite, tourmaline and rutile common, zircon sparse; sillimanite altered by late-stage retogressive metamorphism to pseudomorphous acicular aggregates of sericite.

STRUCTURE

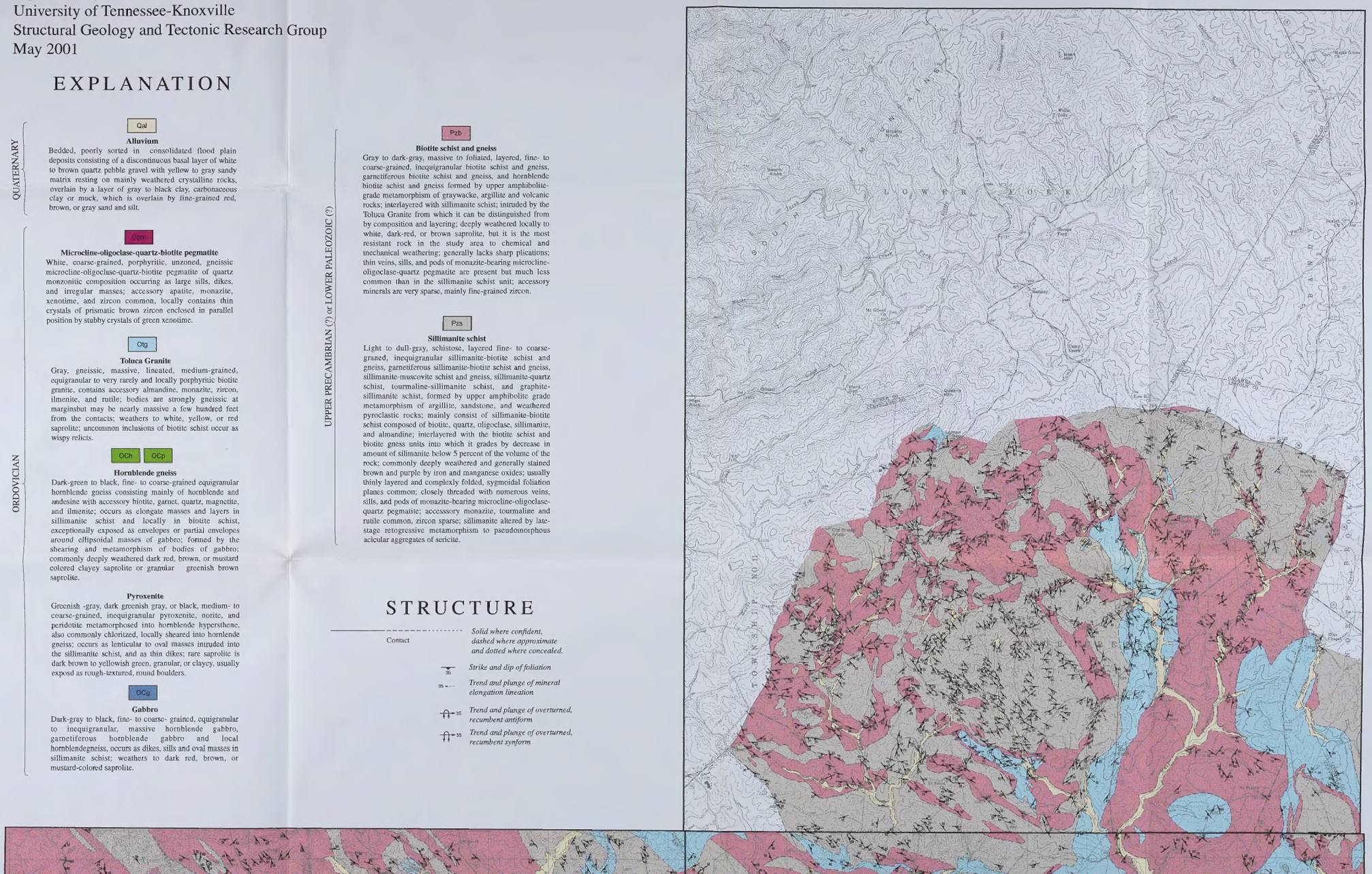
Contact — *Solid where confident, dashed where approximate and dotted where concealed.*

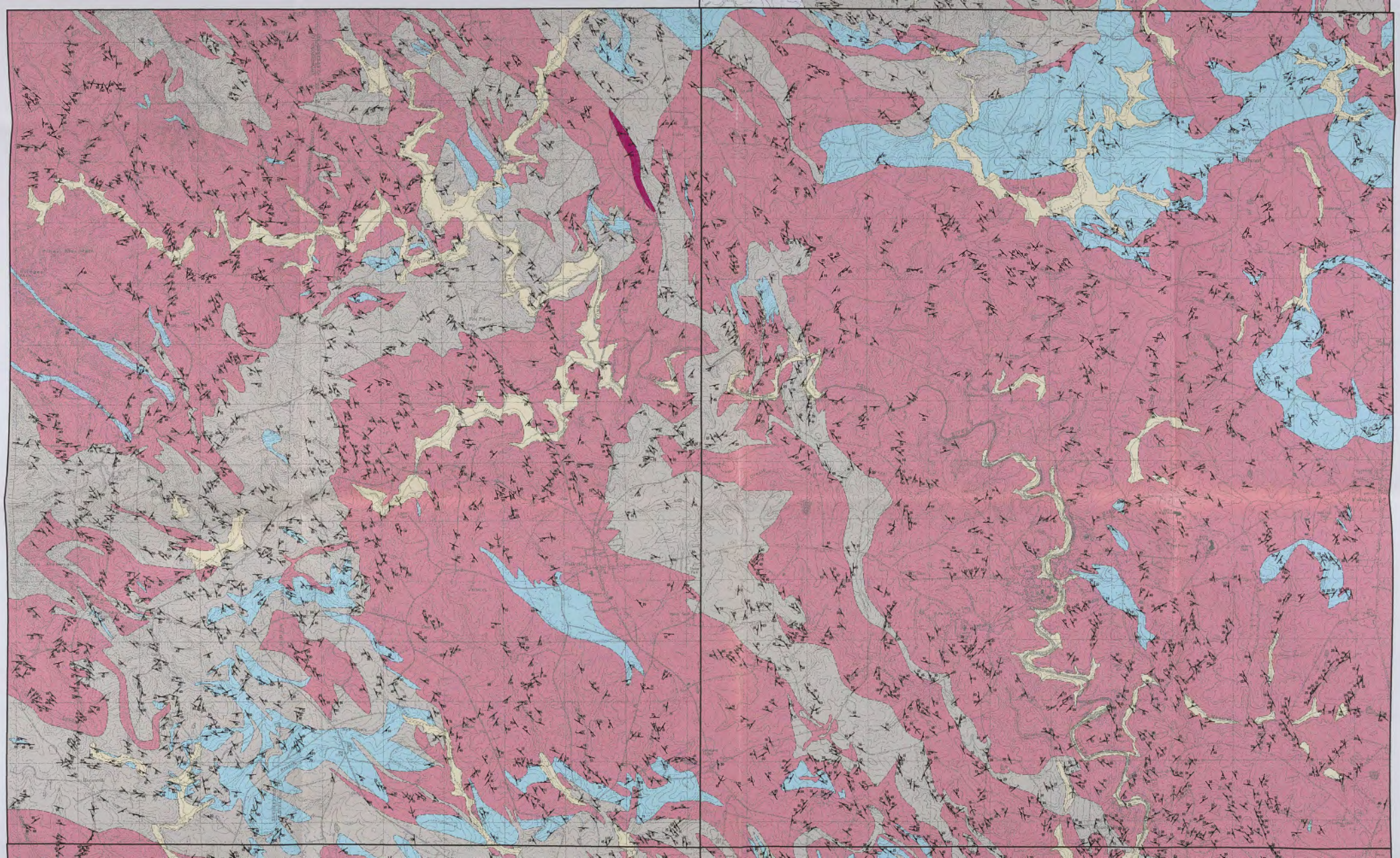
Strike and dip of foliation

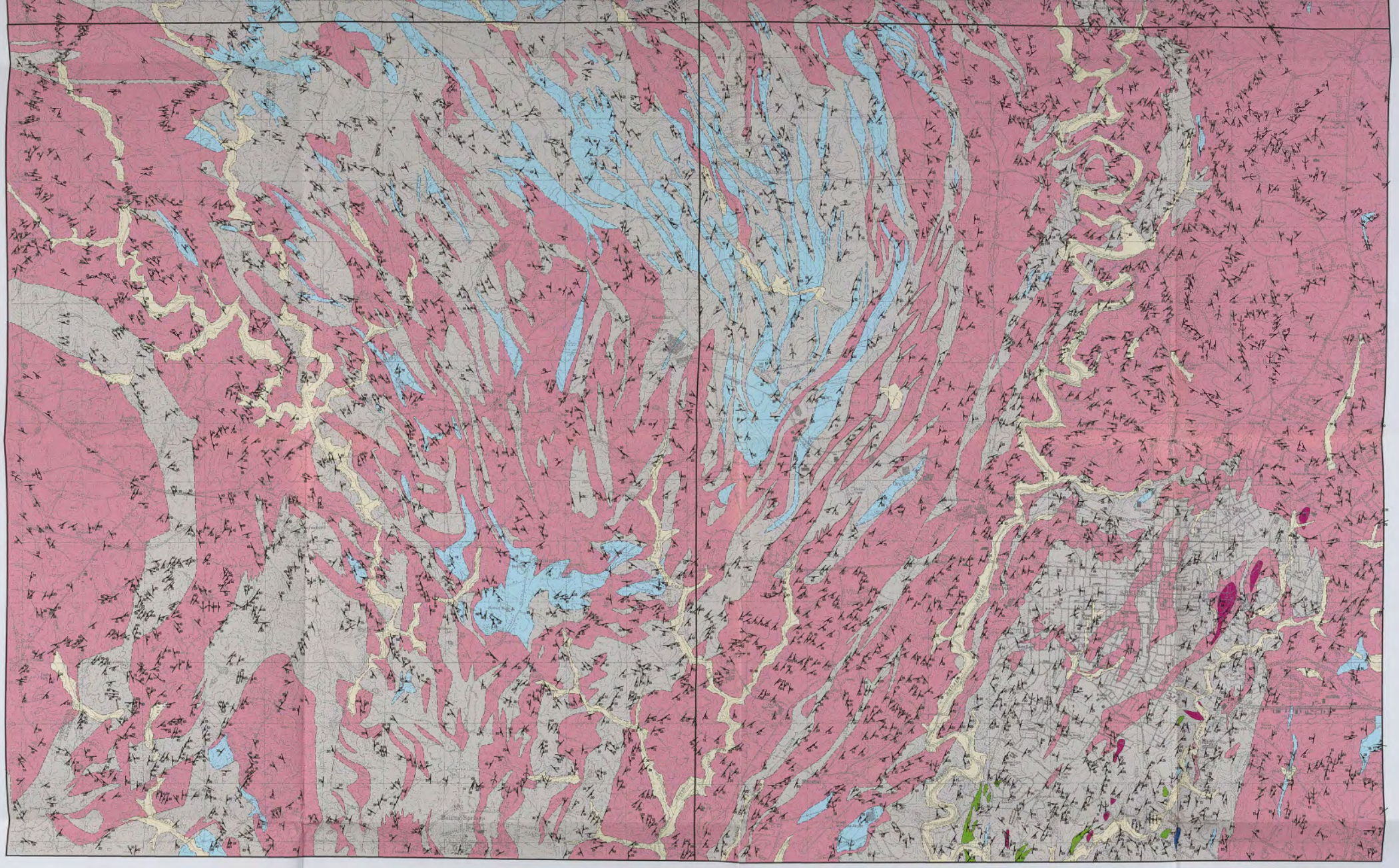
Trend and plunge of mineral elongation lineation

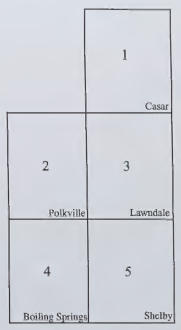
Trend and plunge of overturned, recumbent antiform

Trend and plunge of overturned, recumbent synform





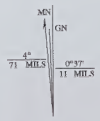


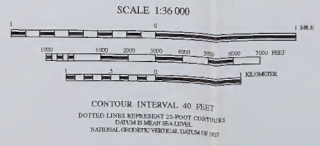


7.5-minute quadrangle index



QUADRANGLE LOCATION





CONTOUR INTERVAL 40 FEET
DOTTED LINES REPRESENT 25-FOOT CONTOURS
DATUM IS MEAN SEA LEVEL
NATIONAL GEODETIC VERTICAL DATUM OF 1929

SOURCES OF DATA

1. CASAR
Compiled from Overstreet, W. C., Whitlow, J. W., White, A. M., and Griffitts, W. C., 1963, Geologic map of the southern portion of the Casar quadrangle, Cleveland, Lincoln, and Burke Counties, North Carolina, showing areas mined for monazite and mica. U. S. Geological Survey Field Studies Map MF-257, 1:24,000.

2. POLKVILLE
Compiled from Yates, R. G., 1963, Preliminary geologic map of the northwest quarter of the Shelby quadrangle, Cleveland and Rutherford Counties, North Carolina, U. S. Geological Survey Field Studies Map MF-258, 1:24,000.

3. LAWNDALE
Compiled from Yates, R. G. 0and Overstreet, W. C., 1962, Preliminary geologic map of the northeast quarter of the Shelby quadrangle, Cleveland County, North Carolina, U. S. Geological Survey Field Studies Map MF-249, 1:24,000.

4. BOILING SPRINGS
Compiled from Griffits, W. C., Yates, R. G., and Overstreet, W. C., 1962, Preliminary geologic map of the southwest quarter of the Shelby quadrangle, Cleveland and Rutherford Counties, North Carolina. U. S. Geological Suvey Field Studies Map MF-252, 1:24,000.

5. SHELBY
Compiled from Griffits, W. C. and Overstreet, W. C., 1962, Preliminary geologic map of the southeast quarter of the Shelby quadrangle, Cleveland County, North Carolina, U. S. Geological Survey Field Studies Map MF-250, 1:24,000.

Plate IV. Station map of the Casar, Polkville, Lawndale, Boiling Springs, and Shelby 7.5-minute quadrangles, North Carolina

compiled by Sara Bier
supervised by Robert D. Hatcher, Jr.
University of Tennessee-Knoxville
Structural Geology and Tectonic Research Group
May 2001

EXPLANATION

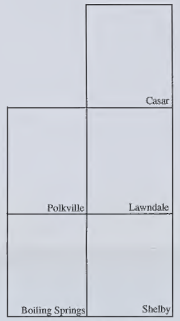
20 Compiled from Overstreet, W. C., Whitlow, J. W., White, A. M., and Griffitts, W. R., 1963, Geologic map of the southern portion of the Casar quadrangle, Cleveland, Lincoln, and Burke Counties, North Carolina, showing areas mined for monazite and mica. U. S. Geological Survey Field Studies Map MF-257, 1:24,000.

161 Compiled from Yates, R. G., 1963, Preliminary geologic map of the northwest quarter of the Shelby quadrangle, Cleveland and Rutherford Counties, North Carolina, U. S. Geological Survey Field Studies Map MF-258, 1:24,000.

371 Compiled from Yates, R. G. and Overstreet, W. C., 1962, Preliminary geologic map of the northeast quarter of the Shelby quadrangle, Cleveland County, North Carolina, U. S. Geological Survey Field Studies Map MF-249, 1:24,000.

1080 Compiled from Griffits, W. C., Yates, R. G., and Overstreet, W. C., 1962, Preliminary geologic map of the southwest quarter of the Shelby quadrangle, Cleveland and Rutherford Counties, North Carolina. U. S. Geological Survey Field Studies Map MF-252, 1:24,000.

405 Compiled from Griffits, W. C. and Overstreet, W. C., 1962, Preliminary geologic map of the southeast quarter of the Shelby quadrangle, Cleveland County, North Carolina, U. S. Geological Survey Field Studies Map MF-250, 1:24,000.



7.5-minute quadrangle index





CONTOUR INTERVAL 40 FEET
DOTTED LINES REPRESENT 20-FOOT CONTOURS
DATUM IS MEAN SEA LEVEL
NATIONAL GEODETIC VERTICAL DATUM OF 1927



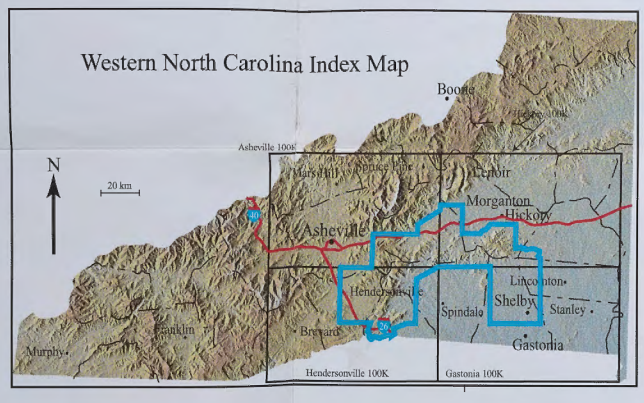
QUADRANGLE LOCATION


Belwood
Fairbanks
Double Mtns
Chestry Mountain
Mount Magnet
New Haven
Belwood
RIVER
ROAD

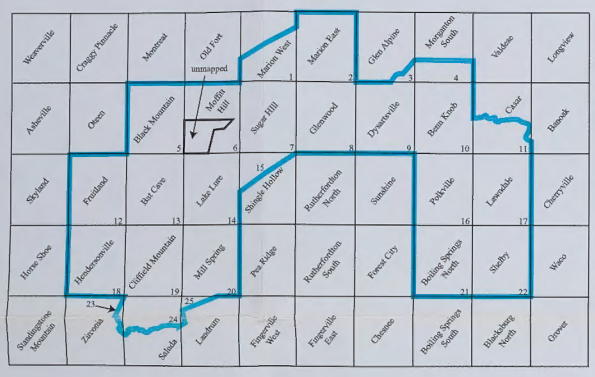

Boiling Springs
Shelby

Plate V. Detailed Geologic Mapping in the Western and Central Inner Piedmont, North Carolina

Version 3.5, May 2001
compiled by B. R. Bream and S. E. Bier
supervised by Robert D. Hatcher

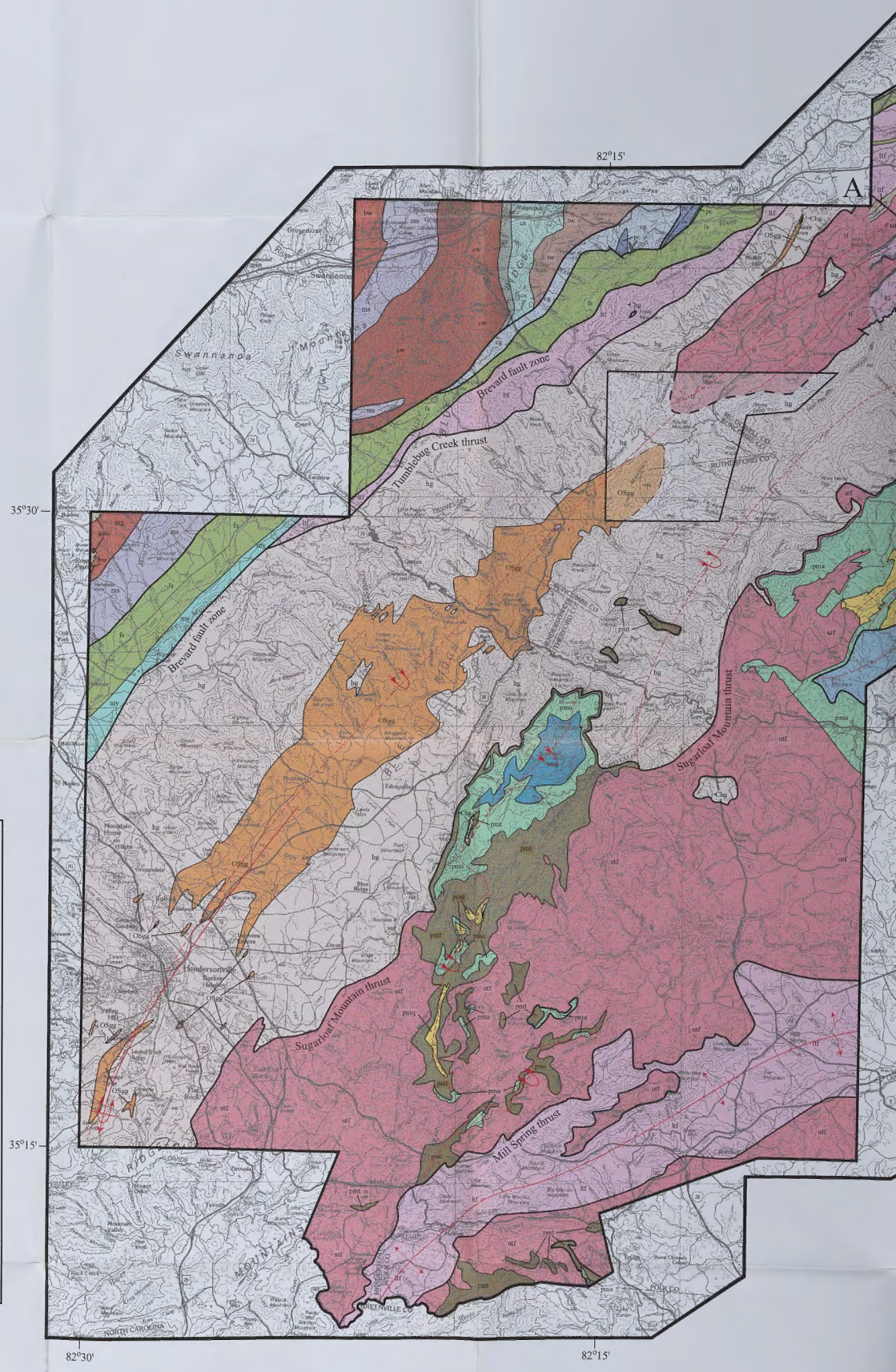


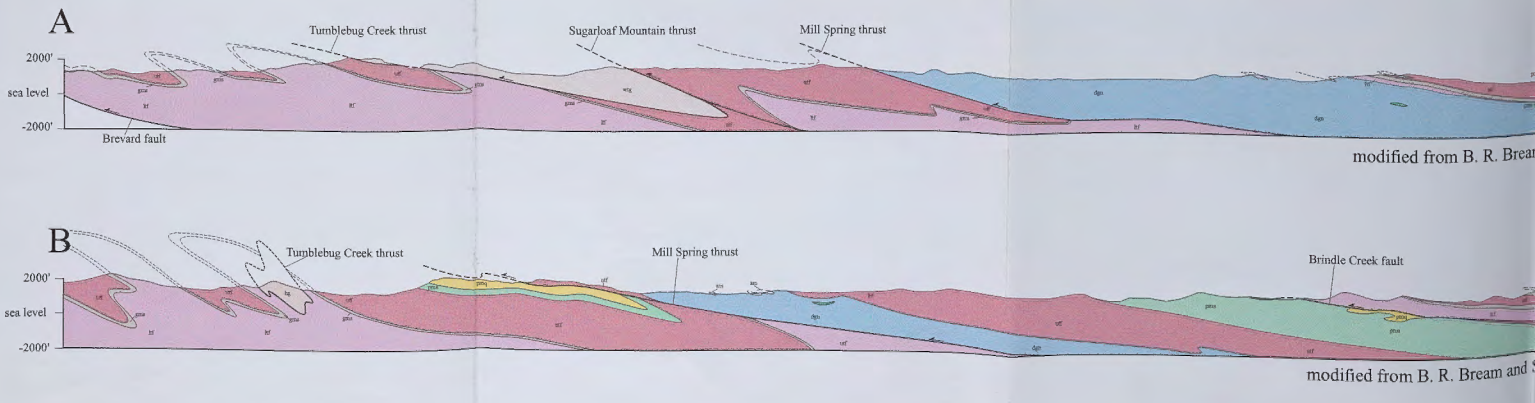
7.5' Quadrangle Index



Sources of data

1. Marion West
   - Bream, B.R., and Hill, J.C., in preparation, Geologic map of part of the Marion West quadrangle, North Carolina: North Carolina Department of Environment and Natural Resources open file report, scale 1:24,000.
   - Conley, J.F., and Drummond, R.N., 1981, Geologic map and mineral resources summary of the northeast 1/4 Marion Quadrangle, North Carolina: North Carolina Department of Natural Resources and Community Development and Tennessee Valley Authority GM 210–NE, scale 1:24,000.
2. Marion East
   - Hill, J.C., in preparation, Geologic map of the Marion East quadrangle, North Carolina: North Carolina Department of Environment and Natural Resources open file report, scale 1:24,000.
3. Glen Alpine
   - Giorgis, S.D., in preparation, Geologic map of part of the Glen Alpine quadrangle, North Carolina: North Carolina Department of Environment and Natural Resources open file report, scale 1:24,000.
4. Morganton South
   - Giorgis, S.D., and Riedel, J.J., in preparation, Geologic map of the Morganton South quadrangle, North Carolina: North Carolina Department of Environment and Natural Resources open file report, scale 1:24,000.
5. Black Mountain
   - Butler, J.R., 1972, Geologic map and mineral resources summary of the Black Mountain quadrangle, North Carolina: North Carolina Department of Natural and Economic Resources Map-GM 201–SE, scale 1:24,000.
6. Moffitt Hill
   - Hurley, B.W., 1974, Geology of the Old Fort area, McDowell County, North Carolina (unpublished M.S. thesis): Chapel Hill, University of North Carolina, 66 p.
   - Yanagihara, G.M., 1994, Structure, stratigraphy, and metamorphism of a part of the Columbus Promontory, western Inner Piedmont, North Carolina (unpublished M.S. thesis): Knoxville, University of Tennessee, 214 p.
7. Sugar Hill
   - Bream, B.R., in preparation, Geologic map of the Sugar Hill quadrangle, North Carolina: North Carolina Department of Environment and Natural Resources open file report, scale 1:24,000.
   - Whisnant, J.S., 1979, Geologic map of the SE 1/4 of the Marion quadrangle, North Carolina: North Carolina Geological Survey and Tennessee Valley Authority GM 210–SE, scale 1:24,000.
   - Yanagihara, G.M., 1994, Structure, stratigraphy, and metamorphism of a part of the Columbus Promontory, western Inner Piedmont, North Carolina (unpublished M.D. thesis): Knoxville, University of Tennessee, 214 p.
8. Glenwood
   - Bream, B.R., and Williams, S.T., in preparation, Geologic map of the Glenwood quadrangle, North Carolina: North Carolina Department of Environment and Natural Resources open file report, scale 1:24,000.
9. Dysartsville
   - Giorgis, S.D., and Williams, S.T., in progress, Geologic map of the Dysartsville quadrangle, North Carolina: North Carolina Department of Environment and Natural Resources open file report, scale 1:24,000.
10. Bean Knob
    - Giorgis, S.D., and Bier, S.E., in progress, Geologic map of the Bean Knob quadrangle, North Carolina: North Carolina Department of Environment and Natural Resources open file report, scale 1:24,000.
11. Casar
    - Bier, S.E., in progress, Geologic map of part of the Casar quadrangle, North Carolina: North Carolina Department of Environment and Natural Resources open file report, scale 1:24,000.
    - Overstreet, W.C., Whitlow, J.W., White, A. W., and Griffits, W.R., 1963, Geologic map of the southern part of the Casar quadrangle, Cleveland, Lincoln, and Burke counties, North Carolina showing areas mined for monazite and mica: U.S. Geological Survey, scale 1:24,000.
12. Fruitland
    - Lemmon, R.E., and Dunn, D.E., 1973, Geologic map and mineral resources of the Fruitland quadrangle, North Carolina: North Carolina Department of Natural Resources and Community Development Map GM 202–NW, scale 1:24,000.
13. Bat Cave
    - Lemmon, R.E., and Dunn, D.E., 1973, Geologic map and mineral resources of the Bat Cave quadrangle, North Carolina: North Carolina Department of Natural Resources and Community Development Map GM–NW, scale 1:24,000.
14. Lake Lure
    - Tabor, J.R., 1990, Geologic map of the Lake Lure quadrangle, North Carolina (unpublished mapping): Knoxville, University of Tennessee, scale 1:24,000.
    - Yanagihara, G.M., 1994, Structure, stratigraphy, and metamorphism of a part of the Columbus Promontory, western Inner Piedmont, North Carolina (unpublished M.S. thesis): Knoxville, University of Tennessee, 214 p.
    - Jayne, C.C., 1991, Geologic map of part of the Lake Lure quadrangle, North Carolina (unpublished mapping): Knoxville, University of Tennessee, scale 1:24,000.
15. Shingle Hollow
    - Yanagihara, G.M., 1994, Structure, stratigraphy, and metamorphism of a part of the Columbus Promontory, western Inner Piedmont, North Carolina (unpublished M.S. thesis): Knoxville, University of Tennessee, 214 p.
16. Polkville
17. Lawndale
    - Overstreet, W.C., Yates, R.G., Griffits, W.R., 1951 Geologic map of the Shelby 15' quadrangle: U.S. Geological Survey, scale 1:64,000.
18. Hendersonville
    - Lemmon, R.E., 1975, Geology of the Hendersonville quandrangle, North Carolina (unpublished mapping): University of North Carolina, Chapel Hill, scale 1:24,000.
19. Cliffield Mountain
    - Davis, T.L., 1993, Lithostratigraphy, structure, and metamorphism of a crystalline thrust terrane, western Inner Piedmont, North Carolina (unpublished Ph.D. dissertation): Knoxville, University of Tennessee, 245 p.
20. Mill Spring
    - Tabor, J.R., 1990, Geologic map of the Mill Spring quadrangle, North Carolina (unpublished mapping): Knoxville, University of Tennessee, scale 1:24,000.
21. Boiling Spring North
22. Shelby
    - Overstreet, W.C., Yates, R.G., Griffits, W.R., 1951 Geologic map of the Shelby 15' quadrangle: U.S. Geological Survey 1:62,500.
23. Zirconia
24. Saluda
25. Landrum
    - Davis, T.L., 1993, Lithostratigraphy, structure, and metamorphism of a crystalline thrust terrane, western Inner Piedmont, North Carolina (unpublished Ph.D. dissertation): Knoxville, University of Tennessee, 245 p.





STRUCTURE

Trace of axial surface of F_{2b} overturned, recumbent anticline

Trace of axial surface of F_{2b} overturned, recumbent syncline

Trace of axial surface of F_{2c} overturned, recumbent anticline

Trace of axial surface of F_{2c} overturned, recumbent anticline

Hinge of F_{3c} sheath fold

Trace of axial surface of F_3 open, upright anticline

Trace of axial surface of F_3 open, upright syncline

82°00'

35°45'

35°30'

35°15'

81°30'

A

A'

B

B'

C

C'

D

D'

Amblebug Creek thrust

Sugarloaf Mountain thrust

Mill Spring thrust

N

SCALE 1:100 000

1 CENTIMETER ON THE MAP REPRESENTS 1 KILOMETER ON THE GROUND

Kilometers 1 0 1 2 3 4 5 6 7 8 9 10 11 12 13 14 15 16 17 18 19 20

Miles 1 0 1 2 3 4 5 6 7 8 9 10 11 12 13

Supported by the National Cooperative Mapping Program (EDMAP) under Assistance Awards 97HQAG1720, 98HQAG2026, 99HQAG0026, and 00HQAG0035

Supported by National Science Foundation Grant No. EAR-9004604

Compiled from Overstreet et al. (1951, 1963)

Cross Sections

Scale: 1: 50 000

A'

ified from B. R. Bream

C

Brindle Creek fault

C'

2000'

sea level

-2000'

modified from S. G. Giorgis

B'

ault

rom B. R. Bream and S. T. Williams

D

D'

2000'

sea level

-2000'

NORTHWEST OF

AGE UNCERTAIN

ORDOVICIAN-SILURIAN

UPPER PRECAMBRIAN (?) or LOWER PALEOZOIC (?)

EXPLANATION

NORTHWEST OF BREVARD FAULT ZONE | BREVARD FAULT ZONE | SOUTHEAST OF BREVARD FAULT ZONE

AGE UNCERTAIN

ORDOVICIAN-SILURIAN

UPPER PRECAMBRIAN (?) or LOWER PALEOZOIC (?)

Poor Mountain Formation

Tallulah Falls Formation

mylt

Porphyroclastic mylonite and ultramylonite
Porphyroclastic mylonite, medium bluish gray to light gray, fine-grained, thinly laminated, well-foliated; contains rounded to lenticular feldspar porphyroclasts. Groundmass composed mainly of quartz 15%, plagioclase (albite) 10%, microcline 1-5%, muscovite-sericite as much as 75%, biotite-chlorite less than 5%, and opaque minerals. Grades into cataclastic schist and phyllonite. Ultramylonite, medium-gray, very fine grained, highly siliceous; flintlike appearance. Highly fractured; some fractures cemented by silica. Description from Lemmon and Dunn (1973b).

cs

Cataclastic schist, phyllonite, and mylonite
Cataclastic schist and phyllonite, light olive gray to dark gray, medium- to fine-grained; with variable development of "fish-scale" texture formed by curved mica flakes. Major minerals are quartz 15-40%, muscovite-sericite 45-75%, biotite-chlorite 2-24%, garnet, opaque minerals, and locally graphite and staurolite. Interlayered calcareous zones from a few inches to several meters thick. Mylonite, light bluish-gray; fine-grained groundmass with rounded to lenticular feldspar porphyroclasts; strongly foliated. Composition generally the same as the my unit. Description from Lemmon and Dunn (1973b).

cm

Marble
Marble, light-gray to light-bluish-gray, fine- to medium-grained; as discontinuous pods and calcareous layers within the cataclastic schist. Maximum thickness 43 meters. Major minerals are calcite-dolomite 50-55%, muscovite-sericite 30-40%, quartz 1-5%, and opaque minerals. Description from Lemmon and Dunn (1973b).

pl pg

Pegmatite
Pegmatite, coarse-grained (locally finer grained). Composed of quartz, plagioclase, microcline, and muscovite, with minor amounts of biotite and garnet. Mainly concordant lenticular, tabular, or pod-shaped bodies; as much as 16 meters thick. Description from Lemmon and Dunn (1973b).

tg

Toluca Granite
Granitic gneiss, light-gray, medium-grained, granoblastic; poorly to non-foliated. Major minerals include plagioclase (An_{20-30}) 38-42%, quartz 17-25%, microcline 15-44%, biotite 1-16%, and muscovite 2-22%. Accessory minerals include garnet, monazite, limenite, zircon, and opaque minerals. Weathers to white and tan saprolite, and contains xenoliths of biotite gneiss. Description from the Bent Knob 7.5' quadrangle.

wl

Walker top orthogneiss
Biotite granitic gneiss (granite to granodiorite in composition), light-gray, massive, weakly foliated, megacrystic. Microcline and plagioclase megacrysts are often rimmed with myrmekite. Matrix is composed of fine to medium grained quartz 14-16 %, biotite 13-22%, plagioclase (An_{25-30})15-26%, and muscovite 1-3%. Accessory minerals include garnet, zircon, epidote, and opaques. Description from the Bent Knob 7.5' quadrangle.

OSgg

Granitic gneiss
Biotite granitic gneiss (granite to granodiorite in composition), light-gray, medium-grained, poorly foliated. Contains plagioclase (oligoclase) 26%, quartz 33%, microcline 30%, biotite 6%, muscovite, sphene, epidote, allanite, zircon, and opaque minerals. Differs from the Henderson Gneiss in lack of augen and slightly lighter color. Interlayered with Henderson Gneiss (hg). Equivalent to part of the Henderson Granite. Zircon elongation ratios, from reduced major axes, average 2.8, suggesting an igneous origin. Description modified from Lemmon and Dunn (1973b).

dgn

Dysartsville orthogneiss
Biotite-muscovite granitoid gneiss (tonalite composition), light- to medium-gray, medium-grained, massive to weakly-foliated. Contains plagioclase (An_{25-30}) 40-55%, quartz 30-45%, biotite 4-15%, muscovite 0-10%, epidote/clinozoisite, chlorite, garnet, sphene, and opaque minerals. Weathers to a light-gray granular saprolite. Contains map-scale and smaller hornblende gneiss enclaves. Probably has an igneous protolith. Description from the Glenwood and Sugar Hill 7.5' quadrangles.

hg

Henderson Gneiss
Biotite augen gneiss (granite to granodiorite in composition), medium-gray to medium-bluish-gray; generally massive, homogeneous, and well-foliated, conspicuous feldspar (chiefly microcline) augen in a medium-grained matrix of quartz 25%, plagioclase (An_{15-25}) 31%, microcline (average, including augen) 28%, biotite 14%, muscovite 2%, epidote 1%, allanite, sphene, apatite, zircon, and opaque minerals. Cataclasis increases westward toward the Brevard fault zone. Interlayered with biotite granitic gneiss (OSgg). Zircon elongation ratios, from reduced major axes, average 2.6, suggesting an igneous origin. Description modified from Lemmon and Dunn (1973b).

sbgg

Sugarloaf Mountain gneiss
Biotite-muscovite granitic gneiss (granite composition), light-gray, medium-grained, massive to well-foliated. Weathers to a white to light-gray granular saprolite. Contains quartz 35%, plagioclase (oligoclase-andesine) 26%, microcline 28%, biotite 6%, muscovite 4%, garnet, epidote, zircon, chlorite, and opaque minerals. Cut by numerous pegmatite dikes and locally contains isolated discontinuous lenses of hornblende gneiss. Zircon elongation ratios, from reduced major axes, average 2.0, suggesting a sedimentary origin. Description modified from Lemmon and Dunn (1973a).

um

Ultramafic
Altered ultramafic rock, greenish-gray, medium- to fine-grained, felt to poor schistosity. Composed mainly of chlorite, amphibole, talc, carbonate, and opaque minerals. Probably derived from medium-grained olivine-pyroxene rock. Description from Butler (1972).

am

Amphibolite
Amphibolite and amphibole gneiss, dark-gray to black, medium- to coarse-grained, massive to poorly foliated. Contains hornblende, plagioclase, biotite, and quartz. Locally garnetiferous. Occurs as pods, boudins, or thinlayers within the other rock units. Description from the Glenwood and Sugar Hill 7.5' quadrangles.

pmq

Poor Mountain Quartzite
Feldspathic micaceous quartzite, light-tan to light-gray, fine- to medium-grained, massive to medium-layered, sometimes schistose. Composed of plagioclase (An_{25-30}) 30-60%, quartz 30-45%, biotite 0-20%, muscovite 0-8%, chlorite 0-3%, microcline 0-2%, garnet, epidote/clinozoisite, and opaque minerals. Interlayered with the pma unit. Weathers to a yellowish sand or saprolite. Probably derived from a feldspathic sandstone. Description from the Glenwood and Sugar Hill 7.5' quadrangles.

pma

Poor Mountain Amphibolite
Amphibolite and amphibole gneiss, dark- to medium-gray, fine- to medium-grained, finely laminated, thin- to medium-layered. Composed of hornblende 48-65%, plagioclase (An_{25-35}) 5-45%, epidote/clinozoisite 0-28%, quartz 0-6%, and minor amounts of biotite, sphene, zircon, and opaque minerals. Interlayered with the pmq unit and muscovite schist. Weathers to an orange-ochre saprolite. Chemically has a mid-ocean ridge basalt affinity. Description from the Glenwood and Sugar Hill 7.5' quadrangles.

pmtt

Brevard-Poor Mountain transitional unit
Garnetiferous muscovite schist, dark-gray to medium-light-gray, lustrous, medium-grained. Composed of muscovite 28%, biotite 33%, quartz 28%, plagioclase (oligoclase) 7%, microcline 1%, garnet 2%, and opaque minerals. Grades southeastward from Sugarloaf Mountain to a gray to light-gray, highly lustrous, medium-grained muscovite schist; composed of muscovite, quartz, and feldspar, with a decrease in garnet and a marked increase in magnetite southeastward. A discontinuous layer of coarse-grained, white crystalline marble as much as 0.5 meter thick crops out near the base of Werlds Edge. Description from Lemmon and Dunn (1973a).

tuf **tf**

Upper Tallulah Falls Formation (tuf) and undivided Tallulah Falls (tf)
Metagraywacke-biotite gneiss, light-gray to dark-gray, medium- to fine-grained, massive- to thick-layered, well-foliated, commonly porphyroblastic. Major minerals are quartz 26-46%, plagioclase 28-46% (An_{25-35}), biotite 15-30%, and muscovite 1-7%. Minor constituents are epidote, microcline, chlorite, and opaque minerals. Porphyroclasts are plagioclase and microcline. Layer thickness varies from a few millimeters to several meters. Relations to defined by quartzofeldspathic material medium to fine-metagraywacke and by biotite and muscovite in fine gneiss and schist. Probably derived from a feldspathic sandstone. Description from the Glenwood and Sugar Hill 7.5' quadrangles.

gmts

Tallulah Falls garnet mica schist
Muscovite-biotite-garnet-kyanite (or sillimanite) schist, light- to dark-silver-gray, inequigranular to porphyroblastic. Variable mineralogy contains quartz 7-40%, plagioclase 4-30%, muscovite 3-46%, biotite 0-22%, garnet 8-16%, and kyanite/sillimanite 4-15%. Poikiloblastic subhedral garnet porphyroblasts up to 4 mm in diameter occur in a fine-grained matrix. Weathers to tan and purple saprolite. Probably derived from argillaceous rocks. Description from the Glenwood and Sugar Hill 7.5' quadrangles.

ltf

L ower Tallulah Falls Formation
Metagraywacke-biotite gneiss, light-gray to dark-gray, medium- to fine-grained, massive- to thick-layered, well-foliated, commonly porphyroblastic. Similar to the tuf in dominant mineralogy. Generally contains a larger amount of amphibolite and is commonly more migmatitic than the tuf unit. Probably derived from a feldspathic sandstone. Description from the Glenwood and Sugar Hill 7.5' quadrangles.

am

Amphibolite
Amphibolite, black to dark-gray, medium-grained and foliated. Composed of hornblende 63%, plagioclase (calcic oligoclase) 18%, quartz 10%, epidote 4%, and opaque minerals 4%. Generally occurs as a discontinuous, concordant body. Description from Lemmon and Dunn (1973b).

bv

Thin-layered Metasandstone and Schist
Metasandstone and metasiltstone, yellowish-gray to medium bluish-gray, generally thin-layered but locally medium-layered; schist, lustrous light olive-gray to greenish-gray, fine-grained. Schist locally contains graphite and garnet. Probably derived from thinly bedded sequence of sandstone, siltstone, and mudstone. Description from Butler (1972).

pc **os**

Massive porphyroclastic gneiss (pc) and metasiltstone (os)
Porphyroclastic gneiss (pc), medium-gray, fine-grained (matrix), well-foliated, and unlayered. The fine-grained matrix is composed of recrystallized quartz, biotite, white mica, and newly formed epidote or clinozoisite. Porphyroclasts are dominantly untwinned microcline and plagioclase. Metasiltstone (os), medium to dark gray, very fine-grained, and well-foliated with little compositional layering. Major minerals are quartz, plagioclase, white mica, biotite, garnet and sphene. Quartz, plagioclase, and micas form the fine-grained recrystallized groundmass. Description modified from Hurley (1974).

cg

Cataclastic gneiss
Cataclastic granitic gneiss and biotite gneiss, light-gray to medium dark-gray with conspicuous white porphyroclasts of microcline and plagioclase, coarse- to medium-grained, massive- to thin-layered. Locally included biotite schist and boudins of amphibolite. Degree of cataclasis variable; zones of mylonite up to several meters thick conformable to the gneissic layering. Description from Butler (1972).

ss

Muscovite-Chlorite schist
Muscovite-chlorite schist, light to dark greenish-gray, fine-grained, commonly contains garnet and graphite. Minor thin layers of metasandstone. Probably derived from mudstone with minor silty and sandy layers. Description from Butler (1972).

gs

Graphite-Muscovite schist
Dark graphite-muscovite schist, lustrous medium dark-gray to light-gray, fine-grained with scattered porphyroblasts, commonly contains garnet, biotite, and kyanite, locally contains staurolite or chlorite. Pyrite abundant in places. Minor thin-layered dark-gray metasandstone. Probably derived from carbonaceous mudstone with some silty and sandy layers. Description from Butler (1972).

cgw

Metasandstone, metaconglomerate, and biotite-muscovite schist
Metasandstone, medium light-gray to yellowish-gray, massive- to thin-layered; metaconglomerate, light bluish-gray, massive- to thick-layered, with deformed quartz pebbles as much as five centimeters long; muscovite-biotite-garnet schist, lustrous light olive-gray to greenish-gray, medium- to fine-grained. Schist contains some graphite, particularly near eastern contact. Sequence probably derived from carbonaceous mudstone with some silty and sandy layers. Description from Butler (1972).

mz

Garnetiferous muscovite and muscovite-biotite schist
Muscovite and muscovite-biotite schist, lustrous-white to yellowish-gray, medium-grained; generally contains garnet porphyroblasts. Composed of muscovite-sericite 30-66%, biotite-chlorite 10-30%, quartz 1-30%, garnet 1-5%, and opaque minerals. Interlayered with micaceous feldspathic metasandstone. Probably derived from argillaceous rocks with minor sandy layers. Description from Lemmon and Dunn (1973b).

bw **mg**

Biotite metasandstone (bw) and layered muscovite gneiss and schist (mg)
Biotite metasandstone (bw), medium-bluish-gray to yellowish-gray, medium- to fine-grained, thick- to thin-layered. Major minerals are quartz, feldspar, biotite, and muscovite; locally contains garnet. Probably derived from feldspathic sandstone. Biotite-muscovite gneiss (mg), light- to dark-gray, medium- to coarse-grained. Composition: average quartz 40%, plagioclase (oligoclase) 25%, microcline 10%, muscovite-sericite 10%, biotite 10%, garnet 2%, and opaque minerals. Interlayered with subordinate amounts of garnet-muscovite schist and biotite schist. Probably derived from feldspathic sandstone, interbedded with mudstone, and siltstone.Description from Lemmon and Dunn (1973b).

gms

Garnetiferous muscovite schist
Garnetiferous muscovite schist, lustrous-white to dark-gray, medium-grained. Composed mainly of muscovite, biotite, quartz, garnet, and feldspar. Probably derived from argillaceous rocks with minor sandy layers. Description from Lemmon and Dunn (1973b).

pf gn

Layered gneiss
Biotite gneiss, ranges to biotite schist; compositionally layered, medium- to dark-gray, fine- to medium-grained, equigranular. Composed of quartz, plagioclase, biotite, and minor muscovite; locally garnetiferous. Includes zones layers and masses of granitic mortar and flaser gneiss which contain pink microcline porphyroclasts. Description from Conley and Drummond (1985).

pf wmg

Mica gneiss unit of the Wilson Creek Gneiss
Mica gneiss to augen gneiss, light-gray, poorly foliated, medium- to fine-grained, well-foliated and lineated, inequigranular. Composed of quartz 40-55%, plagioclase 20-30%, muscovite 15-20%, microcline 5-10%, opaque minerals 3%, various amounts of sericite altered from muscovite and feldspar, and chlorite altered from biotite. Weathers to light-tan saprolite and pinkish silty clay soil. Description from Conley and Drummond (1985).

pf wcg

Quartz monzonite unit of the Wilson Creek Gneiss
Quartz monzonite, strongly foliated, gray-green, medium- to coarse-grained, inequigranular to porphyritic. Composed of muscovite 30-35%, plagioclase 20-30%, quartz 20-25%, microcline 10-15%, chlorite 5%, and minor epidote, calcite, biotite, limenite, and leucoxene. Cataclastic textures, ranging from mortar gneiss to mylonite, are present throughout. Description from Conley and Drummond (1985).